Support Information

Dichlorotetrazine-Mediated Peptide Cyclodimerization Enables Exponential Expansion and Topological Diversification of Peptide Libraries

Quan Zuo[a,b,c], Quanshu He[a,b,c], Jie Yan[a,b,c], Ximiao Yang[a,b], Hao Tian[a,b], Hongyi Huang[a,b], Xin Gao[a,b], Jieting Shen[a,b], Yonghui Hu[a,b], Linger Li[a,b], Minzi Lu[a,b], Rui Wang*[a,b], Kuan Hu*[a,b]

[a] Dr. Q. Zuo, Q. He, J. Yan, X. Yang, H. Tian, H. Huang, X. Gao, J. Shen, Y. Hu, L. Li, M. Lu, Prof. Dr. R. Wang, Prof. Dr. K. Hu
State Key Laboratory of Bioactive Substance and Function of Natural Medicines
Institute of Materia Medica, Chinese Academy of Medical Sciences and Peking Union Medical College
Beijing 100050, P. R. China
E-mail: wangrui@lzu.edu.cn; hukuan@imm.ac.cn

[b] Dr. Q. Zuo, Q. He, J. Yan, X. Yang, H. Tian, H. Huang, X. Gao, J. Shen, Y. Hu, L. Li, M. Lu, Prof. Dr. R. Wang, Prof. Dr. K. Hu
Beijing Key Laboratory of Targeted Radiopharmaceutical Development and Translational Nuclear Medicine,
Institute of Materia Medica, Chinese Academy of Medical Sciences & Peking Union Medical College,
Beijing 100050, P. R. China

[c] These authors contributed equally to this work.

Table of contents

1. General information

1.1 Reagents

Commercially available reagents and solvents were purchased from Energy Chemical, J&K Scientific, Innochem or Bidepharm and all these reagents were used directly without further purification unless otherwise noted. All kinds of buffer were purchased from MACKLIN Reagent. RP-HPLC solvents were purchased as HPLC grade from Innochem. Unless stated otherwise, all reactions were carried out in flame-dried glassware. All solvents were purified and dried according to standard methods prior to use. Most peptides were obtained using standard Fmoc SPPS-chemistry, the other peptides were ordered from Genscript Biotech Corporation and Hangzhou Zhuan Tai Biotechnology.

1.2 Instruments

LC-MS spectra were performed on a Waters SQ Detector 2 mass spectrometer coupled to an Acquity ultra-performance liquid chromatography (UPLC) system. Purity analysis was carried out on Waters 2998. Semi-preparative HPLC was carried out on a SHIMADZU Essentia LC-16P using a Waters XBridge® Peptide BEH C18 (5 μm, 19 mm x 150 mm) Column. Small molecule compounds were purified using Biotage IsoleraOne Flash. Additionally, the equipment includes: a constant temperature shaking incubator (model THZ-100) produced by Shanghai Yiheng Scientific Instruments Co., Ltd.; a biosafety cabinet (model MSC1.5) from Thermoscientific in Germany; a constant temperature incubator (model DHP9080B) produced by Shanghai Langxuan Laboratory Equipment Co., Ltd.; a Ge-Ga generator from New Radiomedicine Technology in Chengdu, China; a microPET/CT from Siemens Medical Solutions in Knoxville, Munich, Germany.

2. LC-MS, analytical HPLC and preparative HPLC information

2.1 UPLC-MS analysis

LC–MS was performed on a SQ Detector 2 mass spectrometer coupled to an Acquity highperformance liquid chromatography (UPLC) system, equipped with UPCMA, UPBSM+, and UPSMFTN+. Water (solvent A) and acetonitrile with 0.1% formic acid (solvent B), were used as the mobile phase at a flow rate of 0.3 mL/min.

Low-resolution mass spectrometric measurements were acquired using the following parameters: positive electrospray ionization (ESI), desolvation temperature = 350 °C, source gas flow = 645 L / h, capillary voltage = 3.0 kV, cone voltage = 40 V; negative electrospray ionization (ESI), desolvation temperature = 350 °C, source gas flow = 645 L / h, capillary voltage = 2.2 kV, cone voltage = 50 V.

For UPLC-MS analyses of the reaction mixtures, the photodiode array (PDA/DAD) detector provides two traces simultaneously from a single injection: a full-wavelength total absorbance chromatogram to monitor all UV-active species, and an extracted UV chromatogram at a specific wavelength (220 nm, 270nm, or 285 nm) used for determining the analytical yield of the target products.

Following LC methods were used:

Tab S1. Method A (Column: Waters ACQUITY UPLC® Peptide BEH C18, 2.1 × 100 mm, 1.7 μm, flow rate 0.3 mL/min)

Time (min)	Solvent A (%)	Solvent B (%)
0	95	5
5.50	45	55
8.00	0	100
9.00	0	100
9.01	95	5
10	95	5

2.2 Analytical HPLC

Analytical RP-HPLC analysis was performed on a Waters 2998, equipped with SMFTN-R, and QSM-R. All RP-HPLC analyses were done with 0.1% (v/v) trifluoroacetic acid (TFA) in water (RP-HPLC solvent A) and acetonitrile with 0.1% (v/v) TFA (RP-HPLC solvent B) as mobile phases. Typically, Method B and Method C were used for analytical RP-HPLC analyses.

Tab S2. Method B (CHIRALPAK®IC, 4.6 × 250 mm, 5 μm, flow rate 1 mL/min)

Time (min)	Solvent A (%)	Solvent B (%)
0	95	5
15	10	90

15.01	0	100
17	0	100
17.01	95	5
20	95	5

Tab S3. Method C (Inertsil ODS-SP, 4.6 × 250 mm, 5 µm, flow rate 1 mL/min)

Time (min)	Solvent A (%)	Solvent B (%)
0	95	5
25	35	65
27	5	95
27.01	5	95
35	95	5
35.01	95	5

Tab S4. Method D (Inertsil ODS-SP, 4.6 × 250 mm, 5 µm, flow rate 1 mL/min)

Time (min)	Solvent A (%)	Solvent B (%)
0	100	0
5	100	0
20	70	30
25	35	65
25.01	5	95
27	5	95
27.01	100	0
35	100	0

Tab S5. Method E (CHIRALPAK®IC, 4.6 × 250 mm, 5 µm, flow rate 1 mL/min)

Time (min)	Solvent A (%)	Solvent B (%)
0	90	10
50	80	20
50.01	0	100
55	0	100
55.01	95	5
60	95	5

Tab S6. Method F (Inertsil ODS-SP, 4.6 × 250 mm, 5 µm, flow rate 1 mL/min)

Time (min)	Solvent A (%)	Solvent B (%)
0	90	10
20	0	100

25	0	100
25.01	90	10
30	90	10

2.3 Preparative HPLC

Purification of peptides on a semi-preparative scale was performed on a SHIMADZU Essentia LC-16P using a Waters XBridge® Peptide BEH C18 (5 μm, 19 mm x 150 mm) Column at a flow rate of 6-8 mL/min. All peptides were separated by RP-HPLC using acetonitrile with 0.1% (v/v) TFA and water as mobile phases.

3. Synthesis of peptide substrates

Peptide substrates mainly include unprotected long peptides which are obtained mainly by solid-phase synthesis.

Solid-Phase Peptide Synthesis (SPPS):

Peptide synthesis was carried out manually using standard Fmoc SPPS-chemistry and CTC resin. CTC resin (1.0 equiv., 0.1 mmol) pre-swollen 30 min in CH_2Cl_2 (20 mL). Fmoc-amino acids (2.0 equiv.) was coupled to the resin using HBTU (4.0 equiv.) and DIEA (8.0 equiv.) in CH_2Cl_2 (20 mL, r.t., 1.5 h). After Fmoc deprotection with 20% piperidine/DMF (15 min) and washing (alternating DMF/CH_2Cl_2, 3 times each). Subsequent amino acids were coupled sequentially using HBTU/DIEA in DMF (r.t., 1.5 h per cycle). Kaiser tests confirmed complete deprotection after each step. The remaining steps mainly refer to the literature[1].

Peptide cleavage and deprotection:

Peptides were deprotected and cleaved from the resin under reducing conditions, by treatment with 2.5% v/v water and 2.5% v/v triisopropylsilane in neat trifluoroacetic acid (40 mL). For cysteine-containing peptides, the cleavage conditions typically involve TFA: Tris: Water: EDT, v:v= 92.5%: 2.5%: 2.5%: 2.5%. The resulting mixture was shaken for 3 hours, at room temperature. The resin was removed by filtration and peptides were precipitated in cold diethyl ether (50 mL). Peptides were pelleted by centrifugation at 4000 rpm, at 4 °C, for 5 minutes. Finally, the mother liquors were carefully removed and crude peptides were dried under vacuum.

Peptide purification and analyses:

Peptides were dissolved in water with a minimum amount of organic co-solvent (acetonitrile, dimethylformamide or dimethyl sulfoxide). Peptides were then purified

on preparative RP-HPLC. Fractions containing the desired peptide were lyophilized. The purity was assessed by analyzing using Method C, and low-resolution mass (LRMS) measurements were also acquired using Method A.

Characterization of oligopeptides and long peptides:

H-Cys-Arg-Gly-Asp-{D-Pro}-Pro-Arg-Gly-Asp-Cys-OH (**L1**). Analytical HPLC using Method C, RT = 5.650 min, the HPLC purity is 95%.

<Chromatogram>

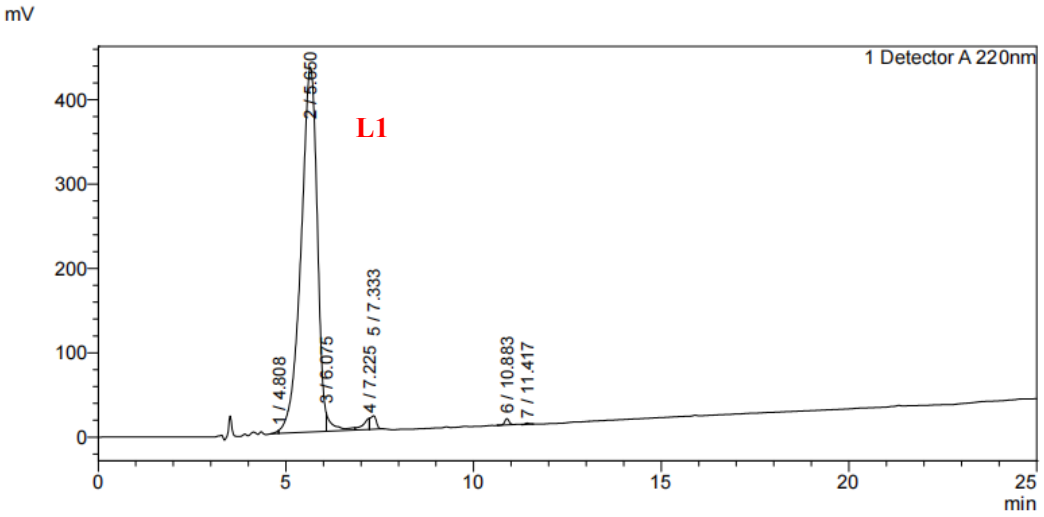

<Peak Table>

Detector A 220nm

Peak#	Ret. Time	Area	Height	Area%
1	4.808	17454	3731	0.129
2	5.650	12880409	432551	95.061
3	6.075	255649	21829	1.887
4	7.225	146419	13036	1.081
5	7.333	178123	15895	1.315
6	10.883	58648	7423	0.433
7	11.417	12988	1545	0.096
Total		13549690	496009	100.000

Fig S1. HPLC-UV chromatogram at 220 nm of **L1**.

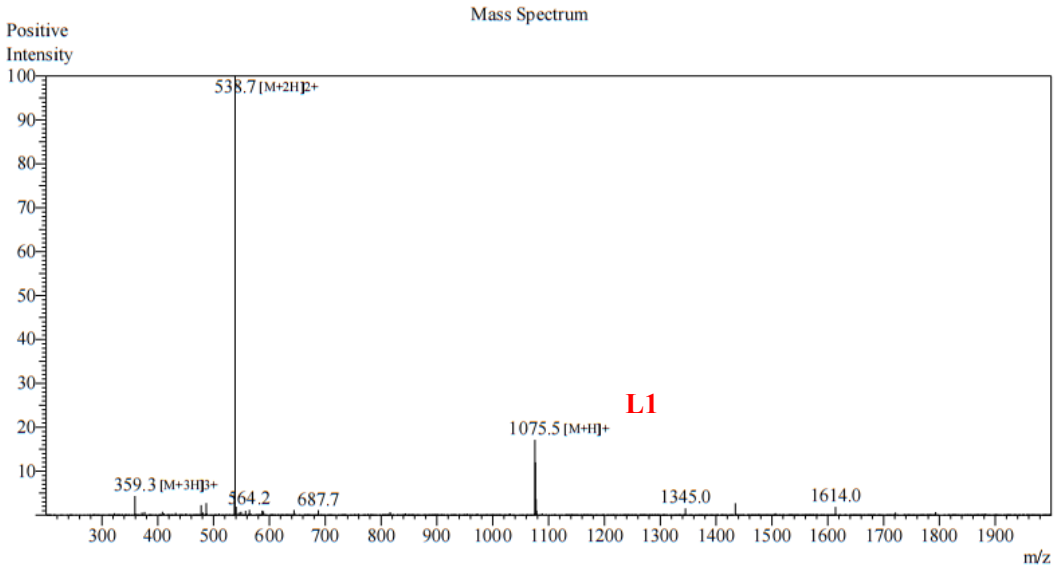

Fig S2. ESI-MS spectrum of **L1**. LRMS (ES+) m/z: $[M+H]^+$ calcd for $C_{40}H_{66}N_{16}O_{15}S_2$ 1075.4, found 1075.5.

Ac-Cys-Arg-Gly-Asp-{D-Pro}-Pro-Arg-Gly-Asp-Cys-OH (L2). Analytical HPLC using Method C, RT = 9.342 min, the HPLC purity is 96%.

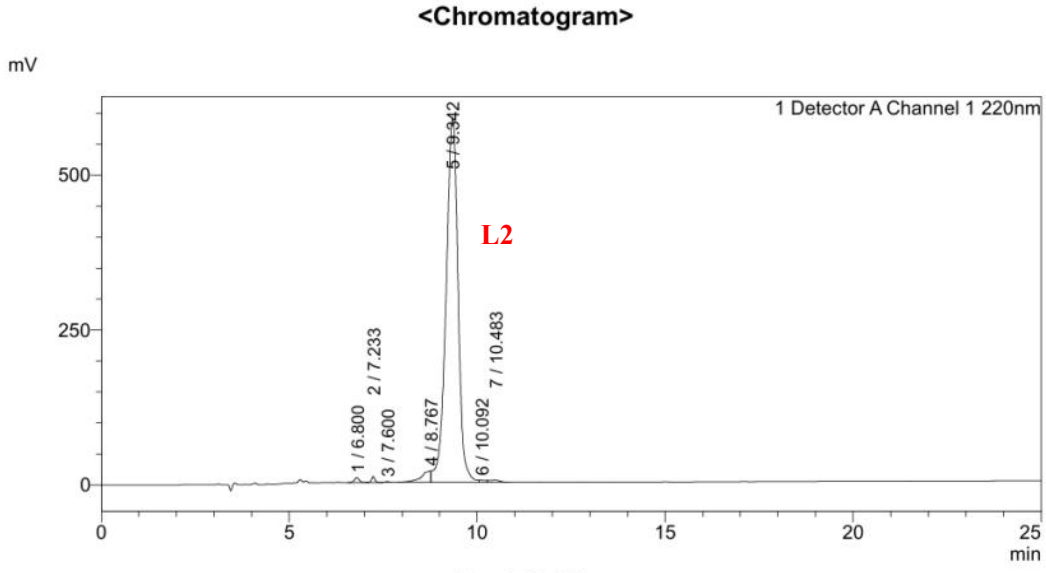

<Peak Table>

Detector A Channel 1 220nm

Peak#	Ret. Time	Area	Height	Area%
1	6.800	76401	8023	0.561
2	7.233	60777	9744	0.446
3	7.600	6756	1248	0.050
4	8.767	322911	18362	2.372
5	9.342	13044587	589025	95.822
6	10.092	37782	3170	0.278
7	10.483	64192	3239	0.472
Total		13613406	632811	100.000

Fig S3. HPLC-UV chromatogram at 220 nm of **L2**.

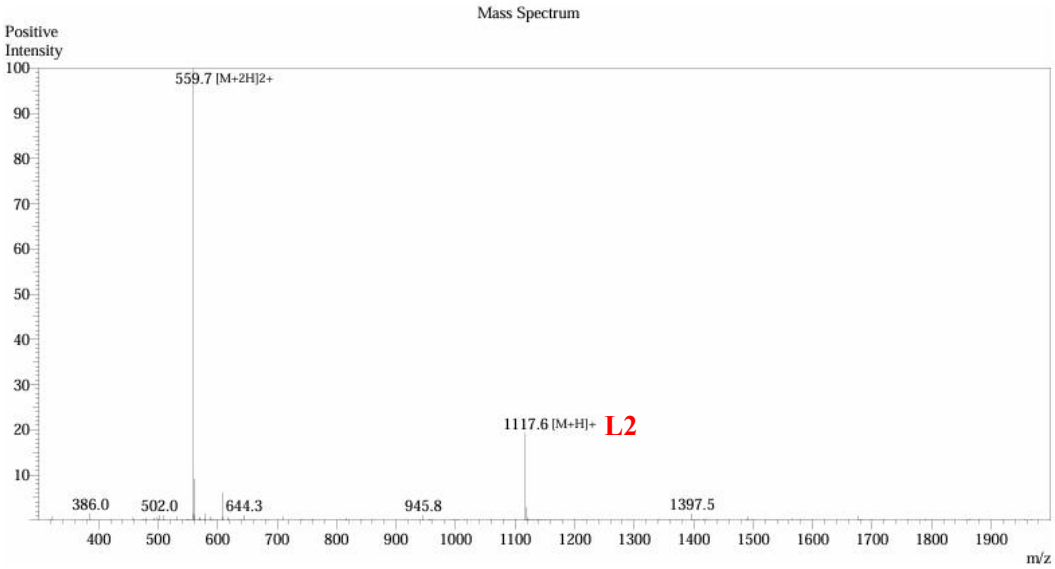

Fig S4. ESI-MS spectrum of **L2**. LRMS (ES+) m/z: $[M+H]^+$ calcd for $C_{42}H_{68}N_{16}O_{16}S_2$ 1117.4, found 1117.6.

H-Cys-Arg-Gly-Asp-{D-Pro}-Pro-Arg-Gly-Asp-Ala-OH (L3). Analytical HPLC using Method C, RT = 8.842 min, the HPLC purity is 99%.

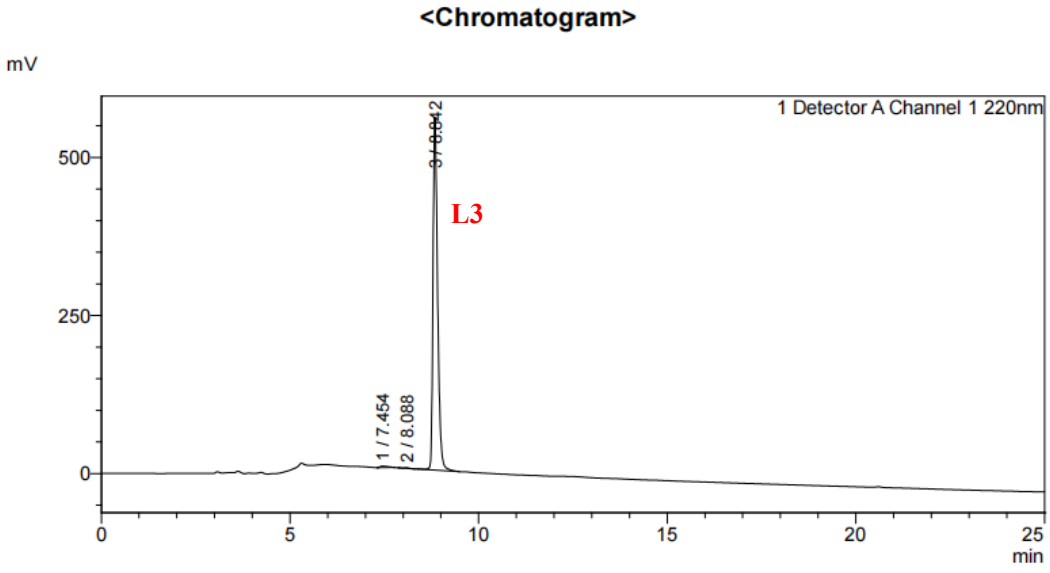

<Peak Table>

Detector A Channel 1 220nm

Peak#	Ret. Time	Area	Height	Area%
1	7.454	34378	2383	0.725
2	8.088	7587	1230	0.160
3	8.842	4698864	558401	99.115
Total		4740829	562014	100.000

Fig S5. HPLC-UV chromatogram at 220 nm of **L3**.

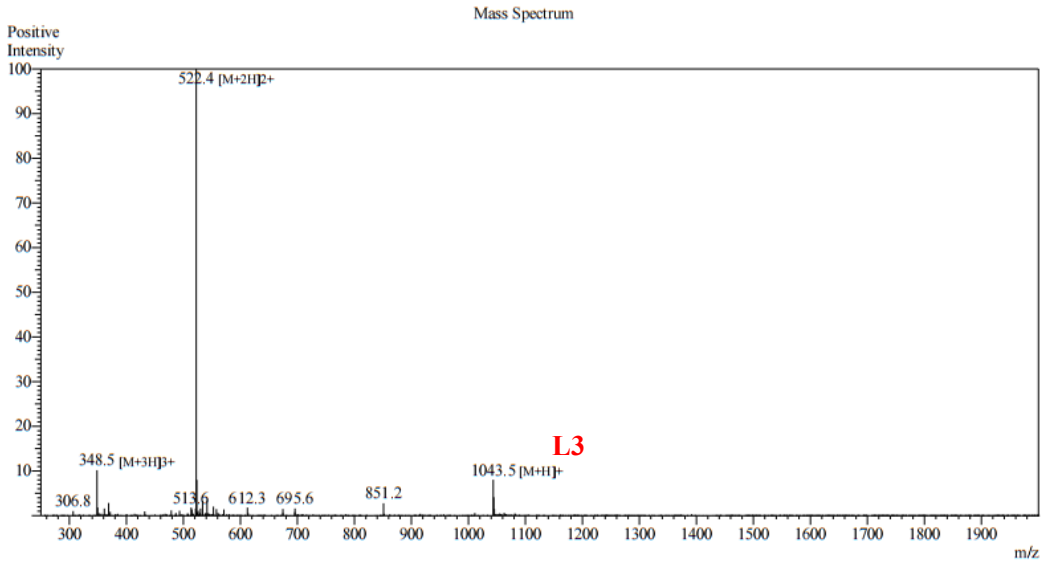

Fig S6. ESI-MS spectrum of **L3**. LRMS (ES+) m/z: $[M+H]^+$ calcd for $C_{40}H_{66}N_{16}O_{15}S_2$ 1043.5, found 1043.5.

H-Cys-Ala-NH$_2$ (L4). Analytical HPLC using Method D, RT = 4.017 min, the HPLC purity is 96%.

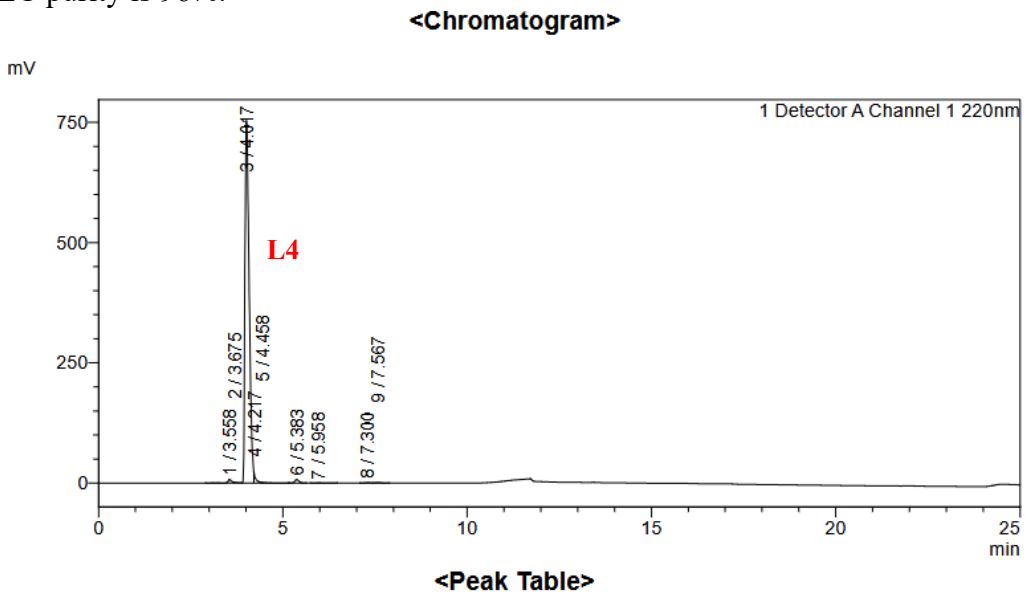

<Peak Table>

Detector A Channel 1 220nm

Peak#	Ret. Time	Area	Height	Area%
1	3.558	52967	7633	0.855
2	3.675	14018	1651	0.226
3	4.017	5960159	754411	96.179
4	4.217	80475	23910	1.299
5	4.458	9648	1031	0.156
6	5.383	56638	7480	0.914
7	5.958	3610	227	0.058
8	7.300	8411	832	0.136
9	7.567	11010	1125	0.178
Total		6196936	798300	100.000

Fig S7. HPLC-UV chromatogram at 220 nm of **L4**.

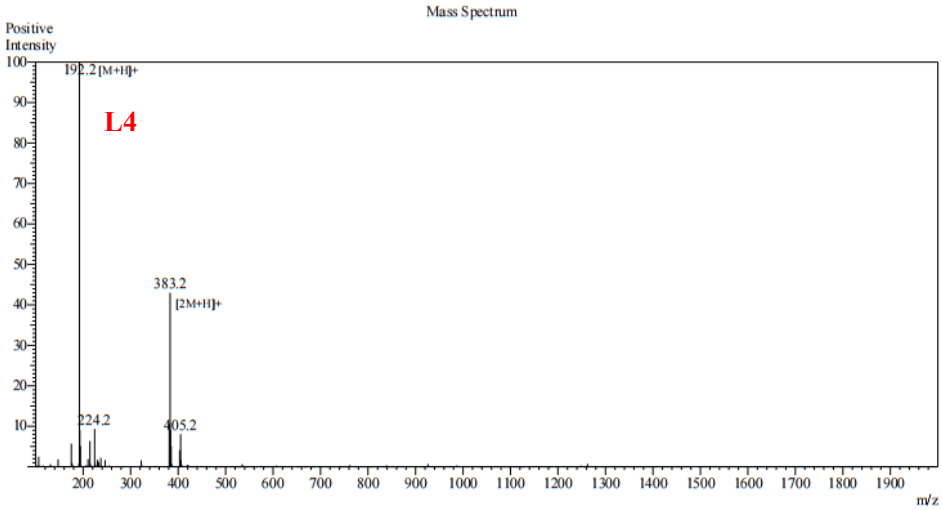

Fig S8. ESI-MS spectrum of **L4**. LRMS (ES+) m/z: $[M+H]^+$ calcd for $C_6H_{14}N_3O_2S$ 192.1, found 192.2.

H-Ala-Arg-Gly-Asp-pro-Pro-Arg-Gly-Asp-Cys-OH (**L5**). Analytical HPLC using Method C, RT = 7.561 min, the HPLC purity is 99%.

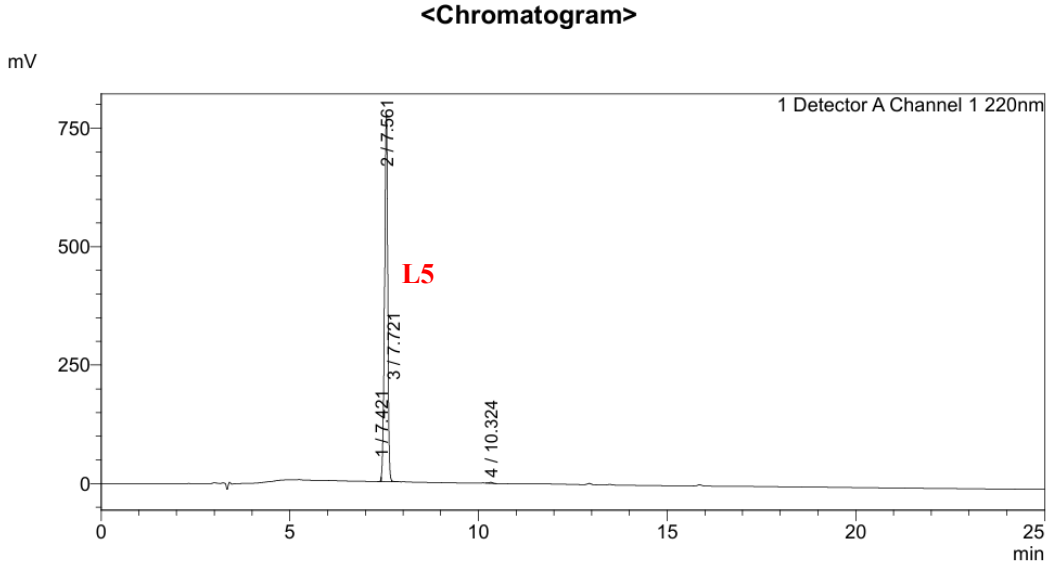

<Peak Table>

Detector A Channel 1 220nm

Peak#	Ret. Time	Area	Height	Area%
1	7.421	9663	5000	0.210
2	7.561	4586561	774340	99.437
3	7.721	3634	1645	0.079
4	10.324	12655	2266	0.274
Total		4612513	783252	100.000

Fig S9. HPLC-UV chromatogram at 220 nm of **L5**.

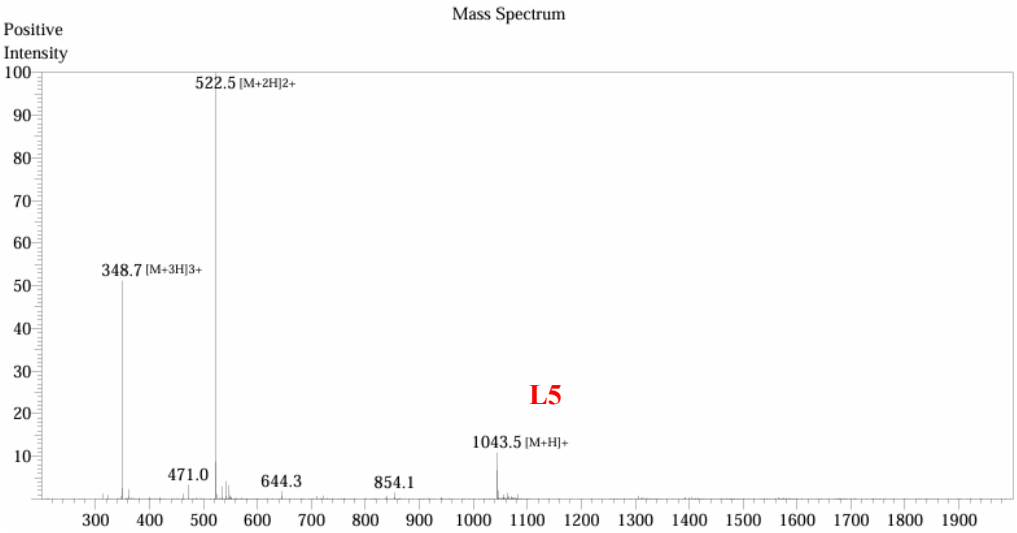

Fig S10. ESI-MS spectrum of **L5**. LRMS (ES+) m/z: $[M+H]^+$ calcd for $C_{40}H_{66}N_{16}O_{15}S_2$ 1043.5, found 1043.5.

H-Cys-Arg-Gly-Asp-Ala-Ala-Arg-Gly-Asp-Cys-OH (**L6**). Analytical HPLC using Method C, RT = 6.417 min, the HPLC purity is 90%.

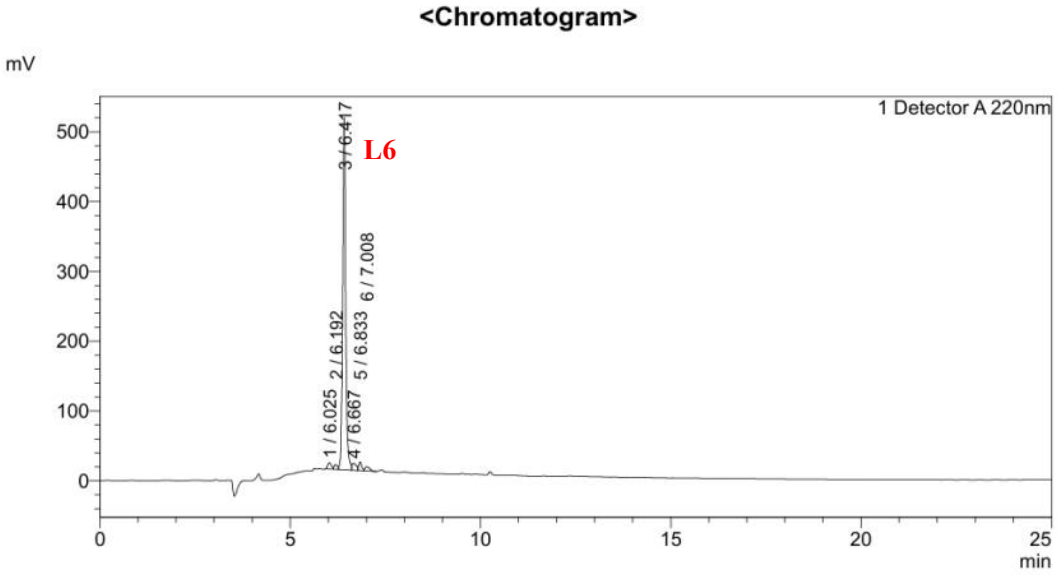

<Peak Table>

Detector A 220nm

Peak#	Ret. Time	Area	Height	Area%
1	6.025	60625	8966	1.959
2	6.192	42654	6755	1.378
3	6.417	2791723	504527	90.211
4	6.667	81204	9856	2.624
5	6.833	68142	12281	2.202
6	7.008	50322	5926	1.626
Total		3094671	548312	100.000

Fig S11. HPLC-UV chromatogram at 220 nm of **L6**.

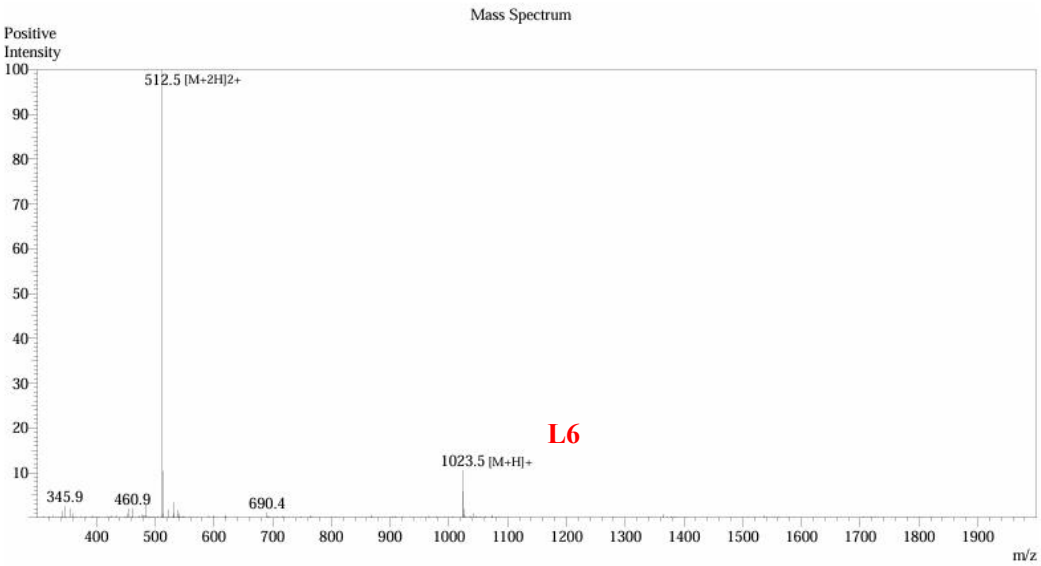

Fig S12. ESI-MS spectrum of **L6**. LRMS (ES+) m/z: $[M+H]^+$ calcd for $C_{36}H_{62}N_{16}O_{15}S_2$ 1023.4, found 1023.5.

H-Cys-Arg-Gly-Asp-Gly-Gly-Arg-Gly-Asp-Cys-OH (**L7**). Analytical HPLC using Method D, RT = 14.003 min, the HPLC purity is 93%.

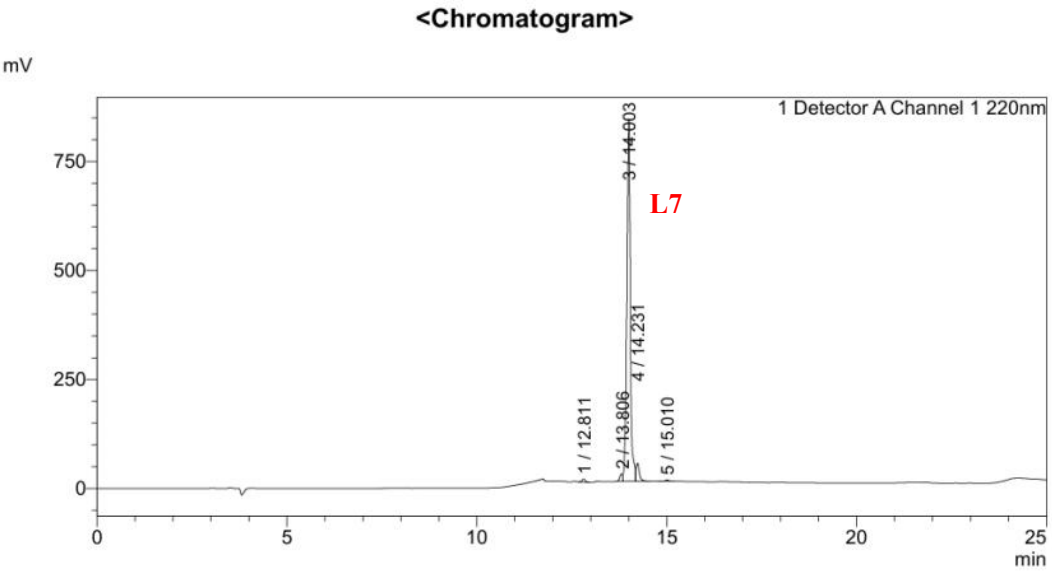

<Peak Table>

Detector A Channel 1 220nm

Peak#	Ret. Time	Area	Height	Area%
1	12.811	36849	6745	0.643
2	13.806	86911	17192	1.517
3	14.003	5341944	832144	93.267
4	14.231	245666	41510	4.289
5	15.010	16190	3185	0.283
Total		5727560	900775	100.000

Fig S13. HPLC-UV chromatogram at 220 nm of **L7**.

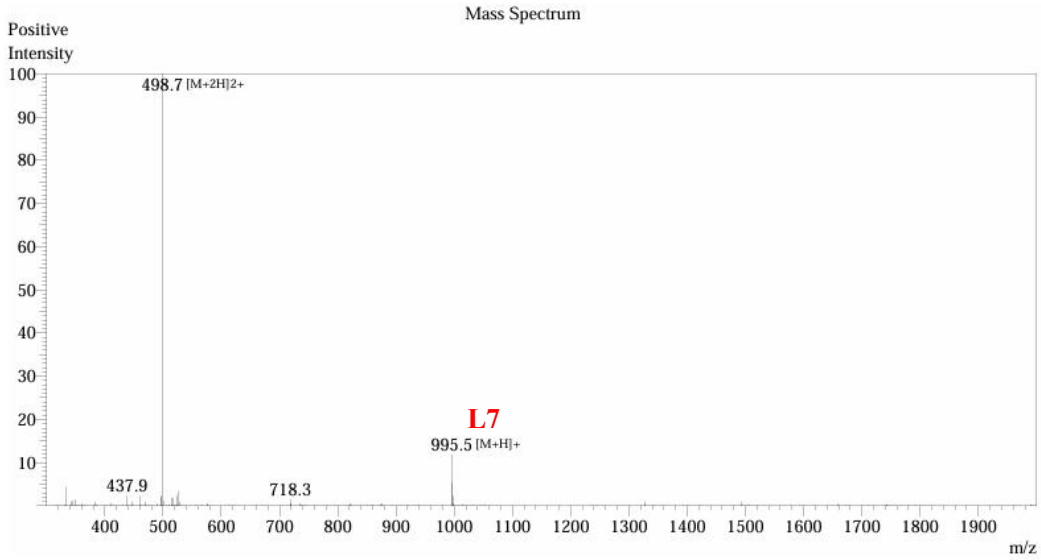

Fig S14. ESI-MS spectrum of **L7**. LRMS (ES+) m/z: $[M+H]^+$ calcd for $C_{34}H_{58}N_{16}O_{15}S_2$ 995.4, found 995.5.

H-Cys-Arg-Gly-Asp-Asn-Gly-Arg-Gly-Asp-Cys-OH (**L8**). Analytical HPLC using Method D, RT = 13.653 min, the HPLC purity is 99%.

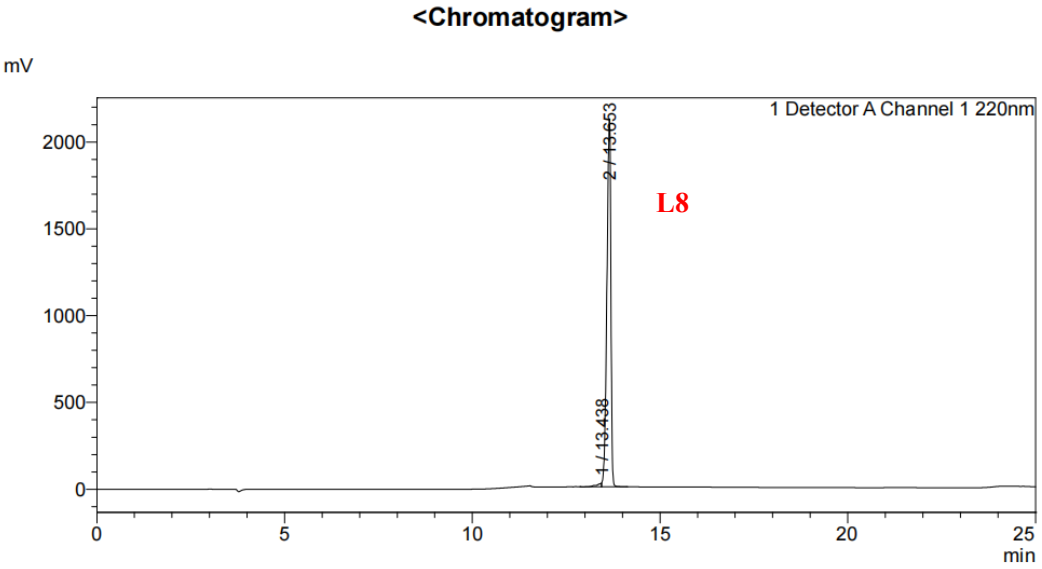

<Peak Table>

Detector A Channel 1 220nm

Peak#	Ret. Time	Area	Height	Area%
1	13.438	178244	19055	1.130
2	13.653	15590577	2120088	98.870
Total		15768821	2139143	100.000

Fig S15. HPLC-UV chromatogram at 220 nm of **L8**.

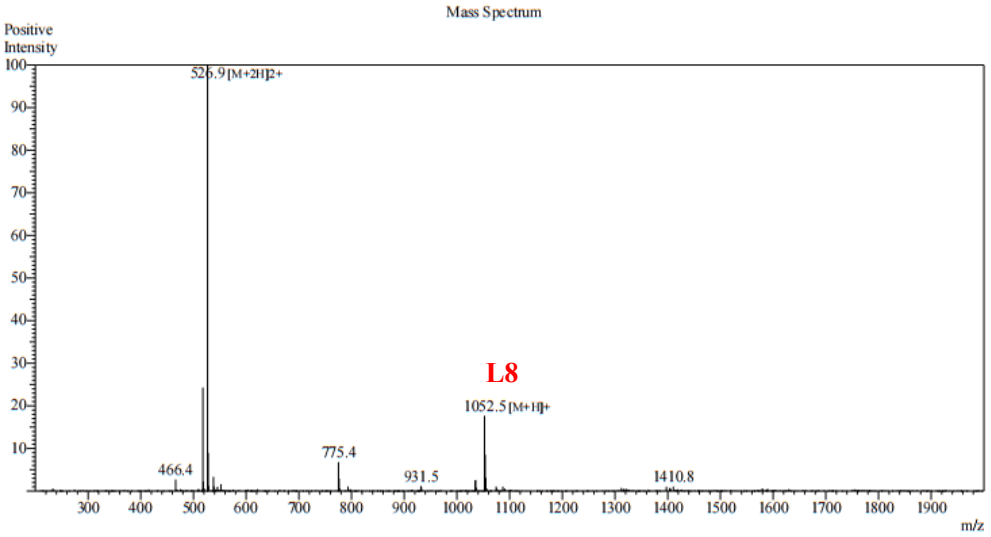

Fig S16. ESI-MS spectrum of **L8**. LRMS (ES+) m/z: $[M+H]^+$ calcd for $C_{36}H_{61}N_{17}O_{16}S_2$ 1052.4, found 1052.5.

H-Cys-Arg-Gly-Asp-pro-Gly-Arg-Gly-Asp-Cys-OH (**L9**). Analytical HPLC using Method C, RT = 7.898 min, the HPLC purity is 98%.

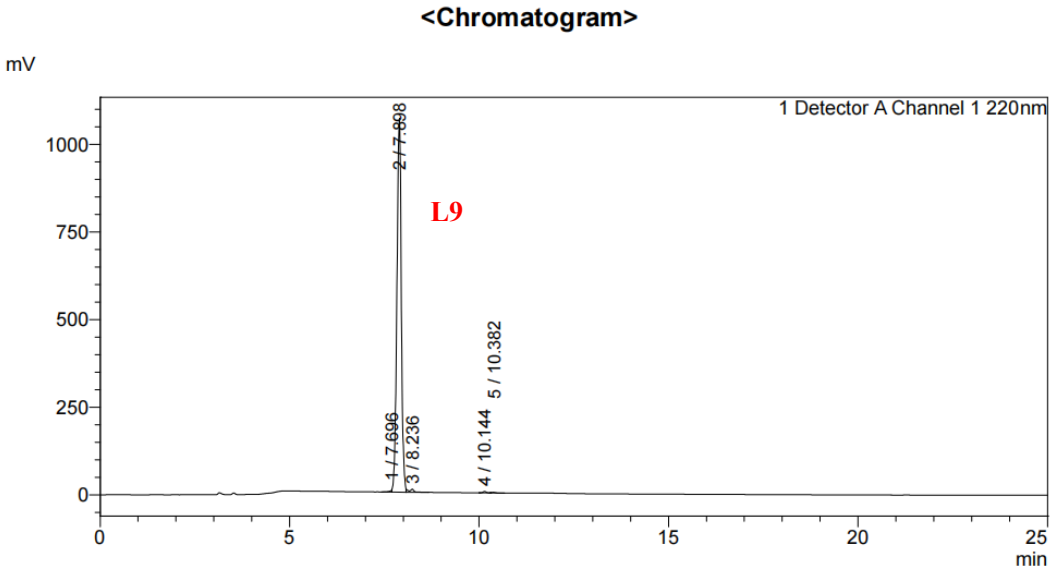

<Peak Table>

Detector A Channel 1 220nm

Peak#	Ret. Time	Area	Height	Area%
1	7.696	27009	5603	0.309
2	7.898	8592883	1066376	98.429
3	8.236	80064	8718	0.917
4	10.144	21102	3789	0.242
5	10.382	8934	1724	0.102
Total		8729992	1086210	100.000

Fig S17. HPLC-UV chromatogram at 220 nm of **L9**.

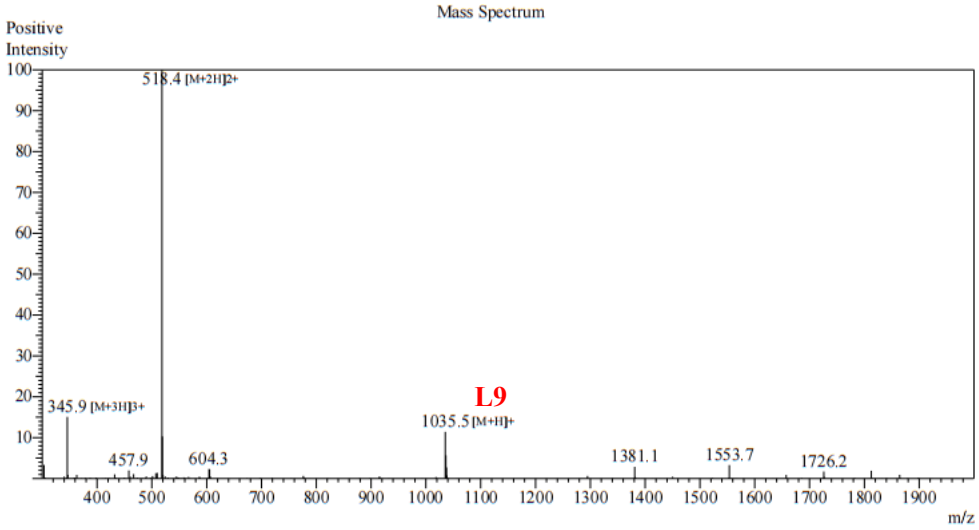

Fig S18. ESI-MS spectrum of **L9**. LRMS (ES+) m/z: $[M+H]^+$ calcd for $C_{37}H_{62}N_{16}O_{15}S_2$ 1035.4, found 1035.5.

H-Cys-Arg-Gly-Asp-Aib-pro-Arg-Gly-Asp-Cys-OH (**L10**). Analytical HPLC using Method D, RT = 12.200 min, the HPLC purity is 98%.

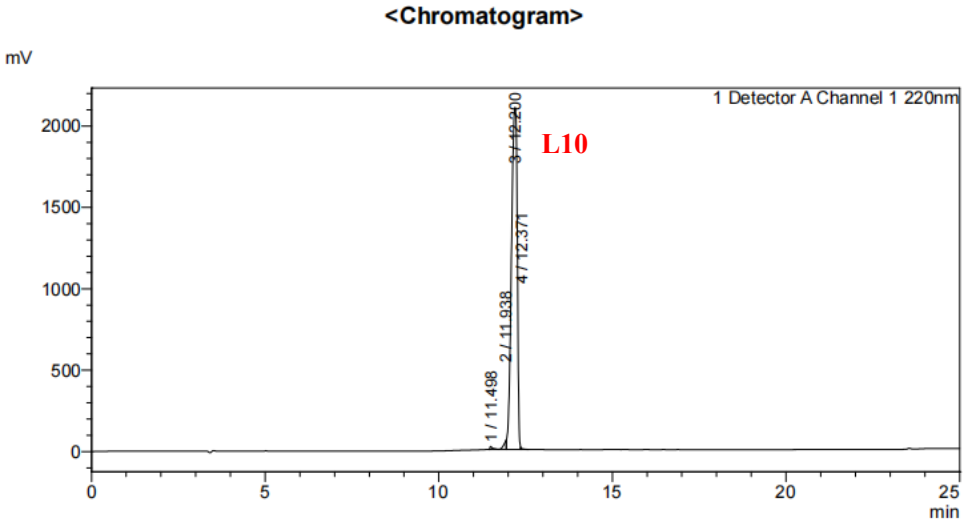

<Peak Table>

Detector A Channel 1 220nm

Peak#	Ret. Time	Area	Height	Area%
1	11.498	109329	18633	0.441
2	11.938	271289	53036	1.094
3	12.200	24388171	2101753	98.350
4	12.371	28649	9646	0.116
Total		24797438	2183068	100.000

Fig S19. HPLC-UV chromatogram at 220 nm of **L10**.

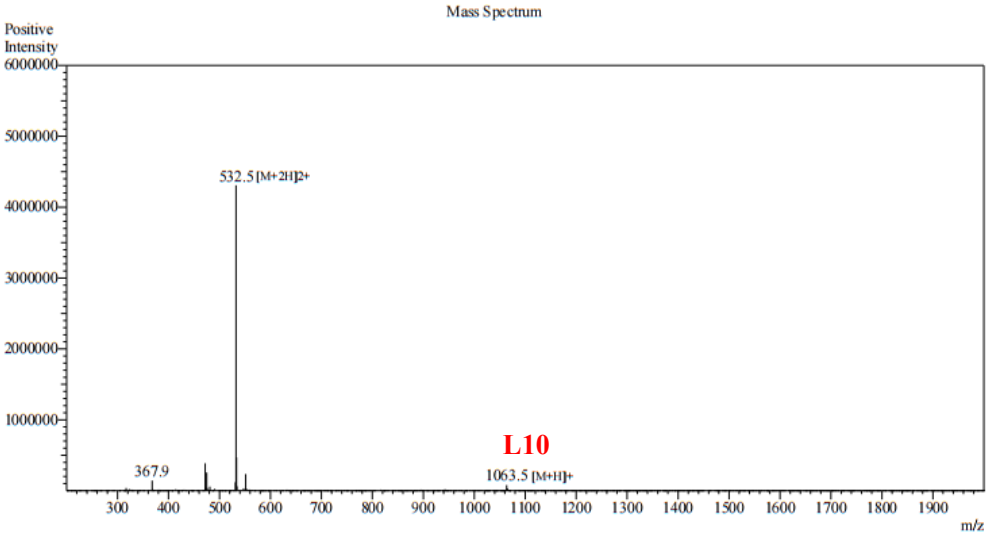

Fig S20. ESI-MS spectrum of **L10**. LRMS (ES+) m/z: $[M+H]^+$ calcd for $C_{39}H_{66}N_{16}O_{15}S_2$ 1063.4, found 1063.5.

H-Cys-Arg-Gly-Asp-Aib-Gly-Arg-Gly-Asp-Cys-OH (**L11**). Analytical HPLC using Method D, RT = 13.725 min, the HPLC purity is 96%.

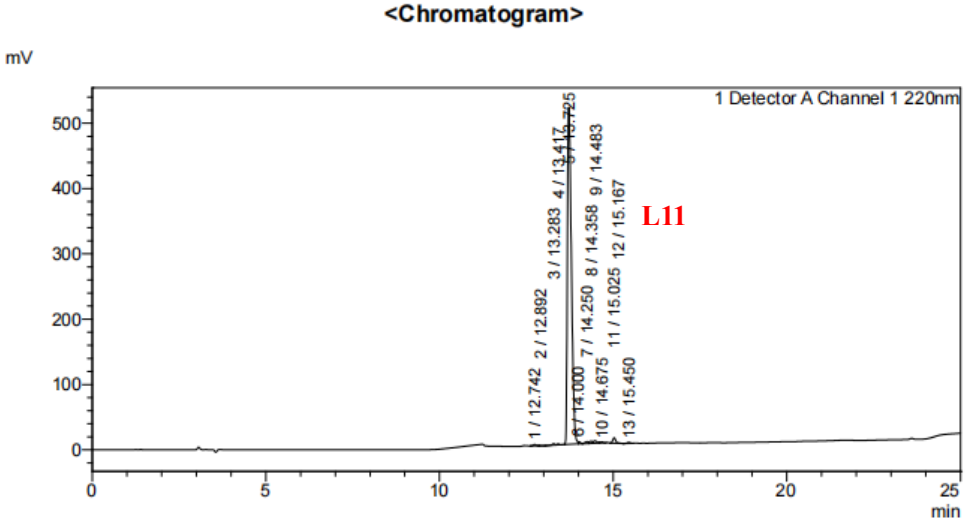

<Peak Table>

Detector A Channel 1 220nm

Peak#	Ret. Time	Area	Height	Area%
1	12.742	10436	2029	0.241
2	12.892	354	88	0.008
3	13.283	12242	2265	0.282
4	13.417	6794	1543	0.157
5	13.725	4156990	516176	95.830
6	14.000	12203	3267	0.281
7	14.250	21574	2999	0.497
8	14.358	20736	3452	0.478
9	14.483	27125	3808	0.625
10	14.675	10529	1745	0.243
11	15.025	48597	8189	1.120
12	15.167	1668	532	0.038
13	15.450	8646	1571	0.199
Total		4337894	547665	100.000

Fig S21. HPLC-UV chromatogram at 220 nm of **L11**.

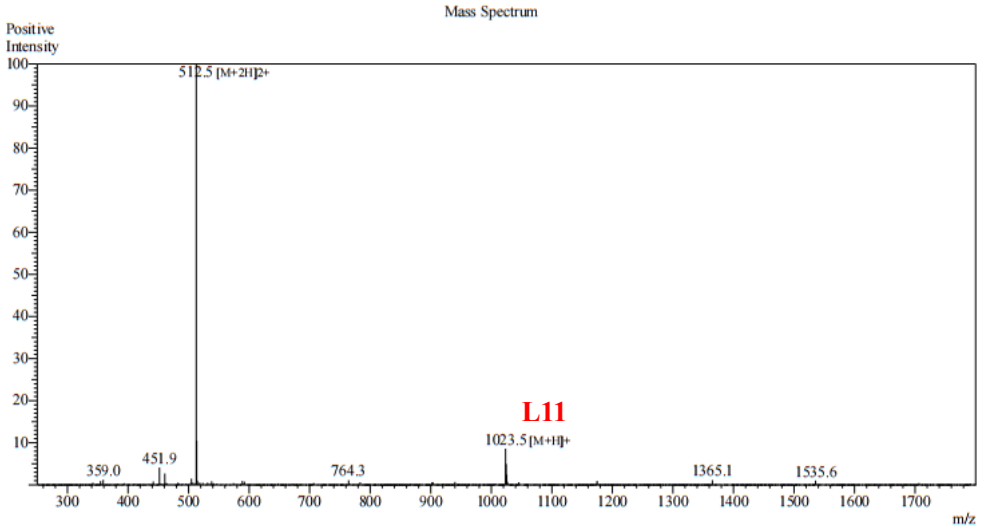

Fig S22. ESI-MS spectrum of **L11**. LRMS (ES+) m/z: $[M+H]^+$ calcd for $C_{36}H_{62}N_{16}O_{15}S_2$ 1023.4, found 1023.5.

Ac-Cys-Arg-Gly-Asp-Ala-Ala-Arg-Gly-Asp-Cys-OH (**L12**). Analytical HPLC using Method C, RT = 7.092 min, the HPLC purity is 90%.

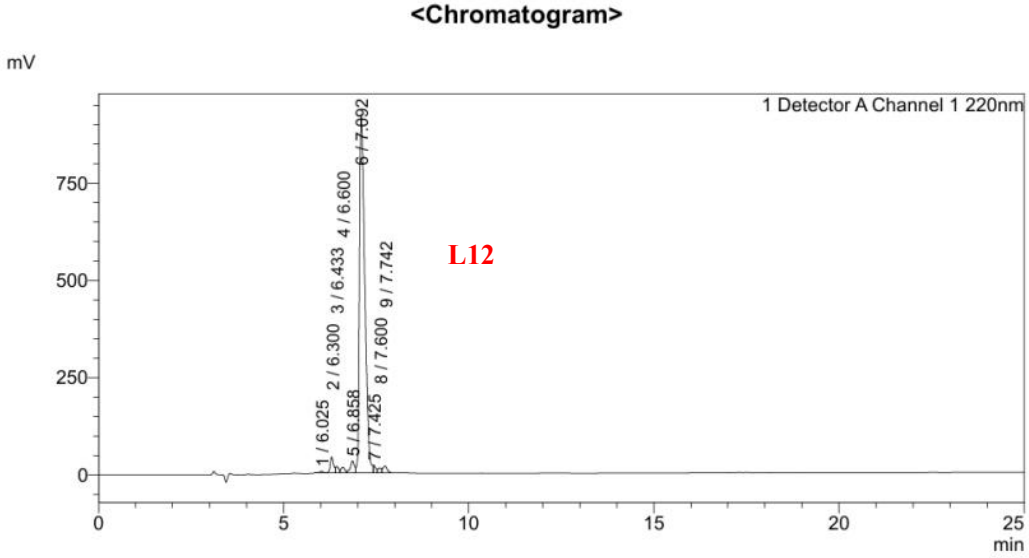

<Peak Table>

Detector A Channel 1 220nm

Peak#	Ret. Time	Area	Height	Area%
1	6.025	26523	4216	0.259
2	6.300	259139	41237	2.528
3	6.433	97596	16147	0.952
4	6.600	112048	14468	1.093
5	6.858	229133	30736	2.235
6	7.092	9227475	921034	90.000
7	7.425	81836	19260	0.798
8	7.600	80731	11974	0.787
9	7.742	138235	16826	1.348
Total		10252716	1075897	100.000

Fig S23. HPLC-UV chromatogram at 220 nm of **L12**.

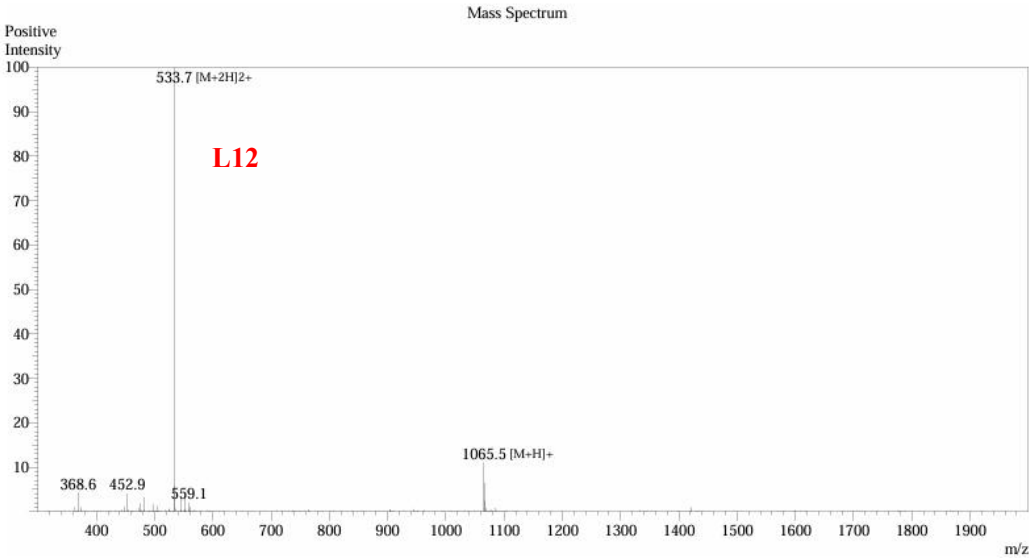

Fig S24. ESI-MS spectrum of **L12**. LRMS (ES+) m/z: $[M+H]^+$ calcd for $C_{38}H_{64}N_{16}O_{16}S_2$ 1065.4, found 1065.5.

Ac-Cys-Arg-Gly-Asp-Gly-Gly-Arg-Gly-Asp-Cys-OH (L13). Analytical HPLC using Method C, RT = 7.174 min, the HPLC purity is 91%.

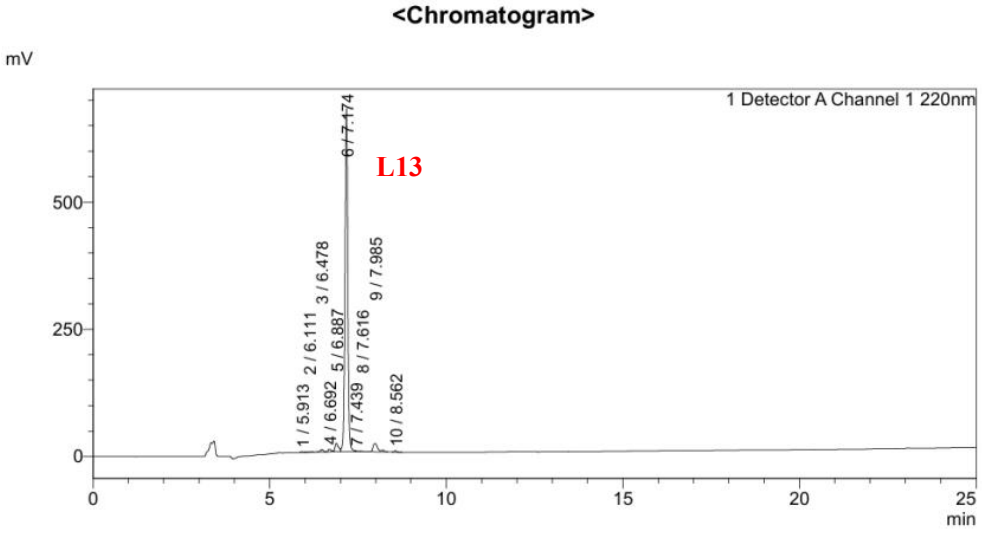

<Peak Table>

Detector A Channel 1 220nm

Peak#	Ret. Time	Area	Height	Area%
1	5.913	2680	621	0.066
2	6.111	3855	507	0.094
3	6.478	28062	4859	0.688
4	6.692	35776	5565	0.877
5	6.887	119965	17258	2.940
6	7.174	3694598	674438	90.555
7	7.439	9233	1945	0.226
8	7.616	5682	1003	0.139
9	7.985	165857	16535	4.065
10	8.562	14235	2844	0.349
Total		4079943	725576	100.000

Fig S25. HPLC-UV chromatogram at 220 nm of **L13**.

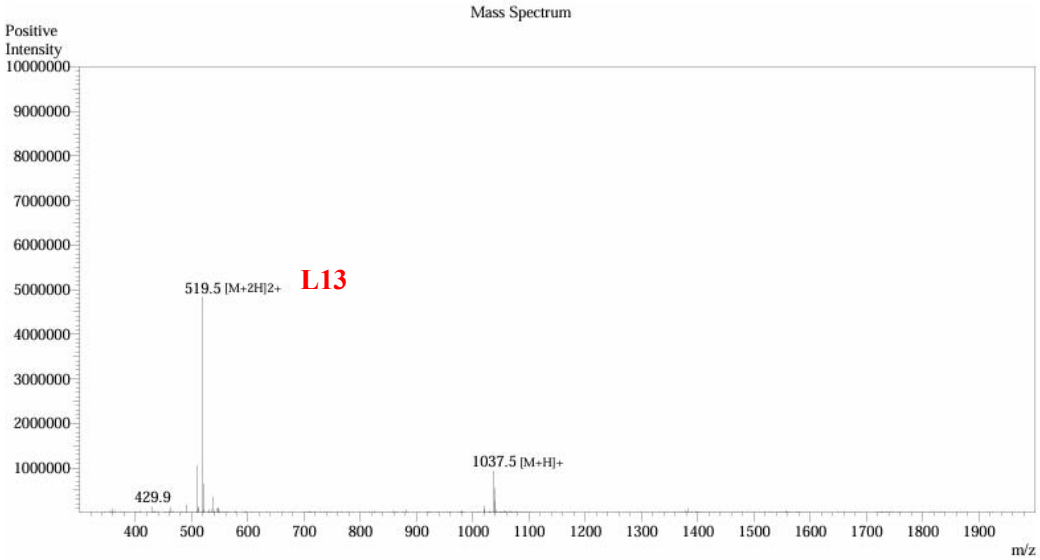

Fig S26. ESI-MS spectrum of **L13**. LRMS (ES+) m/z: $[M+H]^+$ calcd for $C_{36}H_{60}N_{16}O_{16}S_2$ 1037.5, found 1037.4.

Ac-Cys-Arg-Gly-Asp-Asn-Gly-Arg-Gly-Asp-Cys-OH (L14). Analytical HPLC using Method D, RT = 15.408 min, the HPLC purity is 92%.

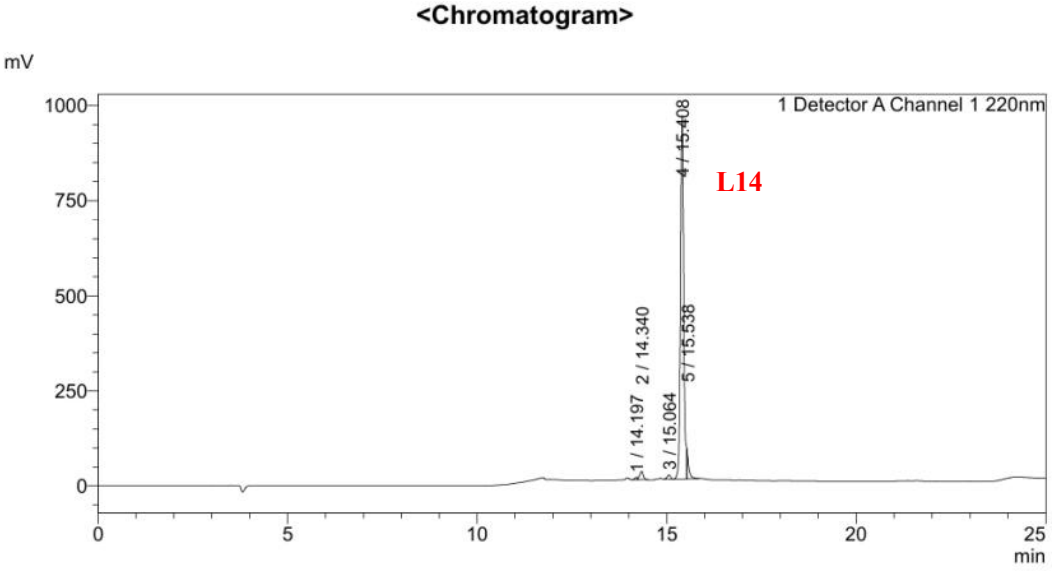

<Peak Table>

Detector A Channel 1 220nm

Peak#	Ret. Time	Area	Height	Area%
1	14.197	28898	6202	0.477
2	14.340	146614	22236	2.419
3	15.064	67120	10970	1.108
4	15.408	5585487	956414	92.169
5	15.538	231928	78338	3.827
Total		6060047	1074161	100.000

Fig S27. HPLC-UV chromatogram at 220 nm of **L14**.

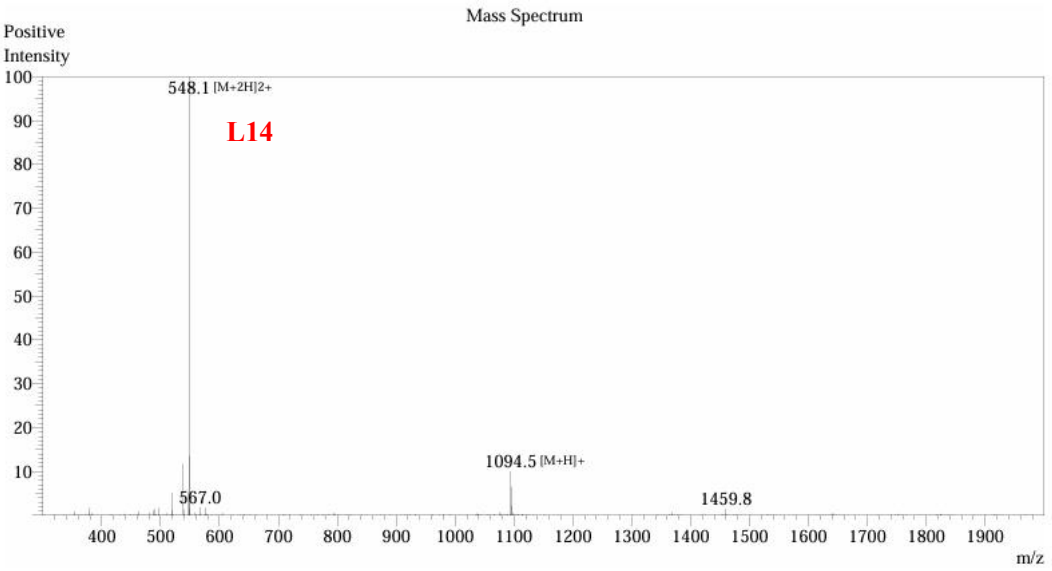

Fig S28. ESI-MS spectrum of **L14**. LRMS (ES+) m/z: $[M+H]^+$ calcd for $C_{38}H_{63}N_{17}O_{17}S_2$ 1094.4, found 1094.5.

Ac-Cys-Arg-Gly-Asp-pro-Gly-Arg-Gly-Asp-Cys-OH (L15). Analytical HPLC using Method C, RT = 5.842 min, the HPLC purity is 93%.

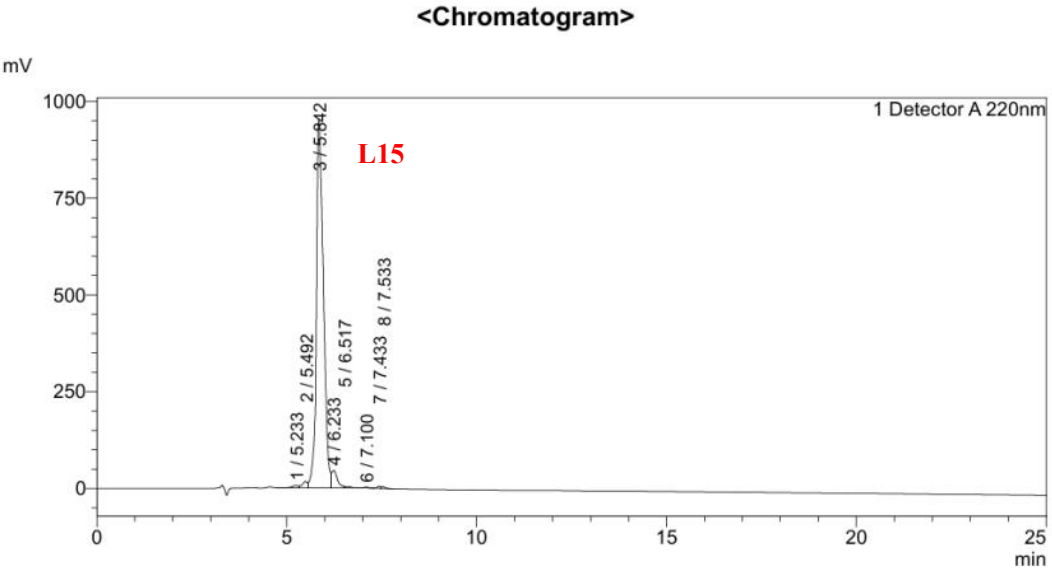

<Peak Table>

Detector A 220nm

Peak#	Ret. Time	Area	Height	Area%
1	5.233	70554	6304	0.540
2	5.492	152449	16524	1.166
3	5.842	12219140	953668	93.463
4	6.233	493092	45052	3.772
5	6.517	42871	3820	0.328
6	7.100	25168	2567	0.193
7	7.433	38573	5337	0.295
8	7.533	31940	4657	0.244
Total		13073786	1037929	100.000

Fig S29. HPLC-UV chromatogram at 220 nm of **L15**.

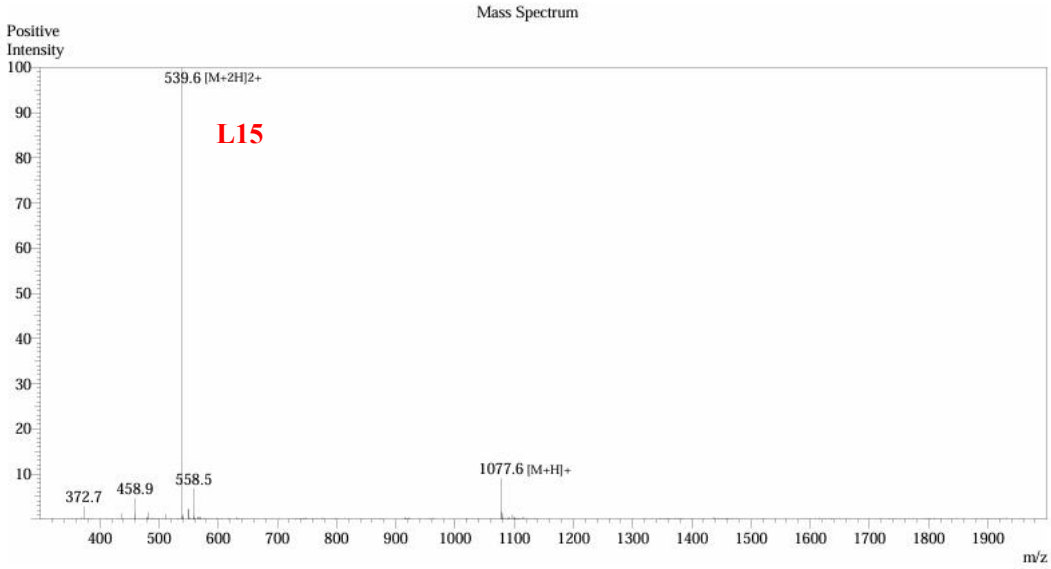

Fig S30. ESI-MS spectrum of **L15**. LRMS (ES+) m/z: $[M+H]^+$ calcd for $C_{39}H_{64}N_{16}O_{16}S_2$ 1077.4, found 1077.6.

Ac-Cys-Arg-Gly-Asp-Aib-pro-Arg-Gly-Asp-Cys-OH (L16). Analytical HPLC using Method C, RT = 5.950 min, the HPLC purity is 92%.

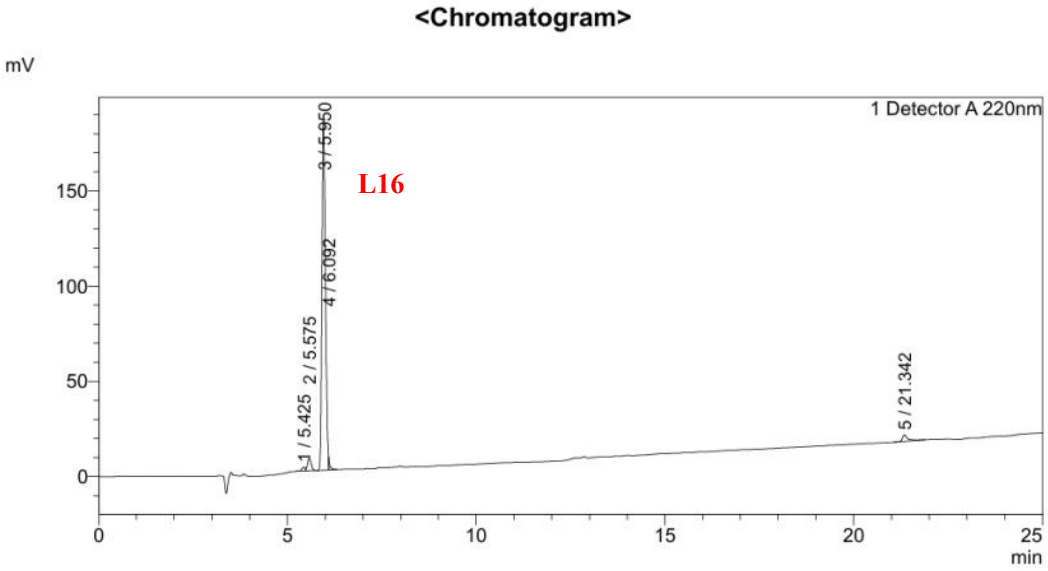

<Peak Table>

Detector A 220nm

Peak#	Ret. Time	Area	Height	Area%
1	5.425	11678	1918	0.907
2	5.575	44009	6582	3.419
3	5.950	1184472	184702	92.014
4	6.092	13613	6589	1.058
5	21.342	33497	3364	2.602
Total		1287269	203154	100.000

Fig S31. HPLC-UV chromatogram at 220 nm of **L16**.

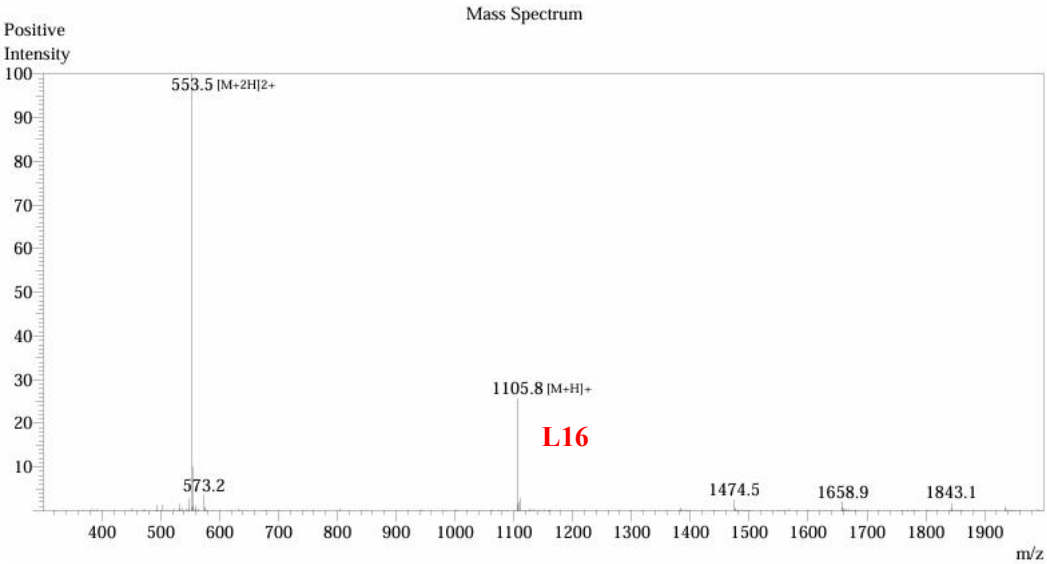

Fig S32. ESI-MS spectrum of **L16**. LRMS (ES+) m/z: $[M+H]^+$ calcd for $C_{41}H_{68}N_{16}O_{16}S_2$ 1105.4, found 1105.8.

Ac-Cys-Arg-Gly-Asp-Aib-Gly-Arg-Gly-Asp-Cys-OH (L17). Analytical HPLC using Method D, RT = 16.042 min, the HPLC purity is 94%.

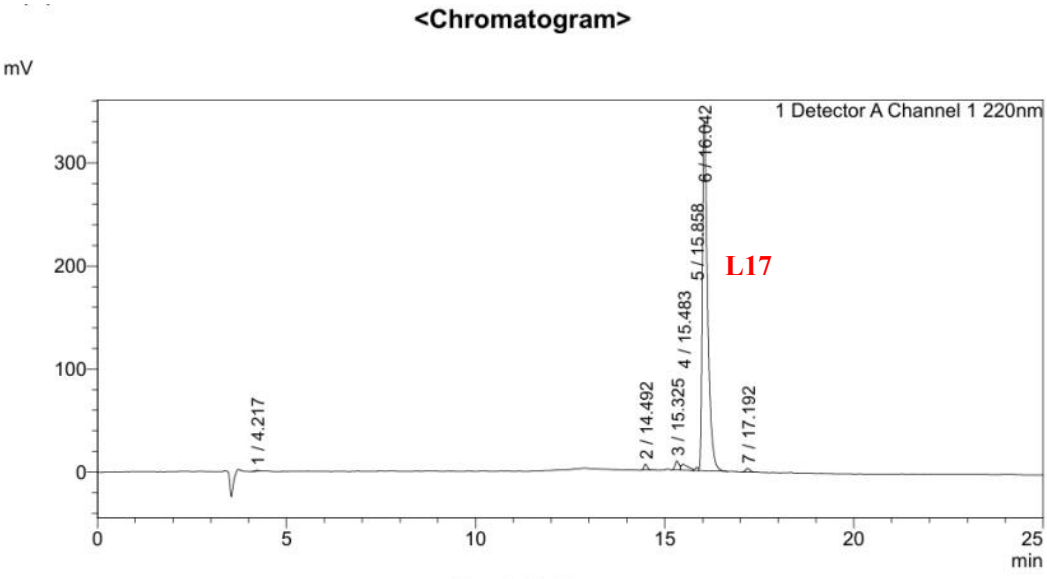

<Peak Table>

Detector A Channel 1 220nm

Peak#	Ret. Time	Area	Height	Area%
1	4.217	5422	1006	0.152
2	14.492	37209	5972	1.045
3	15.325	65552	8773	1.842
4	15.483	74563	5983	2.095
5	15.858	19541	3414	0.549
6	16.042	3328686	339345	93.525
7	17.192	28149	3555	0.791
Total		3559123	368048	100.000

Fig S33. HPLC-UV chromatogram at 220 nm of **L17**.

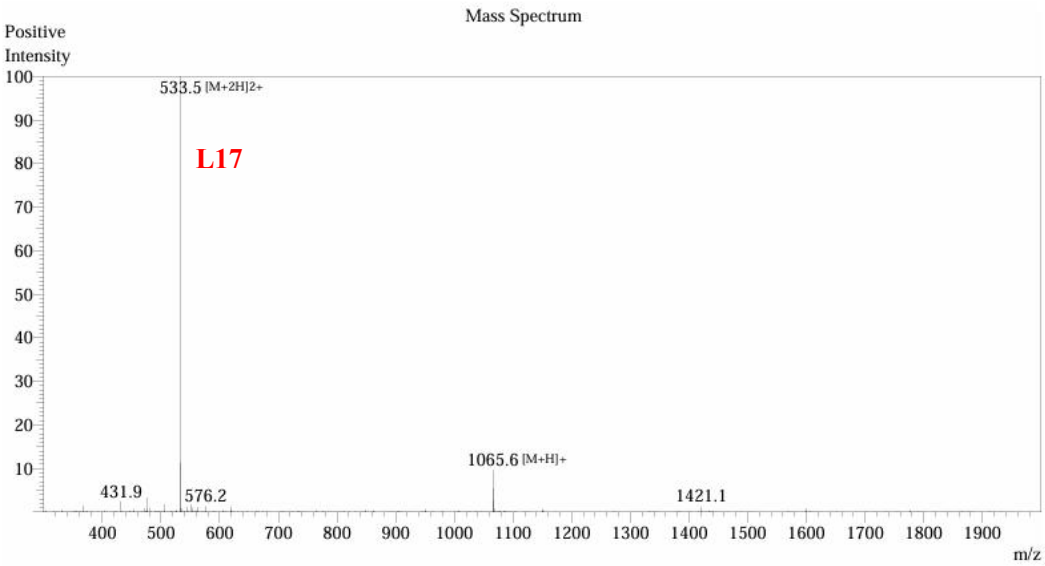

Fig S34. ESI-MS spectrum of **L17**. LRMS (ES+) m/z: $[M+H]^+$ calcd for $C_{38}H_{64}N_{16}O_{16}S_2$ 1065.4, found 1065.6.

H-Cys-Arg-Gly-Asp-Ala-Ala-Arg-Gly-Asp-Cys-Gly-Ser-OH (L18). Analyti cal HPLC using Method C, RT =4.342 min, the HPLC purity is 97%.

<Chromatogram>

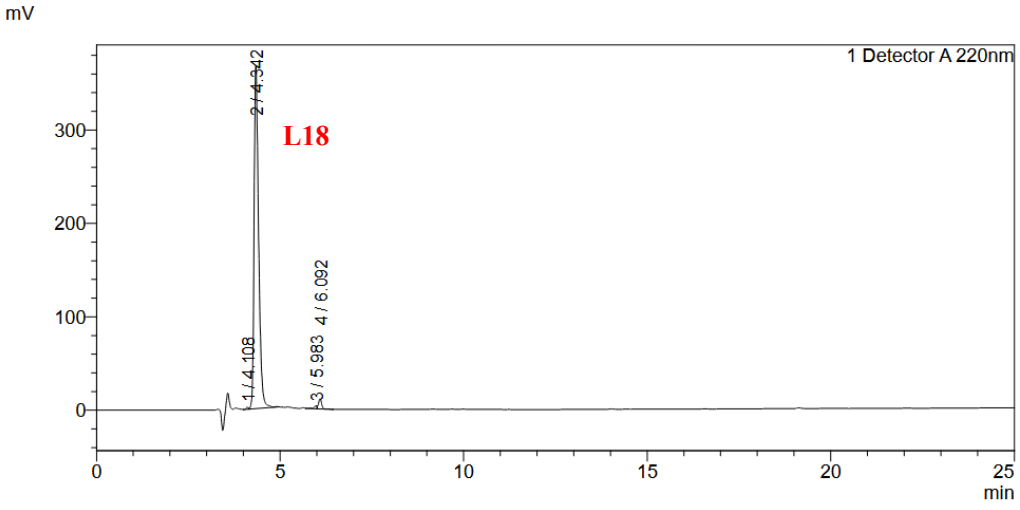

<Peak Table>

Detector A 220nm

Peak#	Ret. Time	Area	Height	Area%
1	4.108	8368	2222	0.261
2	4.342	3116176	367488	97.304
3	5.983	16171	3159	0.505
4	6.092	61788	10850	1.929
Total		3202503	383719	100.000

Fig S35. HPLC-UV chromatogram at 220 nm of **L18**.

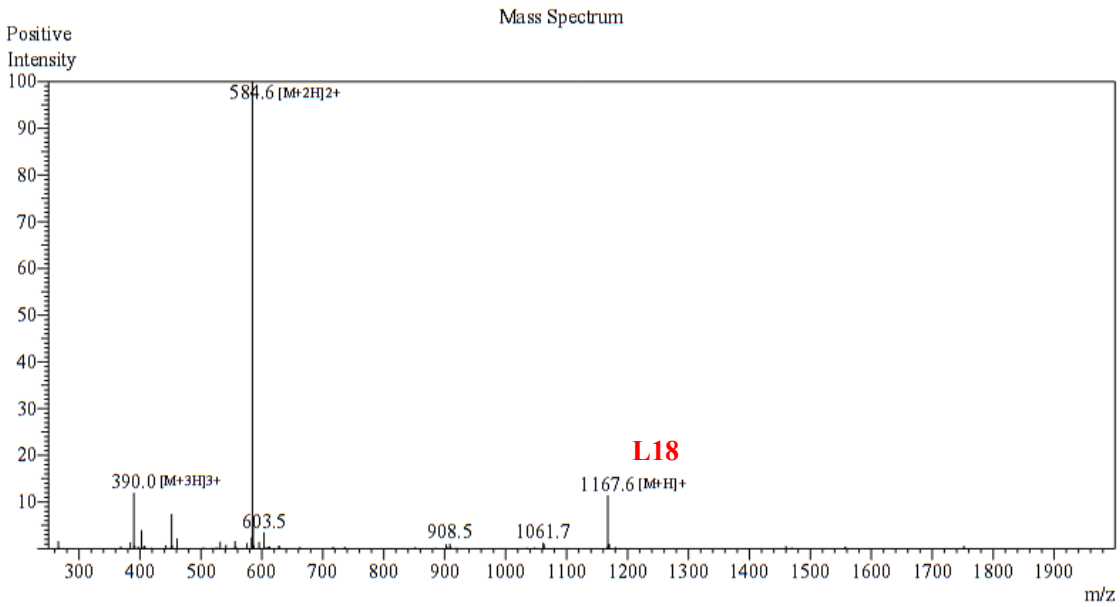

Fig S36. ESI-MS spectrum of **L18**. LRMS (ES+) m/z: $[M+H]^+$ calcd for $C_{41}H_{70}N_{18}O_{18}S_2$ 1167.5, found 1167.6.

Gly-Ser-Cys-Arg-Gly-Asp-Ala-Ala-Arg-Gly-Asp-Cys-OH (L19). Analytical HPLC using Method D, RT = 16.453 min, the HPLC purity is 95%.

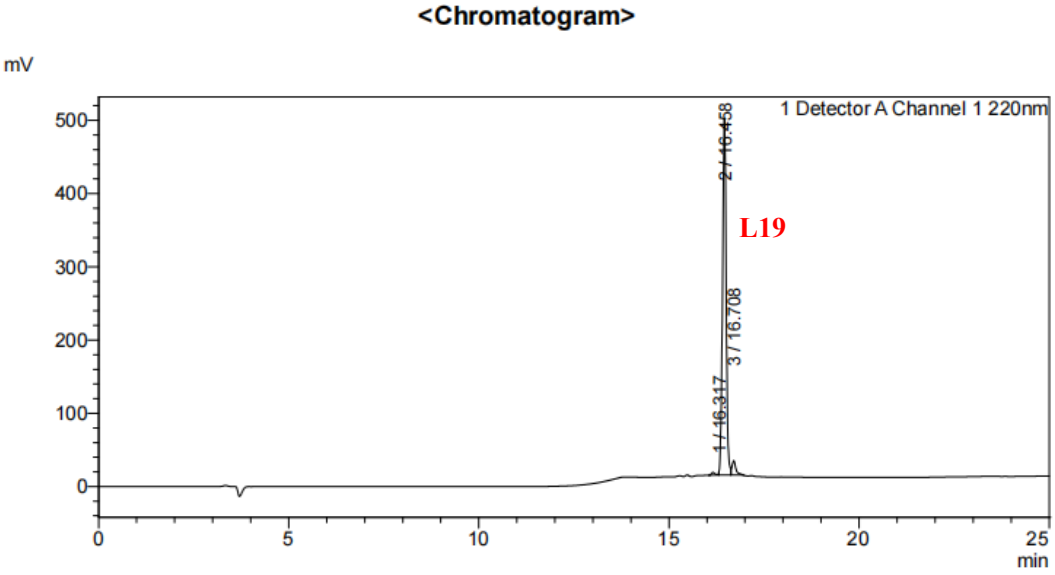

<Peak Table>

Detector A Channel 1 220nm

Peak#	Ret. Time	Area	Height	Area%
1	16.317	26160	4526	0.763
2	16.458	3261215	487471	95.182
3	16.708	138913	19627	4.054
Total		3426288	511624	100.000

Fig S37. HPLC-UV chromatogram at 220 nm of **L19**.

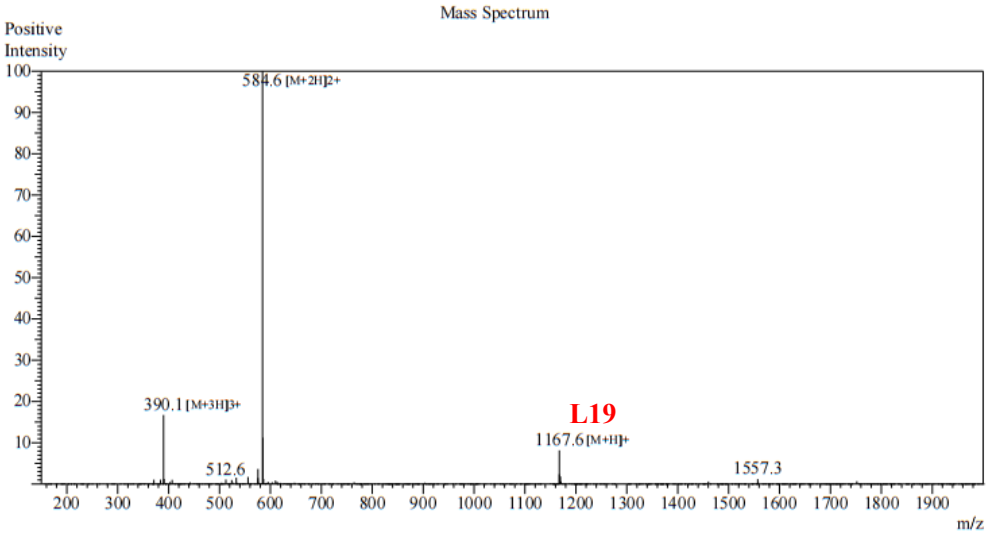

Fig S38. ESI-MS spectrum of **L19**. LRMS (ES+) m/z: $[M+H]^+$ calcd for $C_{41}H_{70}N_{18}O_{18}S_2$ 1167.5, found 1167.6.

Gly-Ser-Cys-Arg-Gly-Asp-Ala-Ala-Arg-Gly-Asp-Cys-Gly-Ser-OH (L20). Analytical HPLC using Method C, RT = 5.712 min, the HPLC purity is 95%.

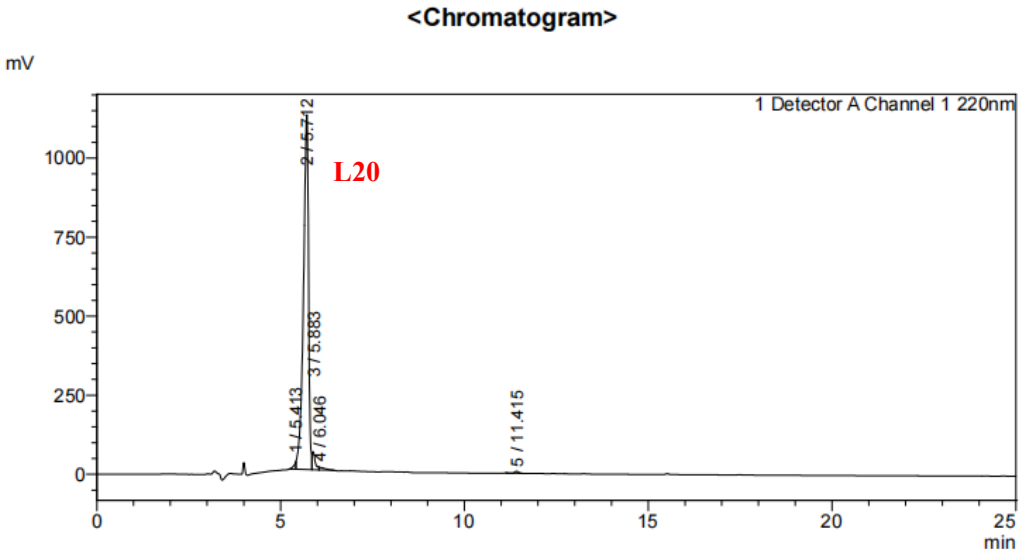

<Peak Table>

Detector A Channel 1 220nm

Peak#	Ret. Time	Area	Height	Area%
1	5.413	97517	21785	0.861
2	5.712	10772948	1122590	95.154
3	5.883	324841	57287	2.869
4	6.046	89035	9018	0.786
5	11.415	37246	6040	0.329
Total		11321587	1216720	100.000

Fig S39. HPLC-UV chromatogram at 220 nm of **L20**.

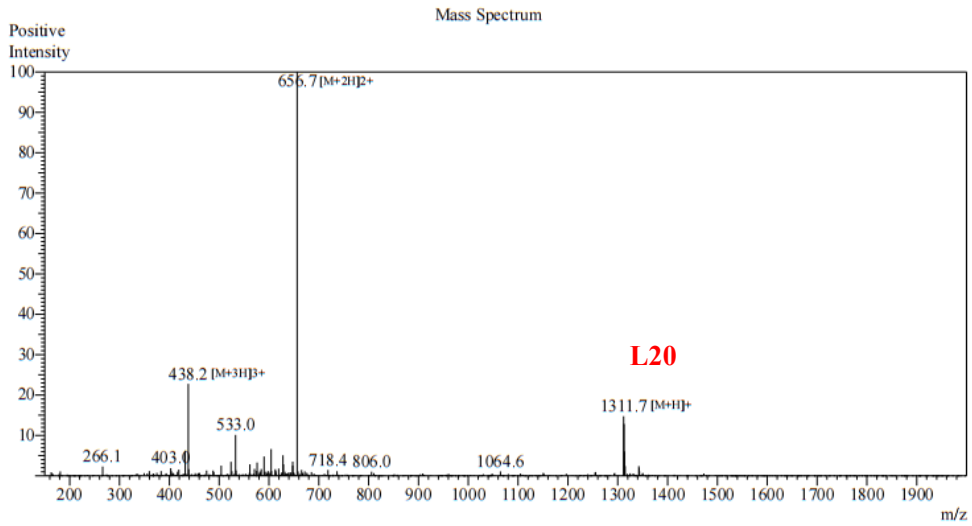

Fig S40. ESI-MS spectrum of **L20**. LRMS (ES+) m/z: $[M+H]^+$ calcd for $C_{46}H_{78}N_{20}O_{21}S_2$ 1311.5, found 1311.7.

H-Cys-Asp-Gly-Arg-Ala-Ala-Asp-Gly-Arg-Cys-OH (L21). Analytical HPLC using Method C, RT =6.433 min, the HPLC purity is 96%.

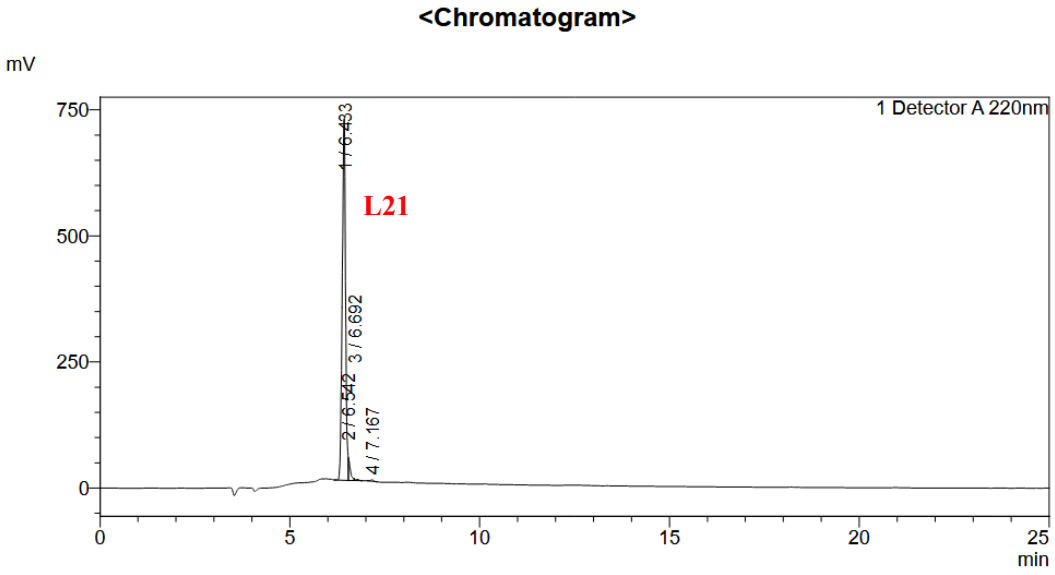

<Peak Table>

Detector A 220nm

Peak#	Ret. Time	Area	Height	Area%
1	6.433	4384577	717654	95.905
2	6.542	150577	44976	3.294
3	6.692	21440	3966	0.469
4	7.167	15210	2859	0.333
Total		4571804	769456	100.000

Fig S41. HPLC-UV chromatogram at 220 nm of **L21**.

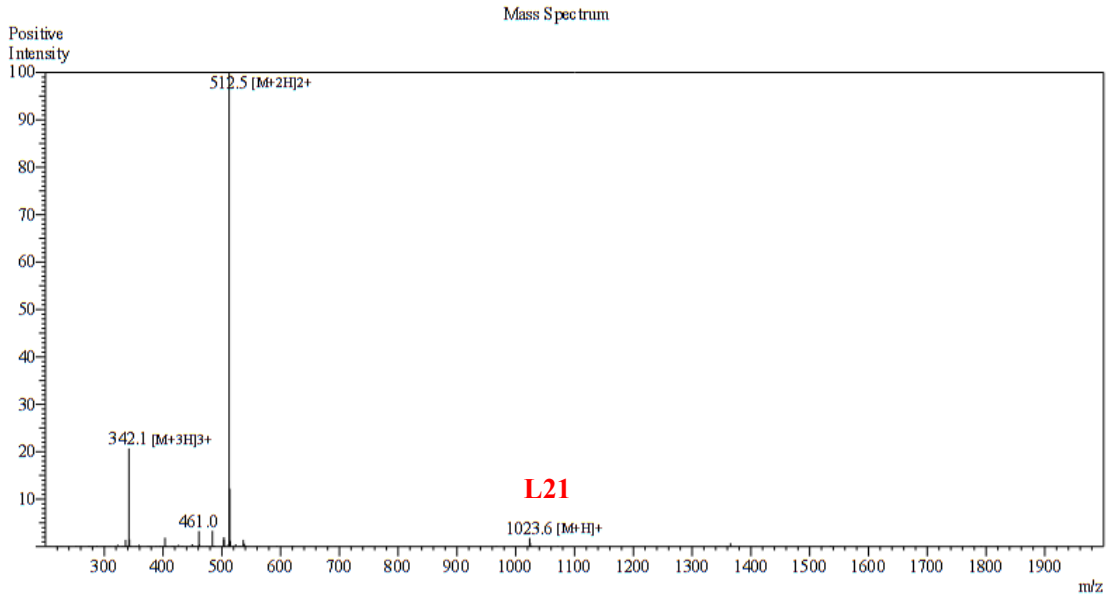

Fig S42. ESI-MS spectrum of **L21**. LRMS (ES+) m/z: $[M+H]^+$ calcd for $C_{36}H_{62}N_{16}O_{15}S_2$ 1023.5, found 1023.6.

H-Cys-Arg-Gly-Asp-Ala-Ala-Asp-Gly-Arg-Cys-OH (L22). Analytical HPLC using Method D, RT =10.857 min, the HPLC purity is 99%.

<Chromatogram>

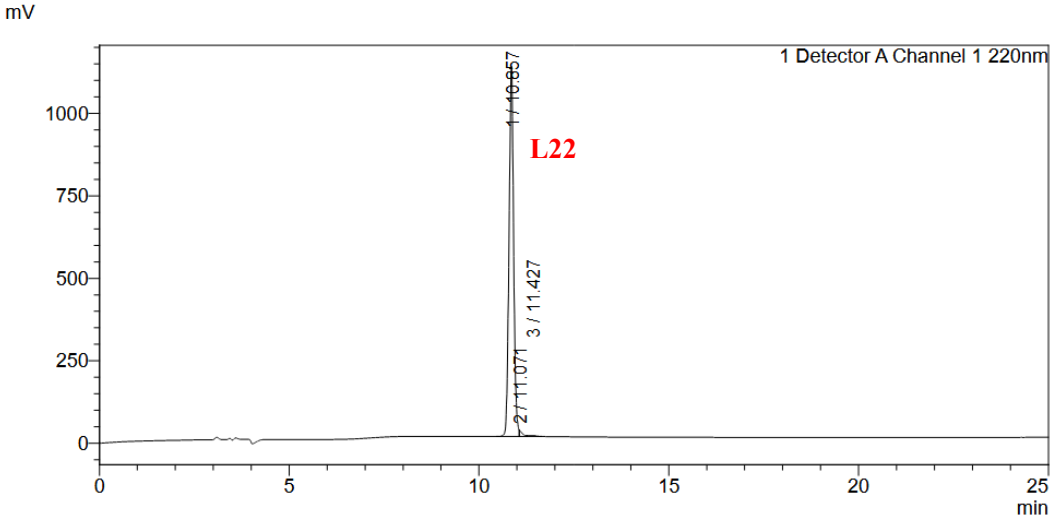

<Peak Table>

Detector A Channel 1 220nm

Peak#	Ret. Time	Area	Height	Area%
1	10.857	9460151	1121816	98.573
2	11.071	97815	18429	1.019
3	11.427	39097	2775	0.407
Total		9597063	1143020	100.000

Fig S43. HPLC-UV chromatogram at 220 nm of **L22**.

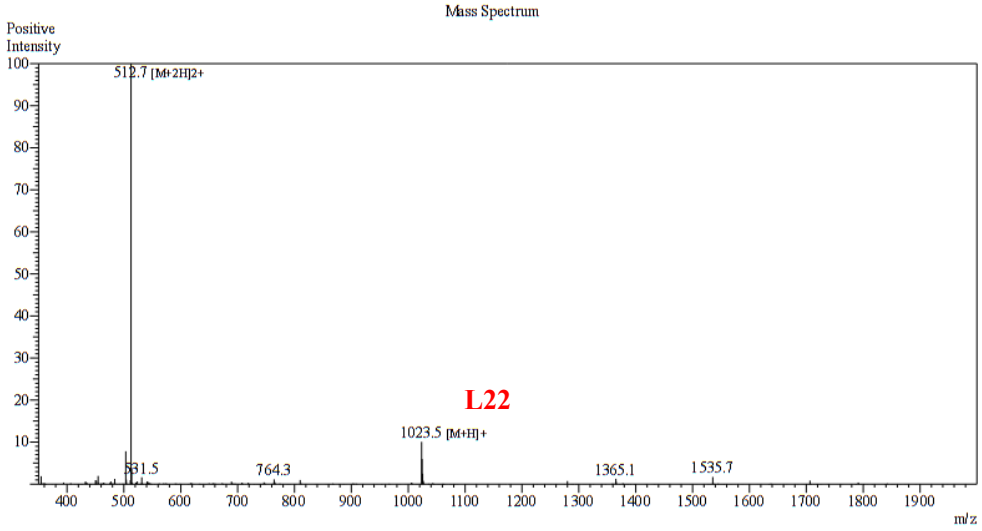

Fig S44. ESI-MS spectrum of **L22**. LRMS (ES+) m/z: $[M+H]^+$ calcd for $C_{36}H_{62}N_{16}O_{15}S_2$ 1023.5, found 1023.5.

H-Cys-Asp-Gly-Arg-Ala-Ala-Arg-Gly-Asp-Cys-OH (L23). Analytical HPLC using Method C, RT =6.249 min, the HPLC purity is 99%.

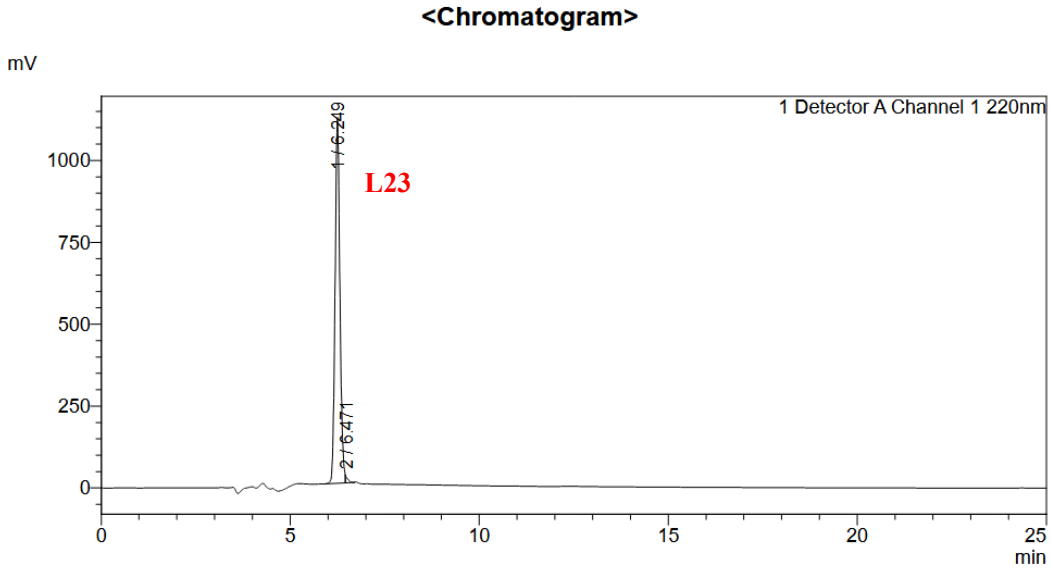

<Peak Table>

Detector A Channel 1 220nm

Peak#	Ret. Time	Area	Height	Area%
1	6.249	9975290	1117378	99.139
2	6.471	86635	20531	0.861
Total		10061926	1137909	100.000

Fig S45. HPLC-UV chromatogram at 220 nm of **L23**.

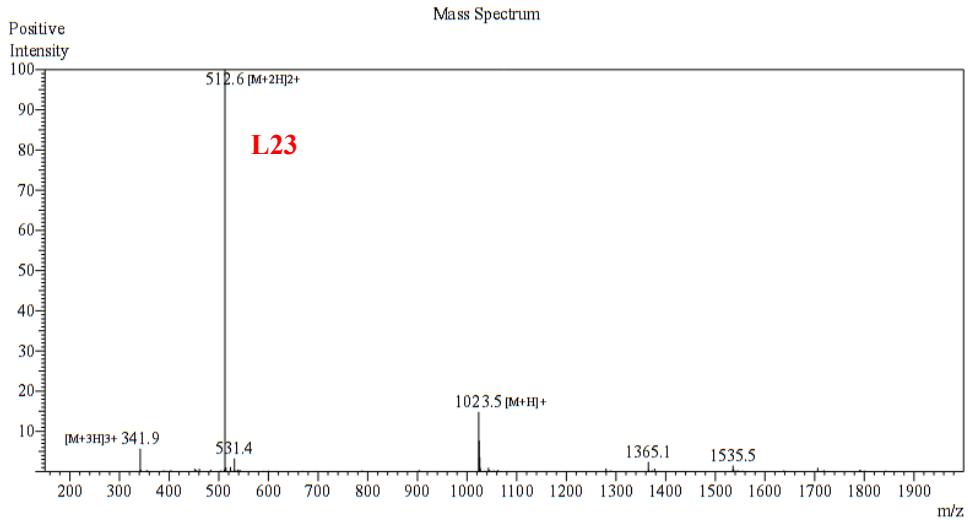

Fig S46. ESI-MS spectrum of **L23**. LRMS (ES+) m/z: $[M+H]^+$ calcd for $C_{36}H_{62}N_{16}O_{15}S_2$ 1023.5, found 1023.5.

H-Cys-Arg-Asp-Ala-Ala-Arg-Asp-Cys-OH (**L24**). Analytical HPLC using Method D, RT =16.375 min, the HPLC purity is 97%.

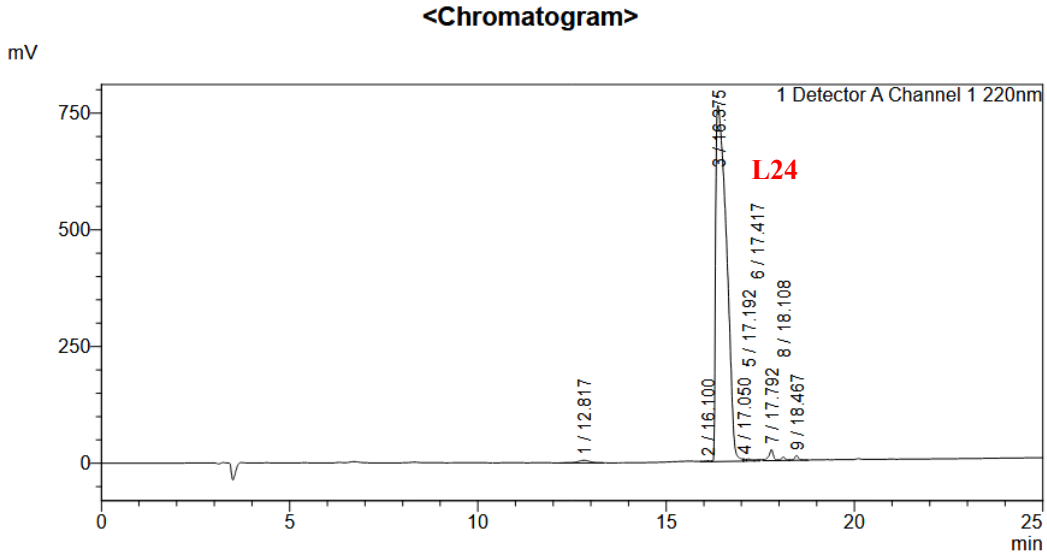

<Peak Table>

Detector A Channel 1 220nm

Peak#	Ret. Time	Area	Height	Area%
1	12.817	116677	5428	0.743
2	16.100	21875	2060	0.139
3	16.375	15163273	762393	96.580
4	17.050	18440	4124	0.117
5	17.192	38459	4291	0.245
6	17.417	18553	2604	0.118
7	17.792	196774	23642	1.253
8	18.108	53918	7357	0.343
9	18.467	72179	9956	0.460
Total		15700147	821856	100.000

Fig S47. HPLC-UV chromatogram at 220 nm of **L24**.

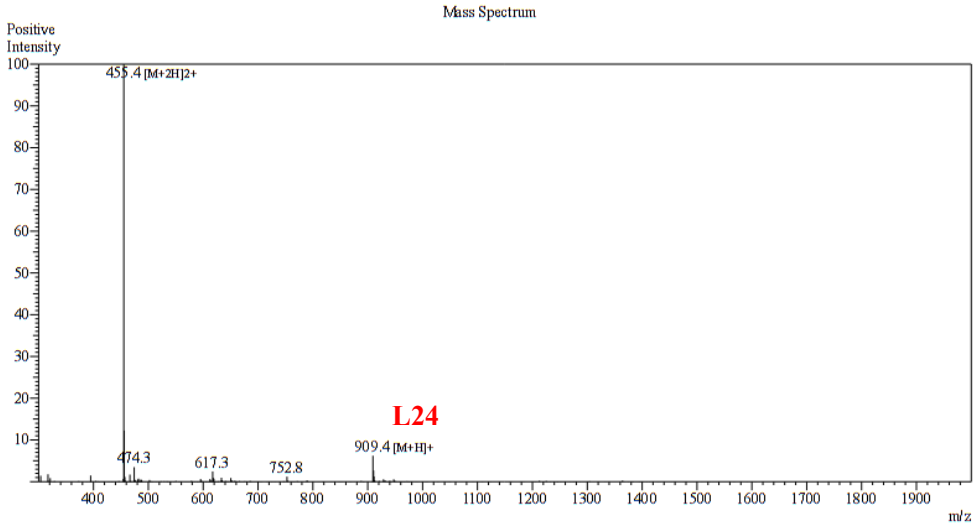

Fig S48. ESI-MS spectrum of **L24**. LRMS (ES+) m/z: $[M+H]^+$ calcd for $C_{32}H_{56}N_{14}O_{13}S_2$ 909.4, found 909.4.

H-Cys-Arg-Gly-Asp-Cys-OH (**L25**). Analytical HPLC using Method D, RT = 13.346 min, the HPLC purity is 98%.

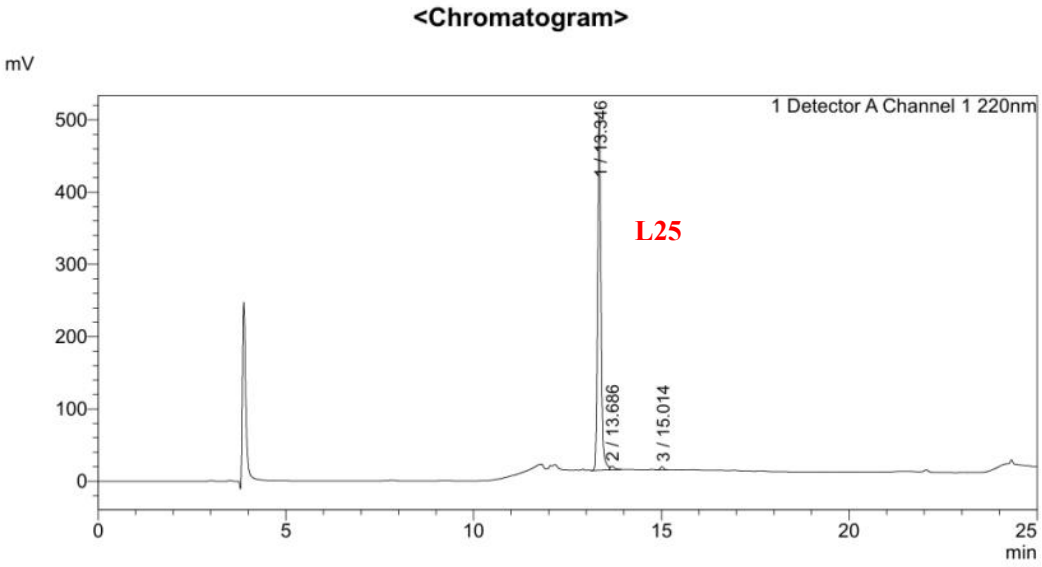

<Peak Table>

Detector A Channel 1 220nm

Peak#	Ret. Time	Area	Height	Area%
1	13.346	3064250	489841	97.987
2	13.686	38647	5071	1.236
3	15.014	24310	4314	0.777
Total		3127207	499226	100.000

Fig S49. HPLC-UV chromatogram at 220 nm of **L25**.

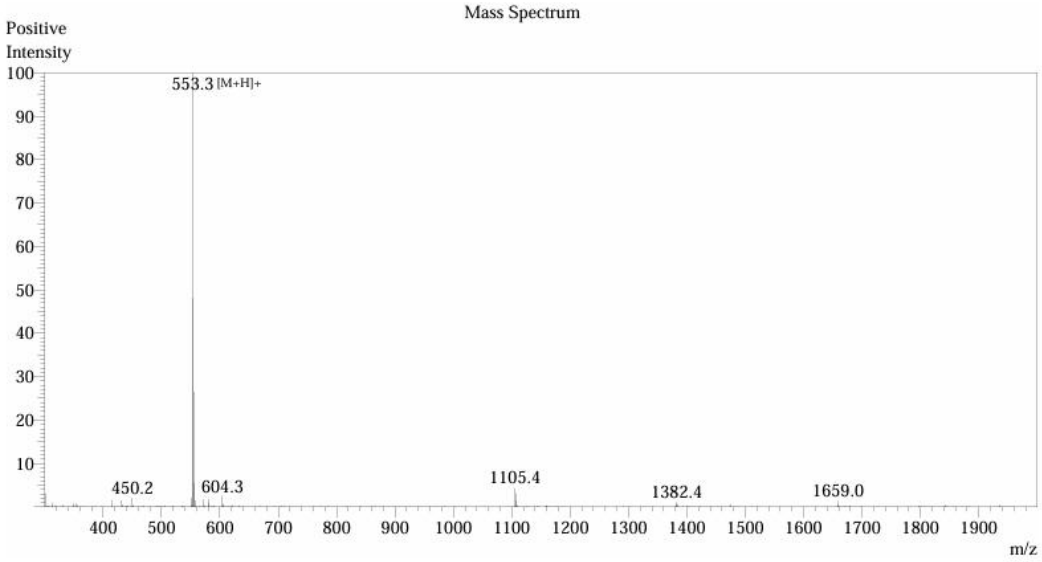

Fig S50. ESI-MS spectrum of **L25**. LRMS (ES+) m/z: $[M+H]^+$ calcd for $C_{18}H_{32}N_8O_8S_2$ 553.2, found 553.3.

H-Cys-Ala-Ala-Cys-OH (L26). Analytical HPLC using Method D, RT = 13.550 min, the HPLC purity is 95%.

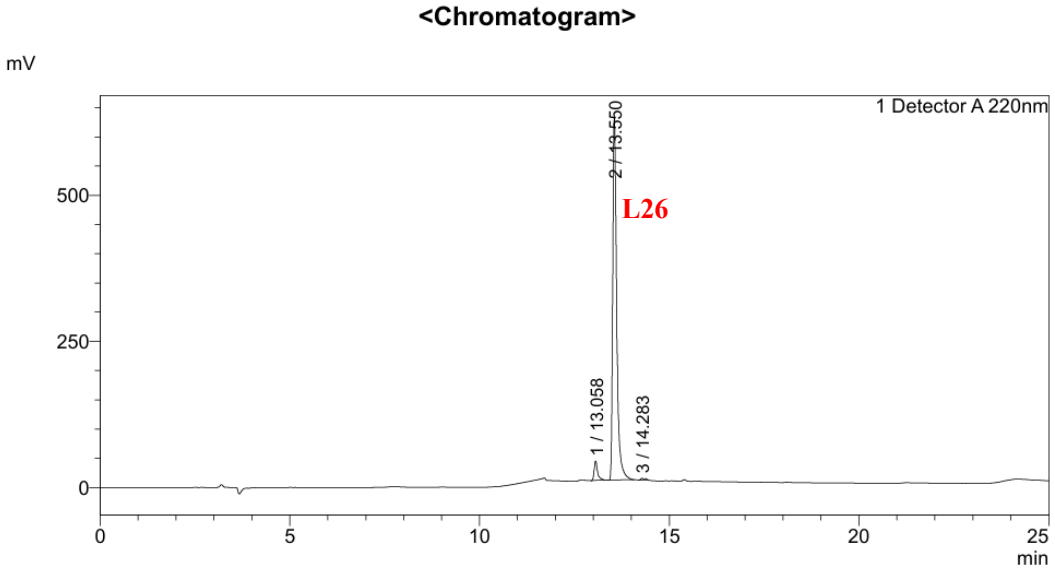

<Peak Table>

Detector A 220nm

Peak#	Ret. Time	Area	Height	Area%
1	13.058	208546	33521	4.386
2	13.550	4522129	621423	95.097
3	14.283	24591	2952	0.517
Total		4755266	657896	100.000

Fig S51 . HPLC-UV chromatogram at 220 nm of **L26**.

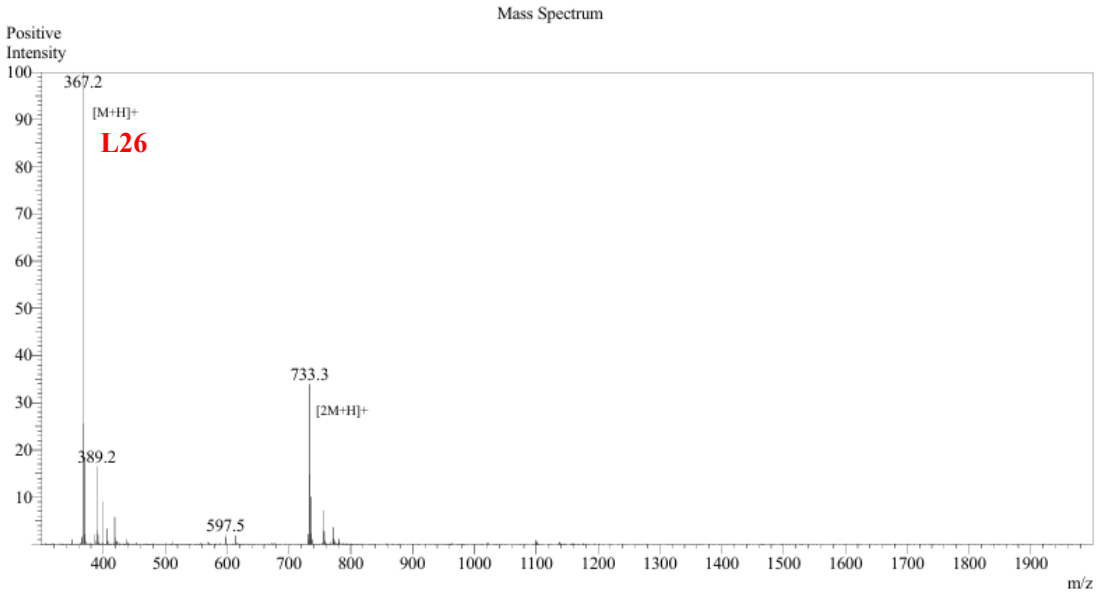

Fig S52 . ESI-MS spectrum of **L26**. LRMS (ES+) m/z: $[M+H]^+$ calcd for $C_{12}H_{22}N_4O_5S_2$ 367.1, found 367.2.

H-Cys-Ala-Ala-Ala-Cys-OH (**L27**). Analytical HPLC using Method C, RT = 5.587 min, the HPLC purity is 99%.

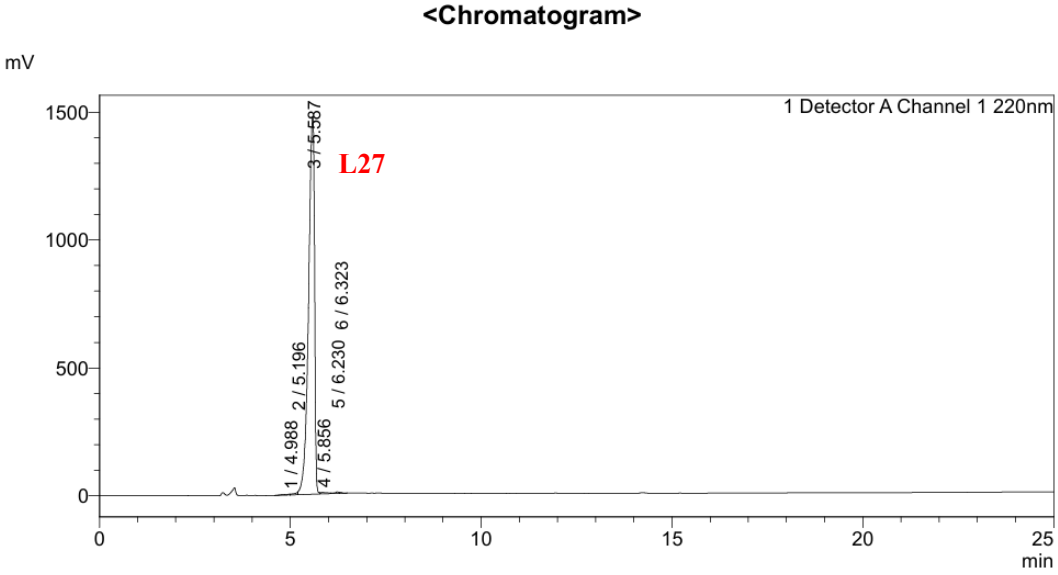

<Peak Table>

Detector A Channel 1 220nm

Peak#	Ret. Time	Area	Height	Area%
1	4.988	41701	3033	0.254
2	5.196	64089	9757	0.390
3	5.587	16182021	1477475	98.505
4	5.856	69169	6272	0.421
5	6.230	50508	6874	0.307
6	6.323	20199	4270	0.123
Total		16427687	1507682	100.000

Fig S53 . HPLC-UV chromatogram at 220 nm of **L27**.

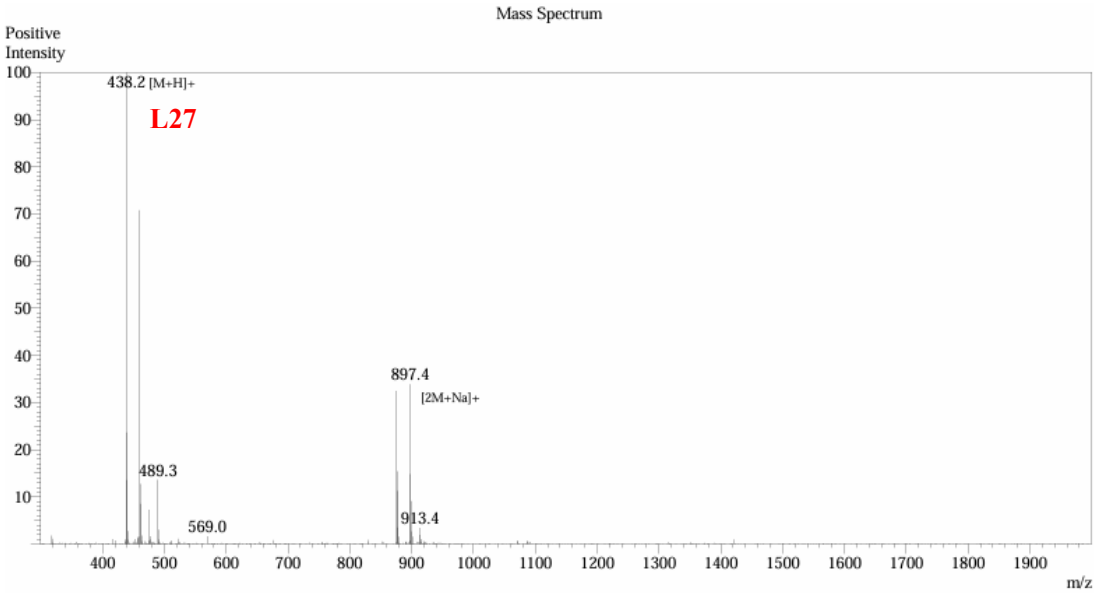

Fig S54 . ESI-MS spectrum of **L27**. LRMS (ES+) m/z: $[M+H]^+$ calcd for $C_{15}H_{27}N_5O_6S_2$ 438.1, found 438.2.

H-Cys-Ala-Ala-Ala-Ala-Cys-OH (L28). Analytical HPLC using Method C, RT = 7.846 min, the HPLC purity is 96%.

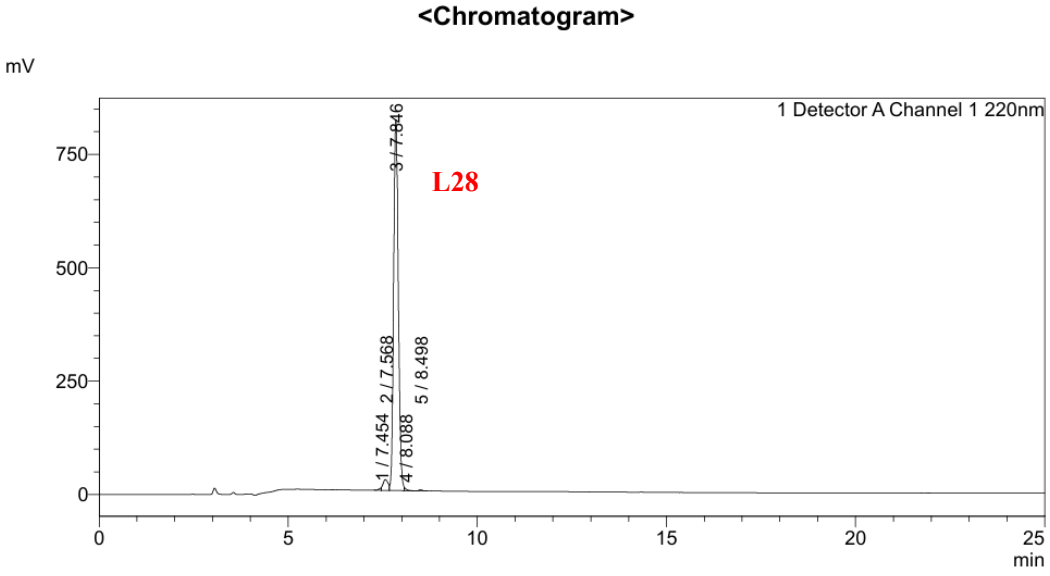

<Peak Table>

Detector A Channel 1 220nm

Peak#	Ret. Time	Area	Height	Area%
1	7.454	19636	4900	0.268
2	7.568	220011	23689	3.005
3	7.846	7053462	817377	96.326
4	8.088	18521	5324	0.253
5	8.498	10878	2014	0.149
Total		7322509	853304	100.000

Fig S55 . HPLC-UV chromatogram at 220 nm of **L28**.

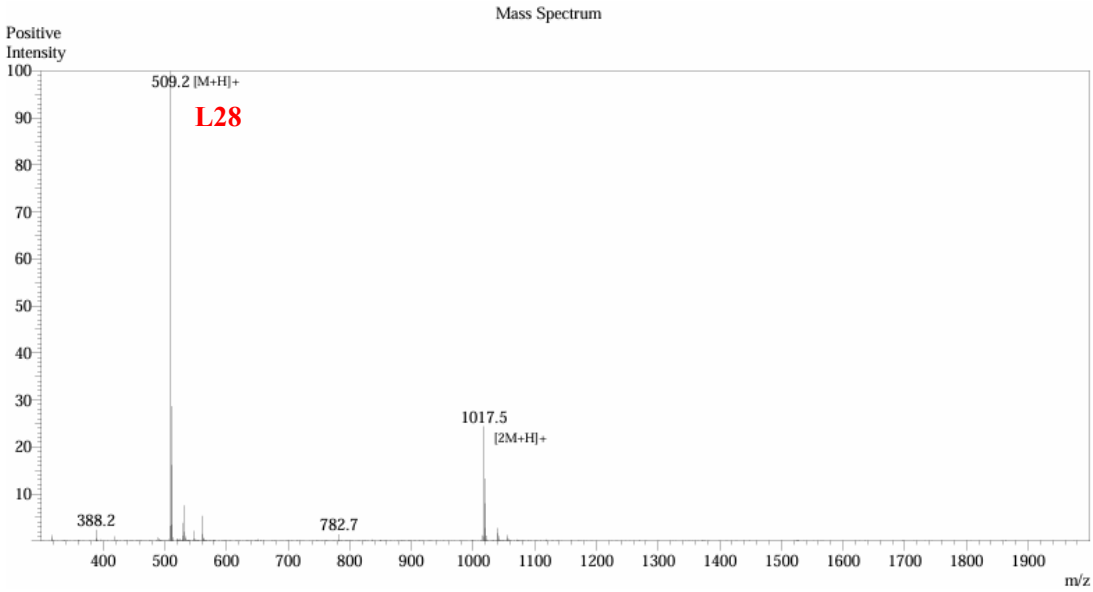

Fig S56 . ESI-MS spectrum of **L28**. LRMS (ES+) m/z: $[M+H]^+$ calcd for $C_{18}H_{32}N_6O_7S_2$ 509.2, found 509.2.

H-Cys-Ala-Ala-Ala-Ala-Ala-Cys-OH (L29). Analytical HPLC using Method C, RT = 6.862 min, the HPLC purity is 95%.

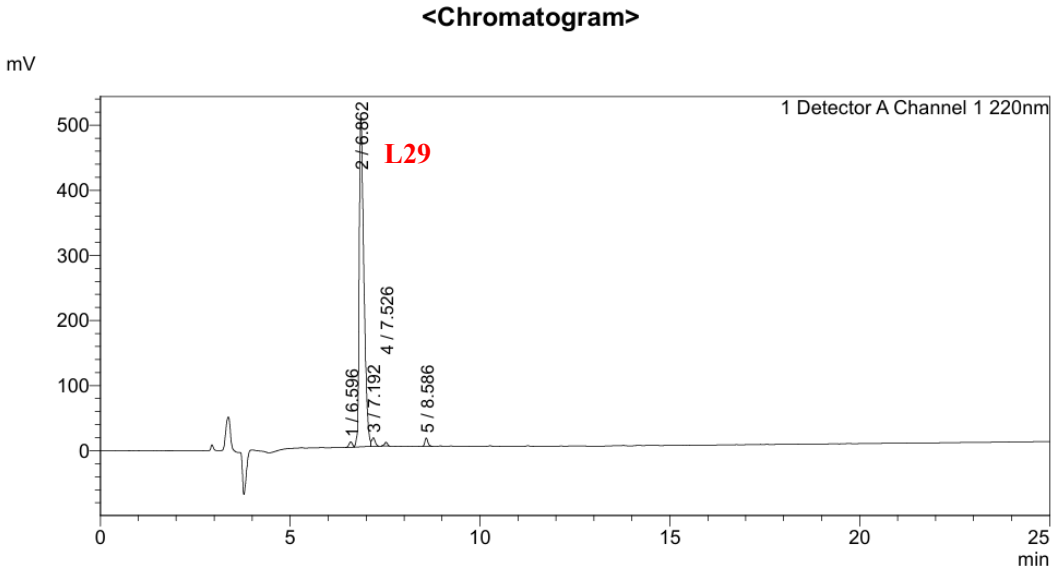

<Peak Table>

Detector A Channel 1 220nm

Peak#	Ret. Time	Area	Height	Area%
1	6.596	49308	8025	1.074
2	6.862	4362322	505782	95.021
3	7.192	82571	12923	1.799
4	7.526	29666	5605	0.646
5	8.586	67018	12531	1.460
Total		4590885	544866	100.000

Fig S57 . HPLC-UV chromatogram at 220 nm of **L29**.

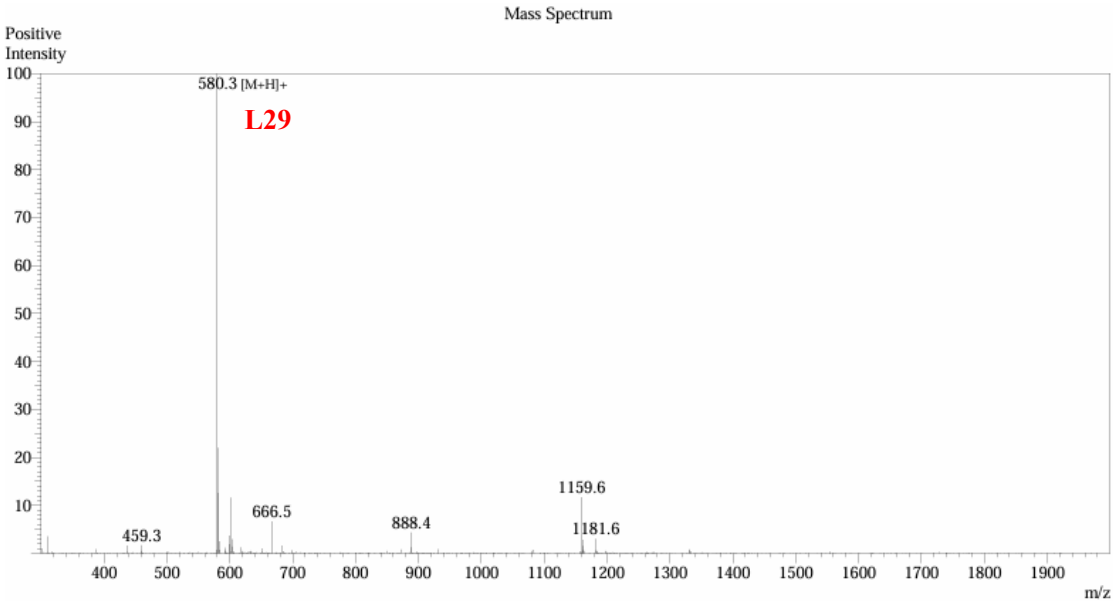

Fig S58 . ESI-MS spectrum of **L29**. LRMS (ES+) m/z: $[M+H]^+$ calcd for $C_{21}H_{37}N_7O_8S_2$ 580.2, found 580.3.

H-Cys-Gly-Ser-Cys-OH (L30). Analytical HPLC using Method C, RT = 5.001 min, the HPLC purity is 99%.

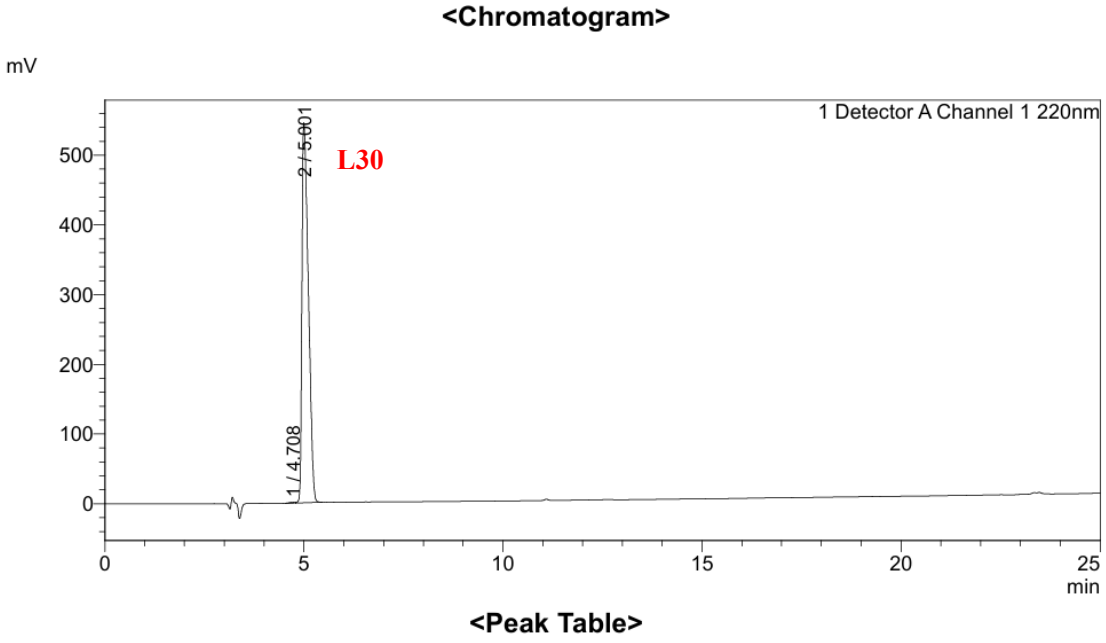

<Peak Table>

Detector A Channel 1 220nm

Peak#	Ret. Time	Area	Height	Area%
1	4.708	11047	1224	0.181
2	5.001	6085951	545983	99.819
Total		6096998	547207	100.000

Fig S59. HPLC-UV chromatogram at 220 nm of **L30**.

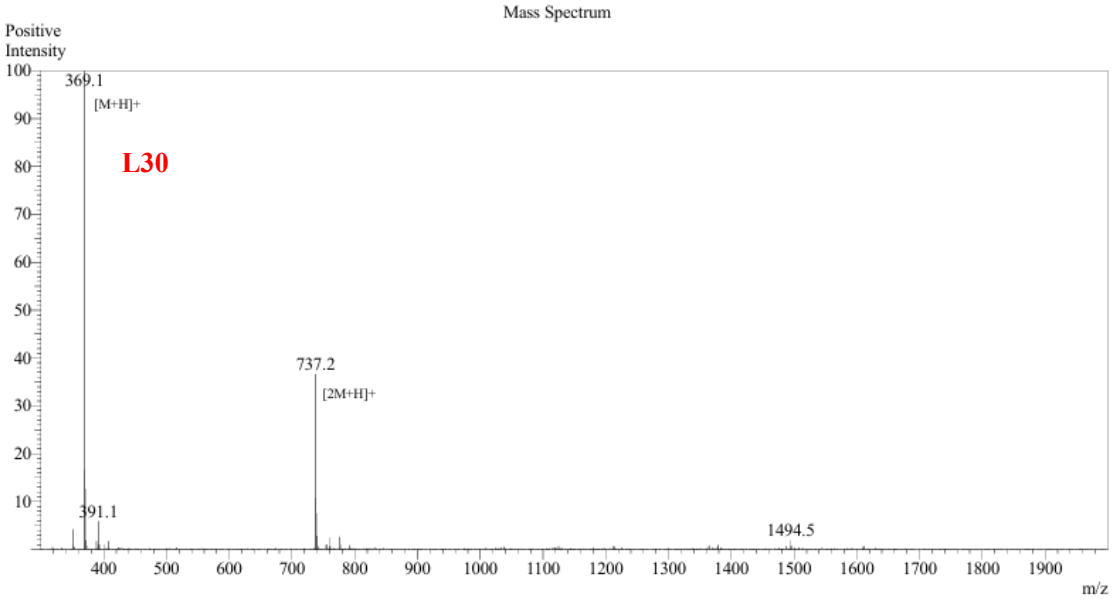

Fig S60. ESI-MS spectrum of **L30**. LRMS (ES+) m/z: $[M+H]^+$ calcd for $C_{11}H_{20}N_4O_6S_2$ 369.1, found 369.1.

H-Cys-Gly-Ser-Gly-Ser-Cys-OH (L31). Analytical HPLC using Method D, RT = 12.318 min, the HPLC purity is 96%.

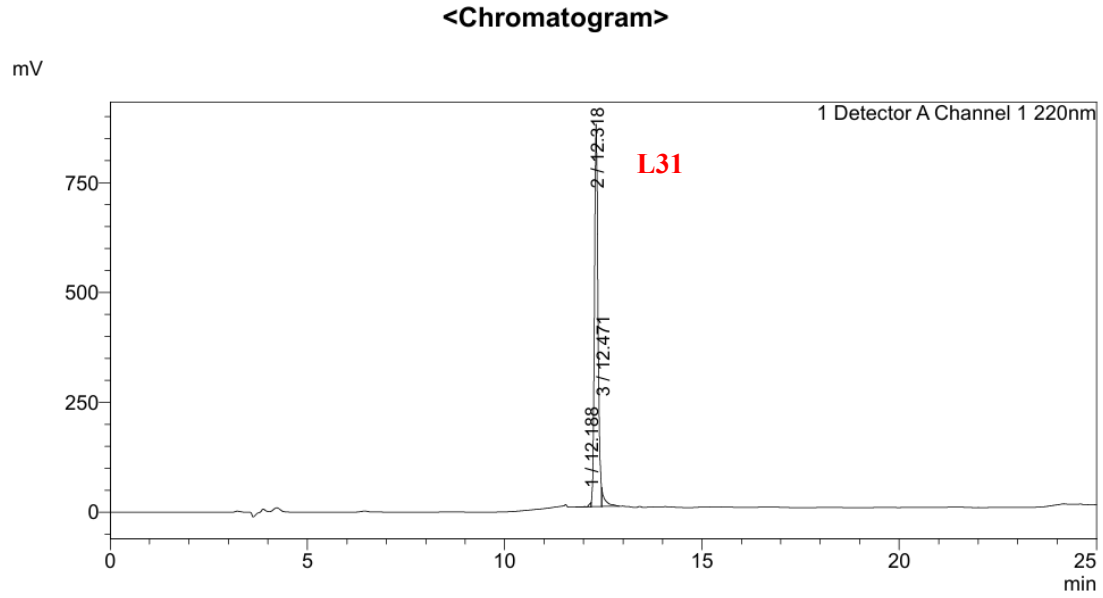

<Peak Table>

Detector A Channel 1 220nm

Peak#	Ret. Time	Area	Height	Area%
1	12.188	34335	8002	0.600
2	12.318	5468257	870602	95.635
3	12.471	215276	37263	3.765
Total		5717868	915867	100.000

Fig S61. HPLC-UV chromatogram at 220 nm of **L31**.

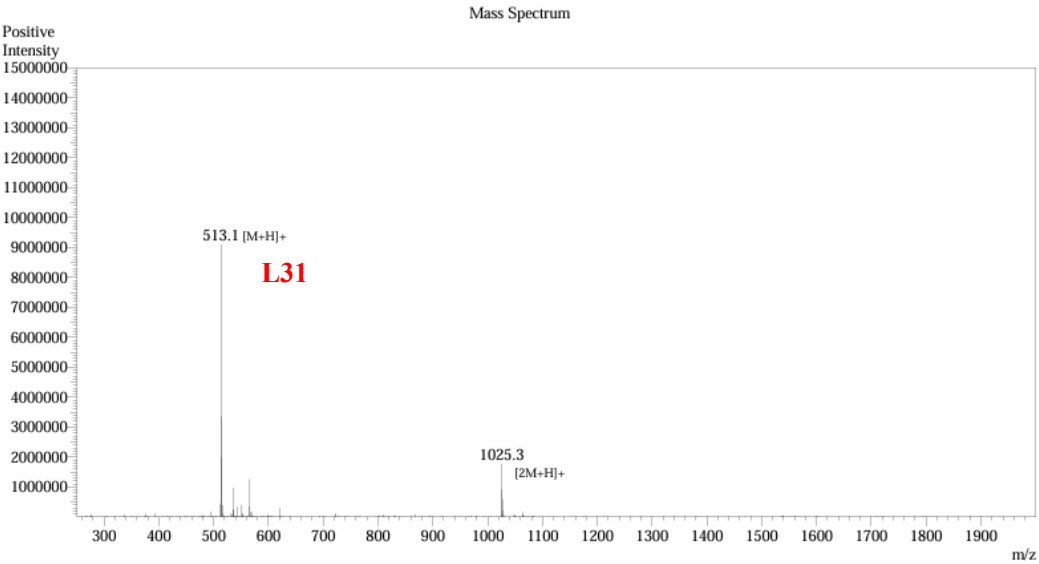

Fig S62. ESI-MS spectrum of **L31**. LRMS (ES+) m/z: $[M+H]^+$ calcd for $C_{16}H_{28}N_6O_9S_2$ 513.1, found 513.1.

H-Cys-Gly-Ser-Gly-Ser-Gly-Ser-Cys-OH (L32). Analytical HPLC using Method D, RT = 13.077 min, the HPLC purity is 97%.

<Chromatogram>

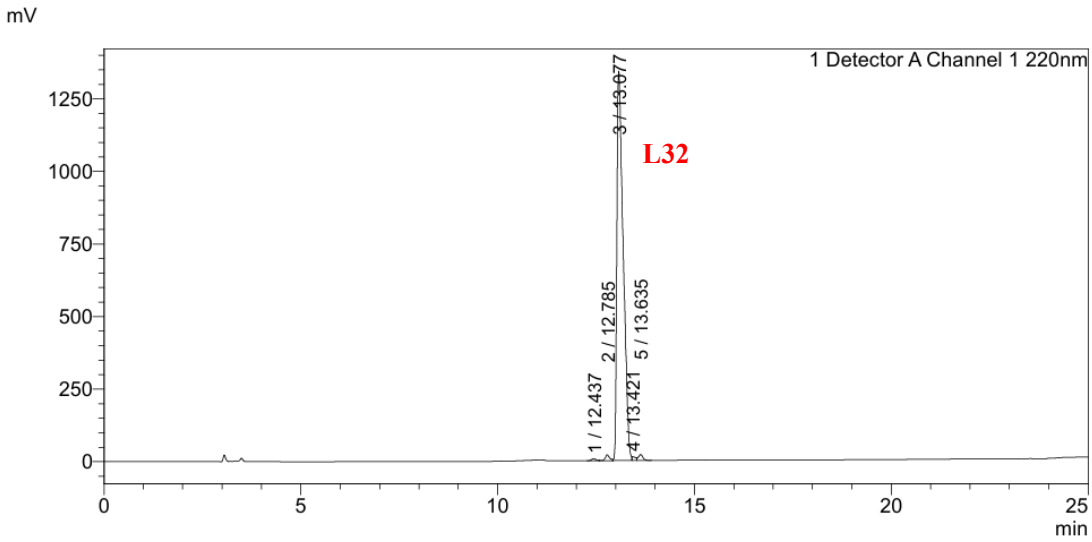

<Peak Table>

Detector A Channel 1 220nm

Peak#	Ret. Time	Area	Height	Area%
1	12.437	50162	6654	0.326
2	12.785	144149	19482	0.936
3	13.077	14968933	1342413	97.180
4	13.421	85590	12690	0.556
5	13.635	154433	19905	1.003
Total		15403267	1401145	100.000

Fig S63. HPLC-UV chromatogram at 220 nm of **L32**.

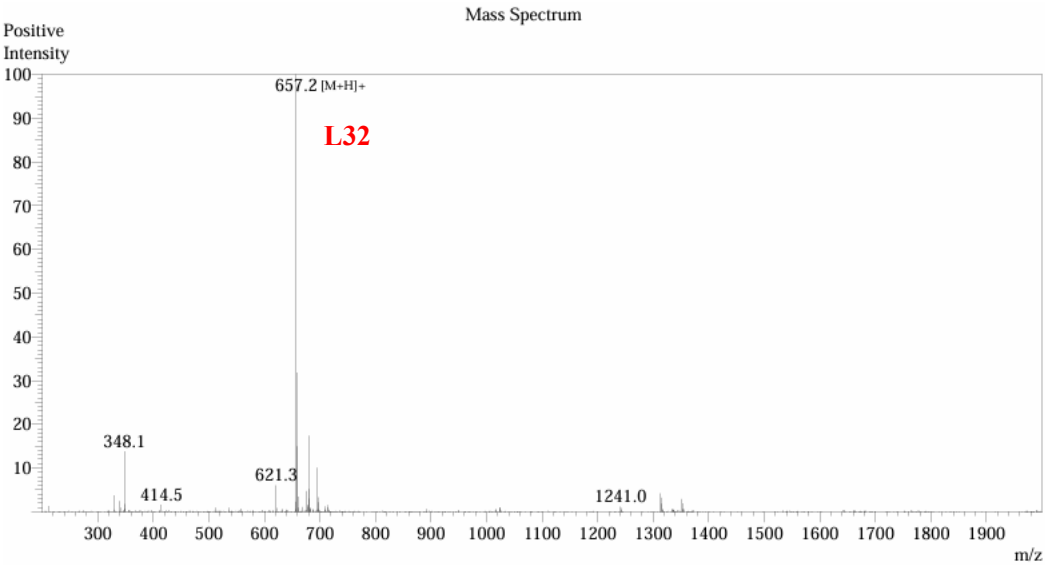

Fig S64. ESI-MS spectrum of **L32**. LRMS (ES+) m/z: $[M+H]^+$ calcd for $C_{21}H_{36}N_8O_{12}S_2$ 657.2, found 657.2.

H-Cys-Gly-Ser-Gly-Ser-Gly-Ser-Gly-Ser-Cys-OH (L33). Analytical HPLC using Method D, RT = 12.813 min, the HPLC purity is 97 %.

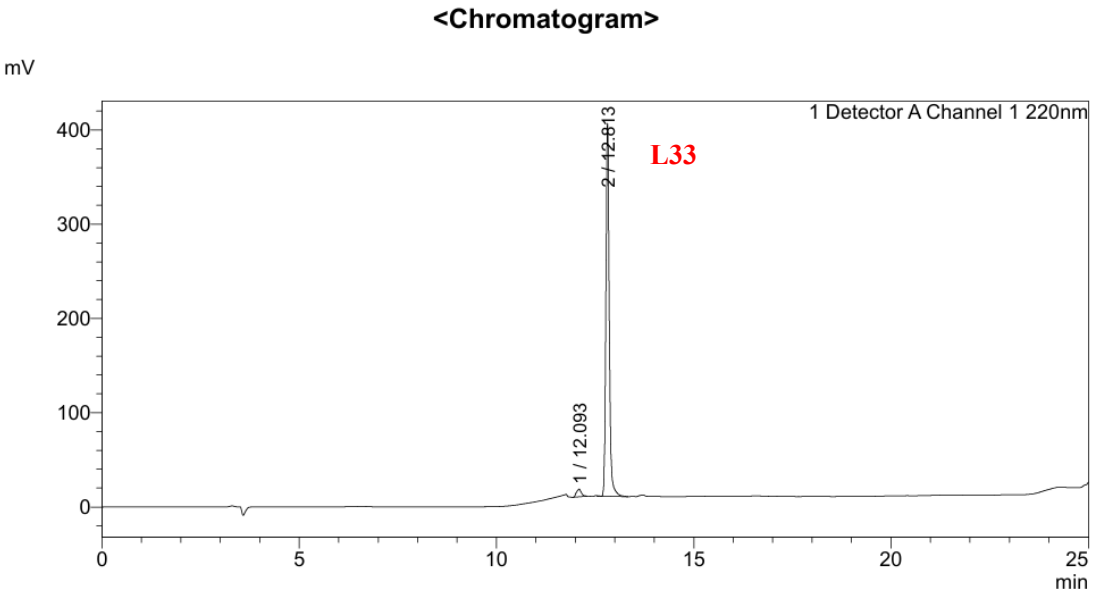

<Peak Table>

Detector A Channel 1 220nm

Peak#	Ret. Time	Area	Height	Area%
1	12.093	67608	7962	2.792
2	12.813	2353947	396105	97.208
Total		2421555	404067	100.000

Fig S65. HPLC-UV chromatogram at 220 nm of **L33**.

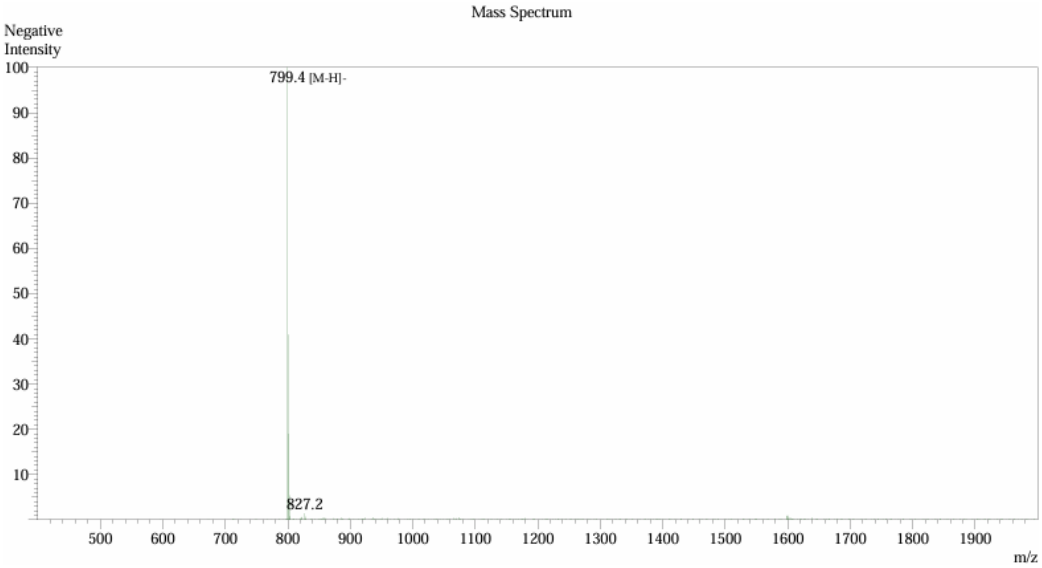

Fig S66. ESI-MS spectrum of **L33**. LRMS (ES+) m/z: $[M+H]^+$ calcd for $C_{26}H_{44}N_{10}O_{15}S_2$ 800.2, found 799.4.

H-Cys-Asn-Gly-Arg-Cys-OH (**L34**). Analytical HPLC using Method C, RT = 13.573 min, the HPLC purity is 97%.

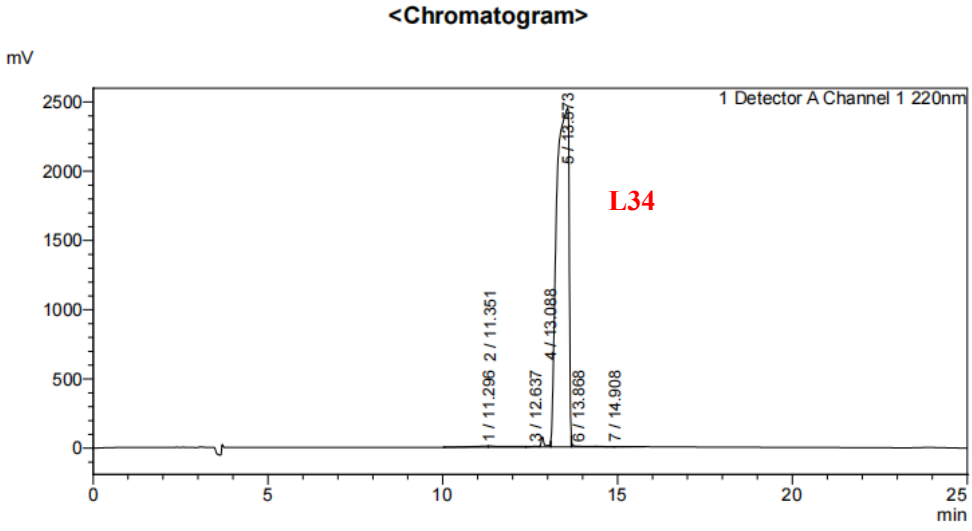

<Peak Table>

Detector A Channel 1 220nm

Peak#	Ret. Time	Area	Height	Area%
1	11.296	263988	8154	0.435
2	11.351	352489	8606	0.580
3	12.637	104759	6680	0.172
4	13.088	494608	28824	0.814
5	13.573	59166785	2450391	97.390
6	13.868	319023	5588	0.525
7	14.908	50520	1704	0.083
Total		60752173	2509946	100.000

Fig S67. HPLC-UV chromatogram at 220 nm of **L34**.

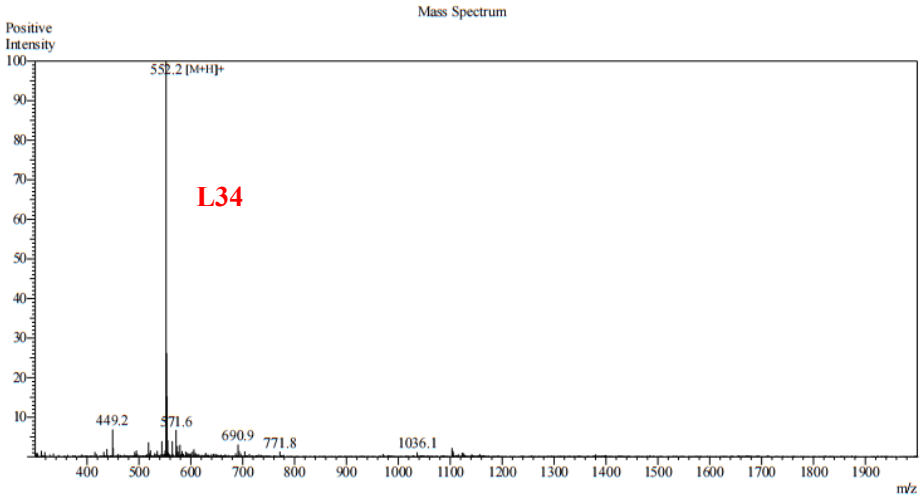

Fig S68. ESI-MS spectrum of **L34**. LRMS (ES+) m/z: $[M+H]^+$ calcd for $C_{18}H_{33}N_9O_7S_2$ 552.2, found 552.2.

H-Cys-Ser-Pro-Tyr-Gly-Arg-Cys-OH (**L35**). Analytical HPLC using Method C, RT = 6.858 min, the HPLC purity is 96%.

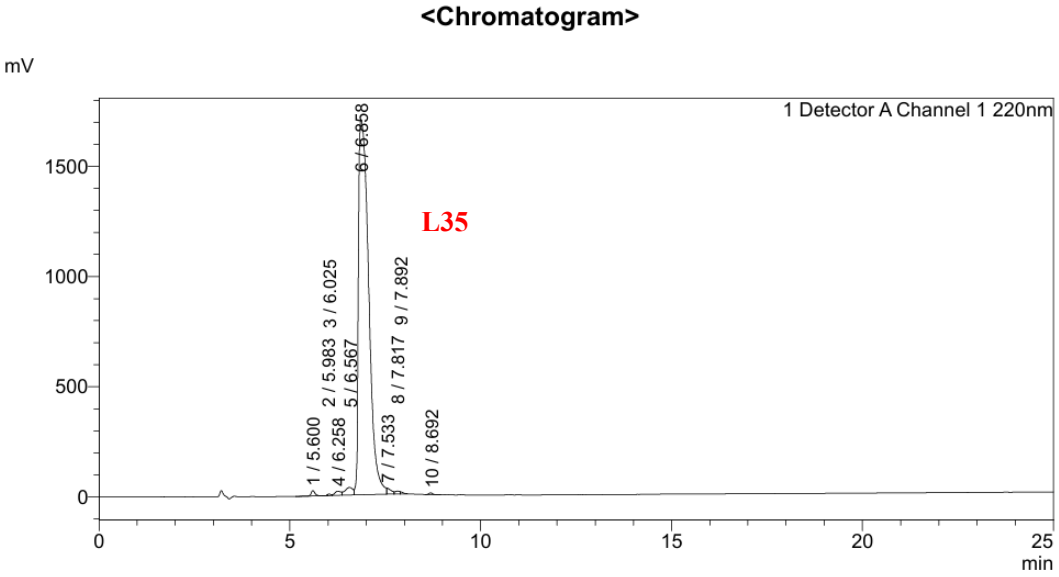

<Peak Table>

Detector A Channel 1 220nm

Peak#	Ret. Time	Area	Height	Area%
1	5.600	156844	24464	0.476
2	5.983	1122	3800	0.003
3	6.025	40913	7548	0.124
4	6.258	204388	19368	0.620
5	6.567	490577	34548	1.489
6	6.858	31597556	1703424	95.911
7	7.533	229614	28196	0.697
8	7.817	110490	13220	0.335
9	7.892	50002	9983	0.152
10	8.692	63152	9044	0.192
Total		32944659	1853596	100.000

Fig S69. HPLC-UV chromatogram at 220 nm of **L35**.

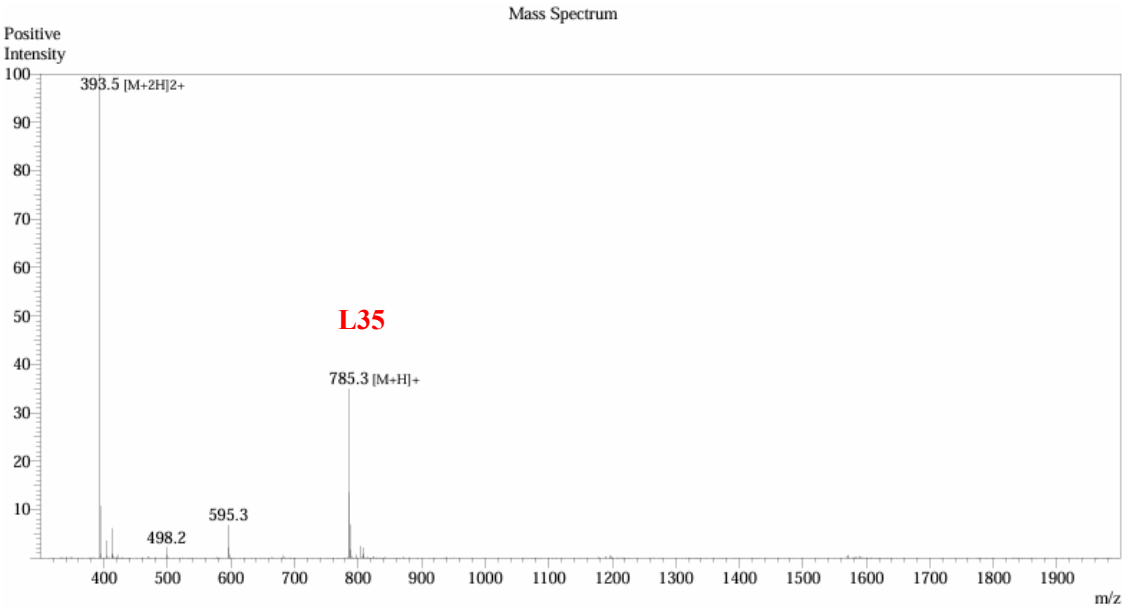

Fig S70. ESI-MS spectrum of **L35**. LRMS (ES+) m/z: $[M+H]^+$ calcd for $C_{31}H_{48}N_{10}O_{10}S_2$ 785.3, found 785.3.

H-Cys-Pro-Pro-Thr-Gln-Phe-Cys-OH (L36). Analytical HPLC using Method C, RT = 10.383 min, the HPLC purity is 96%.

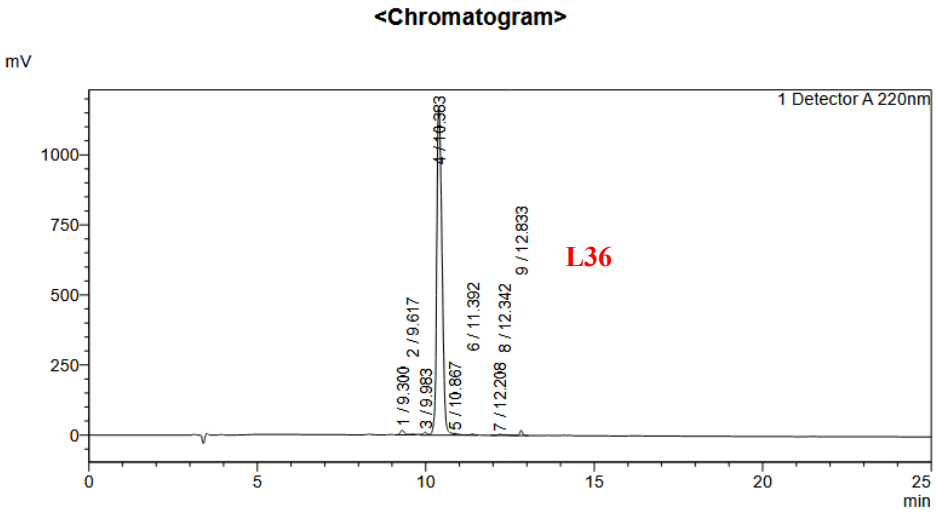

<Peak Table>

Detector A 220nm

Peak#	Ret. Time	Area	Height	Area%
1	9.300	143083	16863	1.079
2	9.617	32011	3307	0.241
3	9.983	80303	10314	0.606
4	10.383	12727825	1165278	95.983
5	10.867	64374	6436	0.485
6	11.392	44499	3960	0.336
7	12.208	34153	4021	0.258
8	12.342	28367	2502	0.214
9	12.833	105840	18907	0.798
Total		13260455	1231587	100.000

Fig S71. HPLC-UV chromatogram at 220 nm of **L36**.

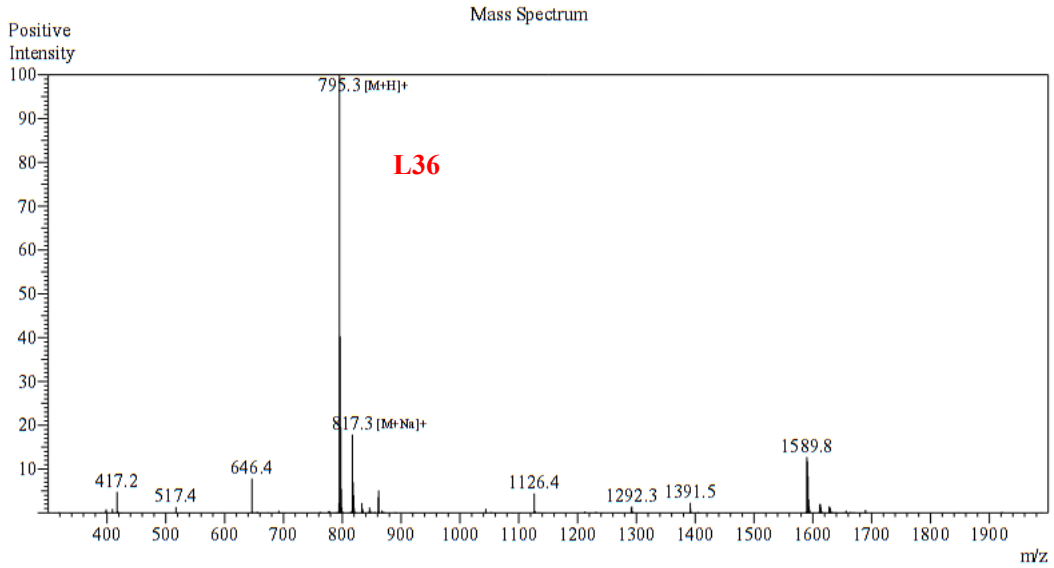

Fig S72. ESI-MS spectrum of **L36**. LRMS (ES+) m/z: $[M+H]^+$ calcd for $C_{34}H_{50}N_8O_{10}S_2$ 795.3, found 795.3.

H-Cys-Tyr-Phe-Gln-Asn-Cys-Pro-Arg-Gly-OH (**L37**). Analytical HPLC using Method C, RT = 10.592 min, the HPLC purity is 96%.

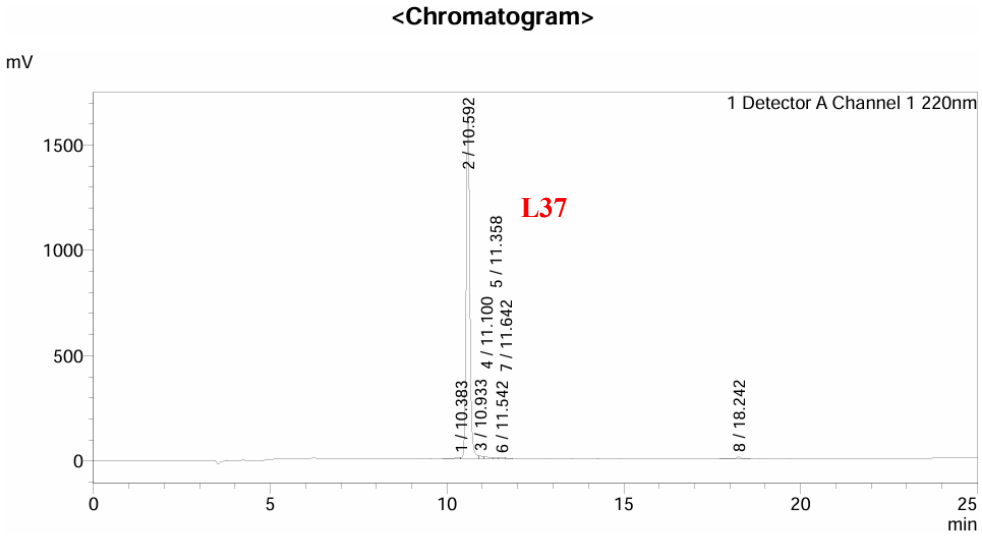

<Peak Table>

Detector A Channel 1 220nm

Peak#	Ret. Time	Area	Height	Area%
1	10.383	73708	7064	0.596
2	10.592	11866984	1646672	95.891
3	10.933	105996	13985	0.857
4	11.100	118253	11510	0.956
5	11.358	35609	4291	0.288
6	11.542	54614	6169	0.441
7	11.642	38040	3772	0.307
8	18.242	82235	10043	0.665
Total		12375441	1703505	100.000

Fig S73. HPLC-UV chromatogram at 220 nm of **L37**.

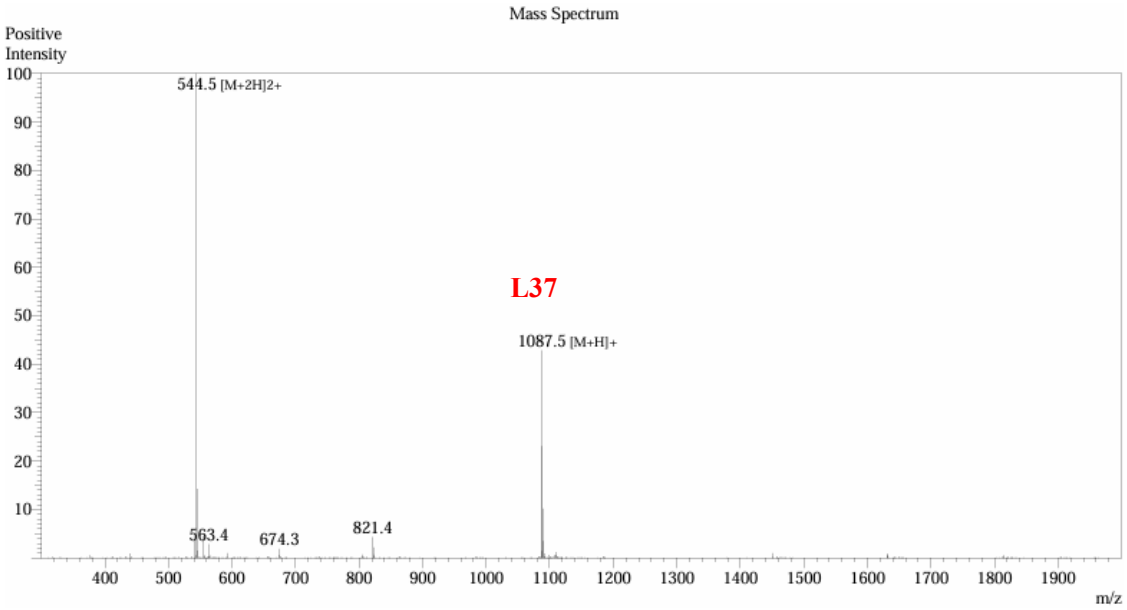

Fig S74. ESI-MS spectrum of **L37**. LRMS (ES+) m/z: $[M+H]^+$ calcd for $C_{46}H_{66}N_{14}O_{13}S_2$ 1087.4, found 1087.5.

H-Cys-Arg-Gly-Asp-Lys-Gly-Pro-Asp-Cys-OH (**L38**). Analytical HPLC using Method C, RT = 4.300 min, the HPLC purity is 96%.

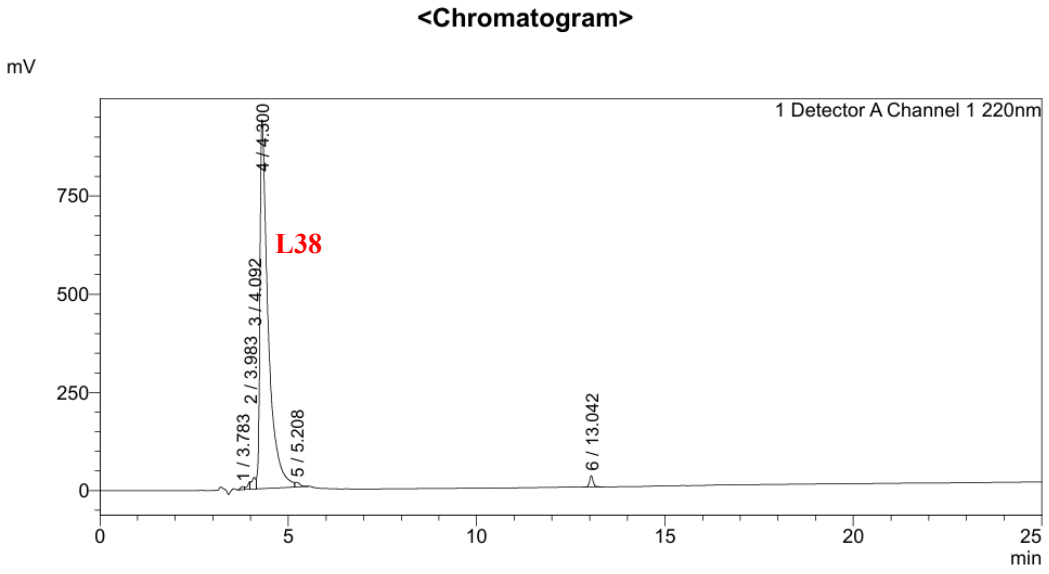

<Peak Table>

Detector A Channel 1 220nm

Peak#	Ret. Time	Area	Height	Area%
1	3.783	47791	7877	0.319
2	3.983	92517	19391	0.618
3	4.092	225821	29709	1.509
4	4.300	14299961	939448	95.561
5	5.208	106677	12070	0.713
6	13.042	191529	29131	1.280
Total		14964296	1037626	100.000

Fig S75. HPLC-UV chromatogram at 220 nm of **L38**.

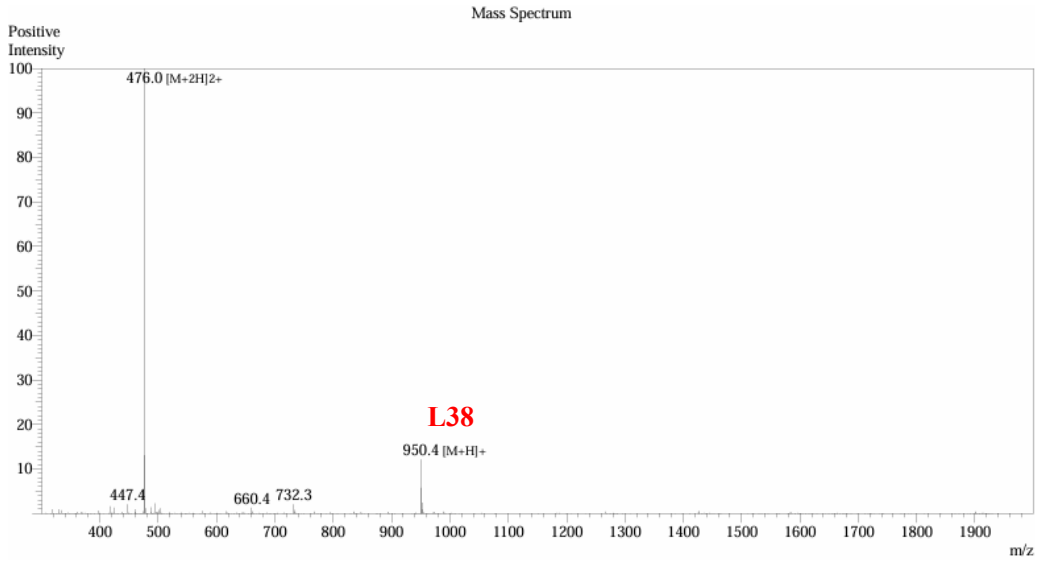

Fig S76. ESI-MS spectrum of **L38**. LRMS (ES+) m/z: $[M+H]^+$ calcd for $C_{35}H_{59}N_{13}O_{14}S_2$ 950.4, found 950.4.

H-Cys-Lys-Ser-{D-Ala}-His-{D-Phe}-Lys-Trp-Cys-OH (**L39**). Analytical HPLC using Method C, RT = 9.706 min, the HPLC purity is 97%.

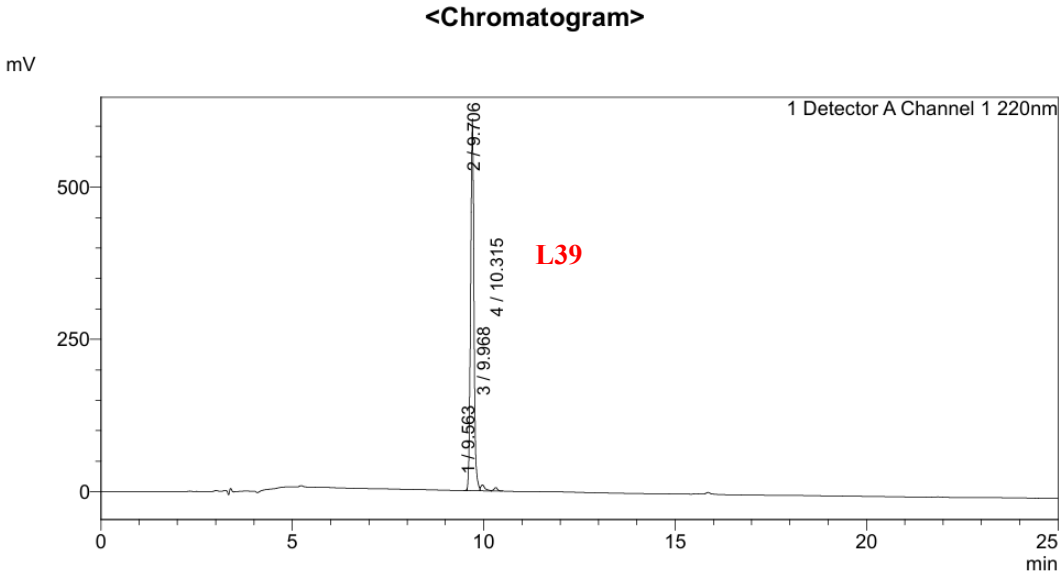

<Peak Table>

Detector A Channel 1 220nm

Peak#	Ret. Time	Area	Height	Area%
1	9.563	3650	1850	0.095
2	9.706	3746516	611406	97.004
3	9.968	75103	9803	1.945
4	10.315	36977	5785	0.957
Total		3862245	628844	100.000

Fig S77. HPLC-UV chromatogram at 220 nm of **L39**.

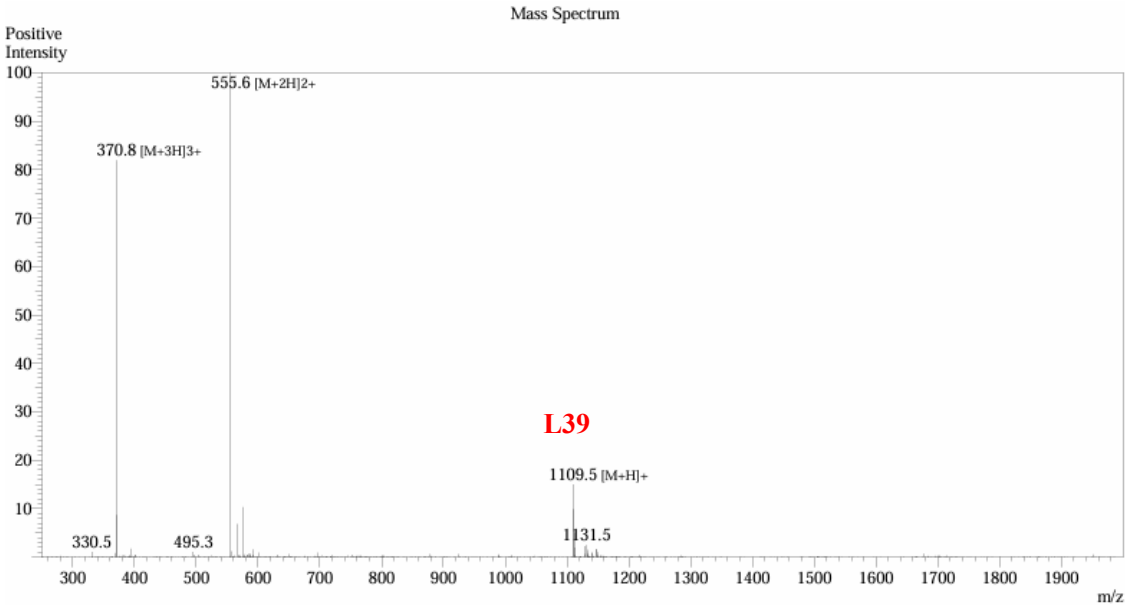

Fig S78. ESI-MS spectrum of **L39**. LRMS (ES+) m/z: $[M+H]^+$ calcd for $C_{50}H_{72}N_{14}O_{11}S_2$ 1109.5, found 1109.5.

H-Cys-Thr-Gly-Arg-Ala-Lys-Arg-Arg-Met-Gln-Tyr-Asn-Arg-Arg-Gly-Cys-OH (**L40**). Analytical HPLC using Method C, RT = 6.001 min, the HPLC purity is 95%.

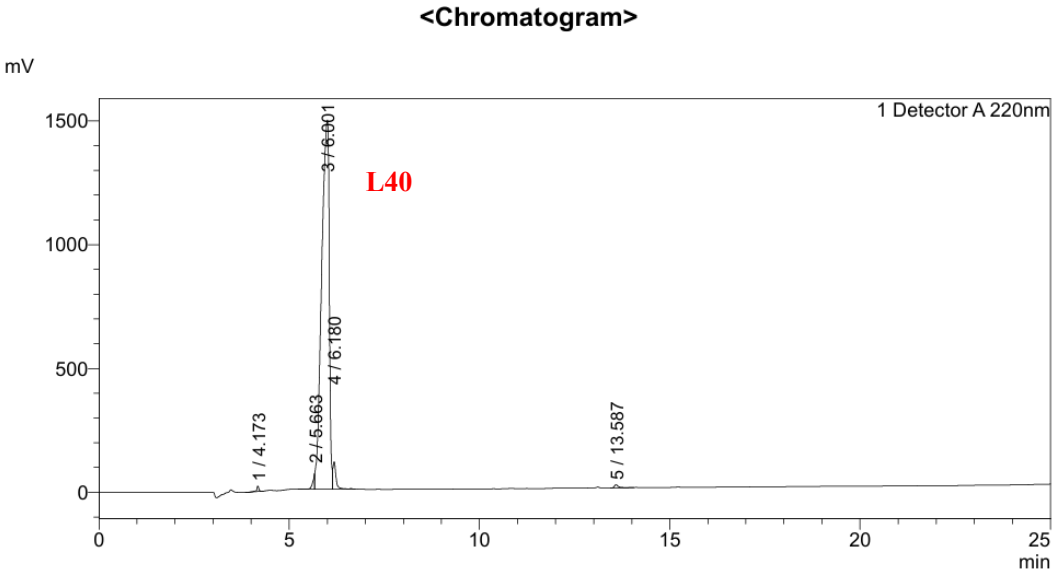

<Peak Table>

Detector A 220nm

Peak#	Ret. Time	Area	Height	Area%
1	4.173	83956	21514	0.386
2	5.663	209527	53780	0.963
3	6.001	20744190	1491703	95.299
4	6.180	637627	110693	2.929
5	13.587	92267	12903	0.424
Total		21767566	1690592	100.000

Fig S79. HPLC-UV chromatogram at 220 nm of **L40**.

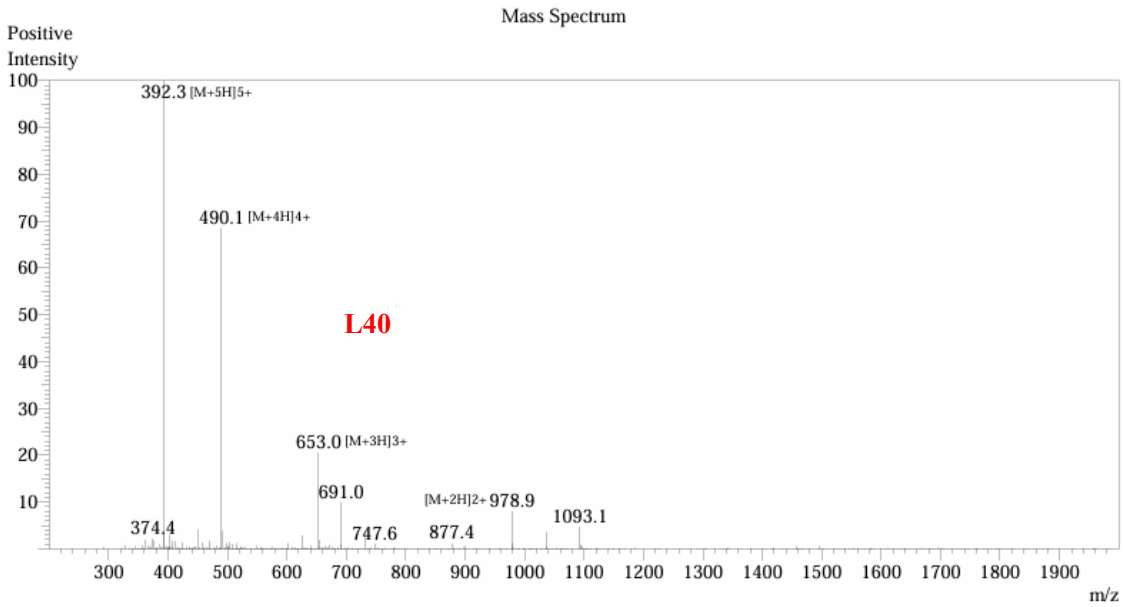

Fig S80. ESI-MS spectrum of **L40**. LRMS (ES+) m/z: $[M+2H]^{2+}$ calcd for $C_{76}H_{134}N_{34}O_{11}S_2$ 978.5, found 978.9.

H-Cys-{D-Tyr}-Arg-Gln-Phe-Asn-Arg-Arg-Thr-His-Glu-Val-Trp-Asn-Leu-Asp-Cys-OH (**L41**). Analytical HPLC using Method C, RT =12.336 min, the HPLC purity is 98%.

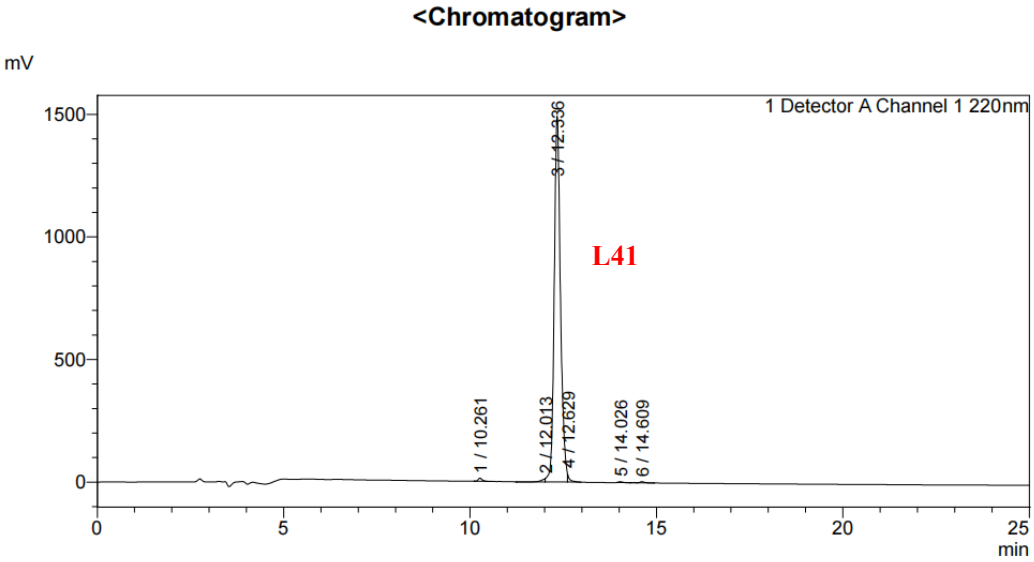

<Peak Table>

Detector A Channel 1 220nm

Peak#	Ret. Time	Area	Height	Area%
1	10.261	97308	13036	0.548
2	12.013	89086	12754	0.502
3	12.336	17389535	1492317	97.963
4	12.629	112923	28062	0.636
5	14.026	25073	3345	0.141
6	14.609	37205	4813	0.210
Total		17751131	1554327	100.000

Fig S81. HPLC-UV chromatogram at 220 nm of **L41**.

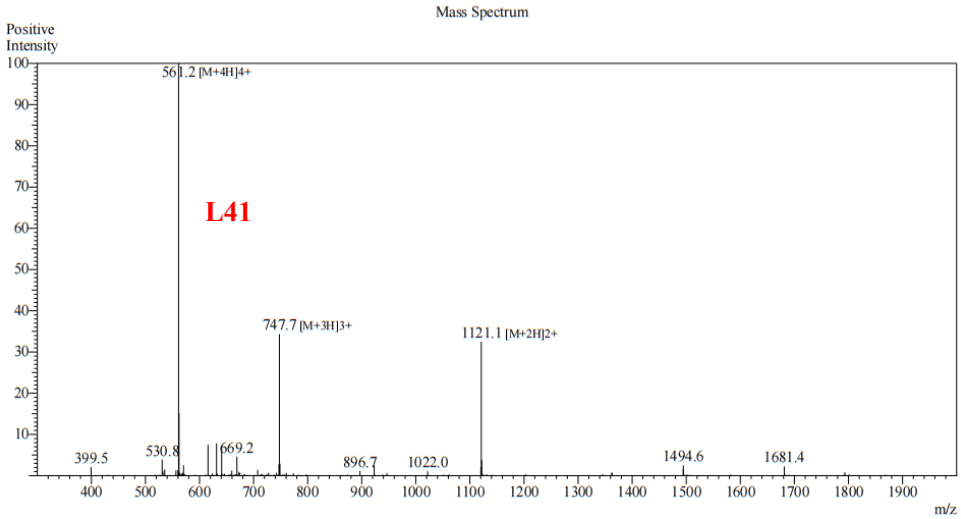

Fig S82. ESI-MS spectrum of **L41**. LRMS (ES+) m/z: $[M+2H]^{2+}$ calcd for $C_{96}H_{142}N_{32}O_{27}S_2$ 1121.0, found 1121.1.

H-Cys-{D-Tyr}-Leu-Ile-Thr-Phe-Arg-Gln-Trp-Ala-Phe-Asn-Leu-Pro-Cys-Gly (**L42**). Analytical HPLC using Method C, RT = 17.283 min, the HPLC purity is 95%.

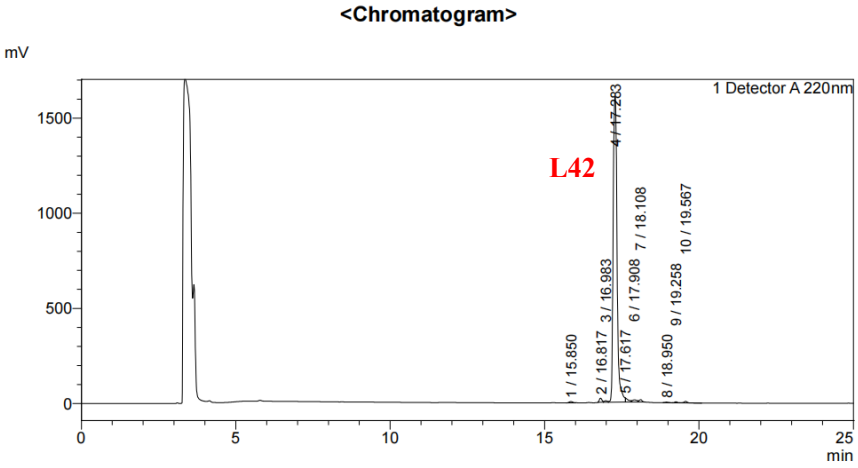

<Peak Table>

Detector A 220nm

Peak#	Ret. Time	Area	Height	Area%
1	15.850	60244	6924	0.409
2	16.817	125873	21848	0.855
3	16.983	52907	8047	0.359
4	17.283	13996994	1605990	95.108
5	17.617	139492	21541	0.948
6	17.908	119523	11133	0.812
7	18.108	79955	12348	0.543
8	18.950	30138	3304	0.205
9	19.258	36996	5294	0.251
10	19.567	74817	8242	0.508
Total		14716939	1704670	100.000

Fig S83. HPLC-UV chromatogram at 220 nm of **L42**.

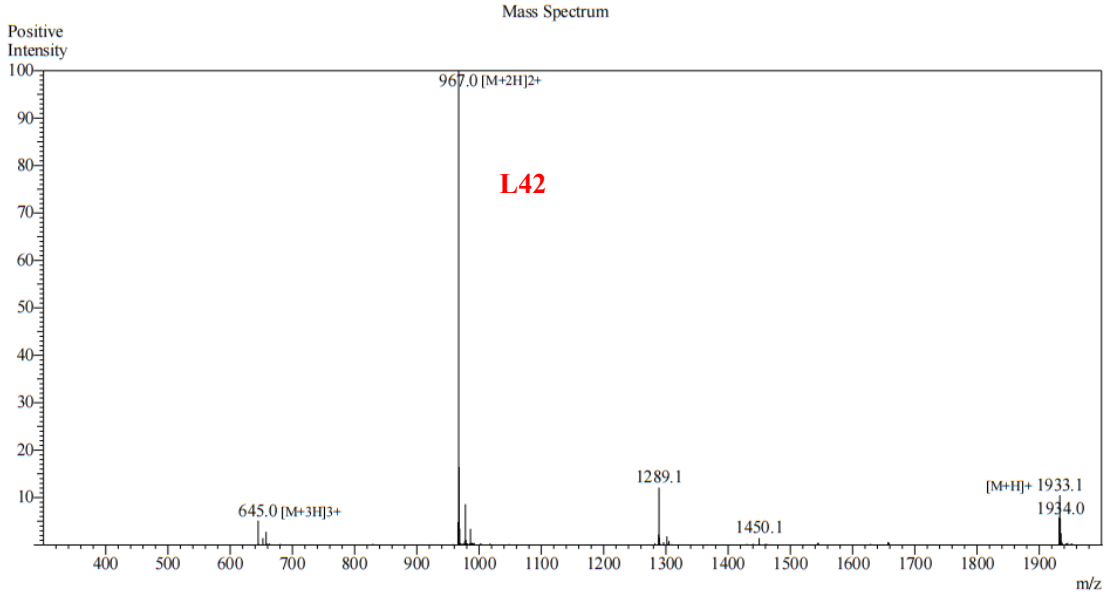

Fig S84. ESI-MS spectrum of **L42**. LRMS (ES+) m/z: $[M+2H]^{2+}$ calcd for $C_{91}H_{130}N_{22}O_{21}S_2$ 966.5, found 967.0.

H-Cys-Asp-Asn-Ile-Lys-His-Val-Pro-Gly-Gly-Gly-Ser-Val-Gln-Ile-Val-Tyr-Lys-Pro-Val-Cys-OH (**L43**). Analytical HPLC using Method C, RT = 9.086 min, the HPLC purity is 98%.

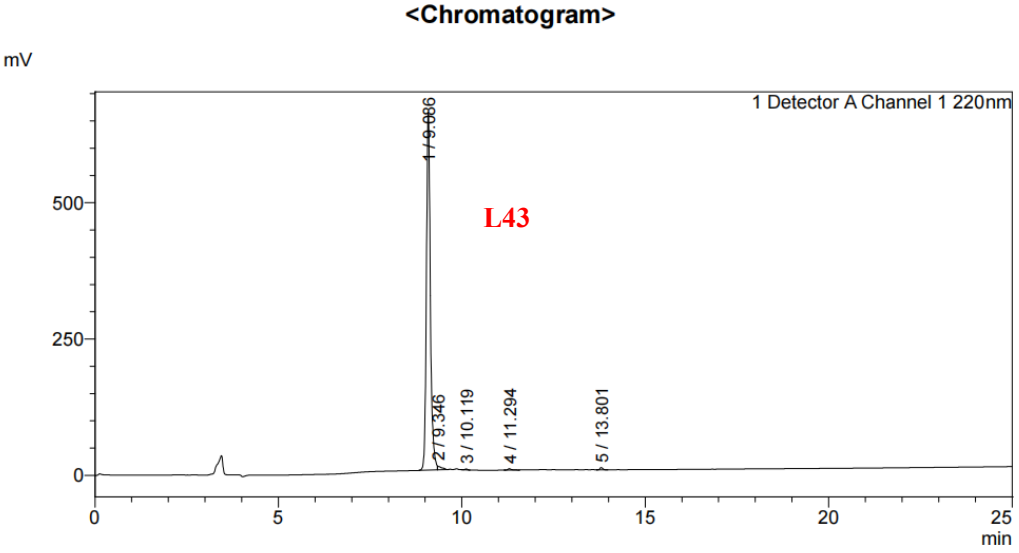

<Peak Table>

Detector A Channel 1 220nm

Peak#	Ret. Time	Area	Height	Area%
1	9.086	4916597	656453	98.054
2	9.346	53442	6621	1.066
3	10.119	7009	1744	0.140
4	11.294	16156	2565	0.322
5	13.801	20967	4185	0.418
Total		5014172	671567	100.000

Fig S85. HPLC-UV chromatogram at 220 nm of **L43**.

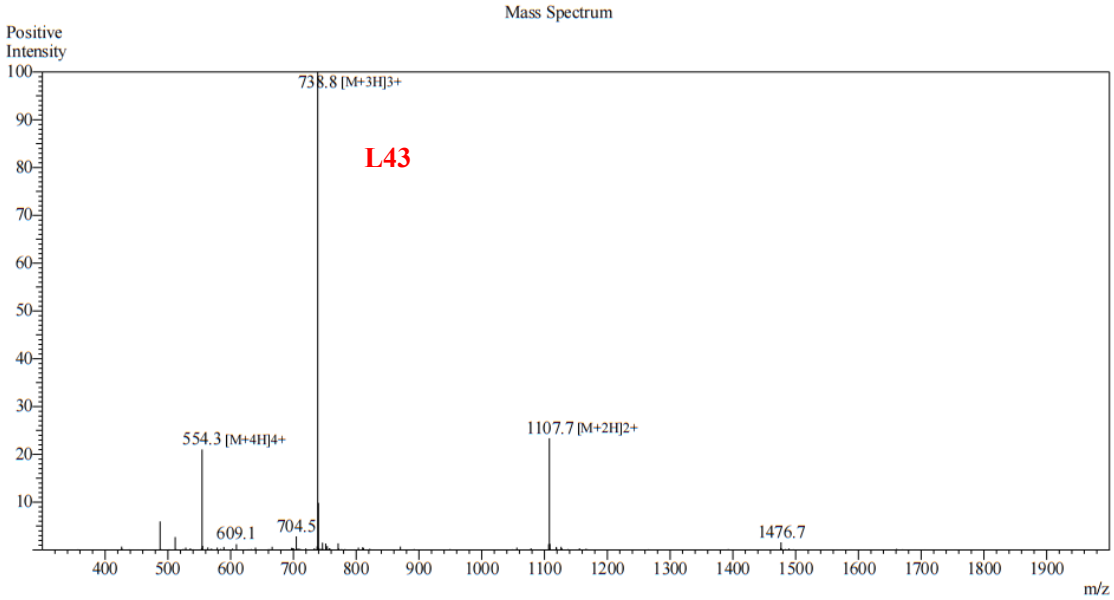

Fig S86. ESI-MS spectrum of **L43**. LRMS (ES+) m/z: $[M+2H]^{2+}$ calcd for $C_{97}H_{157}N_{27}O_{28}S_2$ 1107.1, found 1107.7.

Ac-Cys-Arg-Gly-Asp-Lys-Gly-Pro-Asp-Cys-OH (**L44**). Analytical HPLC using Method C, RT = 7.876 min, the HPLC purity is 96%.

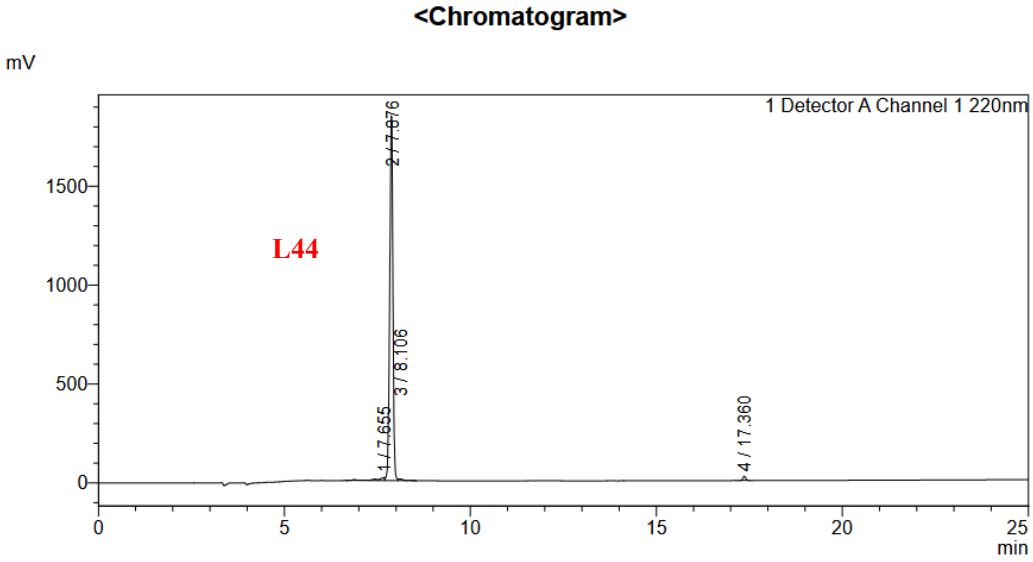

<Peak Table>

Detector A Channel 1 220nm

Peak#	Ret. Time	Area	Height	Area%
1	7.655	249958	15541	2.184
2	7.876	10994088	1845426	96.073
3	8.106	83735	9323	0.732
4	17.360	115706	21473	1.011
Total		11443488	1891764	100.000

Fig S87. HPLC-UV chromatogram at 220 nm of **L44**.

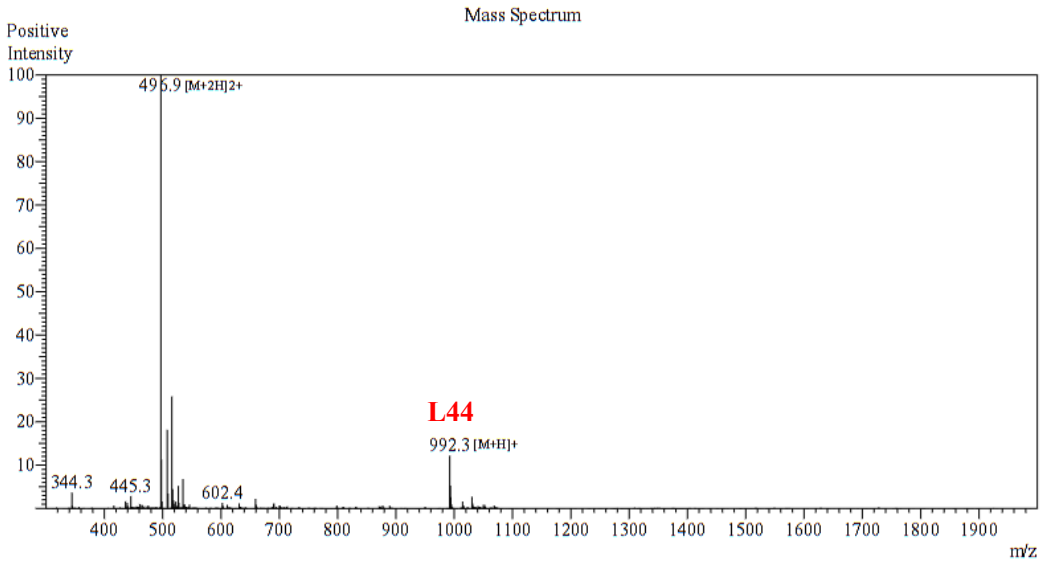

Fig S88. ESI-MS spectrum of **L44**. LRMS (ES+) m/z: $[M+H]^+$ calcd for $C_{37}H_{61}N_{13}O_{15}S_2$ 992.4, found 992.3.

H-Cys-Arg-Gly-Asp-Ala-Arg-Gly-Asp-Cys-OH (**L45**). Analytical HPLC using Method C, RT =14.317 min, the HPLC purity is 96%.

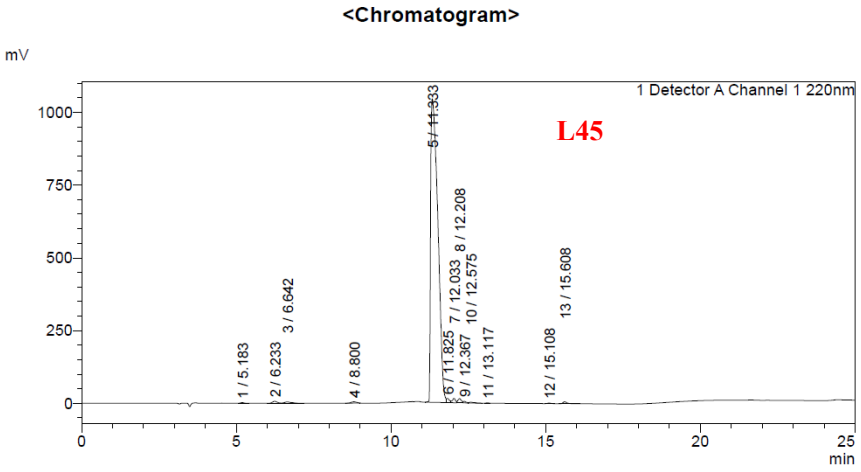

<Peak Table>

Detector A Channel 1 220nm

Peak#	Ret. Time	Area	Height	Area%
1	5.183	19904	2700	0.114
2	6.233	74636	6782	0.426
3	6.642	71854	4568	0.410
4	8.800	56031	4575	0.320
5	11.333	16863021	1043604	96.220
6	11.825	83005	14318	0.474
7	12.033	109233	15179	0.623
8	12.208	110059	14531	0.628
9	12.367	32828	5052	0.187
10	12.575	30251	2683	0.173
11	13.117	7709	1445	0.044
12	15.108	12467	1947	0.071
13	15.608	54415	6366	0.310
Total		17525414	1123751	100.000

Fig S89. HPLC-UV chromatogram at 220 nm of **L45**.

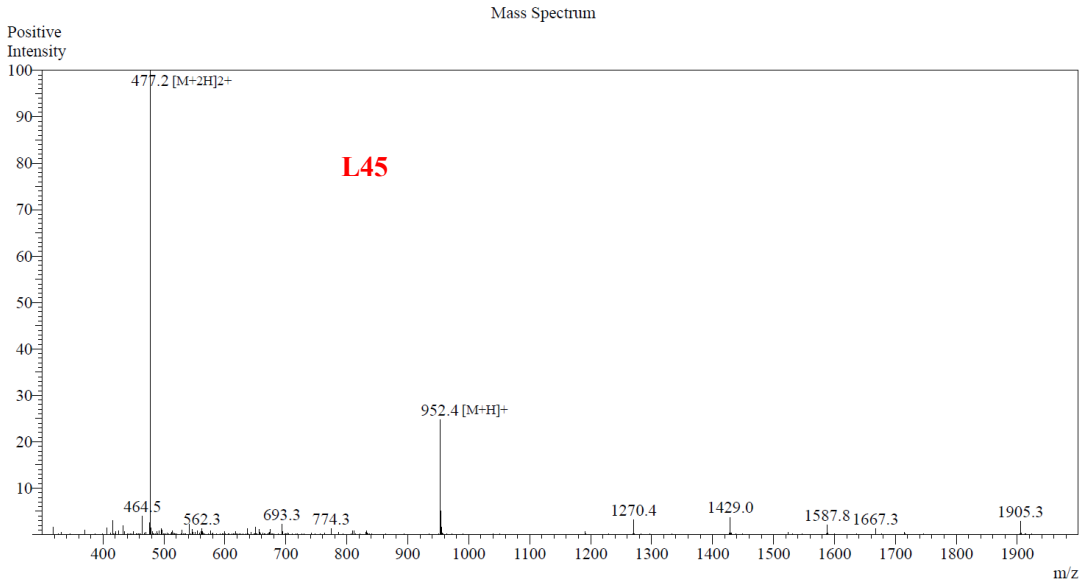

Fig S90. ESI-MS spectrum of **L45**. LRMS (ES+) m/z: $[M+H]^+$ calcd for $C_{33}H_{57}N_{15}O_{14}S_2$ 752.36, found 952.4.

4. Development and optimization of the 3,6-DCT mediated cyclodimerization reaction

4.1 Calibration for LC-MS yield calculation

（1）Establishment of the Quantification Method

To ensure absolute quantification accuracy and address potential variations in absorption coefficients between starting materials and products, purified cyclodimerization product **B1a** was isolated and used as the primary external standard. Standard solutions of **B1a** were prepared in H_2O at concentrations of 0.0625, 0.125, 0.25, 0.5, and 1.0 mM. For each analysis, 10 μL of the solution was injected into the UPLC-MS system under the conditions specified in Method A. Considering that all cyclodimerization products have a 270nm characteristic absorption peak, MassLynx V4.2 software was used to integrate the peak area at 270nm for calibration curve calculation.

A high-precision calibration curve was established within the linear dynamic range of 0.0625 mM to 0.25 mM (3 points), where the UV detector exhibited an excellent linear response (R^2 = 0.9997). Higher concentrations (>= 0.5 mM) were found to approach the detector's saturation limit and were excluded from the global linear regression to maintain the highest precision for low-to-medium concentration samples.

Tab S7. The LC-MS data for B1a at different concentrations

Entry	Concentration of B1a	Peak area of B1a in 270 nm
1	0.0625 mM	51427
2	0.125 mM	100779
3	0.25 mM	192600
4	0.5 mM	301328
5	1 mM	553314

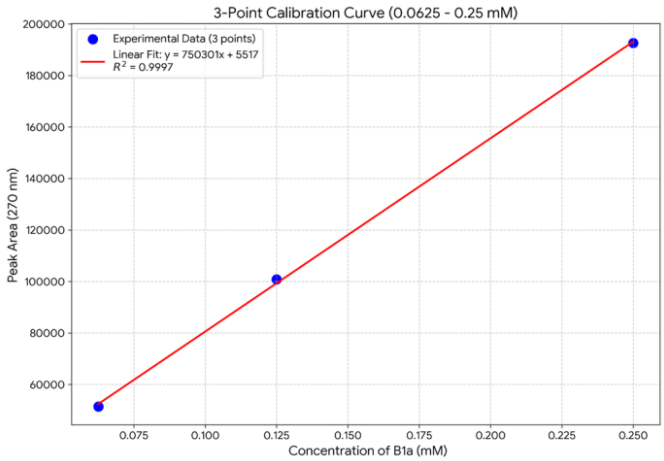

Fig S91. Calibration curve of purified **B1a** (0.0625 to 0.25 mM) at 270 nm (y = 750301x + 5517, R2 = 0.9997).

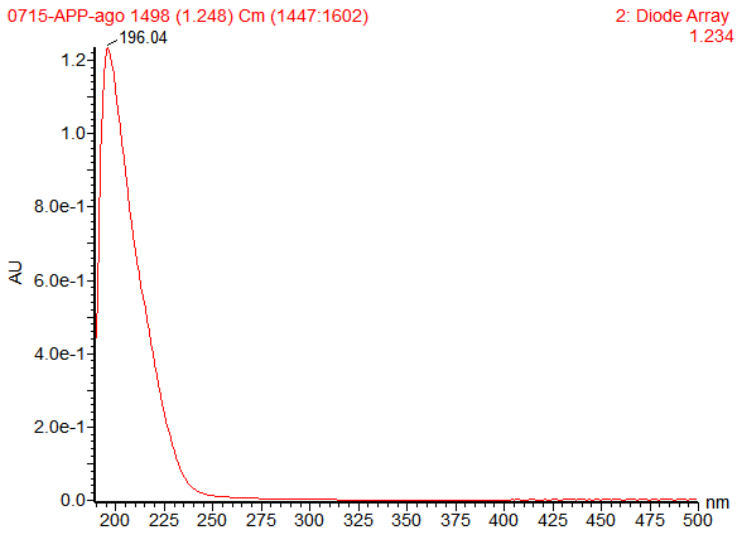

Fig S92. The UV characteristic absorption of **M1-ss**.

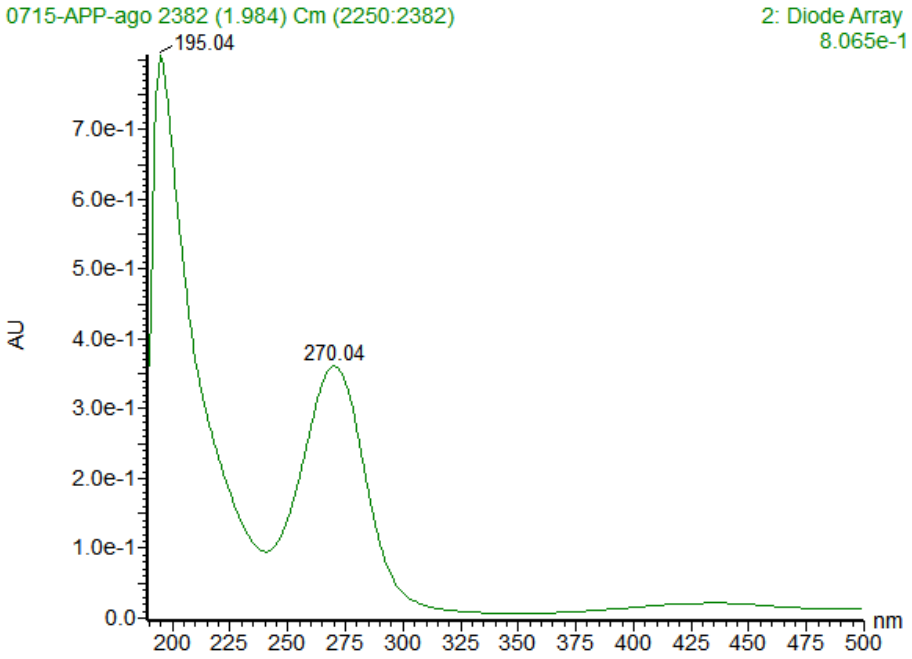

Fig S93. The UV characteristic absorption of **B1a**.

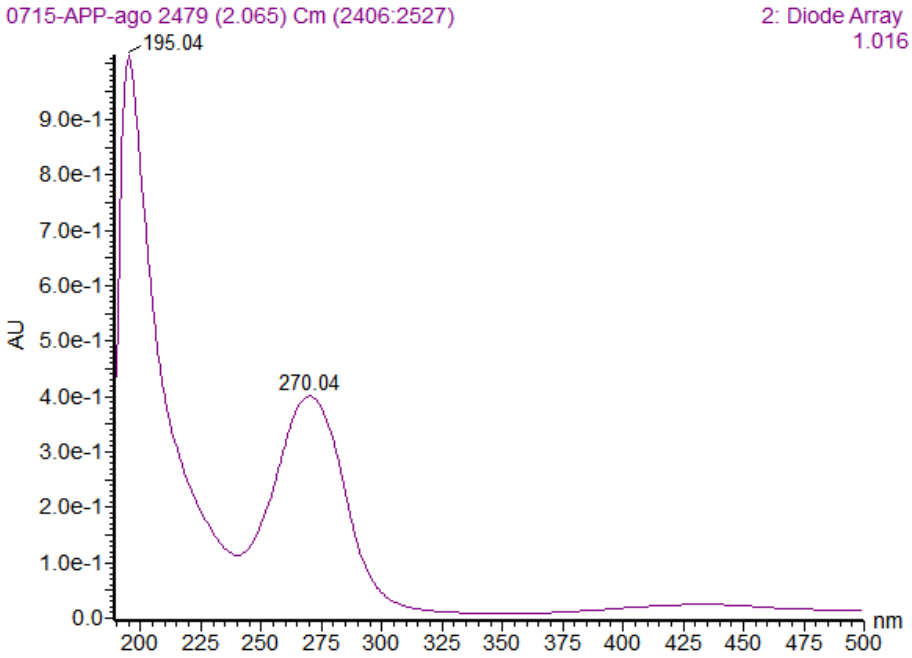

Fig S94. The UV characteristic absorption of **B1b**.

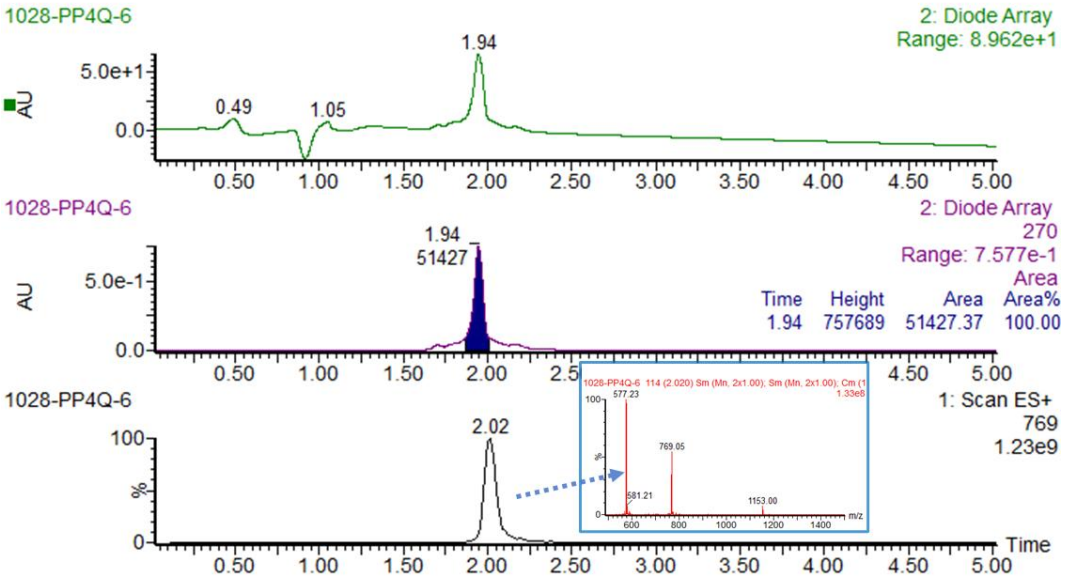

Fig S95. LC-MS for **B1a** (0.0625 mM) including TIC, UV curves (full-wavelength and extracted at 270 nm) and ESI-MS spectrum. Extract mass chromatograms from full scan data.

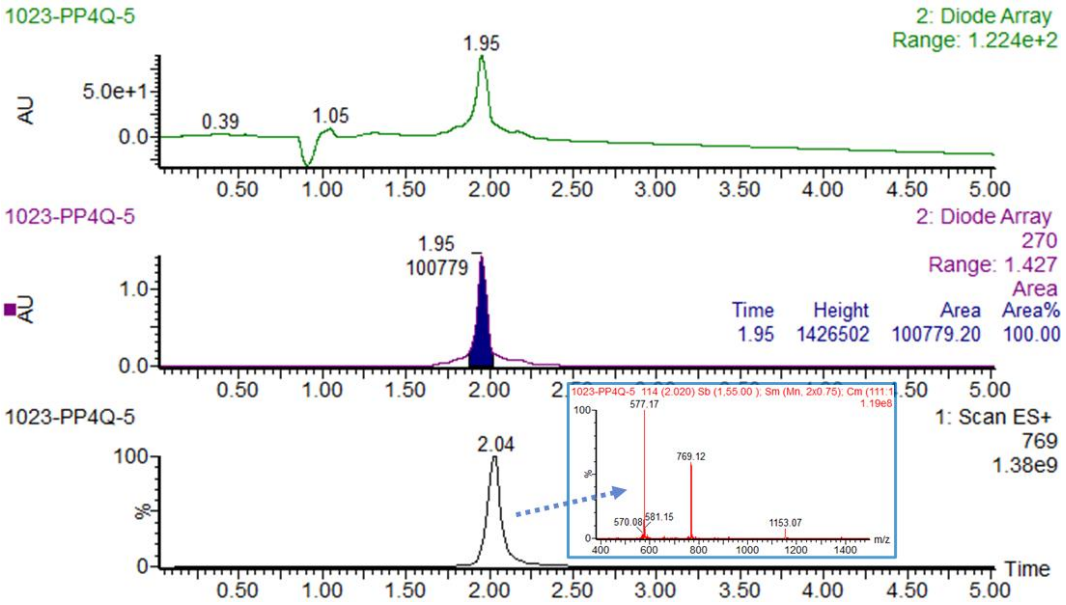

Fig S96. LC-MS for **B1a** (0.125 mM) including TIC, UV curves (full-wavelength and extracted at 270 nm) and ESI-MS spectrum. Extract mass chromatograms from full scan data.

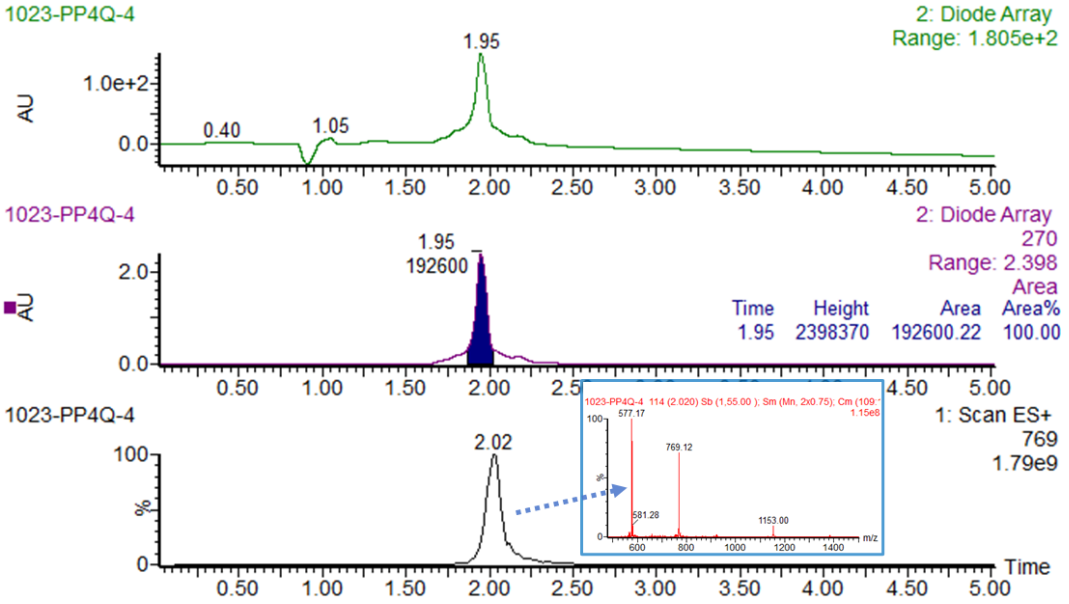

Fig S97 LC-MS for **B1a** (0.25 mM) including TIC, UV curves (full-wavelength and extracted at 270 nm) and ESI-MS spectrum. Extract mass chromatograms from full scan data.

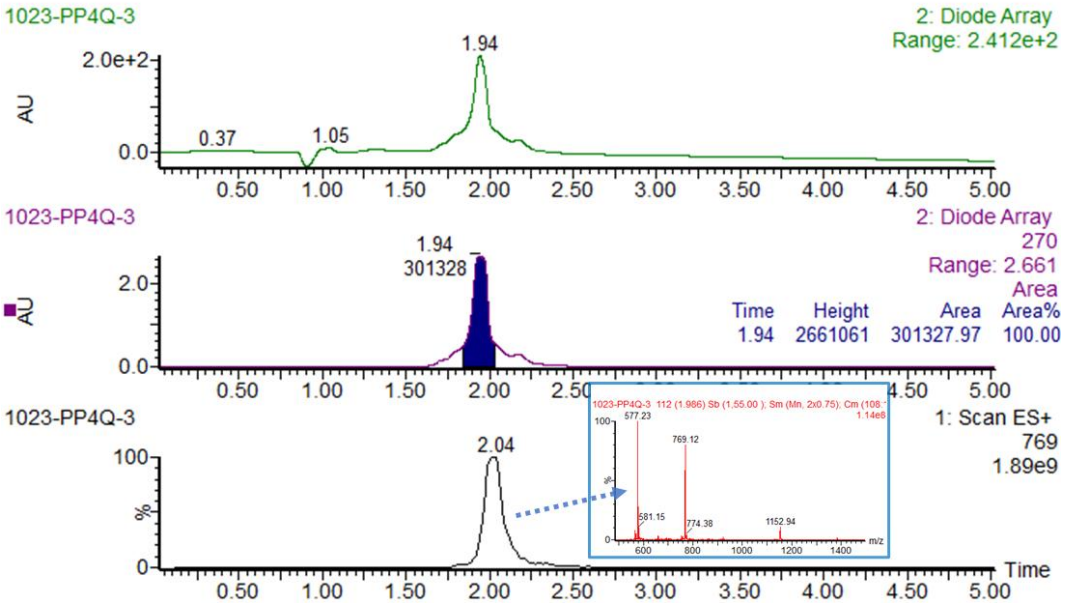

Fig S98 LC-MS for **B1a** (0.5 mM) including TIC, UV curves (full-wavelength and extracted at 270 nm) and ESI-MS spectrum. Extract mass chromatograms from full scan data.

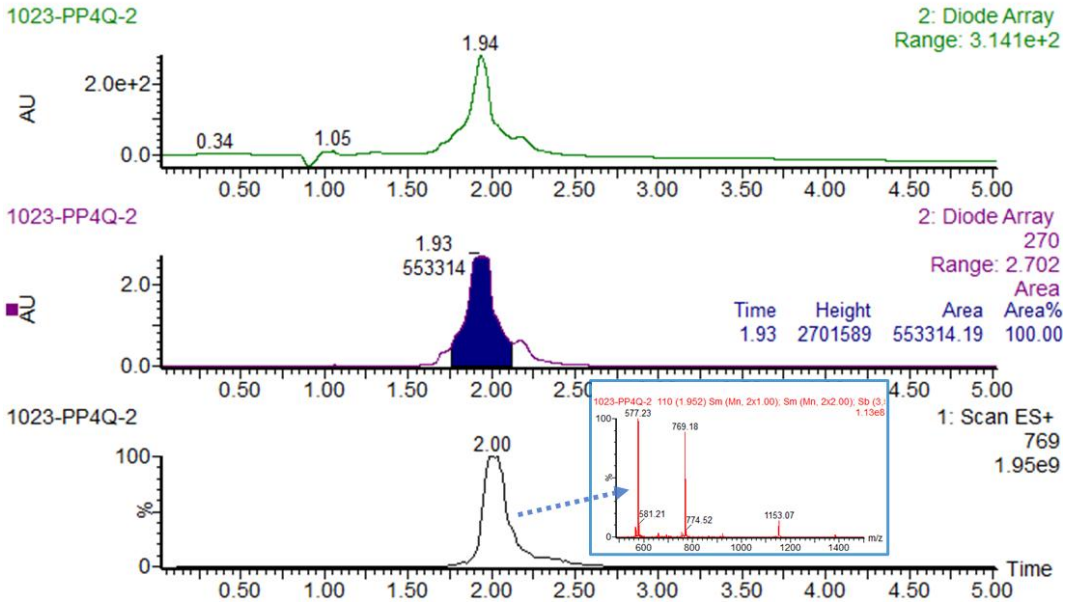

Fig S99 LC-MS for **B1a** (1 mM) including TIC, UV curves (full-wavelength and extracted at 270 nm) and ESI-MS spectrum. Extract mass chromatograms from full scan data.

（2）Calculation Strategies

To mitigate systematic errors arising from detector non-linearity at higher concentrations, a dual-strategy quantification approach was employed.

Strategy A: Linear Regression (for theoretical cyclodimerization product concentrations <= 0.25 mM)：

For reaction conditions where the theoretical maximum cyclodimerization product concentration falls within the linear range (e.g., 0.125, 0.25, and 0.5 mM peptide screenings), the LC-MS yield was calculated using the following **Equation 1**:

$$\text{Yield (\%)} = \frac{(A_{\text{sample}} - 5517)/750301}{C_{\text{theoretical}}} \times 100\%$$

Where A_{sample} is the measured peak area at 270 nm, and $C_{\text{theoretical}}$ is the theoretical maximum cyclodimerization product concentration (mM) based on the starting peptide.

Strategy B: Concentration-Matched Single-Point Calibration (for 1.0 mM peptide):

For high-concentration screenings (1.0 mM peptide, theoretical dimer 0.5 mM), a concentration-matched standard (0.5 mM purified **B1a**) was used as the reference to compensate for detector saturation, **Equation 2**:

$$\text{Yield (\%)} = \frac{A_{\text{sample}}}{A_{\text{std\_at\_0.5\_mM}}} \times 100\%$$

Where $A_{std\_at\_0.5\_mM}$ = 301328 (experimentally determined peak area of the 0.5 mM standard).

4.2 Screening of reaction conditions

Example procedure (Standard reaction conditions, Entry 1):

The dried peptide **L1** (1.0 equiv.) was dissolved in appropriate amount of PBS (20 mM, pH = 9.0) to reach a concentration of 0.56 mM. To this solution, 3,6-DCT (1.0 equiv.) dissolved in acetonitrile (1/9 of the volume of buffer) was added. The final concentrations in the reaction were 0.5 mM peptide, 0.5 mM 3,6-DCT and 10% acetonitrile, followed by thorough mixing. The reaction mixture was shaken at 25 °C and 800 rpm for 1 h on a thermostatic shaker.

Specifically, for Entry 15, the dried peptide **L1** (1.0 equiv.) was dissolved in an appropriate amount of PBS (20 mM, pH = 9.0) to reach a final concentration of 0.5 mM. Separately, 3,6-DCT (1.0 equiv.) was dissolved in an equal volume of $CHCl_3$ and then combined with the peptide solution, followed by thorough mixing. The reaction mixture was shaken at 25 °C and 800 rpm for 1 h on a thermostatic shaker. For Entry 16, the reaction mixture under the standard conditions was supplemented with TCEP (10 equiv.).

After completion, 50 μL of the reaction mixture was collected, and 10 μL was injected into the UPLC-MS for analysis. The peak area of the cyclodimerization products at 270 nm was recorded. Determine the LC-MS yield using **Equation 1** or **2**. Detailed data are shown in **Table S8**.

Tab S8. The LC-MS data for reaction conditions collected using Method A

Entry	Deviation from standard conditions	Peak area of B1a and B1b	Yield (%)[a]
1	None	116206	59.01[b]
2	PBS (pH 5)	28379	12.19[b]
3	PBS (pH 6)	64604	31.50[b]
4	PBS (pH 7)	94525	47.45[b]
5	PBS (pH 7.4)	91930	46.07[b]
6	PBS (pH 8)	98365	49.50[b]
7	0.125 mM peptide	27319	46.50[b]

8	0.25 mM peptide	46418	43.61[b]
9	1 mM peptide	115877	38.46[c]
10	3,6-DCT (1.2 eq.)	103633	52.31[b]
11	3,6-DCT (2 eq.)	0	0
12	Mix 30 minutes	109181	55.26[b]
13	Mix 2 hours	110873	56.17[b]
14	Mix 4 hours	113608	57.62[b]
15	3,6-DCT ($CHCl_3$)	118569	60.27[b]
16	TCEP (10 eq.)	18994	7.18[b]

[a]LC-MS yields represent the conversion yields determined by HPLC analysis. [b]Determined using **Equation 1**. [c]Determined using **Equation 2.**

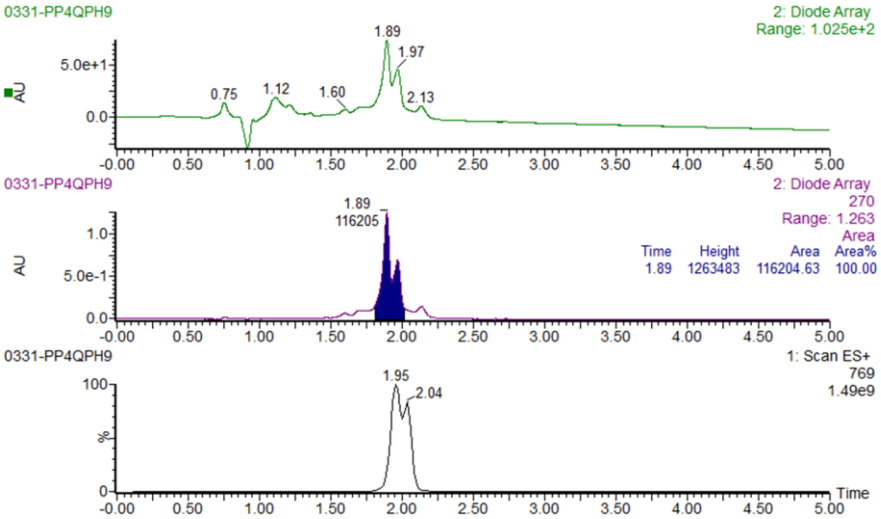

Fig S100. LC-MS of the reaction solution of entry 1 (standard conditions) including TIC and UV curves (full-wavelength and extracted at 270 nm).

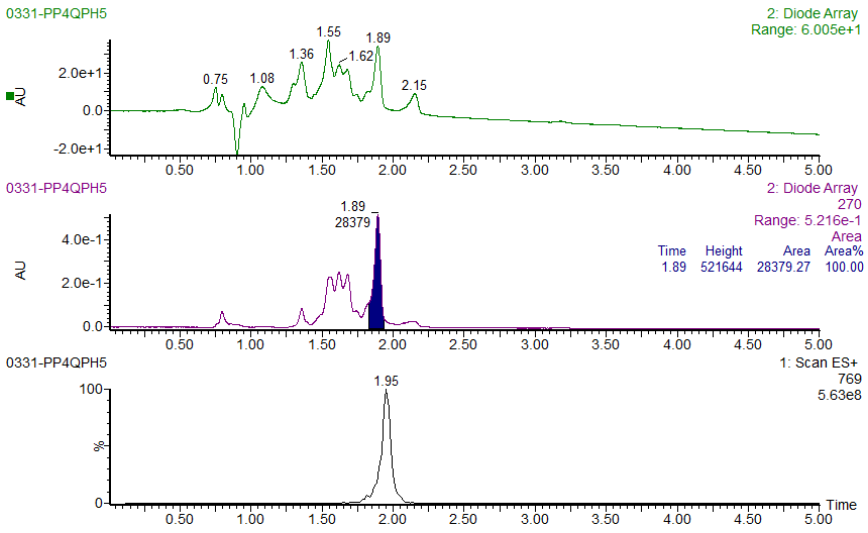

Fig S101. LC-MS of the reaction solution of entry 2 including TIC and UV curves (full-wavelength and extracted at 270 nm).

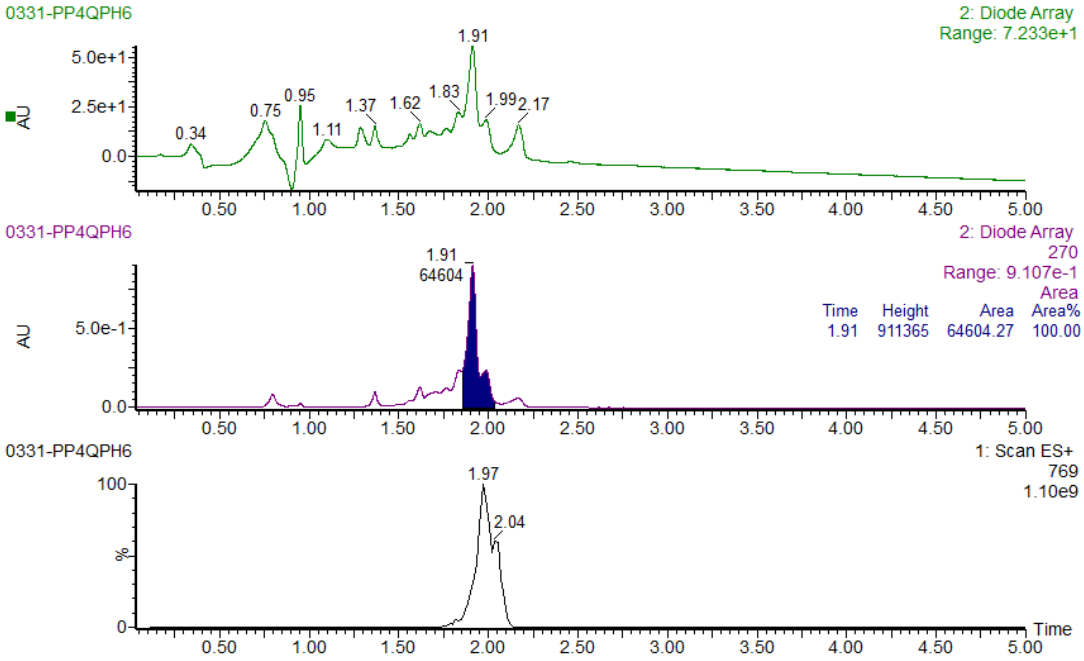

Fig S102. LC-MS of the reaction solution of entry 3 including TIC and UV curves (full-wavelength and extracted at 270 nm).

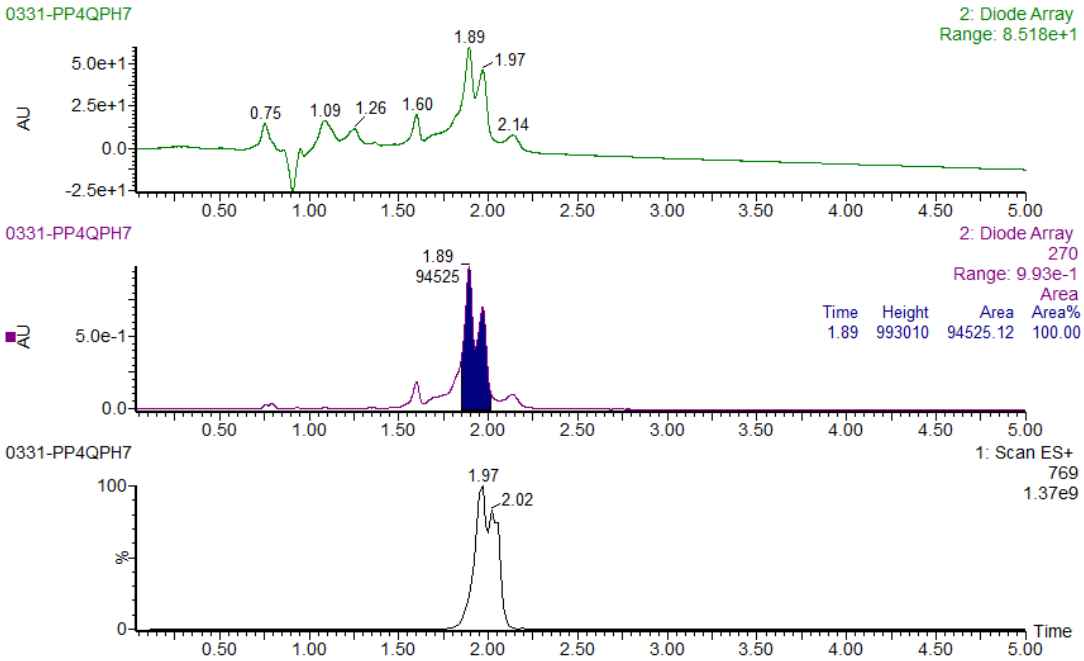

Fig S103. LC-MS of the reaction solution of entry 4 including TIC and UV curves (full-wavelength and extracted at 270 nm).

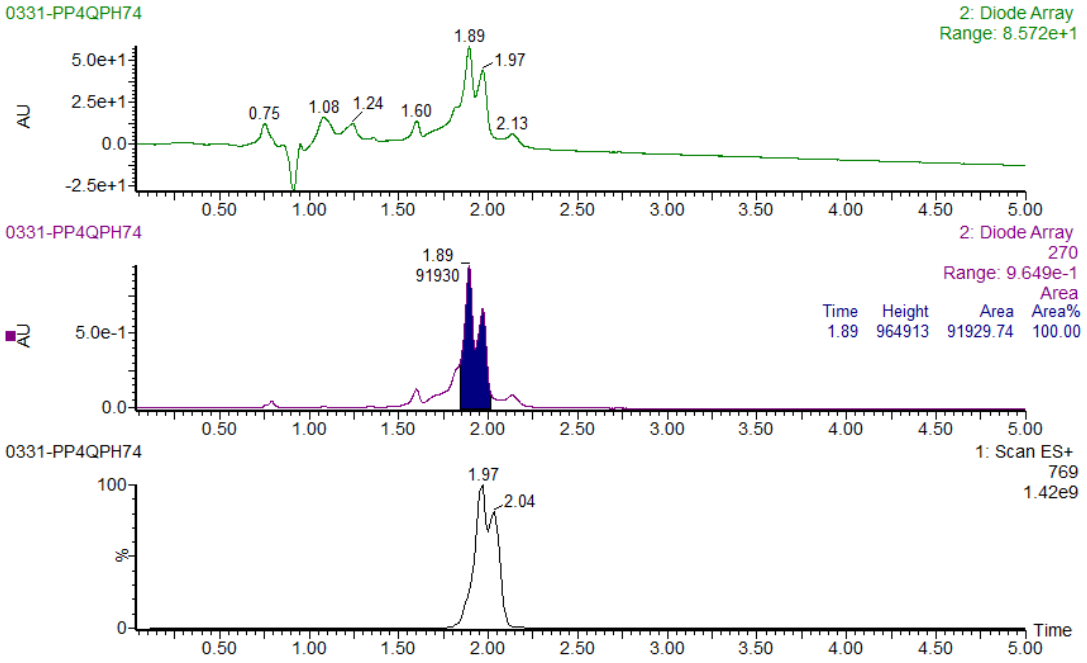

Fig S104. LC-MS of the reaction solution of entry 5 including TIC and UV curves (full-wavelength and extracted at 270 nm).

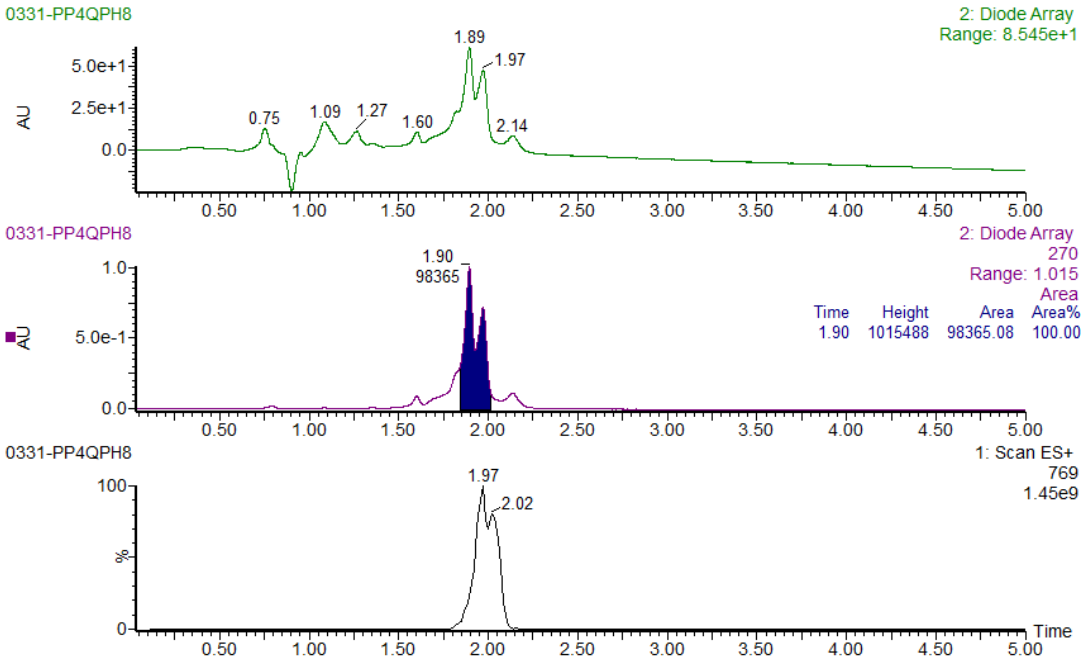

Fig S105. LC-MS of the reaction solution of entry 6 including TIC and UV curves (full-wavelength and extracted at 270 nm).

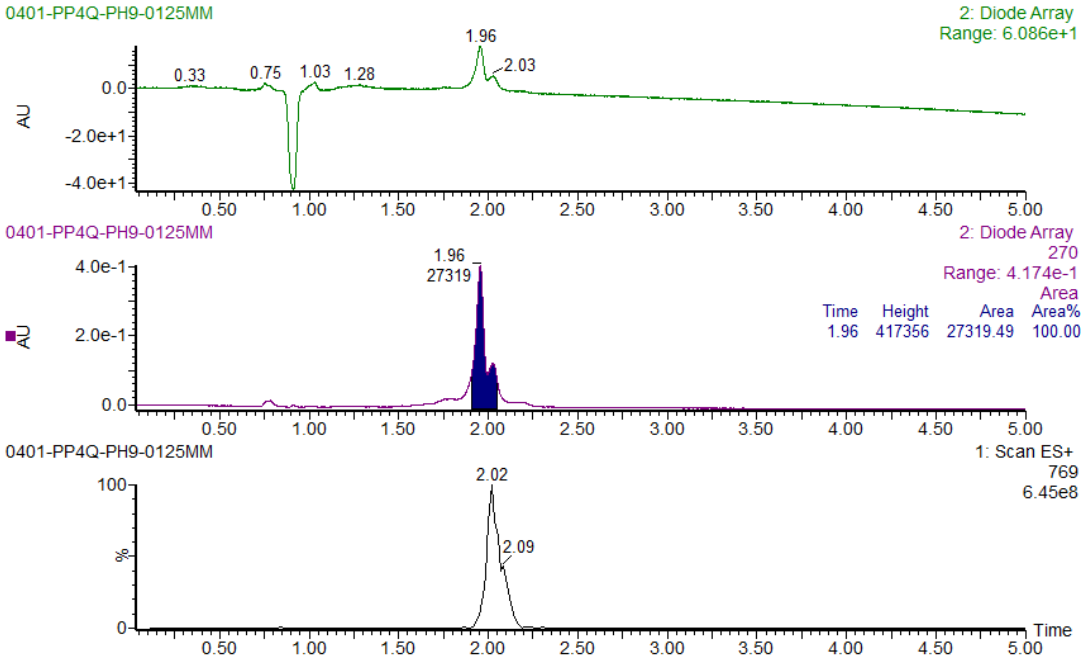

Fig S106. LC-MS of the reaction solution of entry 7 including TIC and UV curves (full-wavelength and extracted at 270 nm).

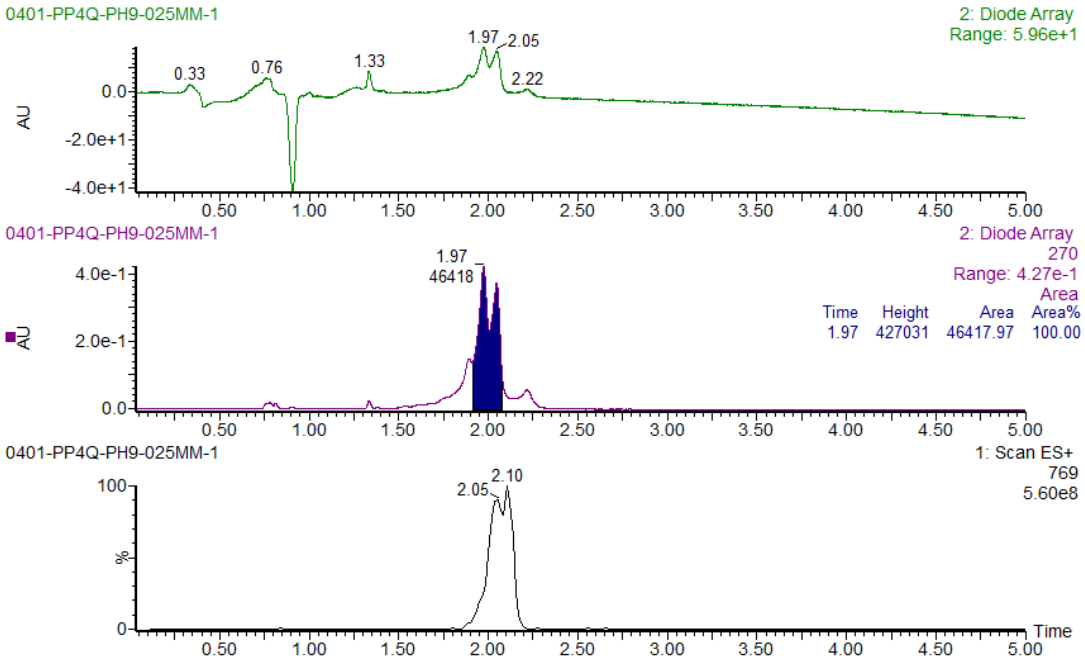

Fig S107. LC-MS of the reaction solution of entry 8 including TIC and UV curves (full-wavelength and extracted at 270 nm).

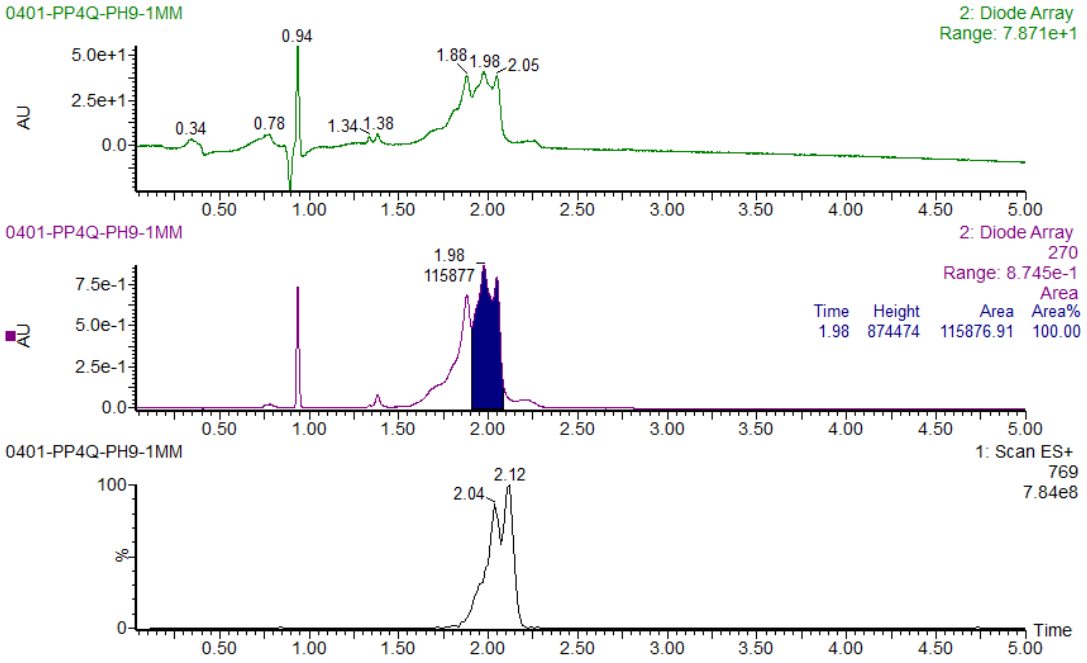

Fig S108. LC-MS of the reaction solution of entry 9 including TIC and UV curves (full-wavelength and extracted at 270 nm).

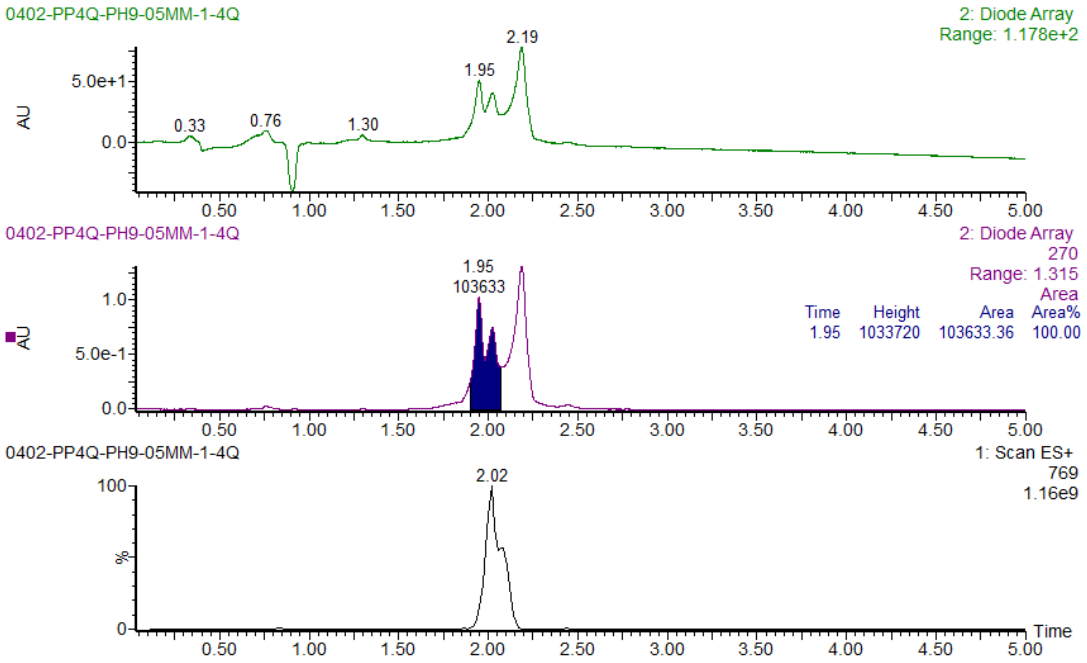

Fig S109. LC-MS of the reaction solution of entry 10 including TIC and UV curves (full-wavelength and extracted at 270 nm).

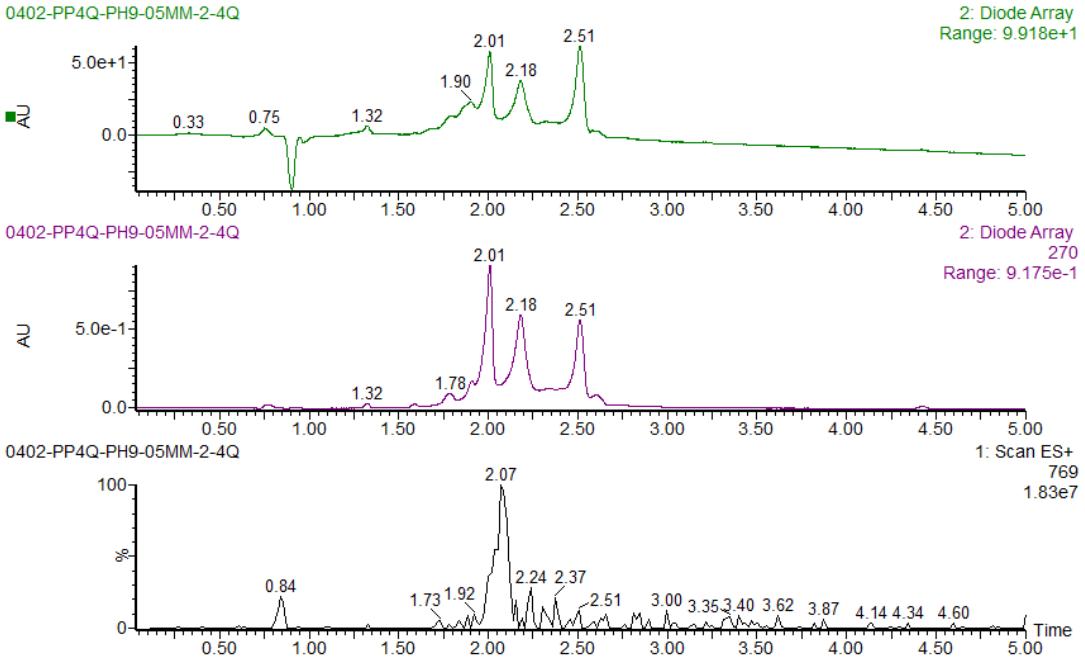

Fig S110. LC-MS of the reaction solution of entry 11 including TIC and UV curves (full-wavelength and extracted at 270 nm).

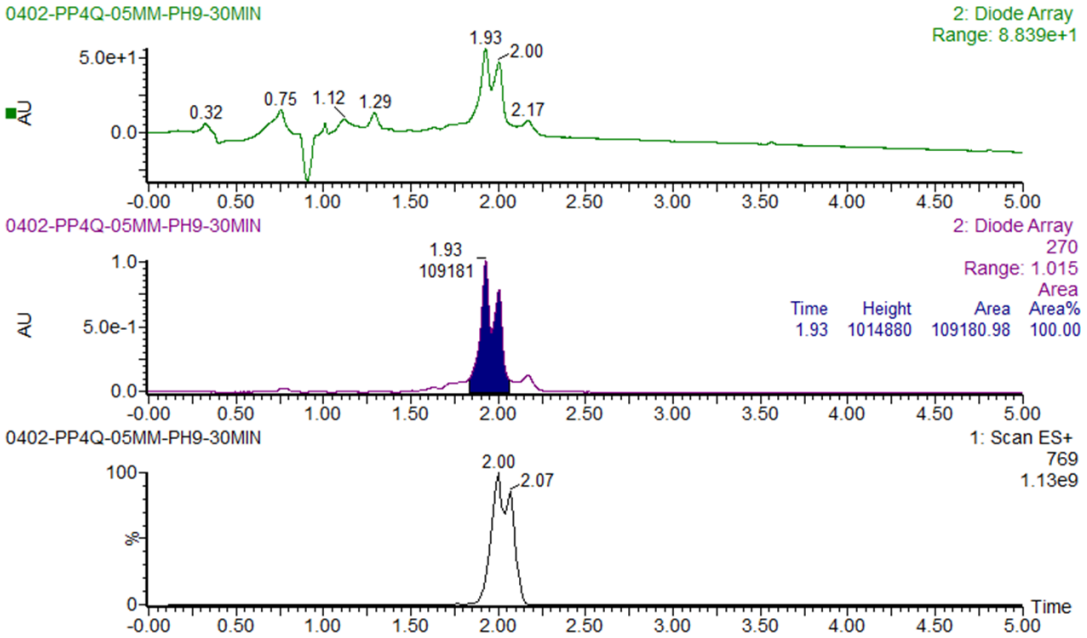

Fig S111. LC-MS of the reaction solution of entry 12 including TIC and UV curves (full-wavelength and extracted at 270 nm).

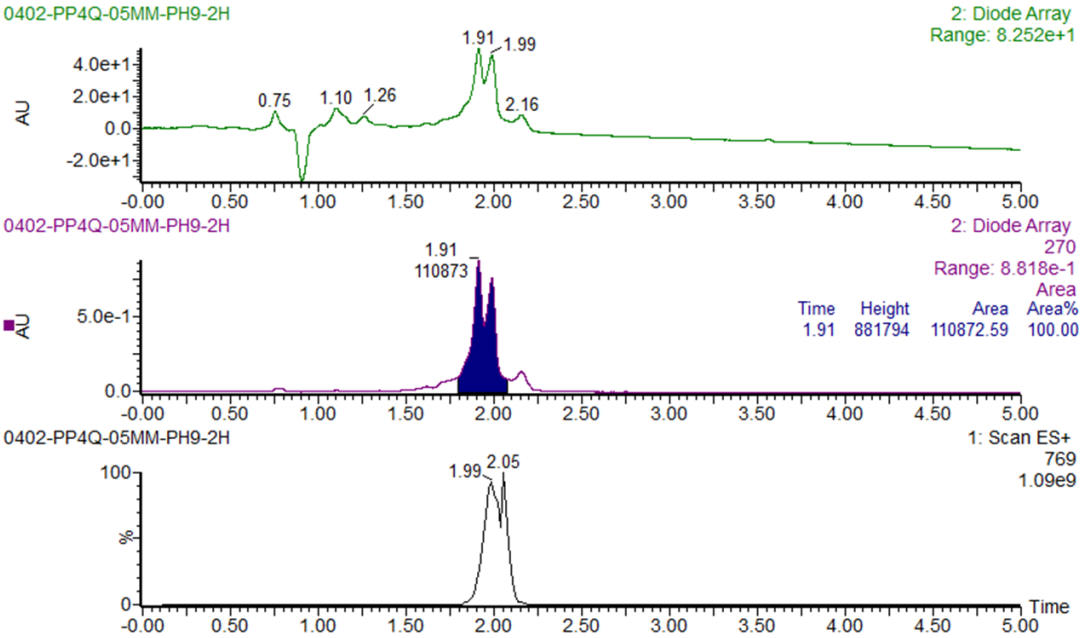

Fig S112. LC-MS of the reaction solution of entry 13 including TIC and UV curves (full-wavelength and extracted at 270 nm).

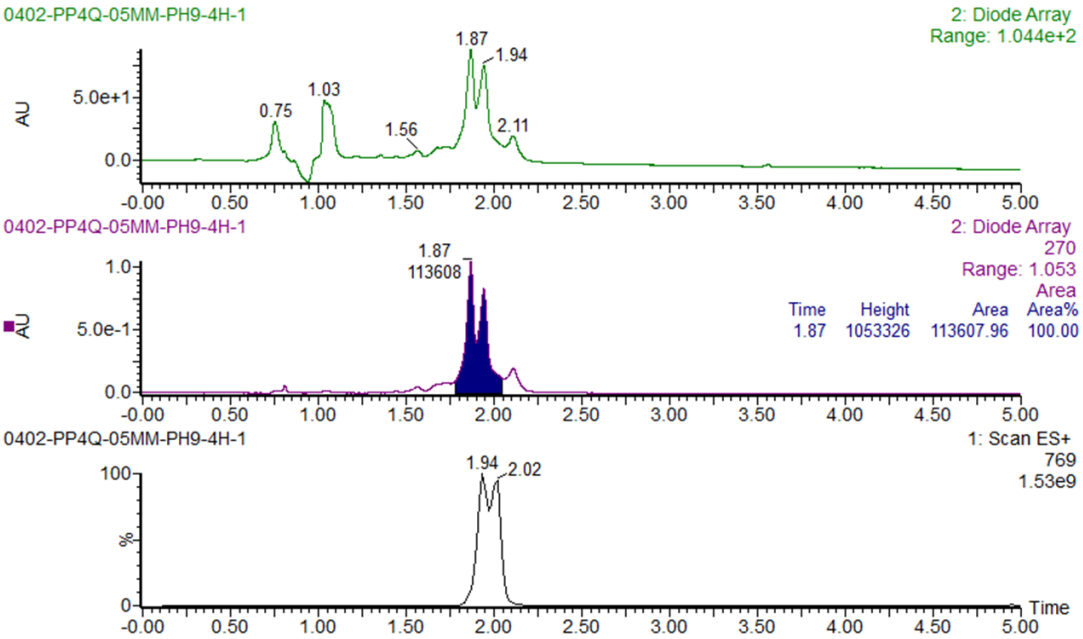

Fig S113. LC-MS of the reaction solution of entry 14 including TIC and UV curves (full-wavelength and extracted at 270 nm).

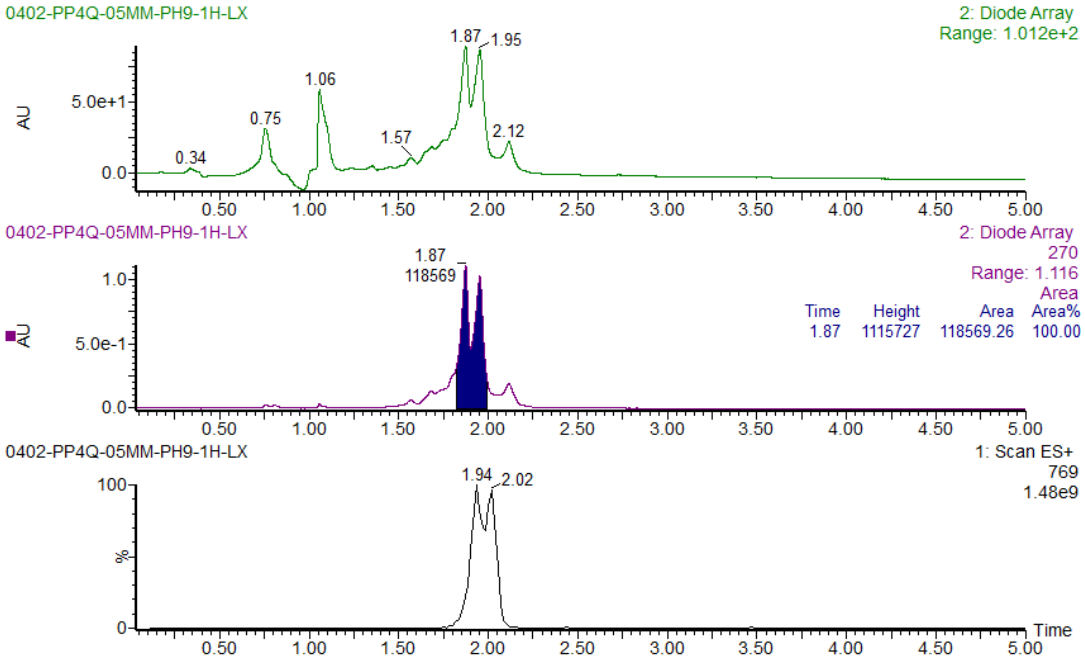

Fig S114. LC-MS of the reaction solution of entry 15 including TIC and UV curves (full-wavelength and extracted at 270 nm).

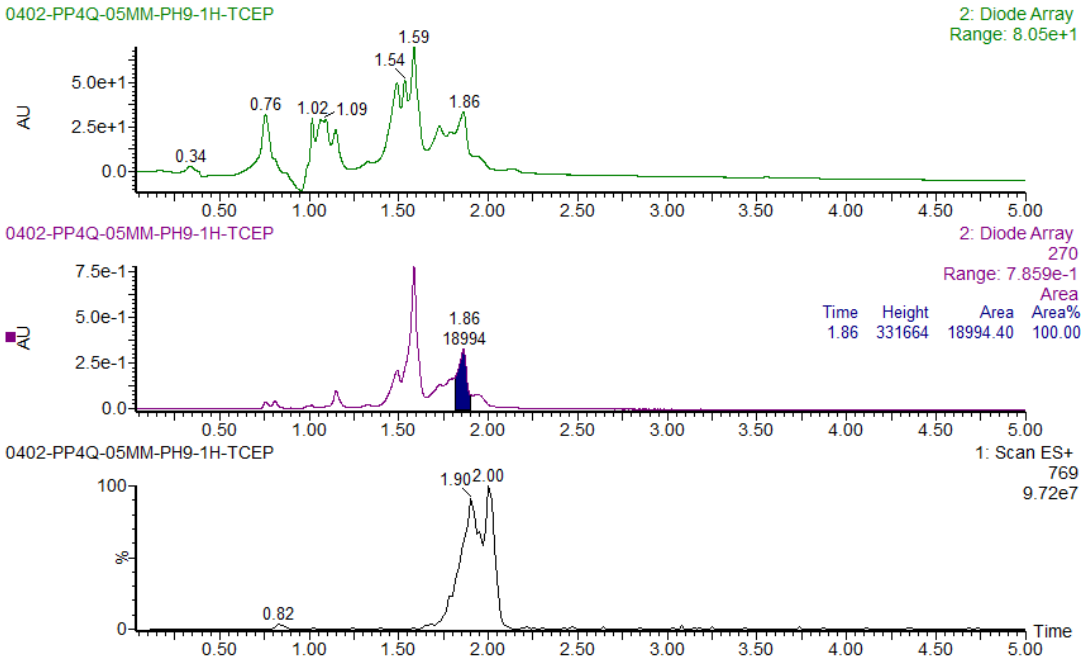

Fig S115. LC-MS of the reaction solution of entry 16 including TIC and UV curves (full-wavelength and extracted at 270 nm).

5. Reaction mechanism investigation and structure confirmation

5.1 Control experiments

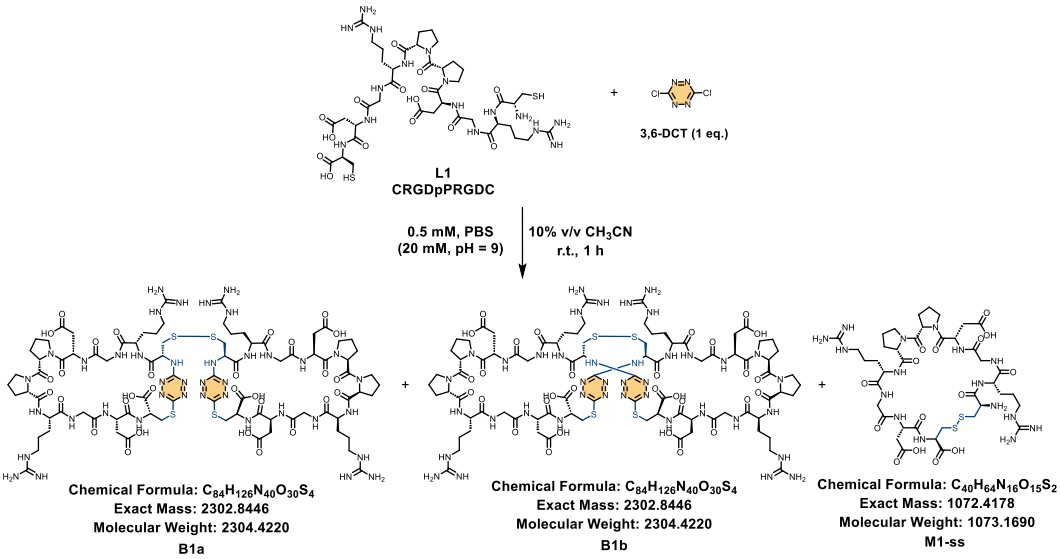

The dried peptide **L1** (1.0 equiv.) was dissolved in appropriate amount of PBS (20 mM, pH = 9.0) to reach a concentration of 0.56 mM. To this solution, 3,6-DCT (1.0 equiv.) dissolved in acetonitrile (1/9 of the volume of buffer) was added. The final concentrations in the reaction were 0.5 mM peptide, 0.5 mM 3,6-DCT and 10% acetonitrile, followed by thorough mixing. The reaction mixture was shaken at 25 °C and 800 rpm for 1 h on a thermostatic shaker.

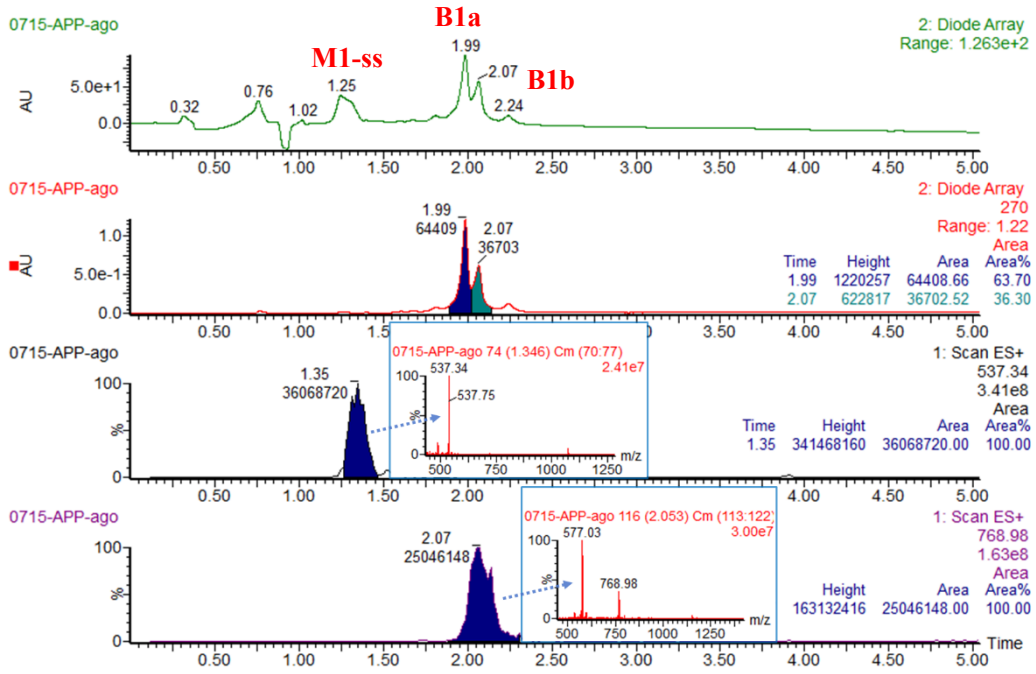

Fig S116. UPLC-MS chromatogram of **B1a** and 3,6-DCT reaction mixture including TIC, UV curves (full-wavelength and extracted at 270 nm) and ESI-MS spectrum. Extract mass chromatograms from full scan data.

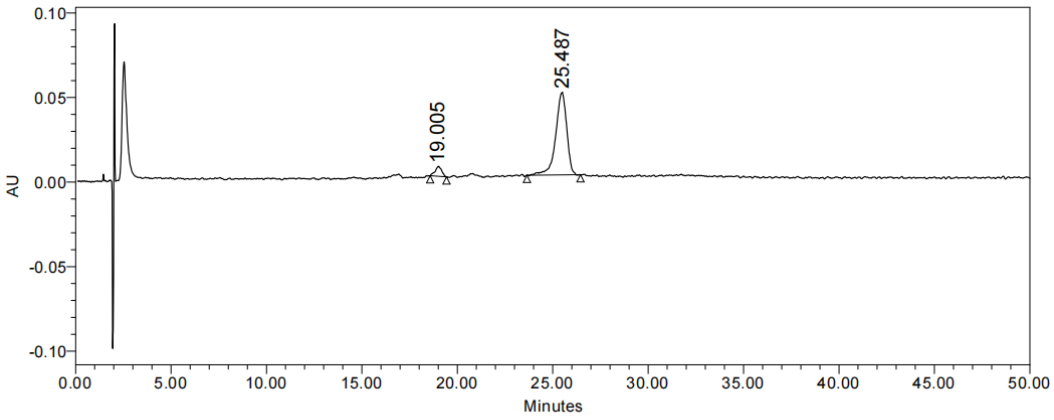

Channel: 2998 Ch1 220nm@4.8nm; Processed Channel: 2998 Ch1 220nm@4.8nm; Result Id: 39149;
Processing Method: PP4QA

Processed Channel Descr.: 2998 Ch1 220nm@4.8nm

	Processed Channel Descr.	RT	Area	% Area	Height
1	2998 Ch1 220nm@4.8nm	19.005	140872	6.69	5850
2	2998 Ch1 220nm@4.8nm	25.487	1964284	93.31	48689

Fig S117. HPLC-UV chromatogram at 220 nm of **B1a**. Analytical HPLC using Method E, RT = 25.487 min, the HPLC purity is 93%.

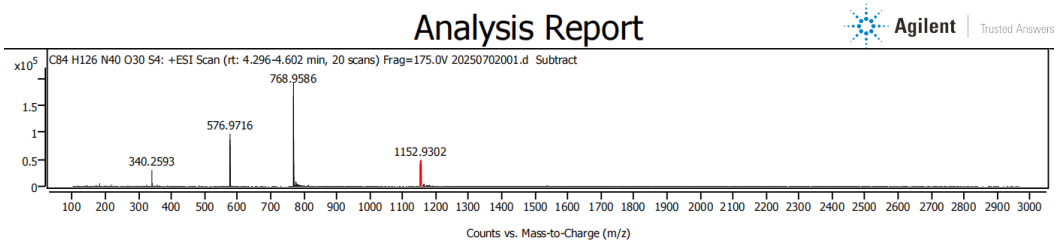

Spectrum Identification Table

Best ID Source	Name	Formula	Species	m/z	Diff (ppm)	CAS	Score	Score (Lib)	Score (DB)	Score (MFG)	Lib/DB
Yes MFG		C84 H126 N40 O30 S4	(M+2H)+2	1152.4291	-0.52		99.89			99.89	

Fig S118. Q-TOF-HRMS spectrum of **B1a**. HRMS (ES+) m/z: $[M+2H]^{2+}$ calcd for $C_{84}H_{126}N_{40}O_{30}S_4$ 1152.4223, found 1152.4291.

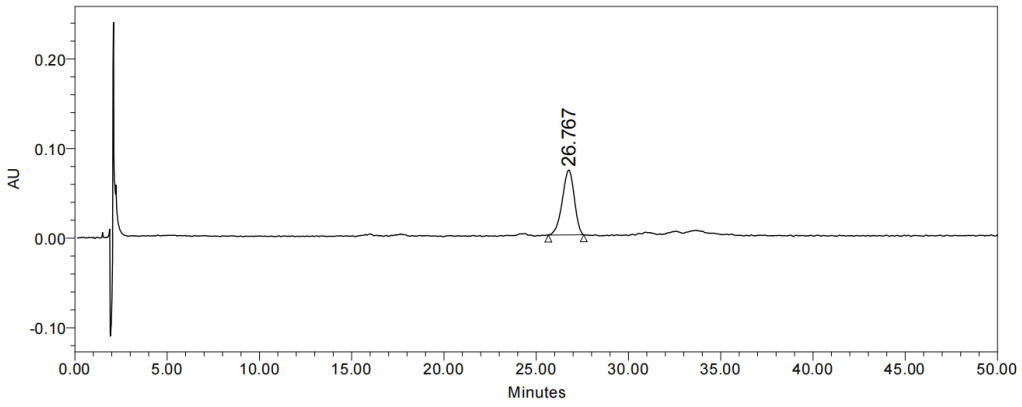

Channel: 2998 Ch1 220nm@4.8nm; Processed Channel: 2998 Ch1 220nm@4.8nm; Result Id: 39151;
Processing Method: PP4QB

Processed Channel Descr.: 2998 Ch1 220nm@4.8nm

	Processed Channel Descr.	RT	Area	% Area	Height
1	2998 Ch1 220nm@4.8nm	26.767	3253882	100.00	72318

Fig S119. HPLC-UV chromatogram at 220 nm of **B1b**. Analytical HPLC using Method E, RT = 26.767 min, the HPLC purity is 99%.

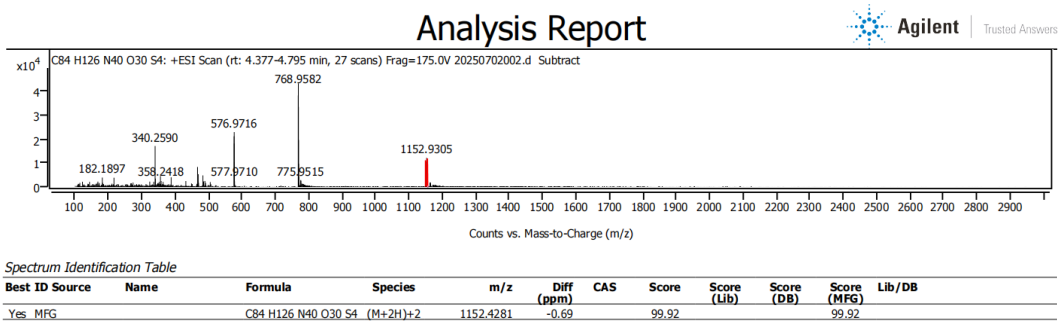

Fig S120. Q-TOF-HRMS spectrum of **B1b**. HRMS (ES+) m/z: $[M+2H]^{2+}$ calcd for $C_{84}H_{126}N_{40}O_{30}S_4$ 1152.4223, found 1152.4281.

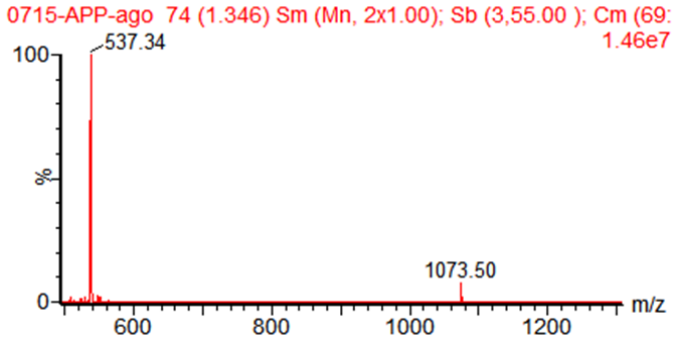

Fig S121. LRMS spectrum of **M1-ss**. LRMS (ESI+) m/z: 1073.50 $[M + H]^+$

Control experiments i:

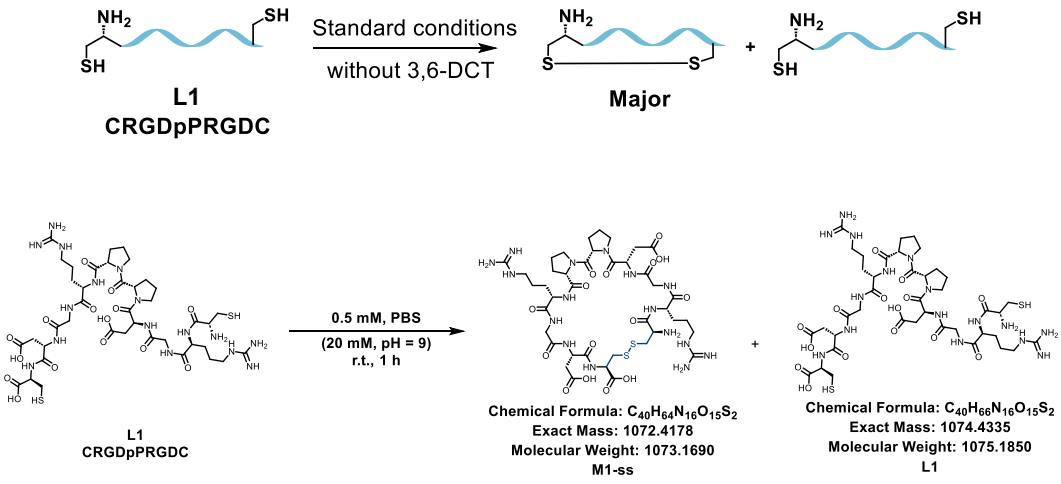

The dried peptide **L1** (1.0 equiv.) was dissolved in appropriate amount of PBS (20 mM, pH = 9.0) to reach a concentration of 0.5 mM. The reaction mixture was shaken at 25 °C and 800 rpm for 1 h on a thermostatic shaker.

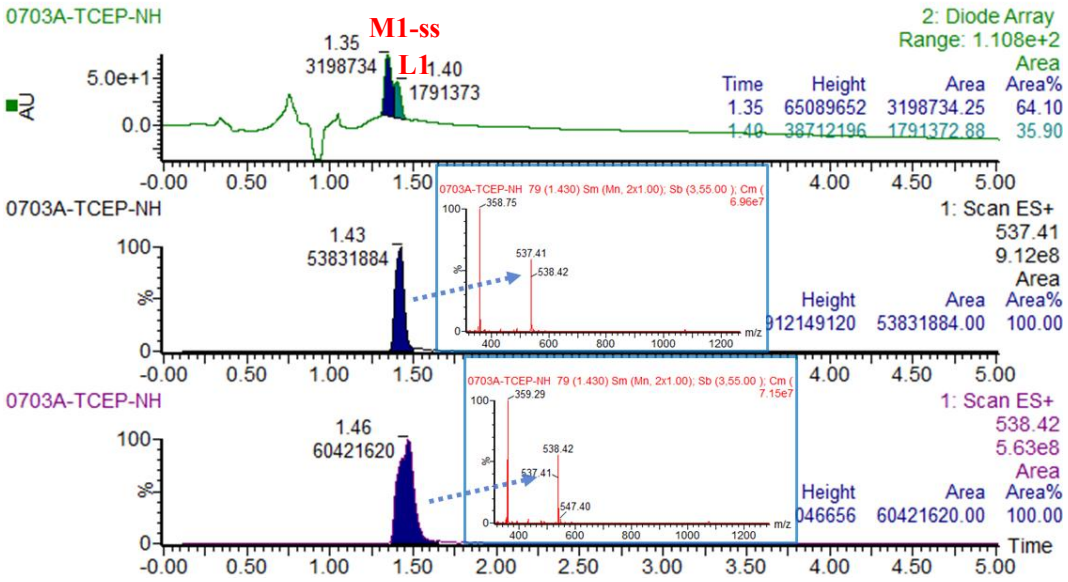

Fig S122. UPLC-MS chromatogram of **L1** without 3,6-DCT reaction mixture including TIC, UV curve (full-wavelength) and ESI-MS spectrum. Extract mass chromatograms from full scan data.

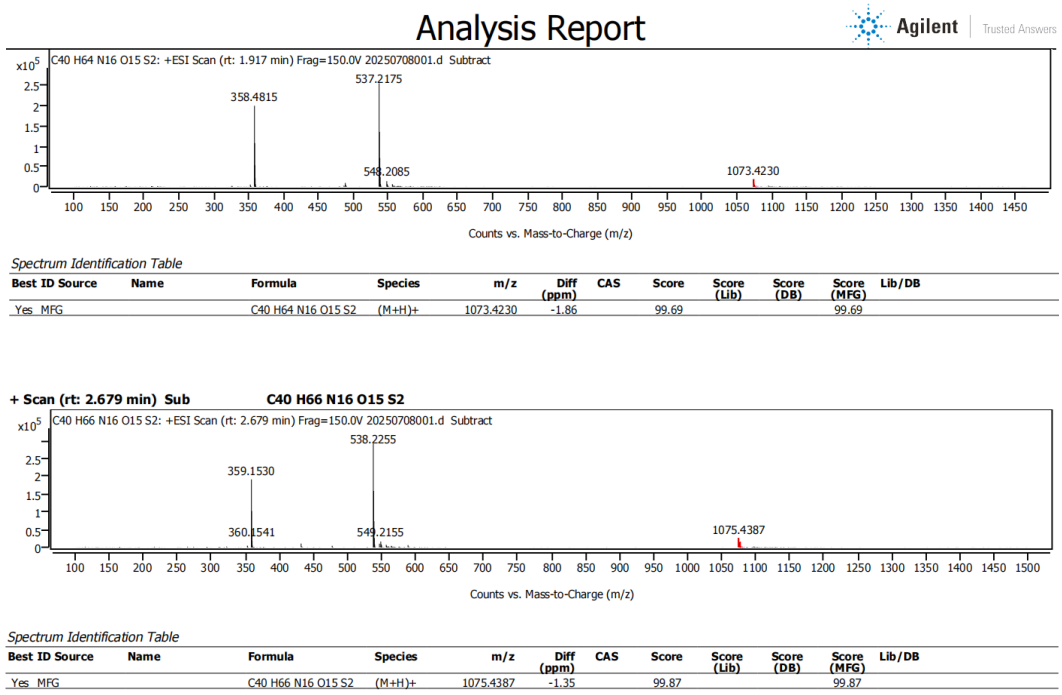

Fig S123. Q-TOF-HRMS spectrum of **L1** without 3,6-DCT reaction mixture. HRMS (ES+) m/z: $[M+H]^+$ calcd for $C_{40}H_{64}N_{16}O_{15}S_2$ 1073.4178, found 1073.4230. HRMS (ES+) m/z: $[M+H]^+$ calcd for $C_{40}H_{66}N_{16}O_{15}S_2$ 1075.4335, found 1075.4378.

Control experiments ii:

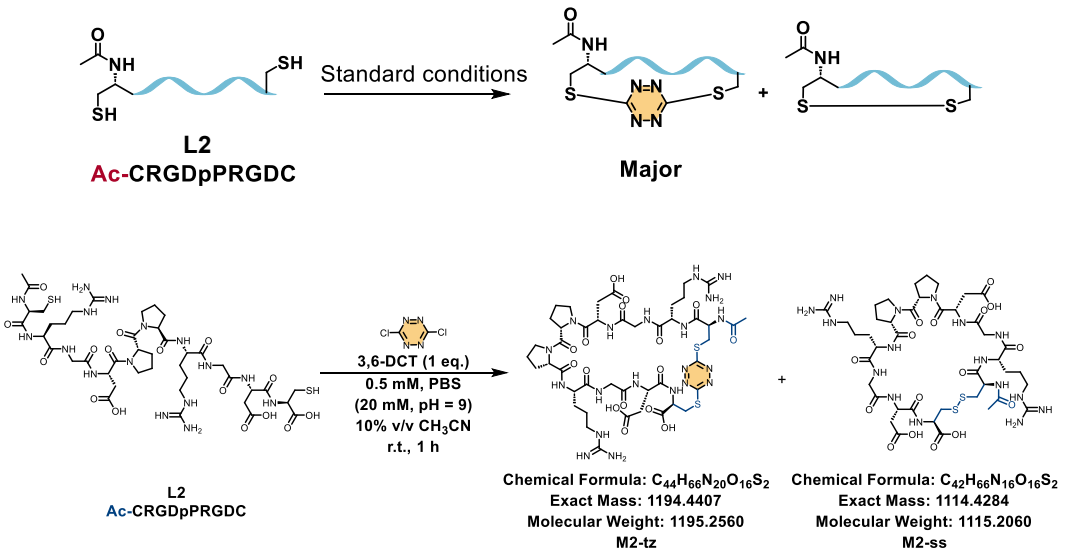

The dried peptide **L2** (1.0 equiv.) was dissolved in appropriate amount of PBS (20 mM, pH = 9.0) to reach a concentration of 0.56 mM. To this solution, 3,6-DCT (1.0 equiv.) dissolved in acetonitrile (1/9 of the volume of buffer) was added. The final concentrations in the reaction were 0.5 mM peptide, 0.5 mM 3,6-DCT and 10% acetonitrile, followed by thorough mixing. The reaction mixture was shaken at 25 °C and 800 rpm for 1 h on a thermostatic shaker.

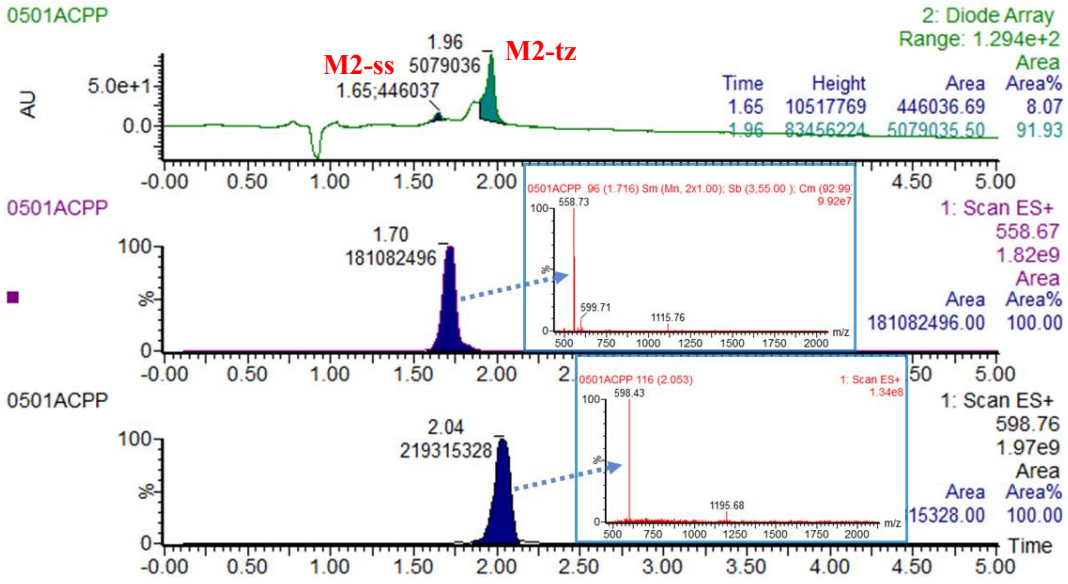

Fig S124. UPLC-MS chromatogram of **L2** and 3,6-DCT reaction mixture including TIC, UV curve (full-wavelength) and ESI-MS spectrum. Extract mass chromatograms from full scan data.

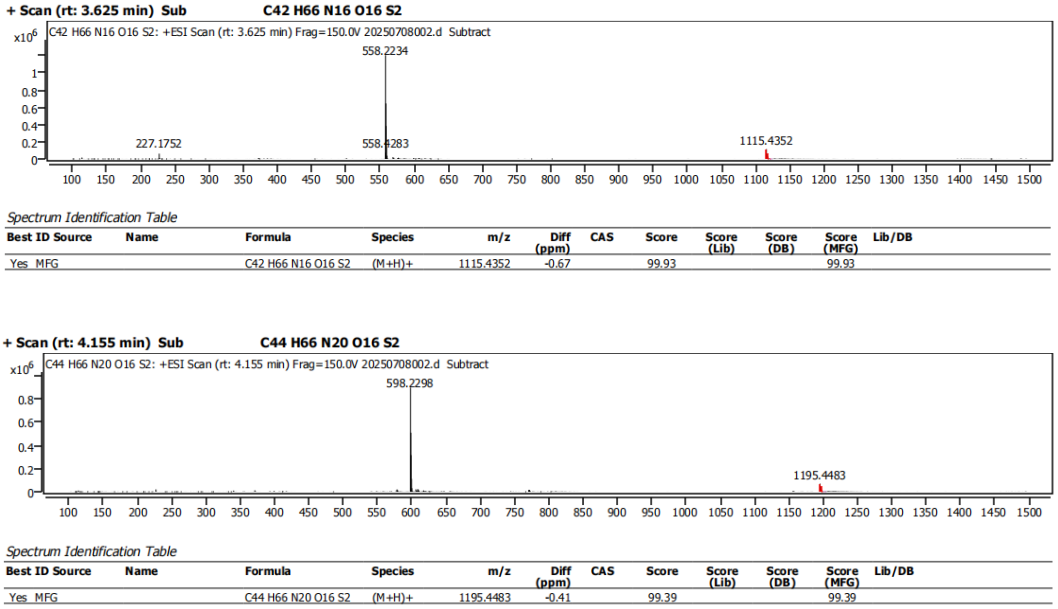

Fig S125. Q-TOF-HRMS spectrum of **L2** and 3,6-DCT reaction mixture. HRMS (ES+) m/z: $[M+H]^+$ calcd for $C_{42}H_{66}N_{16}O_{16}S_2$ 1115.4284, found 1115.4352. HRMS (ES+) m/z: $[M+H]^+$ calcd for $C_{44}H_{66}N_{20}O_{16}S_2$1195.4407, found 1195.4483.

Control experiments iii and iv:

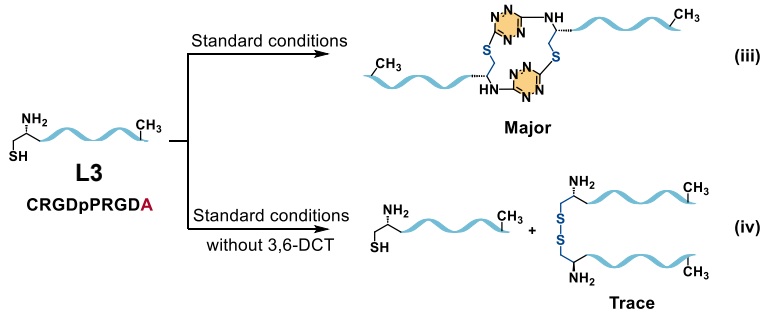

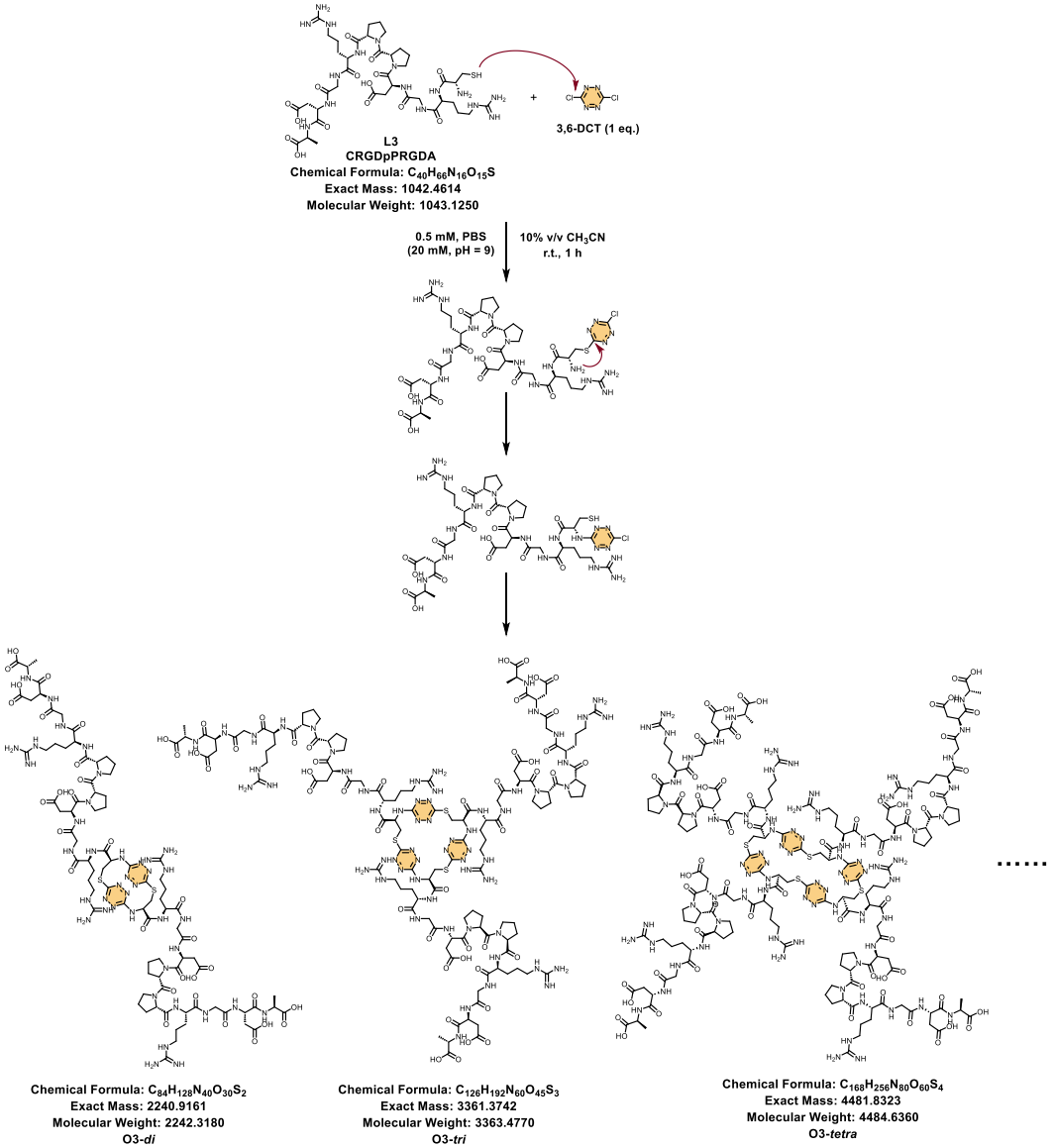

The dried peptide **L3** (1.0 equiv.) was dissolved in appropriate amount of PBS (20 mM, pH = 9.0) to reach a concentration of 0.56 mM. To this solution, 3,6-DCT (1.0 equiv.) dissolved in acetonitrile (1/9 of the volume of buffer) was added. The final concentrations in the reaction were 0.5 mM peptide, 0.5 mM 3,6-DCT and 10% acetonitrile, followed by thorough mixing. The reaction mixture was shaken at 25 °C and 800 rpm for 1 h on a thermostatic shaker.

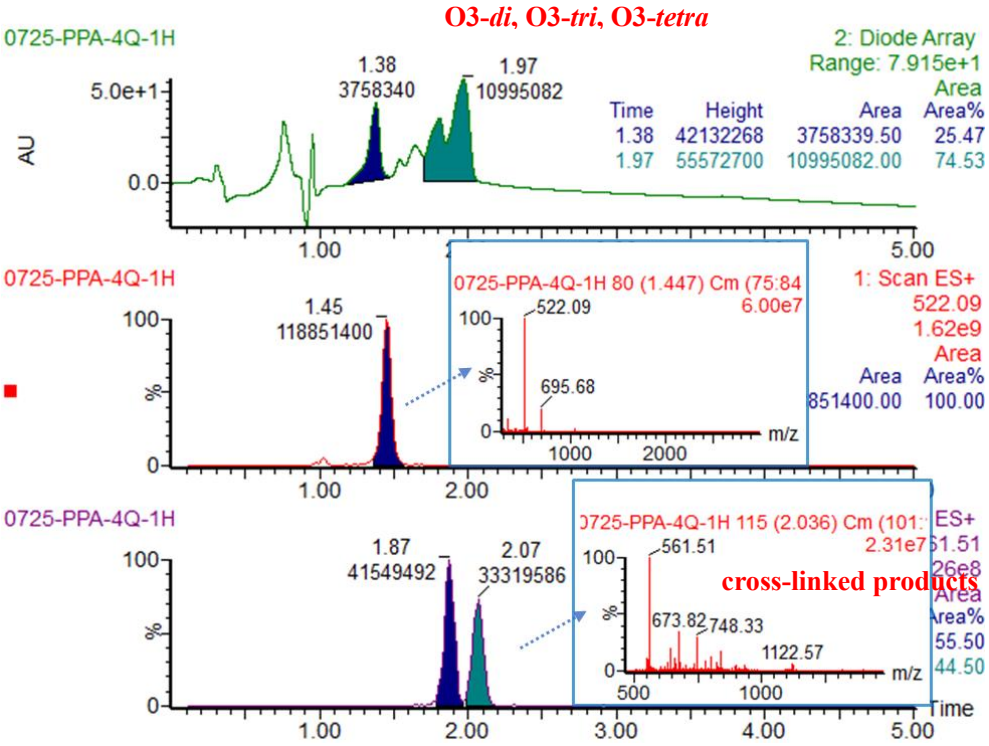

Fig S126. UPLC-MS chromatogram of **L3** and 3,6-DCT reaction mixture including TIC, UV curve (full-wavelength) and ESI-MS spectrum. Extract mass chromatograms from full scan data.

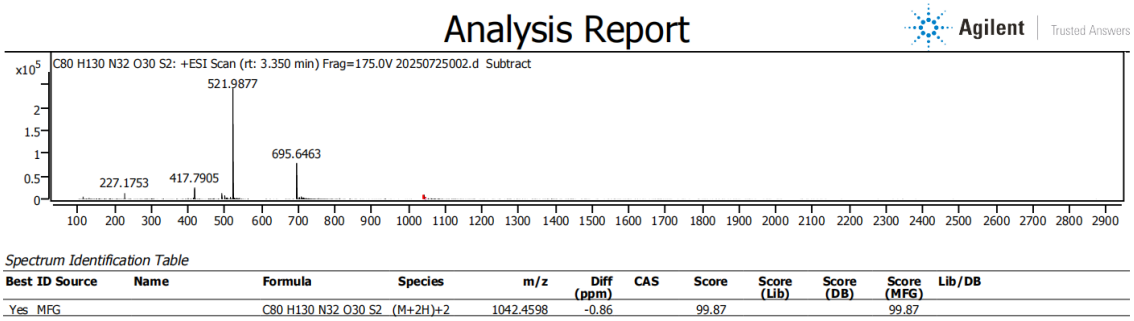

Fig S127. Q-TOF-HRMS spectrum of **L3** and 3,6-DCT reaction mixture. HRMS (ES+) m/z: $[M+2H]^{2+}$ calcd for $C_{80}H_{130}N_{32}O_{30}S_2$ 1042.4536, found 1042.4598.

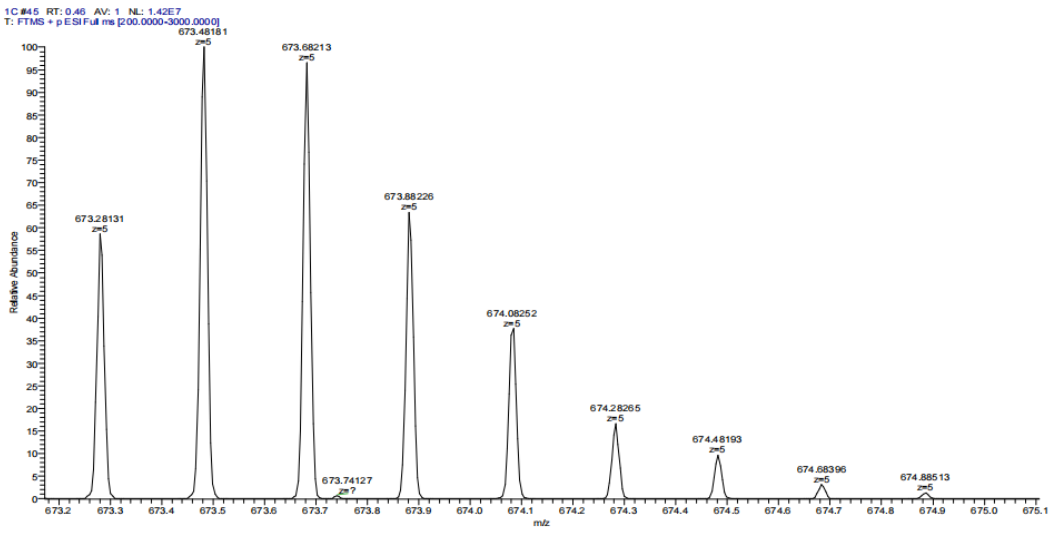

m/z	Theo. Mass	Delta (ppm)	RDB equiv.	Composition	
673.28131	673.28212	-1.2	58.5	C126 H197 O45 N60 S3	$[M+5H]^{5+}$

Fig S128. Q-TOF-HRMS spectrum of **O3-*tri***. HRMS (ES+) m/z: $[M+5H]^{5+}$ calcd for $C_{126}H_{192}N_{60}O_{46}S_3$ 673.27, found 673.28.

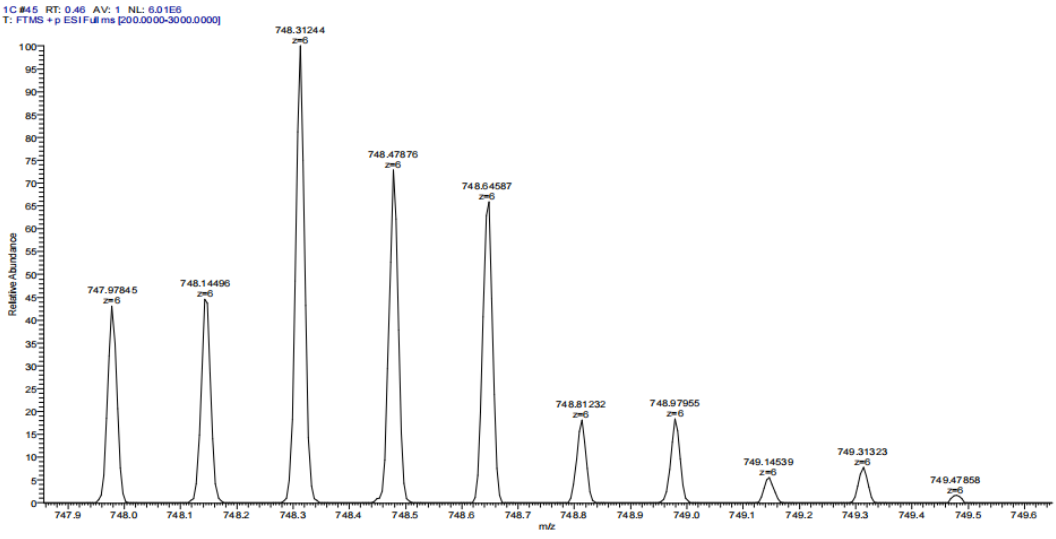

m/z	Theo. Mass	Delta (ppm)	RDB equiv.	Composition	
747.97845	747.97932	-1.17	78	C168 H262 O60 N80 S4	$[M+6H]^{6+}$

Fig S129. Q-TOF-HRMS spectrum of **O3-*tetra***. HRMS (ES+) m/z: $[M+6H]^{6+}$ calcd for $C_{168}H_{256}N_{80}O_{60}S_4$ 747.98, found 747.98.

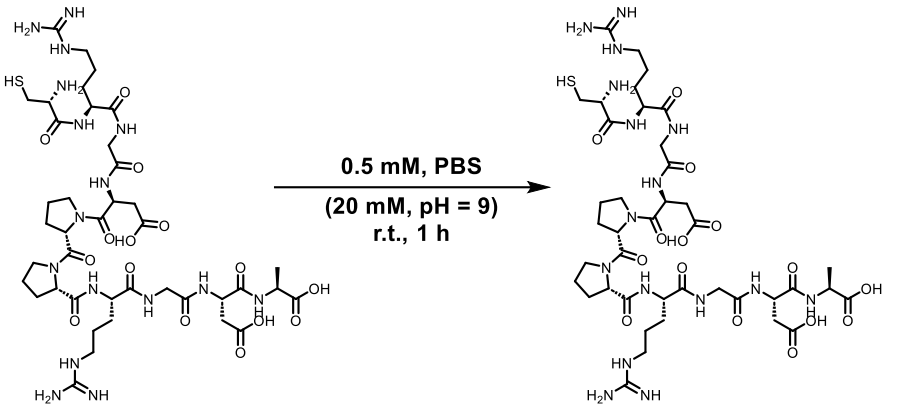

The dried peptide **L3** (1.0 equiv.) was dissolved in appropriate amount of PBS (20 mM, pH = 9.0) to reach a concentration of 0.5 mM. The reaction mixture was shaken at 25 °C and 800 rpm for 1 h on a thermostatic shaker.

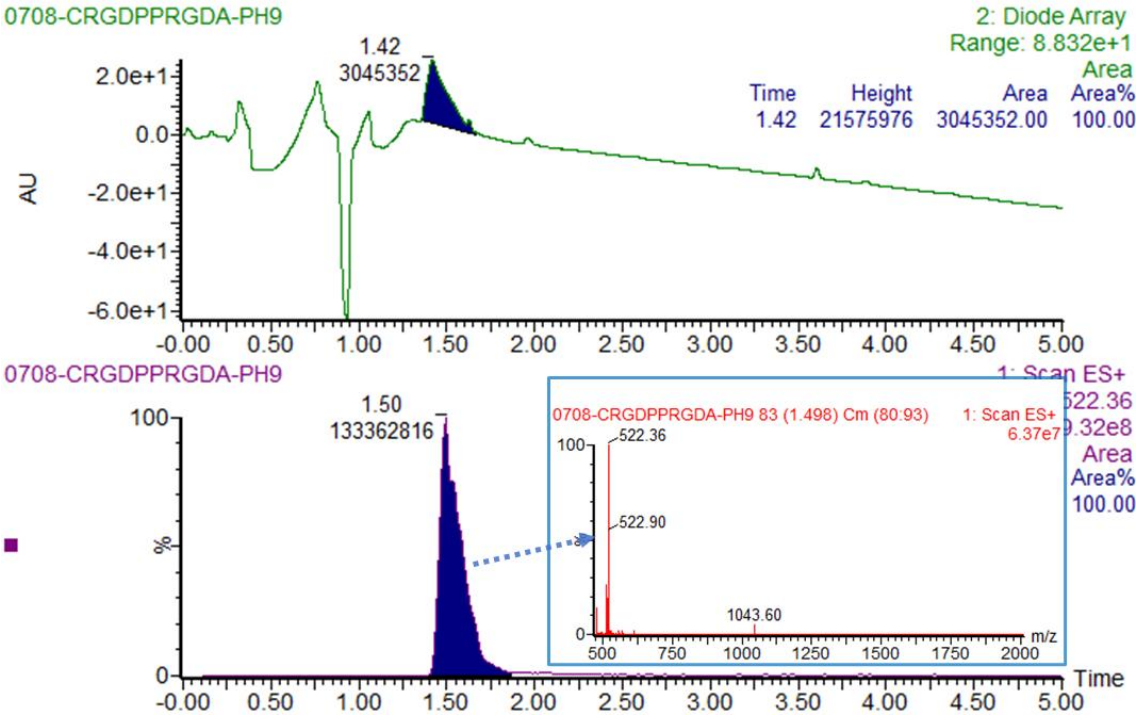

Fig S130. UPLC-MS chromatogram of **L3** without 3,6-DCT reaction mixture including TIC, UV curve (full-wavelength) and ESI-MS spectrum. Extract mass chromatograms from full scan data.

Control experiments with L4:

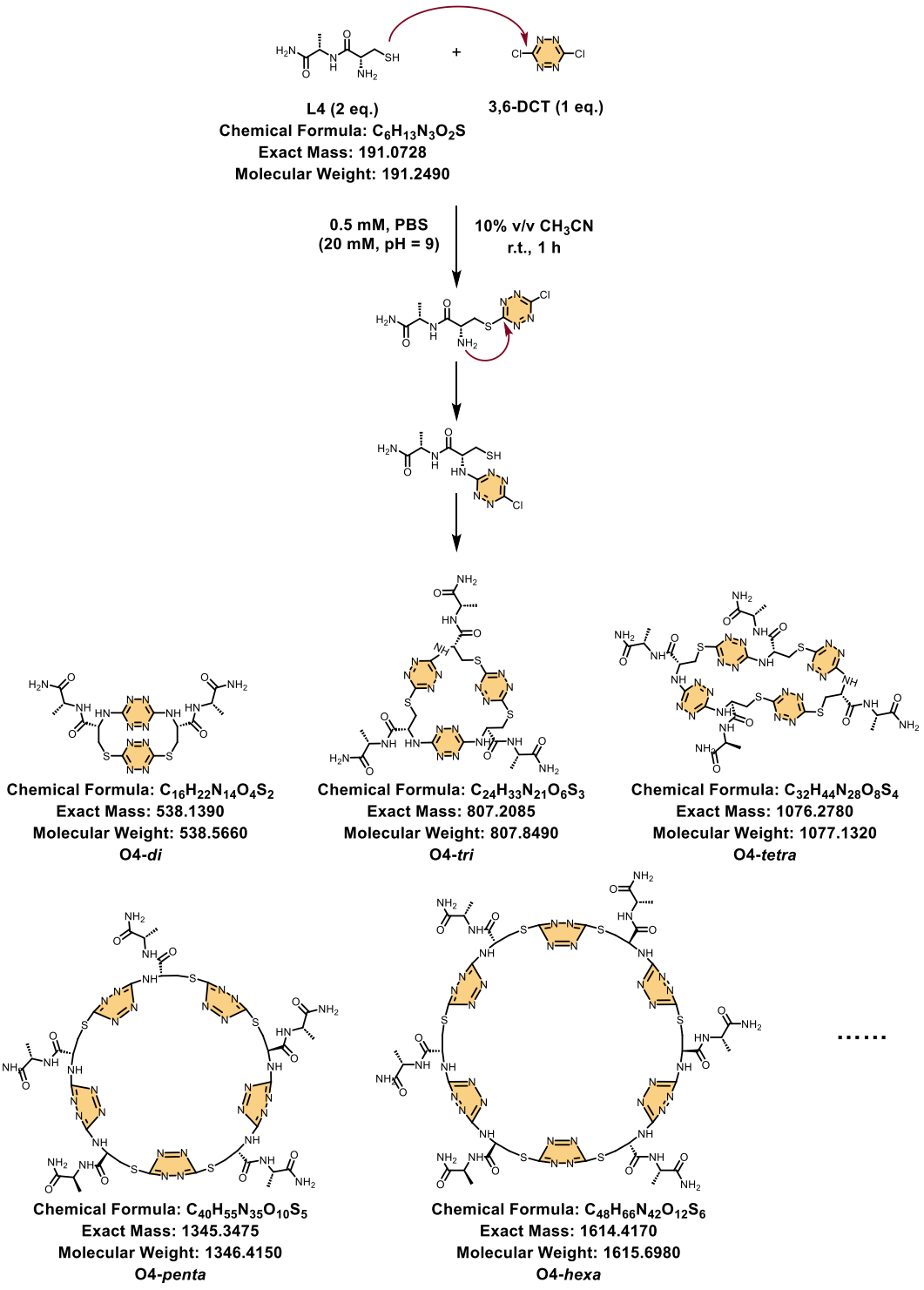

The dried peptide **L4** (2.0 equiv.) was dissolved in appropriate amount of PBS (20 mM, pH = 9.0) to reach a concentration of 0.56 mM. To this solution, 3,6-DCT (1.0 equiv.) dissolved in acetonitrile (1/9 of the volume of buffer) was added. The final concentrations in the reaction were 0.5 mM peptide, 0.5 mM 3,6-DCT and 10% acetonitrile, followed by thorough mixing. The reaction mixture was shaken at 25 °C and 800 rpm for 1 h on a thermostatic shaker.

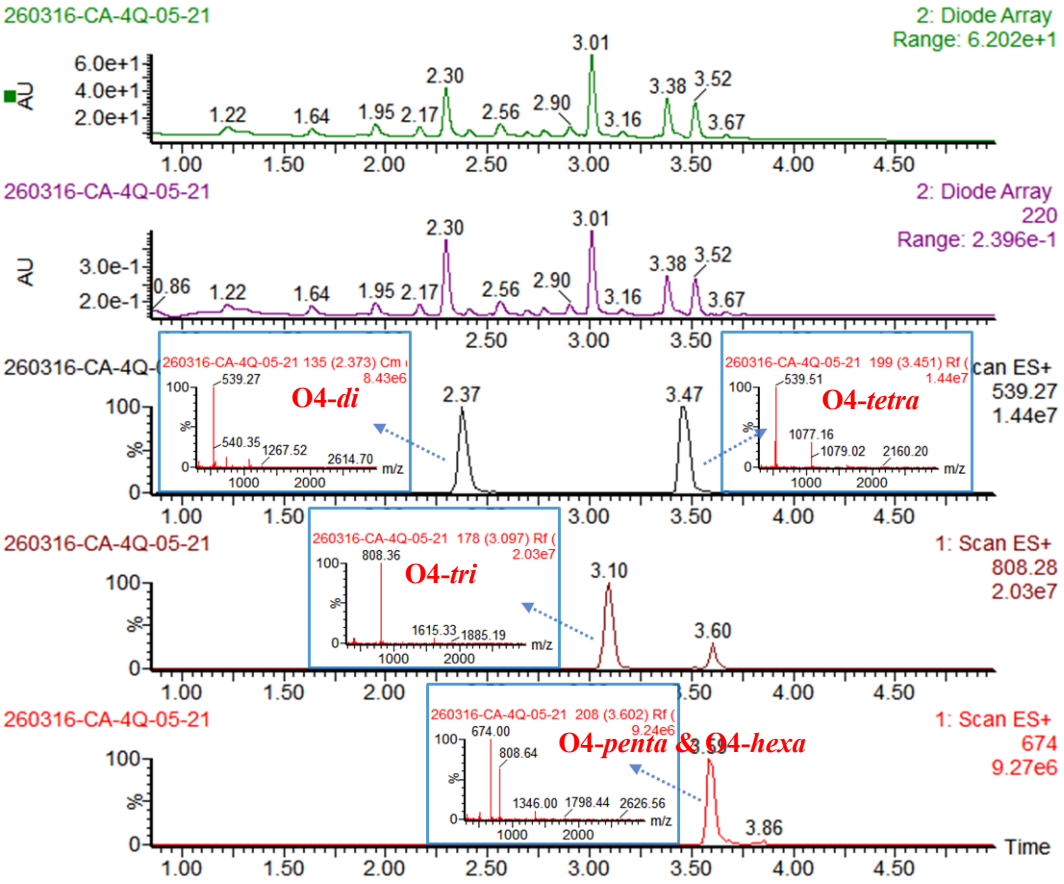

Fig S131. UPLC-MS chromatogram of **L4** (2 eq.) with 3,6-DCT (1 eq.) reaction mixture including TIC, UV curves (full-wavelength and extracted at 220 nm) and ESI-MS spectrum. Extract mass chromatograms from full scan data.

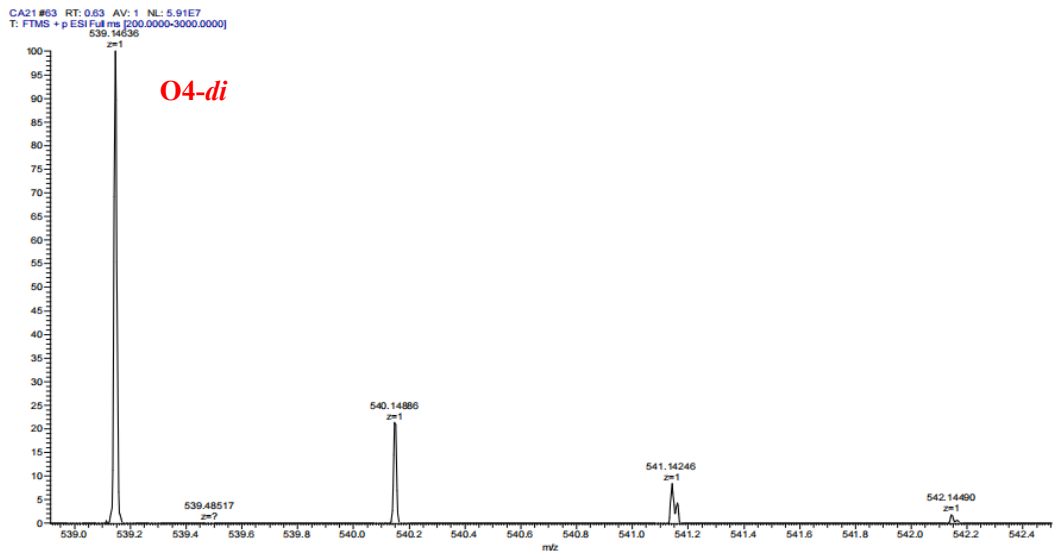

m/z	Theo. Mass	Delta (ppm)	RDB equiv.	Composition	
539.14636	539.14626	0.18	12.5	C16 H23 O4 N14 S2	M+H

Fig S132. Q-TOF-HRMS spectrum of **O4-*di***. HRMS (ES+) m/z: $[M+H]^+$ calcd for $C_{16}H_{23}N_{14}O_4S_2$

539.14, found 539.14.

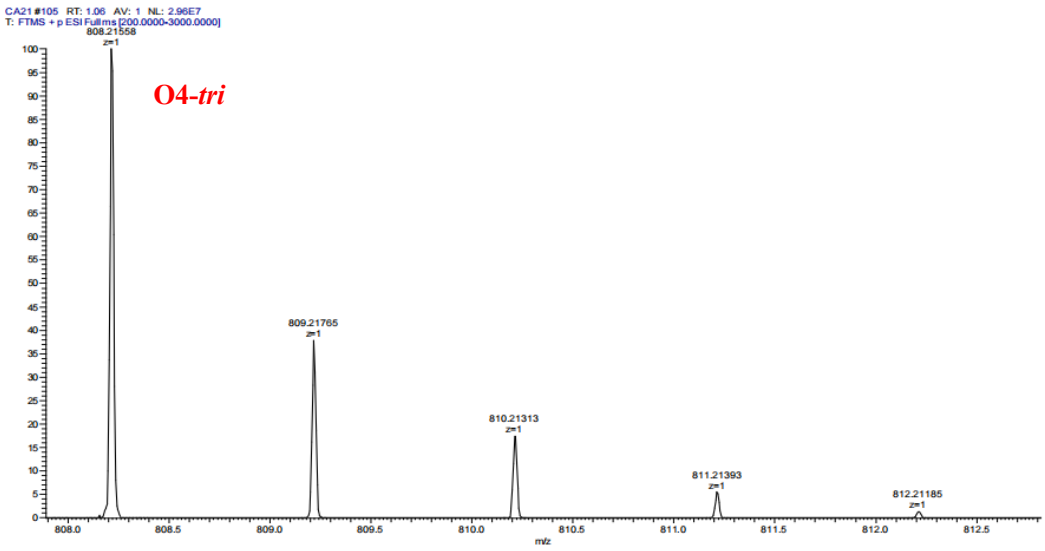

m/z	Theo. Mass	Delta (ppm)	RDB equiv.	Composition	
808.21558	808.21576	-0.22	18.5	C24 H34 O6 N21 S3	M+H

Fig S133. Q-TOF-HRMS spectrum of **O4-*tri.*** HRMS (ES+) m/z: $[M+H]^+$ calcd for $C_{24}H_{33}N_{21}O_6S_3$ 808.21, found 808.21.

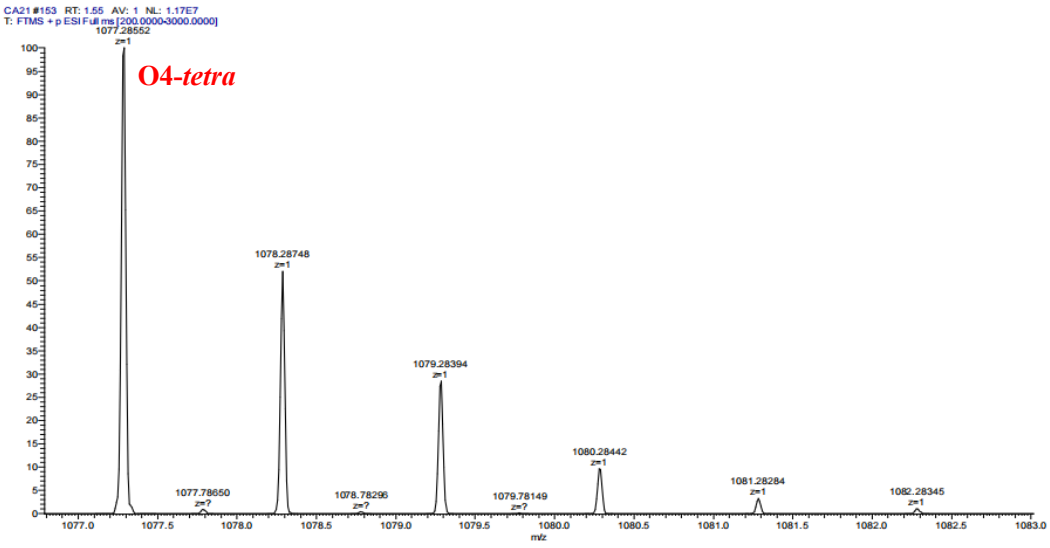

m/z	Theo. Mass	Delta (ppm)	RDB equiv.	Composition	
1077.2855	1077.28525	0.25	24.5	C32 H45 O8 N28 S4	M+H

Fig S134. Q-TOF-HRMS spectrum of **O4-*tetra***. HRMS (ES+) m/z: $[M+H]^+$ calcd for $C_{32}H_{44}N_{28}O_8S_4$ 1077.28, found 1077.29.

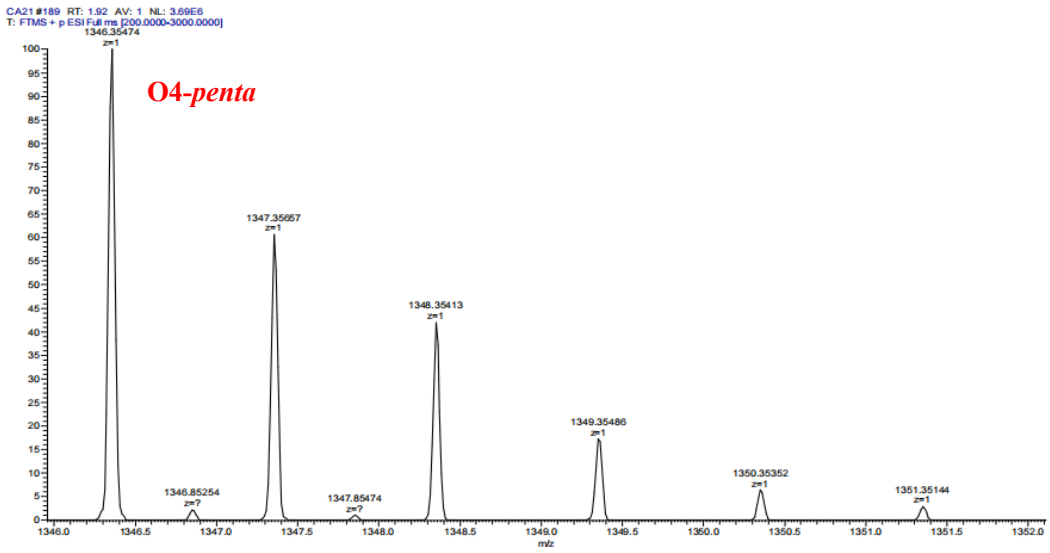

m/z	Theo. Mass	Delta (ppm)	RDB equiv.	Composition	
1346.3547	1346.35474	0	30.5	C40 H56 O10 N35 S5	M+H

Fig S135. Q-TOF-HRMS spectrum of **O4-*penta***. HRMS (ES+) m/z: $[M+H]^+$ calcd for $C_{40}H_{55}N_{35}O_{10}S_5$ 1346.35, found 1346.35.

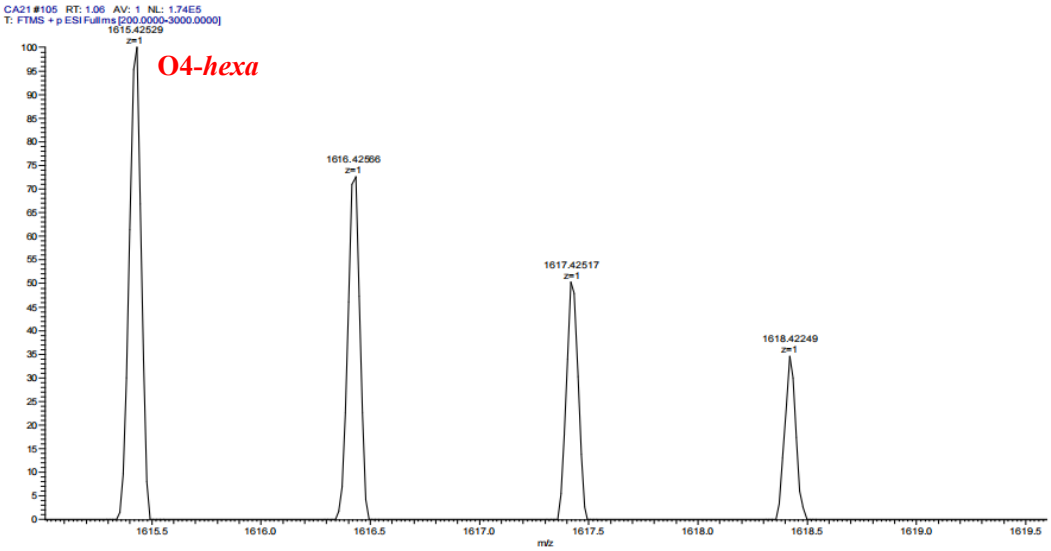

m/z	Theo. Mass	Delta (ppm)	RDB equiv.	Composition	
1615.4253	1615.42424	0.65	36.5	C48 H67 O12 N42 S6	M+H

Fig S136. Q-TOF-HRMS spectrum of **O4-*hexa***. HRMS (ES+) m/z: $[M+H]^+$ calcd for $C_{48}H_{66}N_{42}O_{12}S_6$ 1615.42, found 1615.43.

Control experiments v and vi:

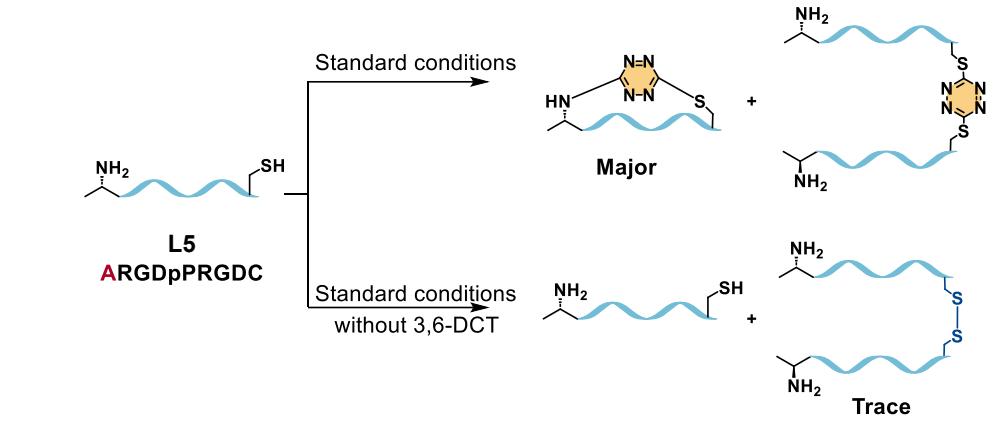

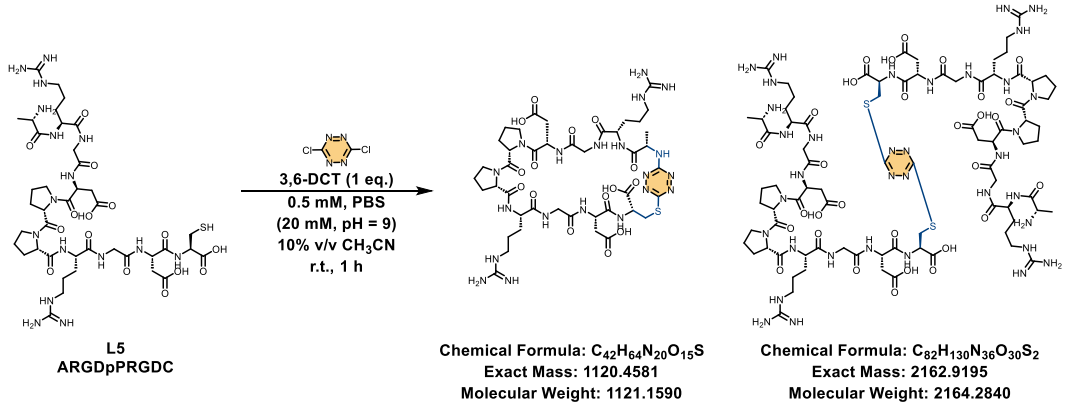

The dried peptide **L5** (1.0 equiv.) was dissolved in appropriate amount of PBS (20 mM, pH = 9.0) to reach a concentration of 0.56 mM. To this solution, 3,6-DCT (1.0 equiv.) dissolved in acetonitrile (1/9 of the volume of buffer) was added. The final concentrations in the reaction were 0.5 mM peptide, 0.5 mM 3,6-DCT and 10% acetonitrile, followed by thorough mixing. The reaction mixture was shaken at 25 °C and 800 rpm for 1 h on a thermostatic shaker.

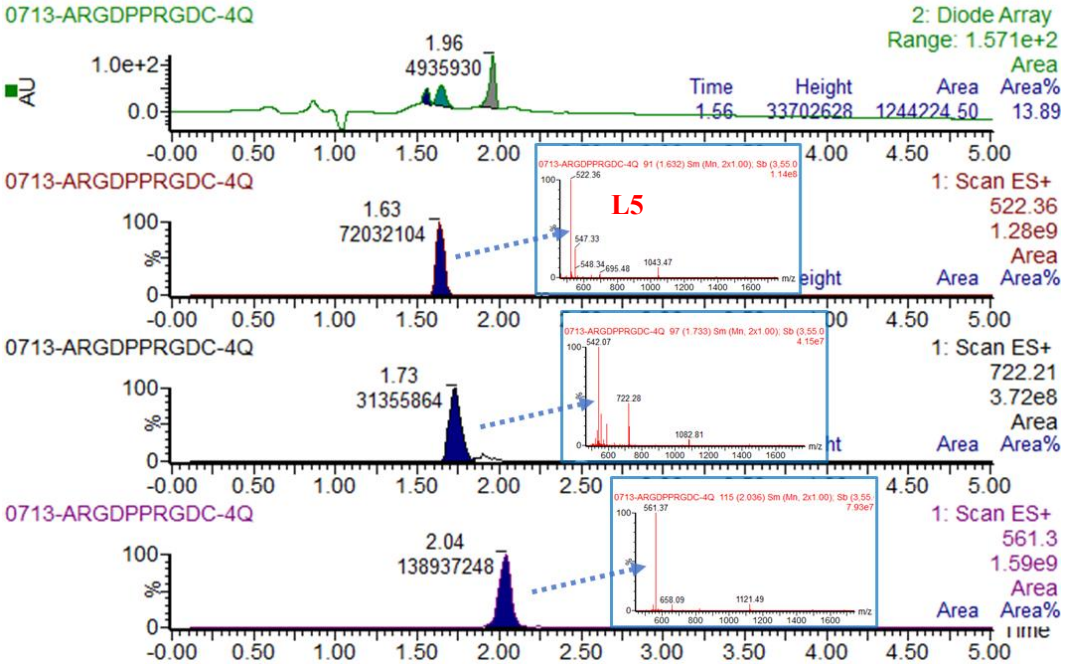

Fig S137. UPLC-MS chromatogram of **L5** and 3,6-DCT reaction mixture including TIC, UV curve (full-wavelength) and ESI-MS spectrum. Extract mass chromatograms from full scan data.

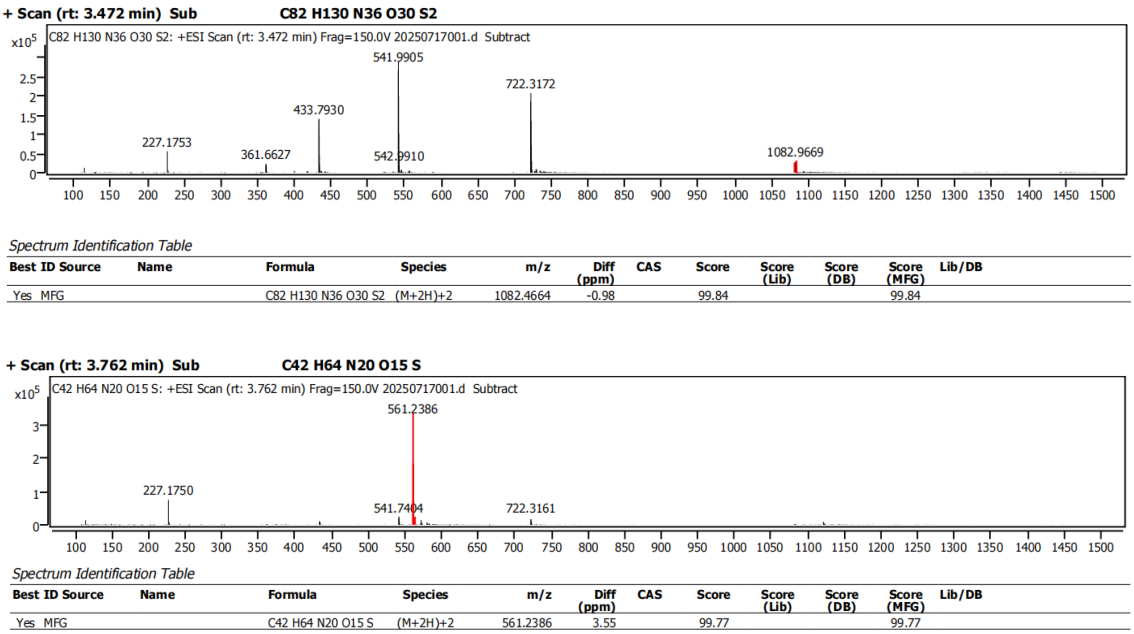

Fig S138. Q-TOF-HRMS spectrum of **L5** and 3,6-DCT reaction mixture. HRMS (ES+) m/z: $[M+2H]^{2+}$ calcd for $C_{82}H_{130}N_{36}O_{30}S_2$ 1082.4598, found 1082.4664. HRMS (ES+) m/z: $[M+2H]^{2+}$ calcd for $C_{42}H_{64}N_{20}O_{15}S$ 561.2291, found 561.2386.

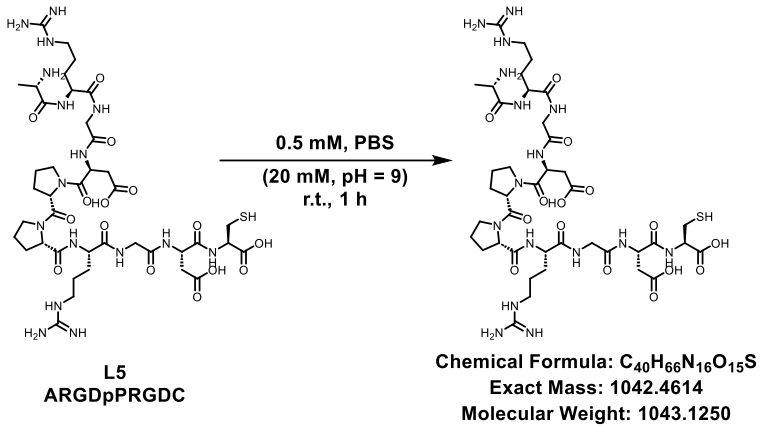

The dried peptide **L5** (1.0 equiv.) was dissolved in appropriate amount of PBS (20 mM, pH = 9.0) to reach a concentration of 0.5 mM. The reaction mixture was shaken at 25 °C and 800 rpm for 1 h on a thermostatic shaker.

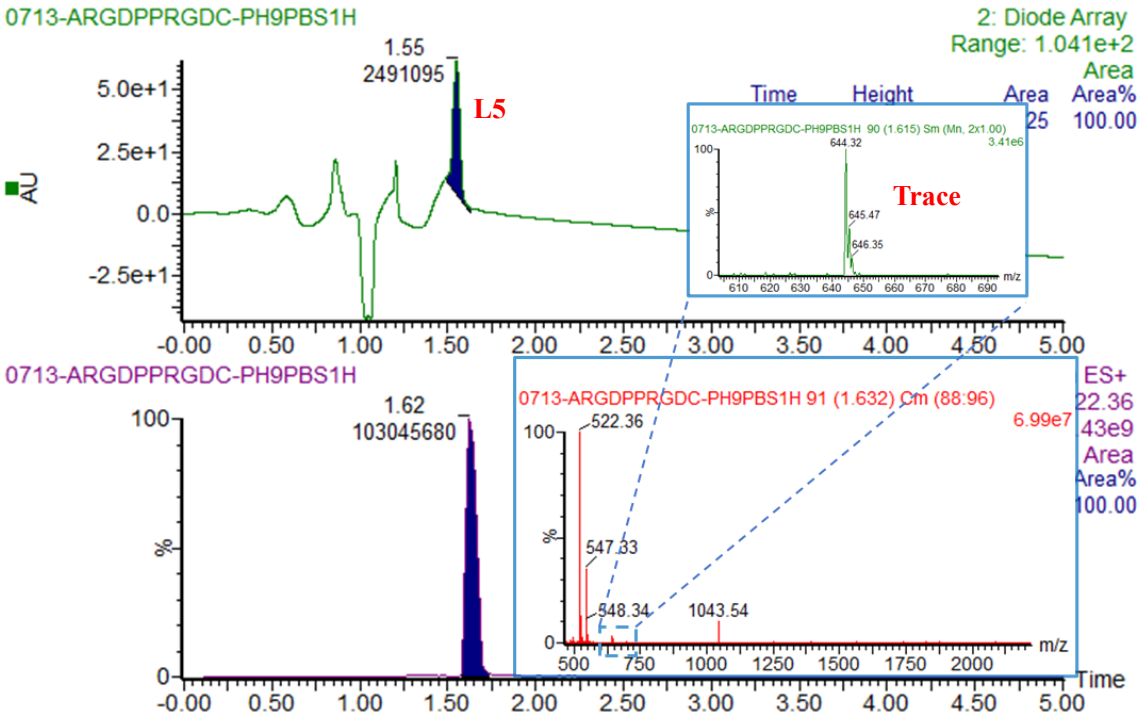

Fig S139. UPLC-MS chromatogram of **L5** without 3,6-DCT reaction mixture including TIC, UV curve (full-wavelength) and ESI-MS spectrum. Extract mass chromatograms from full scan data.

5.2 Structure characterization

Confirmation experiments vii:

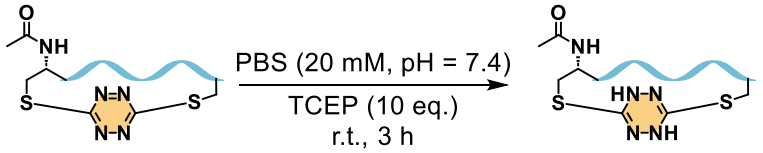

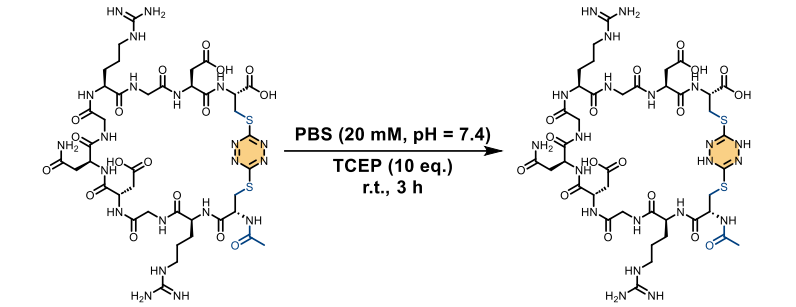

Chemical Formula: $C_{40}H_{61}N_{21}O_{17}S_2$
Exact Mass: 1171.3996
Molecular Weight: 1172.1780
M14-tz

Chemical Formula: $C_{40}H_{63}N_{21}O_{17}S_2$
Exact Mass: 1173.4152
Molecular Weight: 1174.1940
M14-tz-r

The lyophilized monocyclic product (**M14-tz**) was dissolved in PBS (20 mM, pH = 7.4), treated with TCEP (10 equiv.), and reacted at room temperature for 3 h.

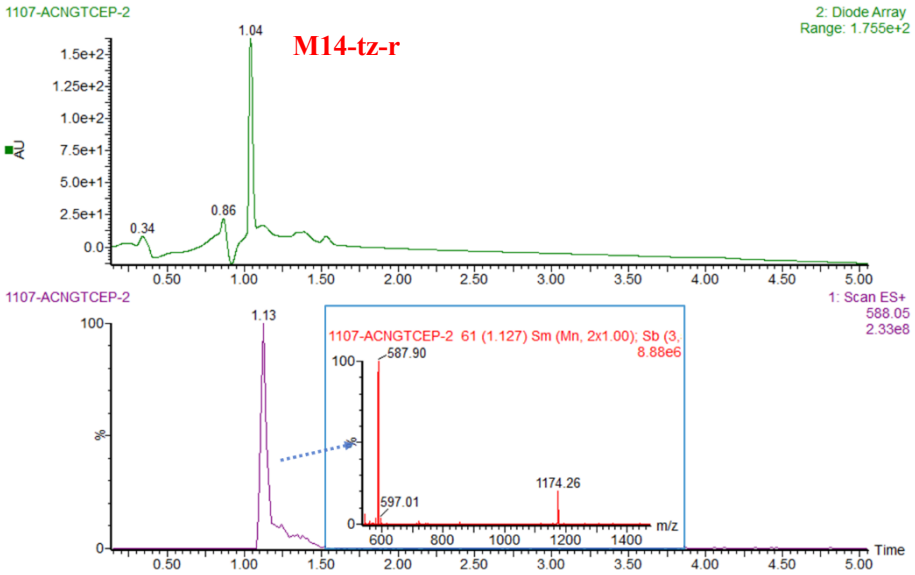

Fig S140. UPLC-MS chromatogram of **M14-tz-r** and TCEP reaction mixture including TIC, UV curve (full-wavelength) and ESI-MS spectrum. Extract mass chromatograms from full scan data.

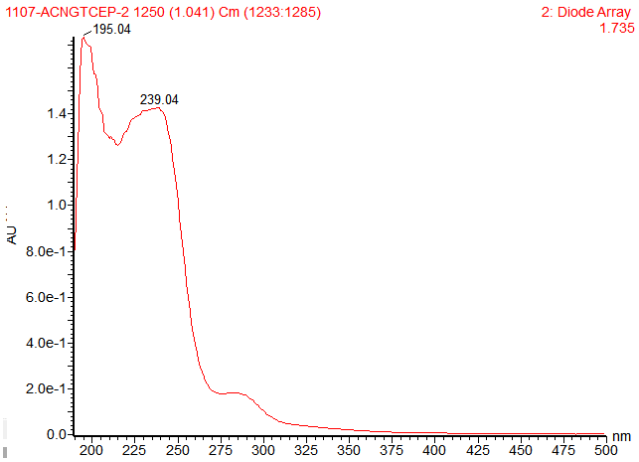

Fig S141. The UV characteristic absorption of **M14-tz-r**.

Confirmation experiments viii:

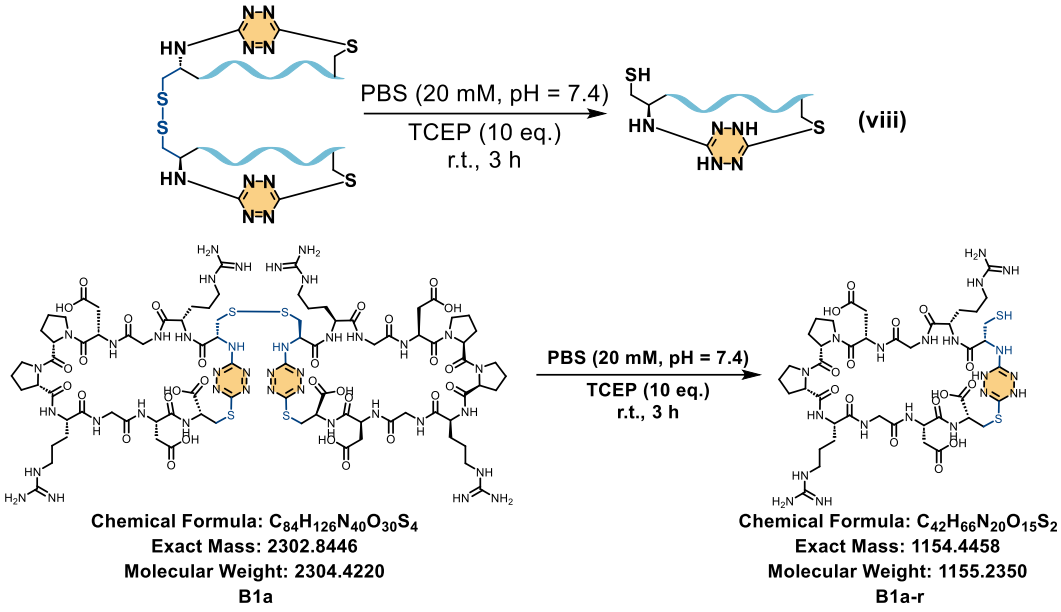

The lyophilized product **B1a** was dissolved in PBS (20 mM, pH = 7.4), treated with TCEP (10 equiv.), and reacted at room temperature for 3 h.

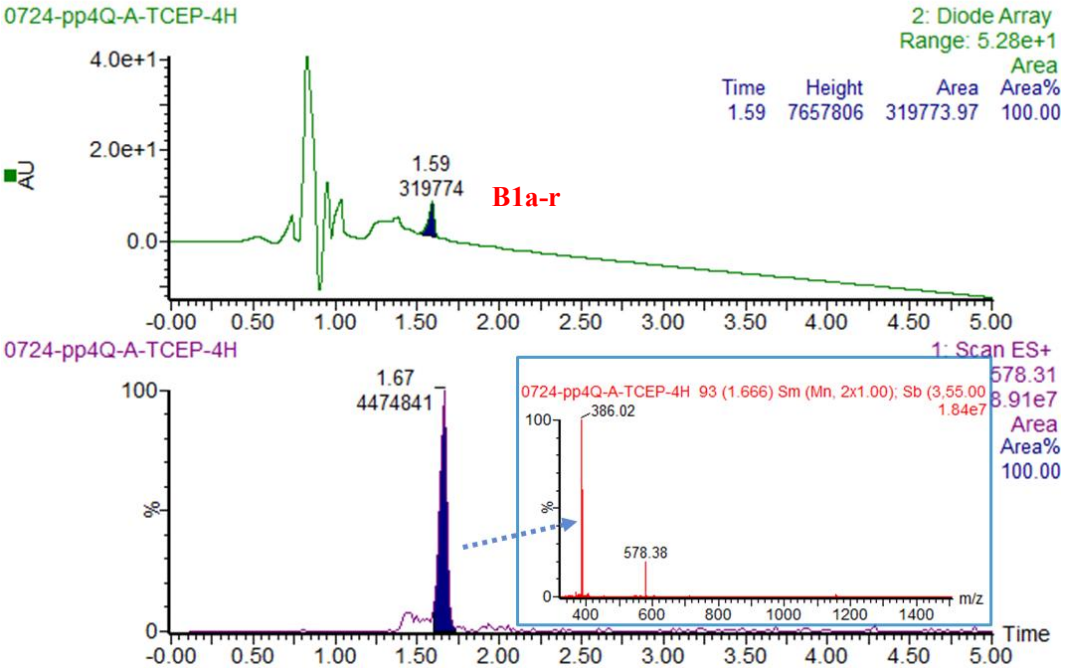

Fig S142. UPLC-MS chromatogram of **B1a** and TCEP reaction mixture including TIC, UV curve (full-wavelength) and ESI-MS spectrum. Extract mass chromatograms from full scan data.

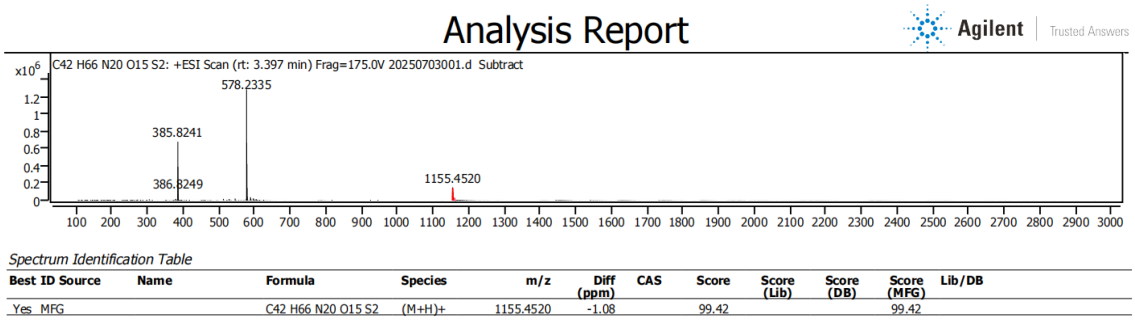

Fig S143. Q-TOF-HRMS spectrum of **B1a-r**. HRMS (ES+) m/z: $[M+H]^+$ calcd for $C_{42}H_{66}N_{20}O_{15}S_2$ 1155.4458, found 1155.4520.

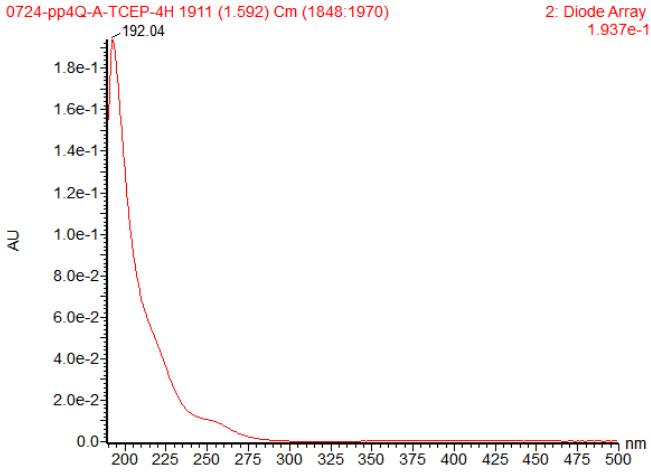

Fig S144. The UV characteristic absorption of **B1a-r**.

Confirmation experiments ix:

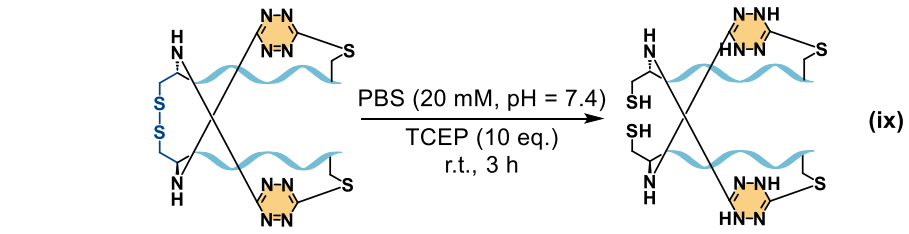

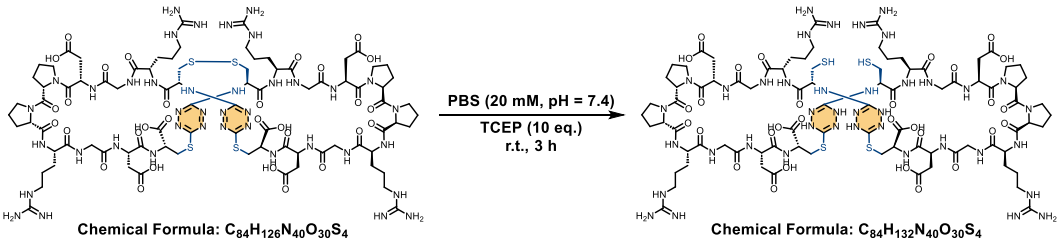

Chemical Formula: $C_{84}H_{126}N_{40}O_{30}S_4$
Exact Mass: 2302.8446
Molecular Weight: 2304.4220
B1b

Chemical Formula: $C_{84}H_{132}N_{40}O_{30}S_4$
Exact Mass: 2308.8916
Molecular Weight: 2310.4700
B1b-r

The lyophilized product **B1b** was dissolved in PBS (20 mM, pH = 7.4), treated with TCEP (10 equiv.), and reacted at room temperature for 3 h.

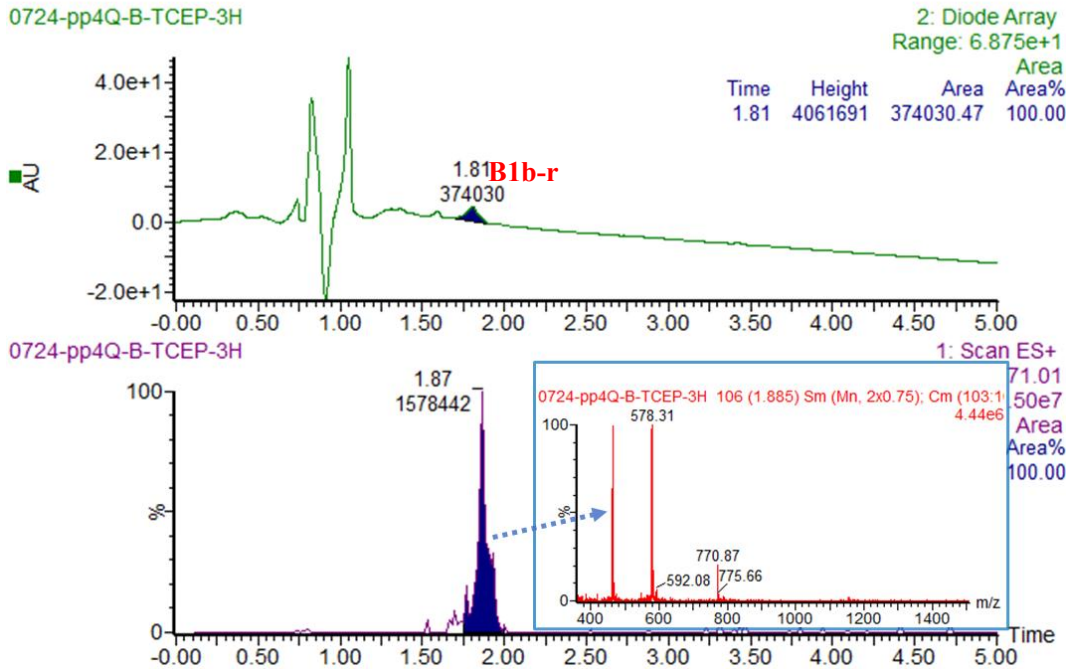

Fig S145. UPLC-MS chromatogram of **B1b** and TCEP reaction mixture including TIC, UV curve (full-wavelength) and ESI-MS spectrum. Extract mass chromatograms from full scan data.

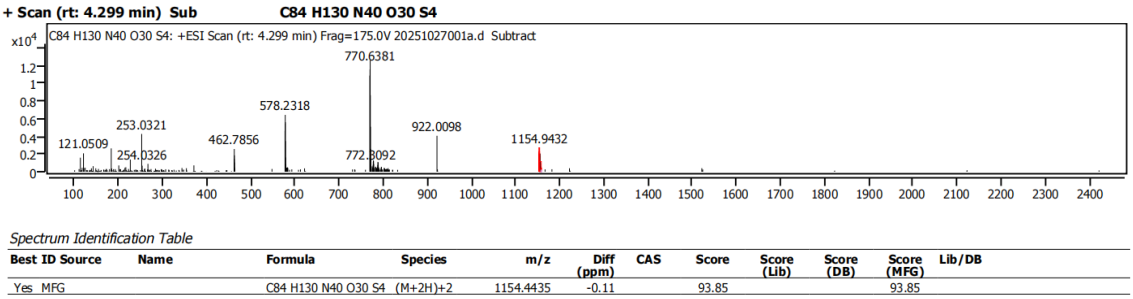

Spectrum Identification Table

Best	ID Source	Name	Formula	Species	m/z	Diff (ppm)	CAS	Score	Score (Lib)	Score (DB)	Score (MFG)	Lib/DB
Yes	MFG		C84 H130 N40 O30 S4	(M+2H)+2	1154.4435	-0.11		93.85			93.85	

Fig S146. Q-TOF-HRMS spectrum of **B1b-r**. HRMS (ES+) m/z: $[M+2H]^{2+}$ calcd for $C_{84}H_{130}N_{40}O_{30}S_4$ 1155.4458, found 1154.9432.

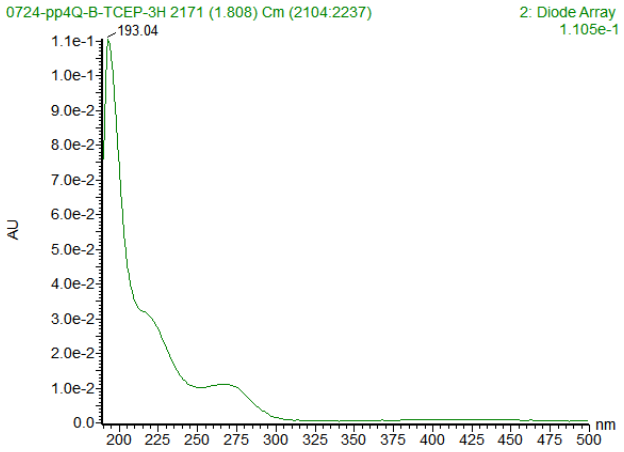

Fig S147. The UV characteristic absorption of **B1b-r**.

5.3 Detailed NMR assignment of key residues in B1a and B1b

The unambiguous determination of the three-dimensional topologies for isomers **B1a** and **B1b** relies heavily on the precise ^{1}H and ^{13}C NMR assignments of three cornerstone residues: the N-terminal Cys1, the C-terminal Cys10, and the sequentially adjacent Asp9. The assignment strategy utilized a rigorous combination of 2D TOCSY, COSY, HSQC, HMBC, and ROESY experiments, employing a bottom-up spin-system extraction and sequential walk approach.

5.3.1 NMR assignment of B1a

Assignment of the C-terminal Cys10:

The assignment was anchored at the C-terminus by identifying the Cys10 spin system. Starting from its distinct amide proton (NH) at 8.32 ppm, TOCSY and COSY spectra revealed intra-residue scalar couplings to its *Hα* (4.45 ppm) and diastereotopic Hβ protons (3.44 and 3.72 ppm). HSQC analysis mapped these Hβ protons to a Cβ chemical shift of 30.9 ppm, a textbook value for an aromatic thioether, confirming the S-Ar linkage. Crucially, HMBC cross-peaks from these Cys10 *Hβ* protons directly to a quaternary carbon at 166.35 ppm (tetrazine core) provided definitive proof of the C-terminal covalent attachment.

Sequential walk and assignment of Asp9:

With Cys10 unambiguously anchored, the adjacent residue (Asp9) was identified via a ROESY sequential walk. A highly intense inter-residue spatial contact ($d_{\alpha N}$) was observed between the Cys10 NH (8.32 ppm) and an *Hα* signal at 4.57 ppm, stereochemically assigning this *Hα* to the preceding residue, Asp9. Using this *Hα* (4.57 ppm) as a starting point in the TOCSY and COSY spectra, the complete Asp9 spin network was extracted: *NH* (8.07 ppm) and two diastereotopic *Hβ* protons (2.42 and 2.60 ppm). HSQC correlations verified the corresponding carbon shifts as *Cα* (49.24 ppm) and *Cβ* (35.98 ppm). The *Cβ* shift at ~36 ppm is an exclusive hallmark of the aspartic acid side chain. Furthermore, HMBC correlations from the Asp9 *Hβ* (2.42 ppm) to its own *Cα* (49.52 ppm) and carbonyl carbon (171.86 ppm) perfectly closed the spin system loop, verifying the residue identity beyond doubt.

Assignment of the N-terminal Cys1:

The N-terminal Cys1 NH was located at an unusually downfield position of 8.84 ppm, characteristic of a proton sterically forced into the deshielding cone of the tetrazine ring in a constrained hairpin. TOCSY cross-peaks linked this NH to its Hα at 4.73 ppm and Hβ at 3.11 ppm. HSQC analysis mapped the Cys1 *Hβ* to a *Cβ* shift of 40.18 ppm. This specific downfield carbon shift confirms that the Cys1 thiol is oxidized, participating in the intermolecular disulfide bond. The N-Ar covalent linkage was verified by a clear $^{3}J_{CH}$ HMBC cross-peak extending from the Cys1 *Hα* (4.73 ppm) across the secondary amine nitrogen to the tetrazine quaternary carbon (~160.83 ppm).

5.3.2 NMR Assignment of B1b

The resonance assignment for **B1b** followed the identical logical pathway, revealing highly conserved chemical environments for the local covalent nodes, but drastic variations reflecting the topological expansion.

Cys10 and Asp9 in B1b:

The C-terminal Cys10 was identified by its *NH* at 8.33 ppm and *Hα* at 4.46 ppm, showing virtually no chemical shift perturbation compared to **B1a**. The sequential ROESY walk from the Cys10 *NH* (8.33 ppm) identified a strong $d_{\alpha N}$ contact to the preceding Asp9 Hα at 4.58 ppm. TOCSY and HSQC extraction of this 4.58 ppm signal yielded an almost identical Asp9 spin network to that of **B1a** (NH: ~8.07 ppm, Hβ: 2.42/2.60 ppm, Cβ: ~36.0 ppm).

Cys1 in B1b:

In stark contrast to the C-terminus, the N-terminal Cys1 experienced significant perturbations. Its NH proton exhibited a prominent upfield shift to 8.59 ppm, and its Hα shifted to 4.83 ppm. While the Cys1 Cβ shift remained at 39.97 ppm (confirming the intact disulfide bond), the critical HMBC signal from Cys1 *Hα* to the tetrazine carbon was completely absent. As discussed in the main text, this absence is indicative of a near-90° dihedral angle specific to the special conformation. The definitive assignment of these **B1b** residues laid the groundwork for identifying the crucial inter-chain Cys1 Hα (4.83 ppm) to Asp9 Hα (4.58 ppm) NOE cross-peak, physically proving the topological crossing.

Tab S9. Detailed ^{1}H and ^{13}C NMR chemical shifts (ppm) of key residues in B1a and B1b

Isomer	Residue	CONH (^{1}H)	Hα (^{1}H)	Cα (^{13}C)	Hβ (^{1}H)	Cβ (^{13}C)	Key 2D Correlations (HMBC/ROESY)
B1a	Cys1	8.84	4.73	54.10	3.11	40.18	HMBC: Hα → Tetrazine C (160.83)
	Asp9	8.07	4.57	49.24	2.42, 2.60	35.98	
	Cys10	8.33	4.45	51.45	3.72 , 3.45	30.9	HMBC: Hβ → Tetrazine C (166.35)
B1b	Cys1	8.59	4.83	54.04	3.20	39.97	
	Asp9	8.08	4.58	50.95	2.44, 2.62	36.15	ROESY: NH → Asp9 Hα (4.58)
	Cys10	8.33	4.45	51.39	3.46, 3.72	30.7	HMBC: Hβ → Tetrazine C (166.69)

6. Sequence determinants impacting the 3,6-DCT mediated cyclodimerization

6.1 Reaction of N-Cys-containing peptides

Example procedure (Standard reaction conditions):

The dried peptide substrate with N-Cys (1.0 equiv.), such as CRGDAARGDC (**L6**), was dissolved in appropriate amount of PBS (20 mM, pH = 9.0) to reach a concentration of 0.56 mM. To this solution, 3,6-DCT (1.0 equiv.) dissolved in acetonitrile (1/9 of the volume of buffer) was added. The final concentrations in the reaction were 0.5 mM peptide, 0.5 mM 3,6-DCT and 10% acetonitrile, followed by thorough mixing. The reaction mixture was shaken at 25 °C and 800 rpm for 1 h on a thermostatic shaker.

After completion, 50 μL of the reaction mixture was collected, and 10 μL was injected into the UPLC-MS for analysis. The peak area of the cyclodimerization products at 270 nm was recorded. Determine the LC-MS yield using **Equation 1**. Meanwhile, the ratio of the cyclodimerization product isomers was calculated based on the peak area ratio at 270 nm or the EIC area ratio. Detailed data are shown in **Table S10**.

Tab S10. The LC-MS data for N-Cys-containing peptides collected using Method A

Peptide sequence	Peak area of	HPLC Yield (%)[a]	Ratio of isomers
CRGDAARGDC	98232	49.43	47/53
CRGDGGRGDC	71033	34.93	54/46
CRGDNGRGDC	49747	23.58	34/66
CRGDpGRGDC	67876	33.24	56/44
CRGDAibpRGDC	84098	41.89	42/58
CRGDAibGRGDC	86036	42.93	67/33
CRGDAARGDCGS	99277	49.99	65/35
CDGRAADGRC	63260	30.78	13/87
CRGDAADGRC	78337	38.82	11/89
CDGRAARGDC	56238	27.04	56/44
CRDAARDC	88645	44.32	65/35
CRGDC	88968	44.49	15/85
CAAC	86282	43.06	54/46
CAAAC	100216	50.49	70/30
CAAAAC	96386	48.44	84/16
CAAAAAC	75384	37.25	77/23
CGSC	88039	43.99	\
CGSGSC	83261	41.45	40/60
CGSGSGSC	94373	47.37	\
CGSGSGSGSC	86586	43.22	\

[a]Yields were determined by LC-MS analysis using **Equation 1**

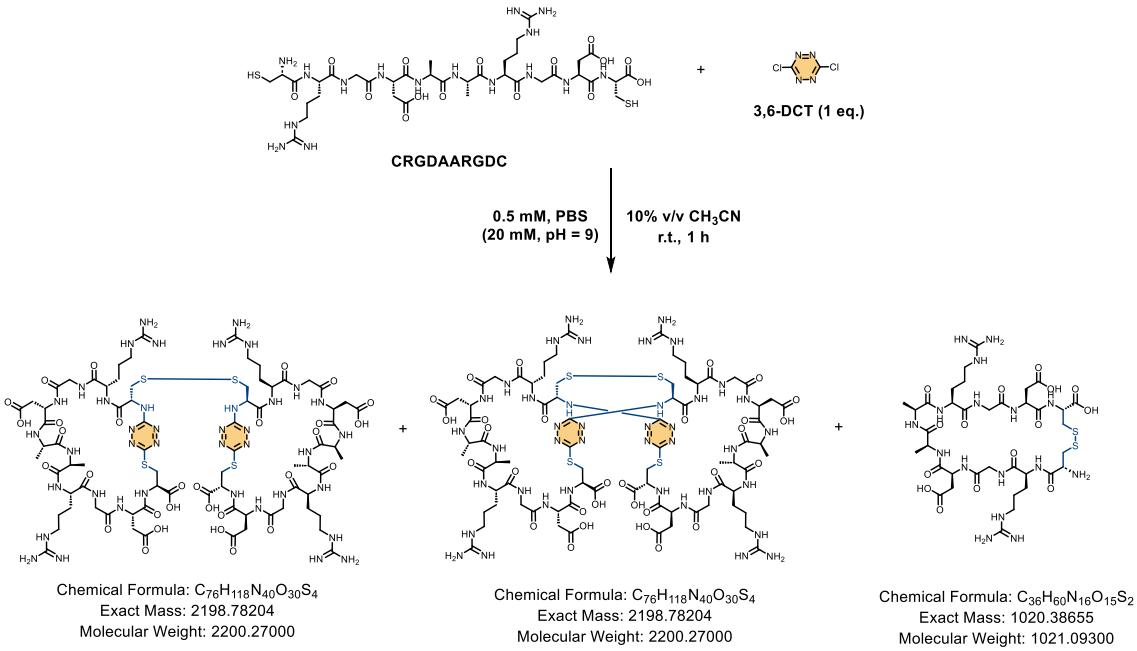

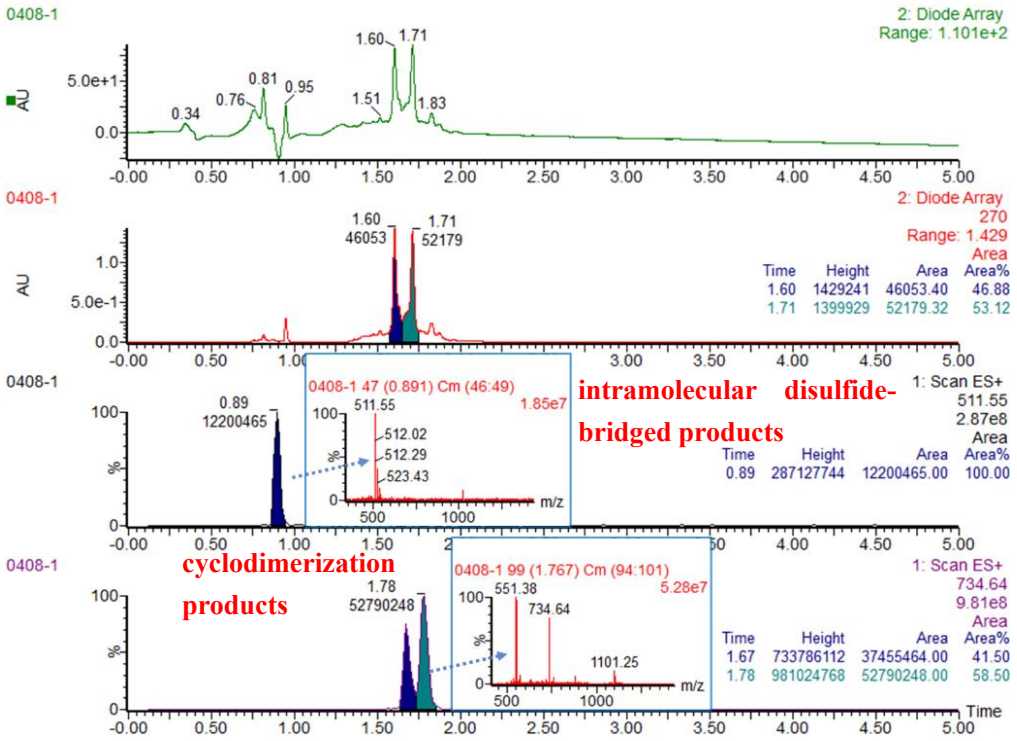

Fig S148. UPLC-MS chromatogram of **L6** and 3,6-DCT reaction mixture including TIC, UV curves (full-wavelength and extracted at 270 nm) and ESI-MS spectrum. Extract mass chromatograms from full scan data. The yield of the corresponding cyclodimerization products was determined to be 49% using equation 1.

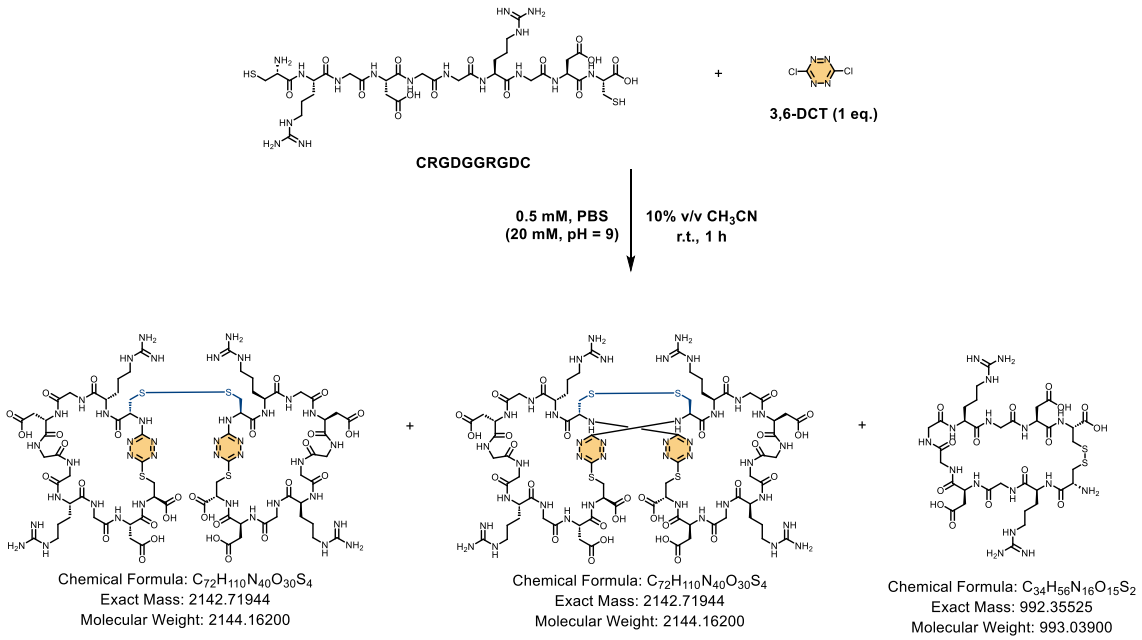

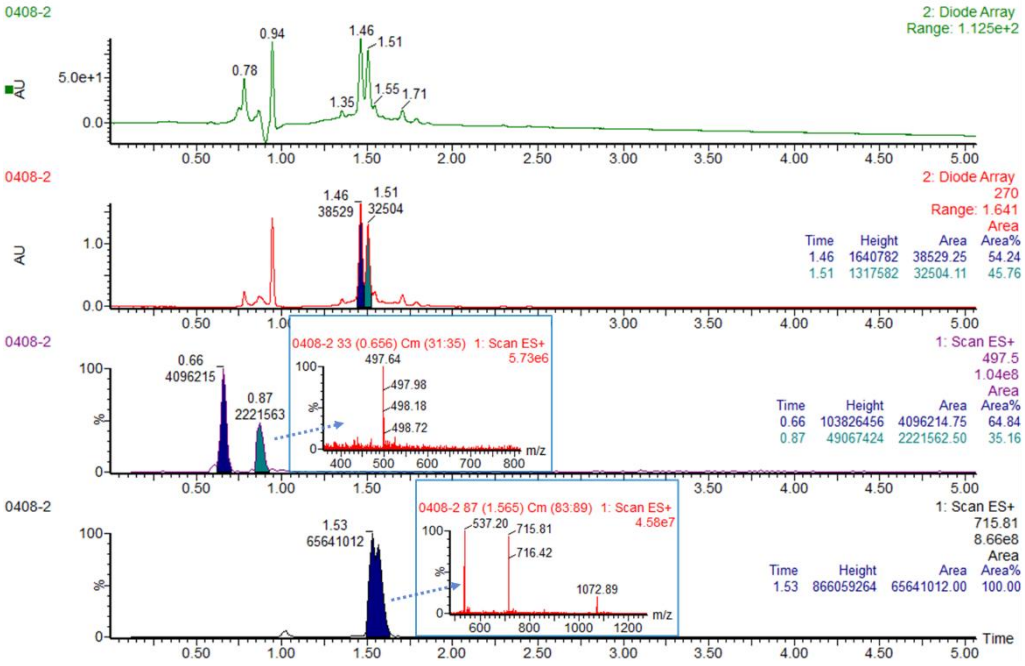

Fig S149. UPLC-MS chromatogram of **L7** and 3,6-DCT reaction mixture including TIC, UV curves (full-wavelength and extracted at 270 nm) and ESI-MS spectrum. Extract mass chromatograms from full scan data. The yield of the corresponding cyclodimerization products was determined to be 35% using equation 1.

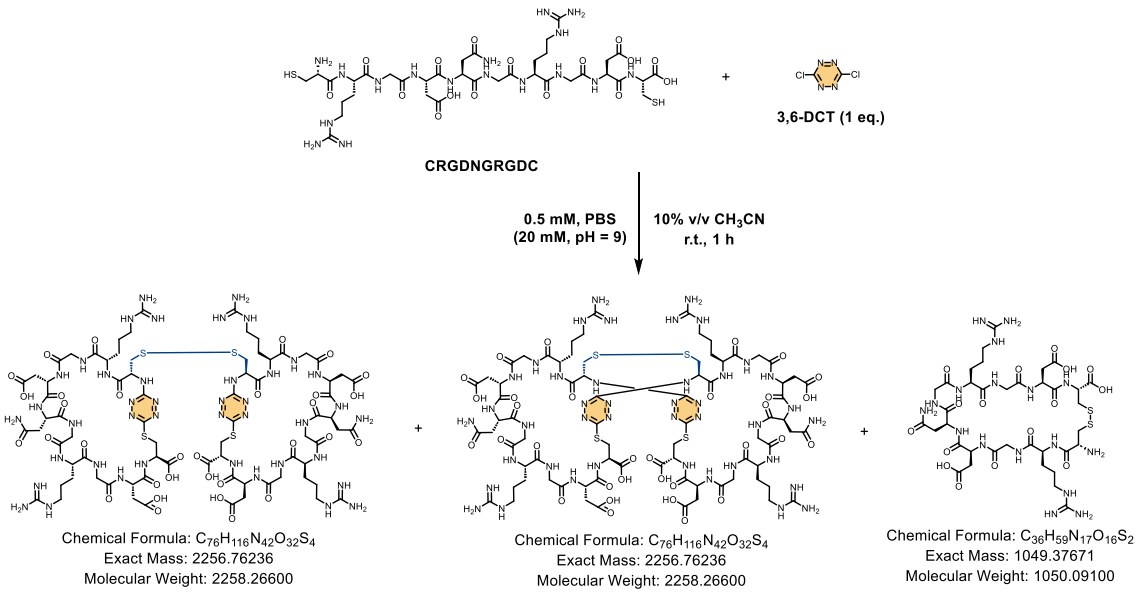

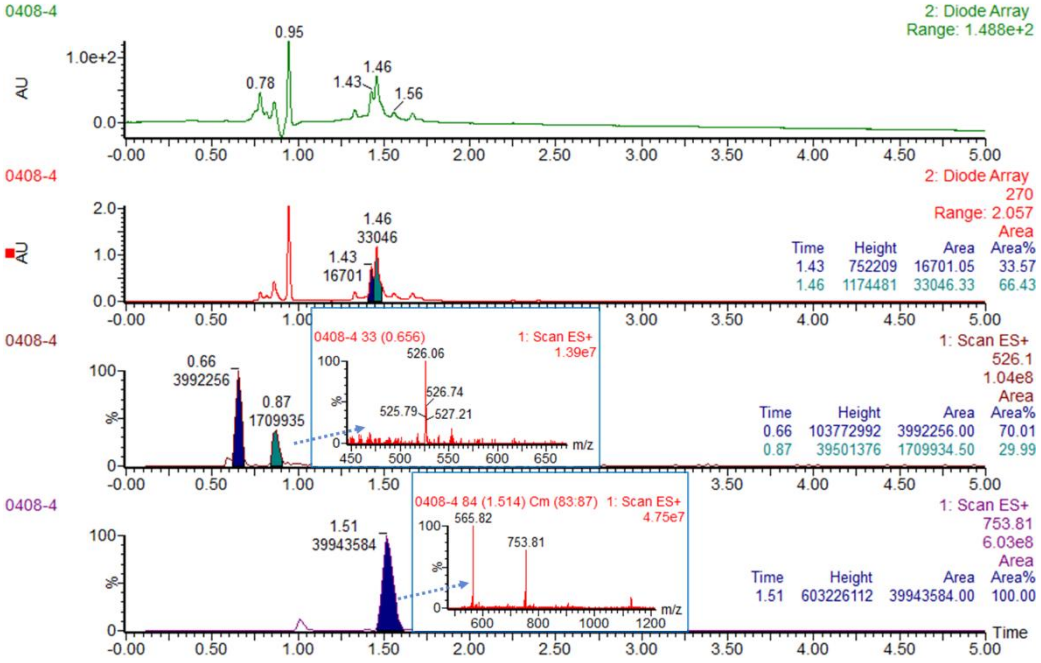

Fig S150. UPLC-MS chromatogram of **L8** and 3,6-DCT reaction mixture including TIC, UV curves (full-wavelength and extracted at 270 nm) and ESI-MS spectrum. Extract mass chromatograms from full scan data. The yield of the corresponding cyclodimerization products was determined to be 24% using equation 1.

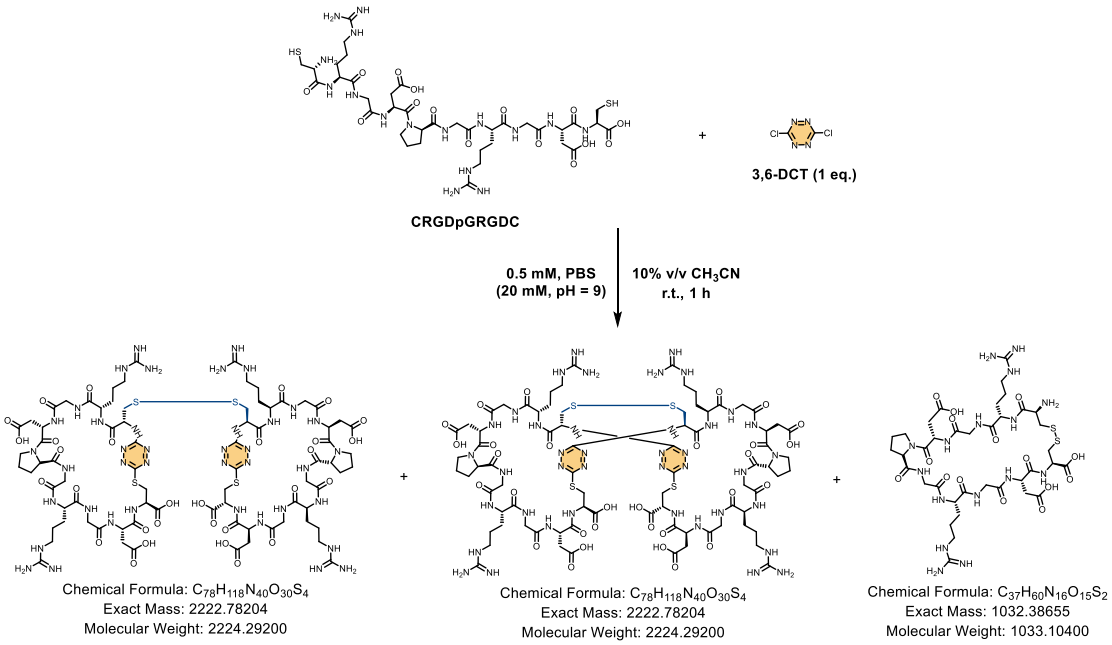

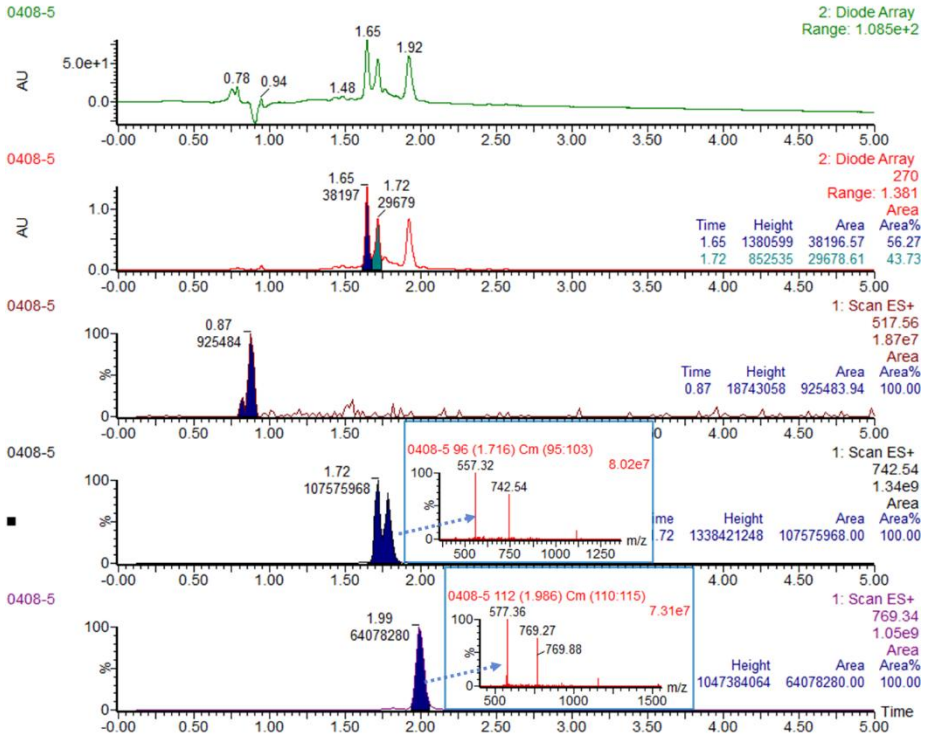

Fig S151. UPLC-MS chromatogram of **L9** and 3,6-DCT reaction mixture including TIC, UV curves (full-wavelength and extracted at 270 nm) and ESI-MS spectrum. Extract mass chromatograms from full scan data. The yield of the corresponding cyclodimerization products was determined to be 33% using equation 1.

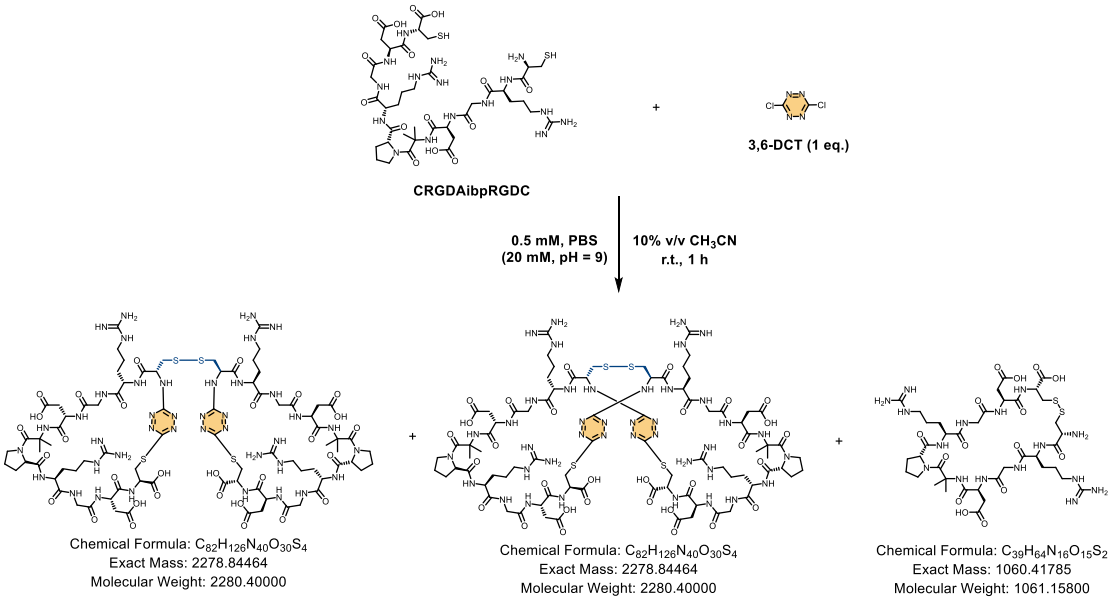

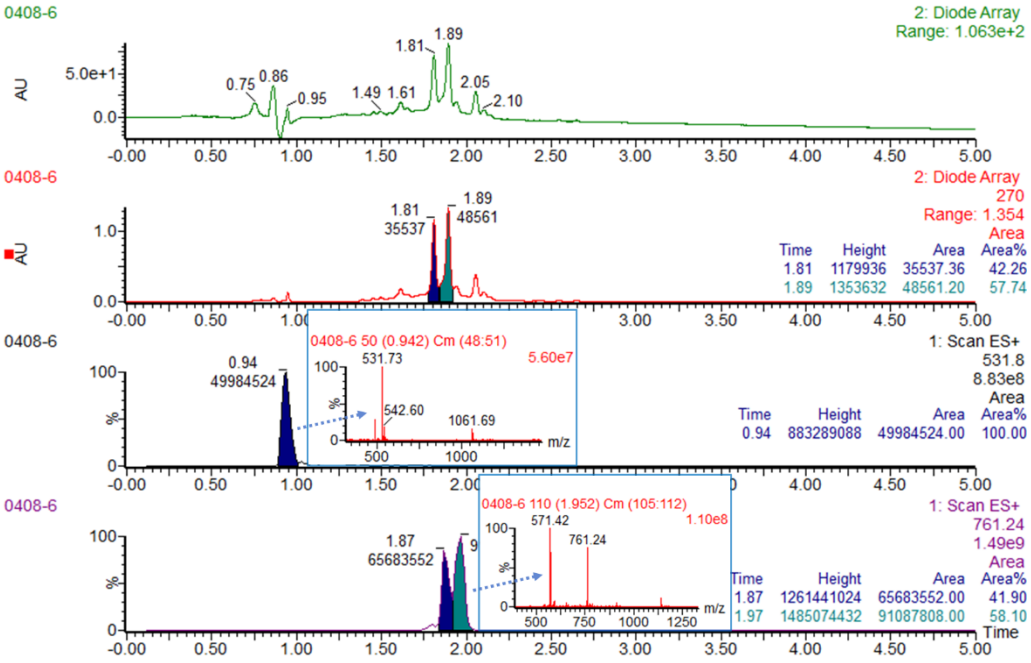

Fig S152. UPLC-MS chromatogram of **L10** and 3,6-DCT reaction mixture including TIC, UV curves (full-wavelength and extracted at 270 nm) and ESI-MS spectrum. Extract mass chromatograms from full scan data. The yield of the corresponding cyclodimerization products was determined to be 42% using equation 1.

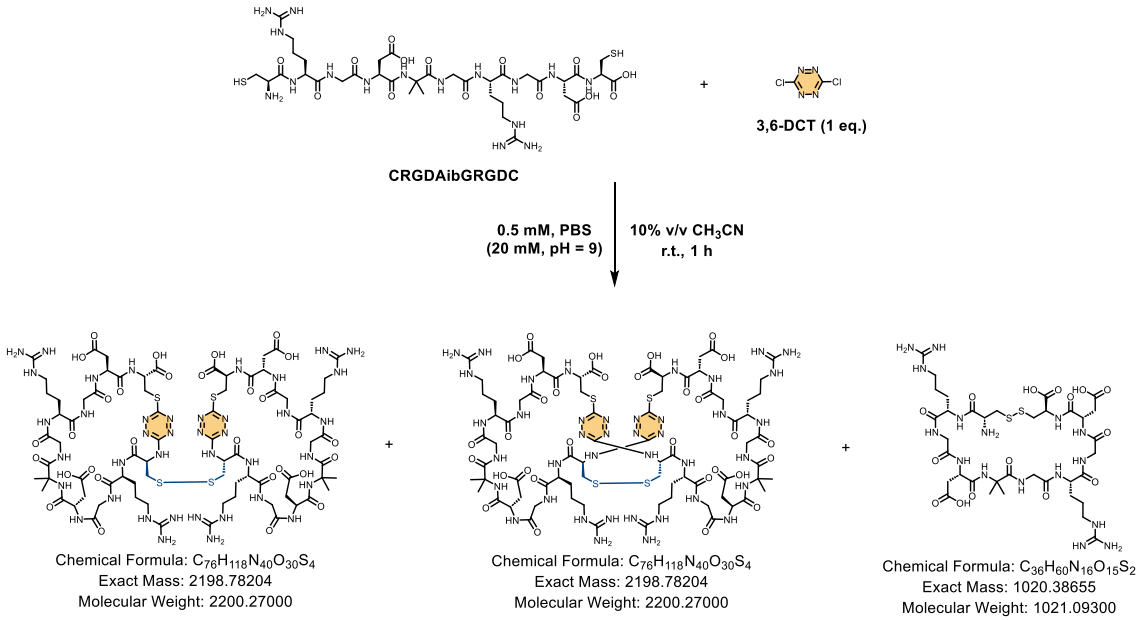

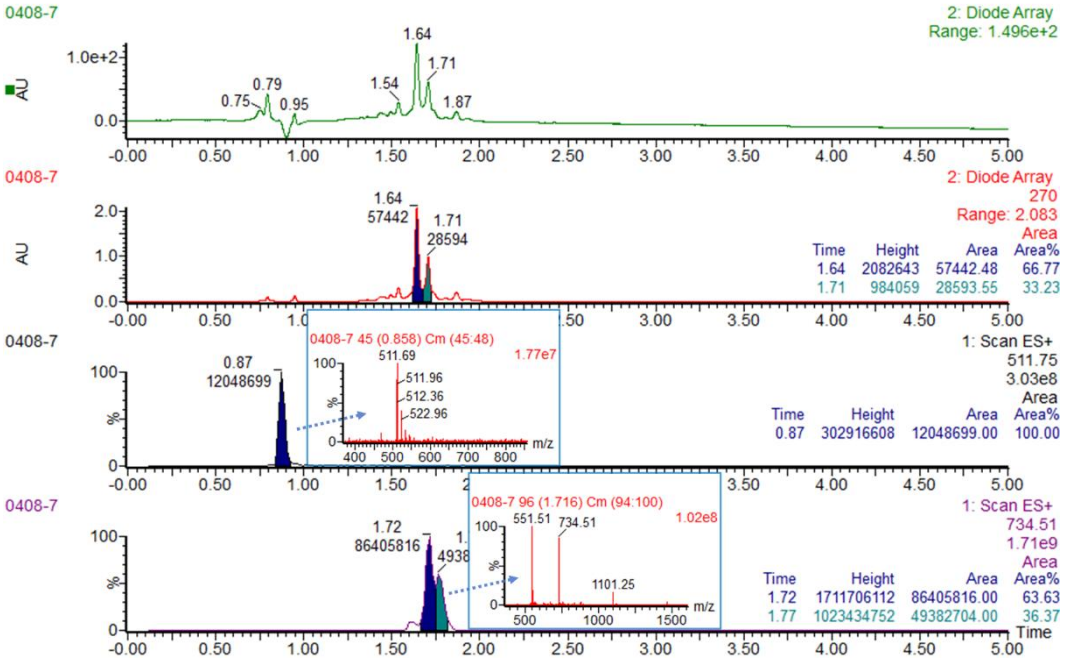

Fig S153. UPLC-MS chromatogram of **L11** and 3,6-DCT reaction mixture including TIC, UV curves (full-wavelength and extracted at 270 nm) and ESI-MS spectrum. Extract mass chromatograms from full scan data. The yield of the corresponding cyclodimerization products was determined to be 43% using equation 1.

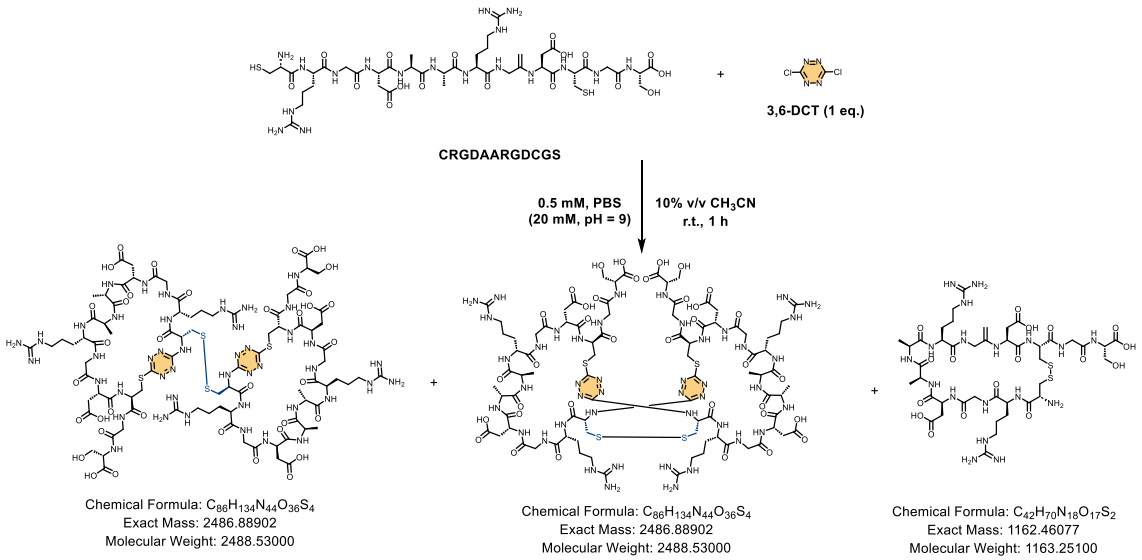

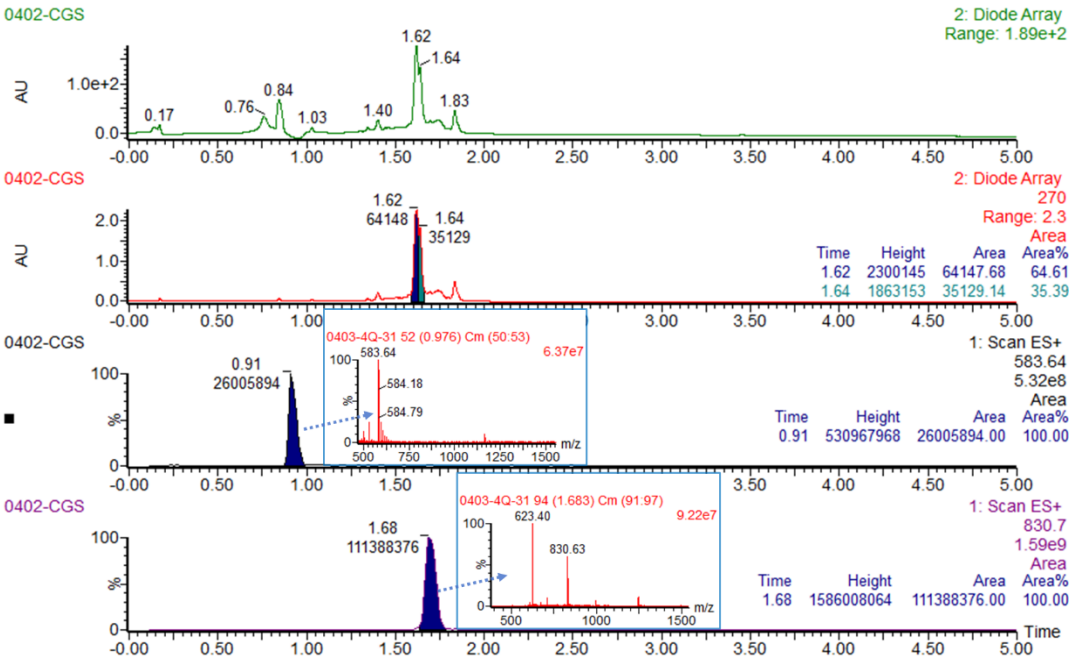

Fig S154. UPLC-MS chromatogram of **L18** and 3,6-DCT reaction mixture including TIC, UV curves (full-wavelength and extracted at 270 nm) and ESI-MS spectrum. Extract mass chromatograms from full scan data. The yield of the corresponding cyclodimerization products was determined to be 50% using equation 1.

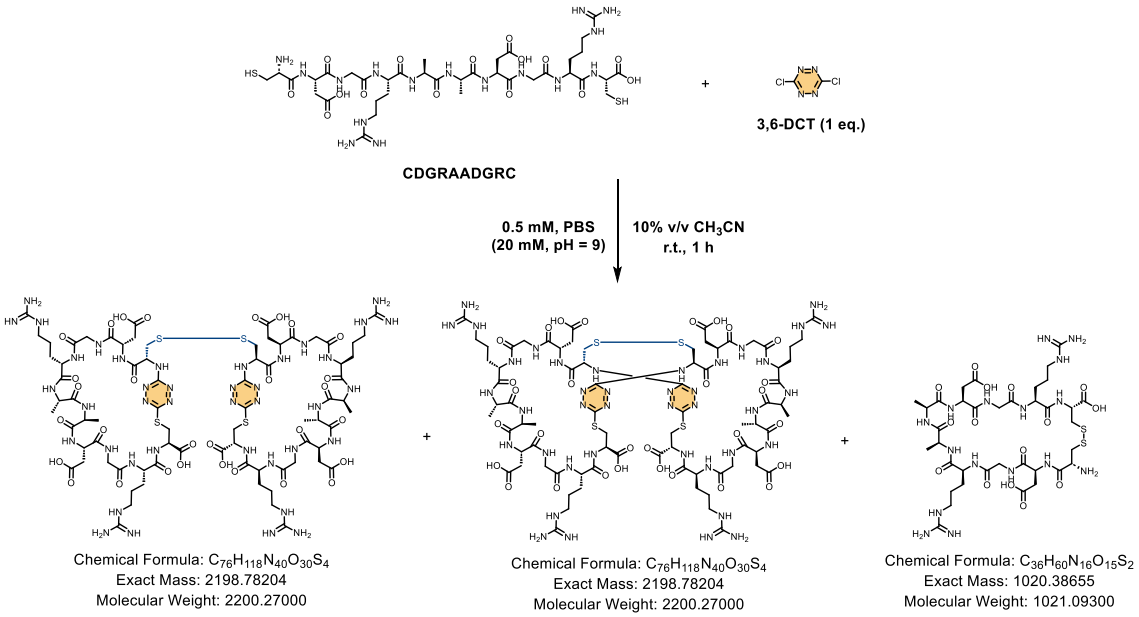

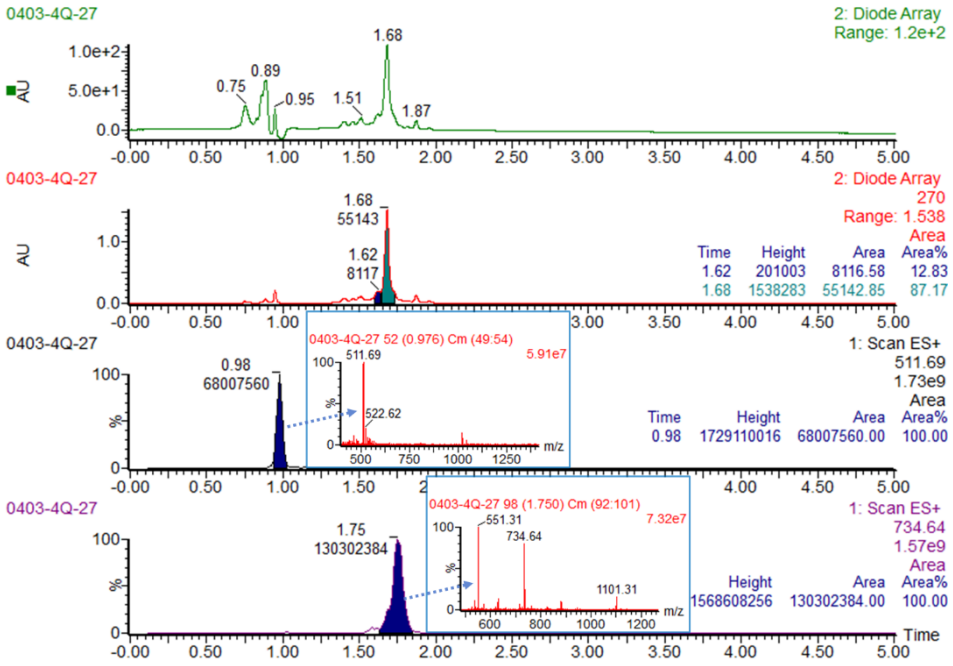

Fig S155. UPLC-MS chromatogram of **L21** and 3,6-DCT reaction mixture including TIC, UV curves (full-wavelength and extracted at 270 nm) and ESI-MS spectrum. Extract mass chromatograms from full scan data. The yield of the corresponding cyclodimerization products was determined to be 31% using equation 1.

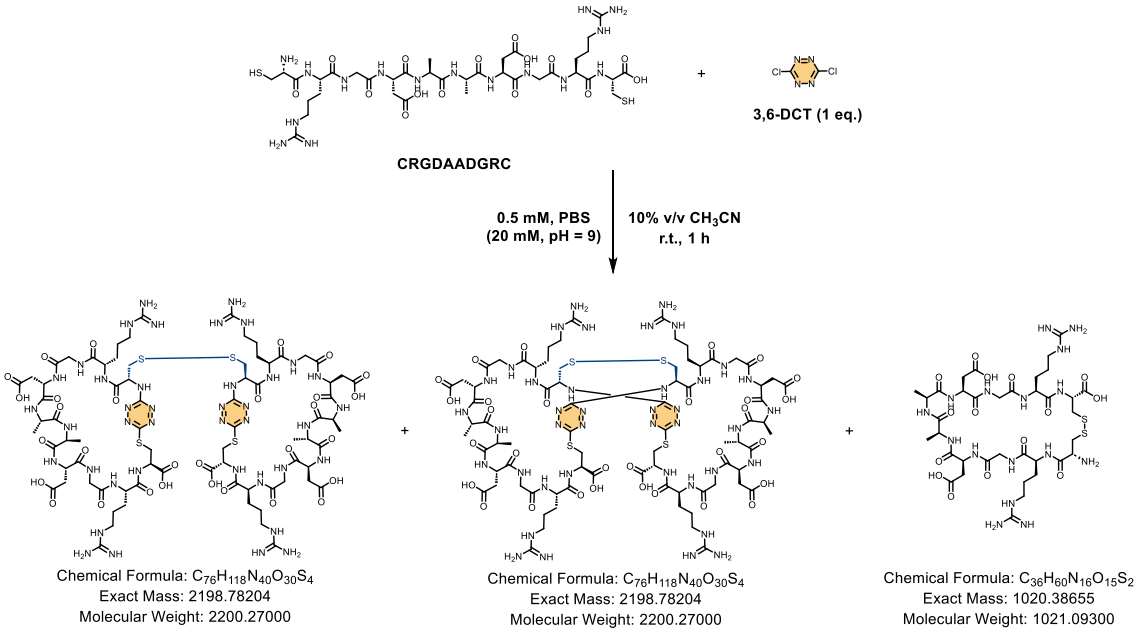

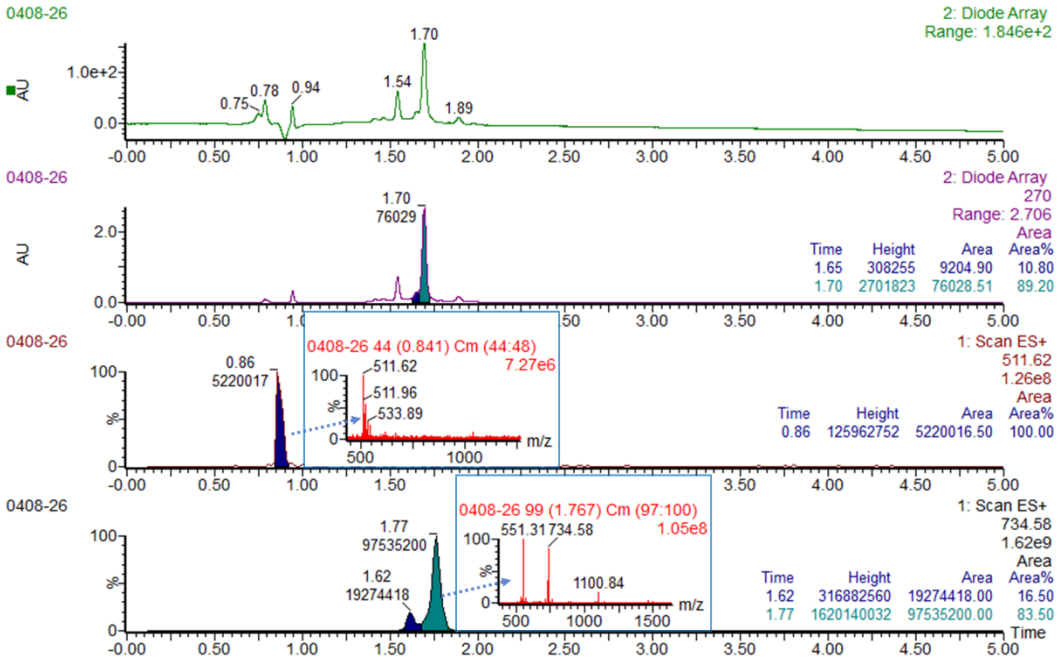

Fig S156. UPLC-MS chromatogram of **L22** and 3,6-DCT reaction mixture including TIC, UV curves (full-wavelength and extracted at 270 nm) and ESI-MS spectrum. Extract mass chromatograms from full scan data. The yield of the corresponding cyclodimerization products was determined to be 39% using equation 1.

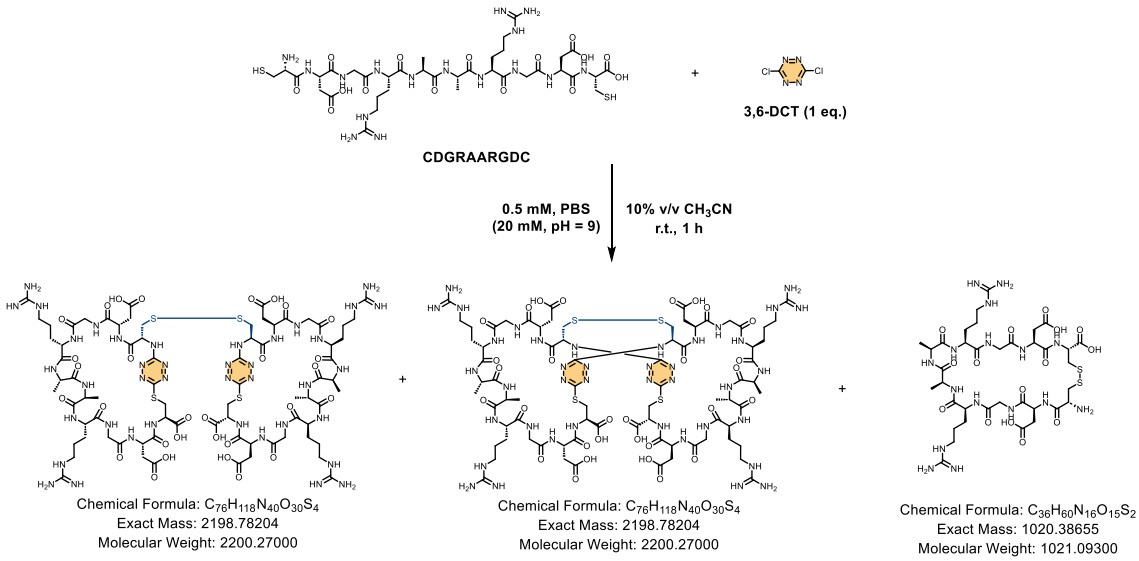

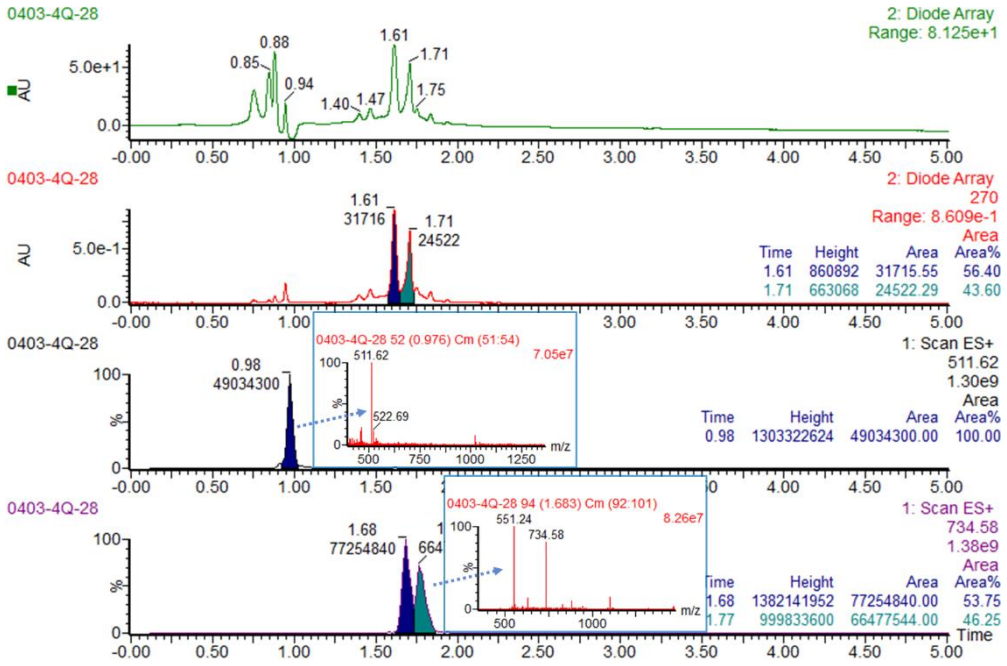

Fig S157. UPLC-MS chromatogram of **L23** and 3,6-DCT reaction mixture including TIC, UV curves (full-wavelength and extracted at 270 nm) and ESI-MS spectrum. Extract mass chromatograms from full scan data. The yield of the corresponding cyclodimerization products was determined to be 27% using equation 1.

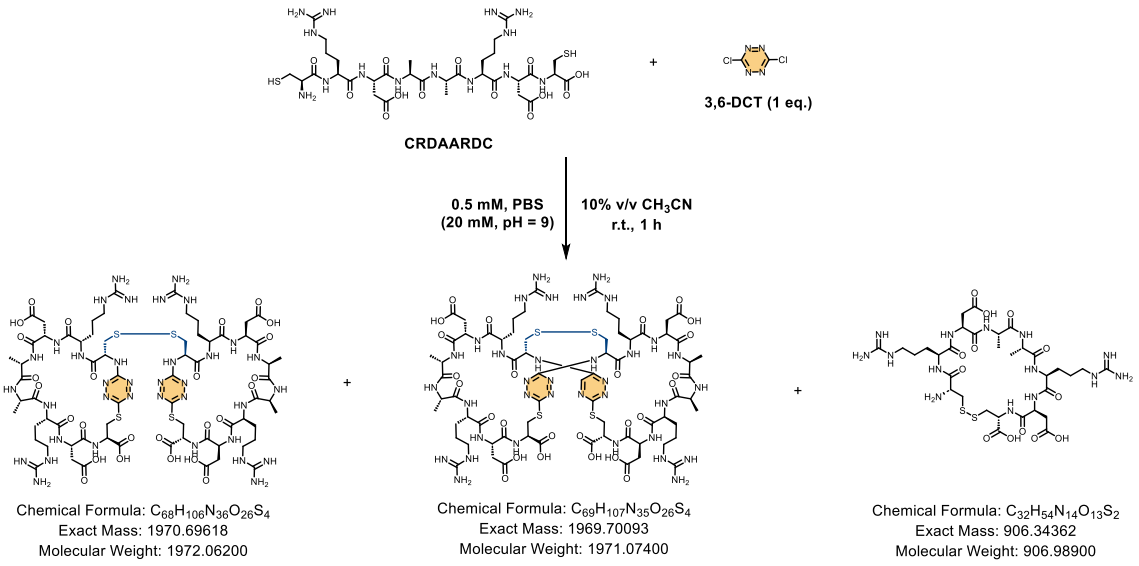

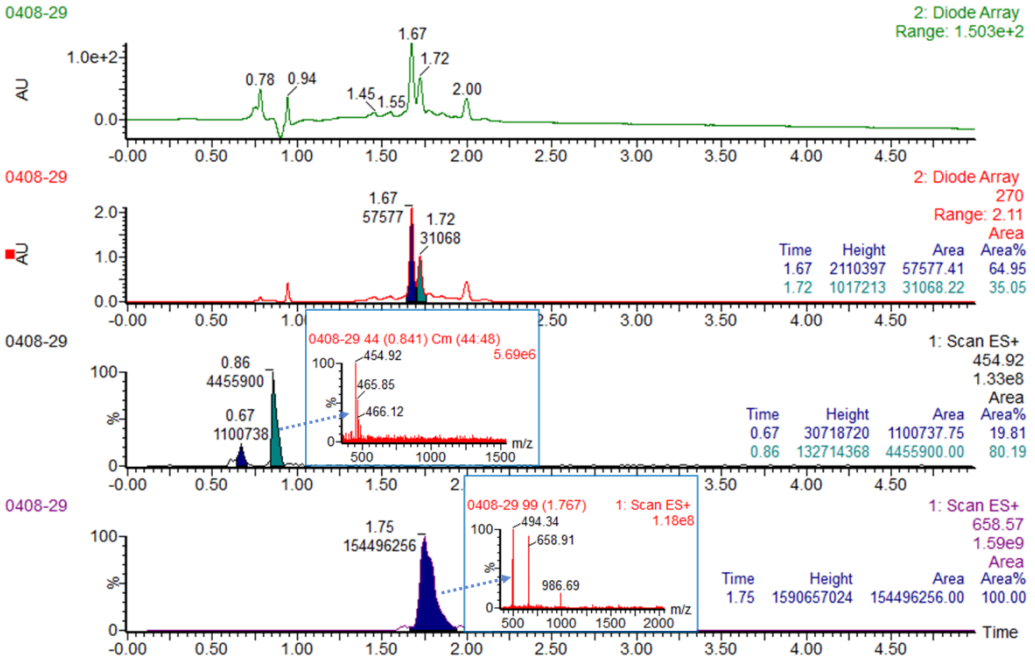

Fig S158. UPLC-MS chromatogram of **L24** and 3,6-DCT reaction mixture including TIC, UV curves (full-wavelength and extracted at 270 nm) and ESI-MS spectrum. Extract mass chromatograms from full scan data. The yield of the corresponding cyclodimerization products was determined to be 44% using equation 1.

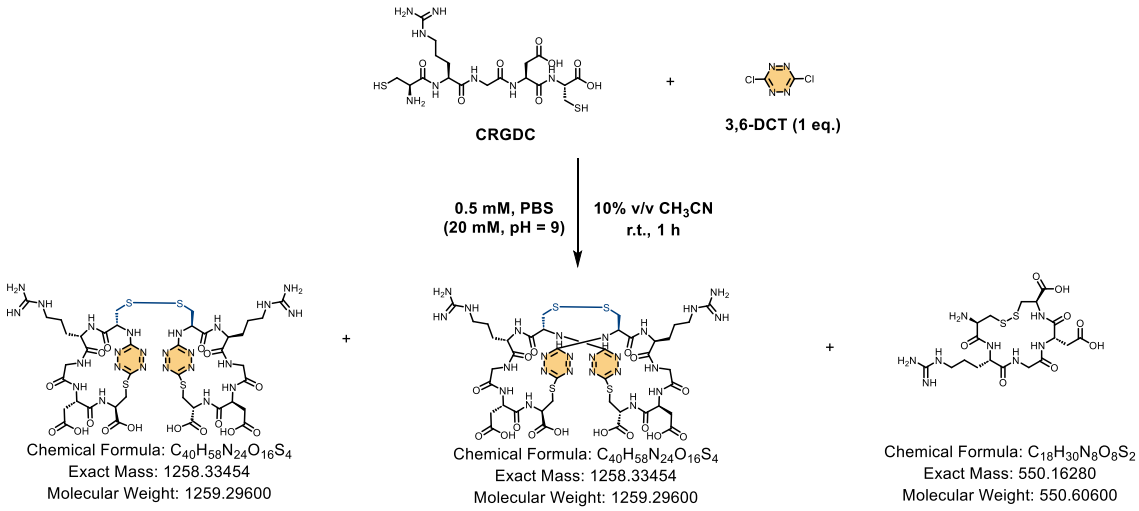

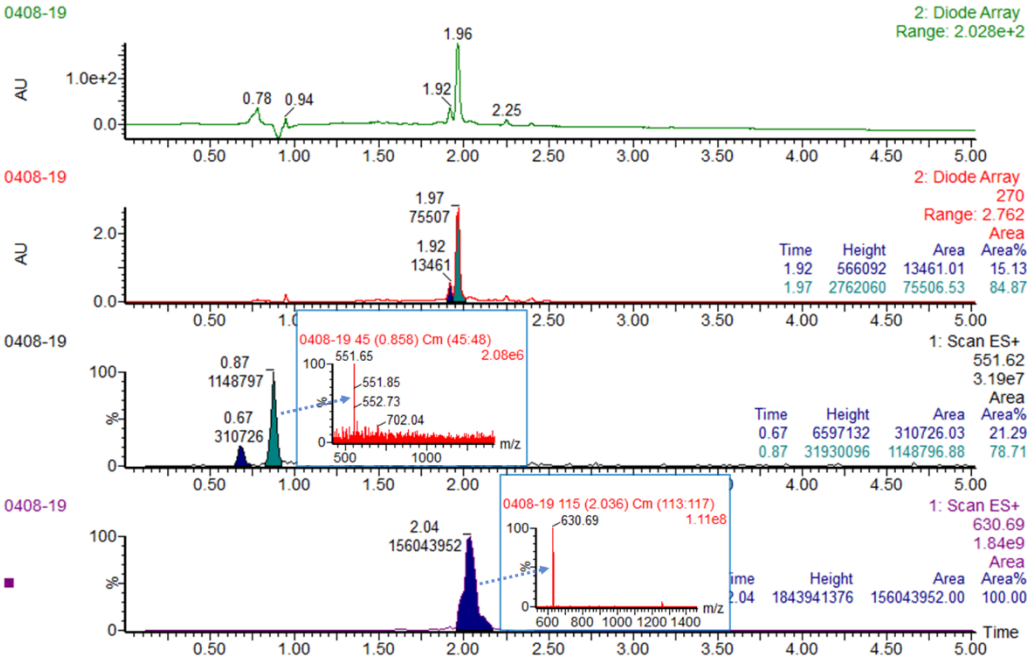

Fig S159. UPLC-MS chromatogram of **L25** and 3,6-DCT reaction mixture including TIC, UV curves (full-wavelength and extracted at 270 nm) and ESI-MS spectrum. Extract mass chromatograms from full scan data. The yield of the corresponding cyclodimerization products was determined to be 44% using equation 1.

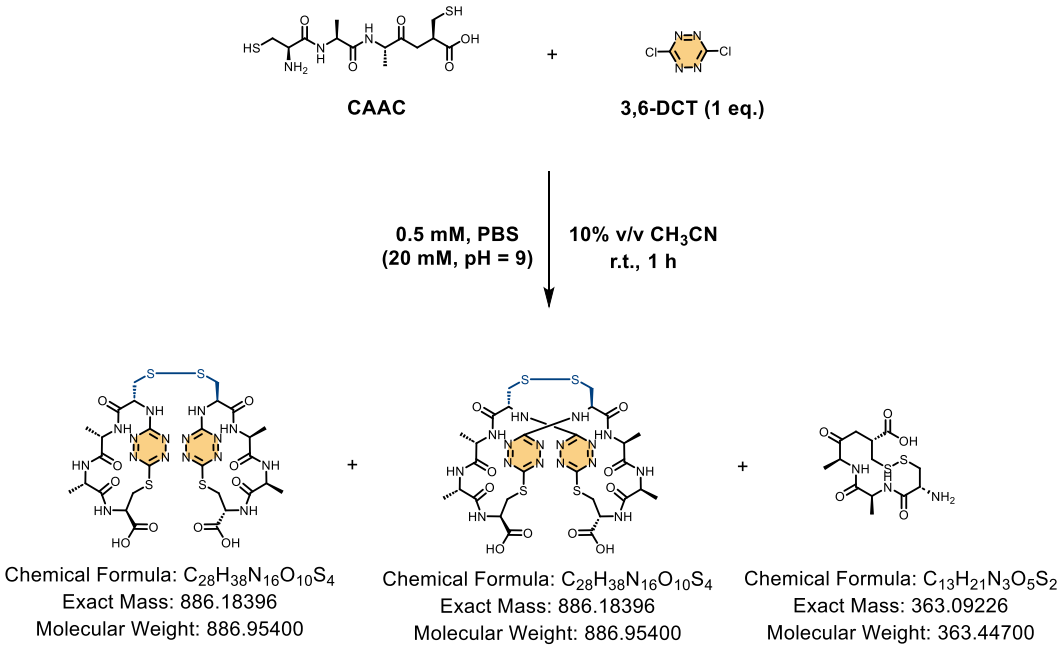

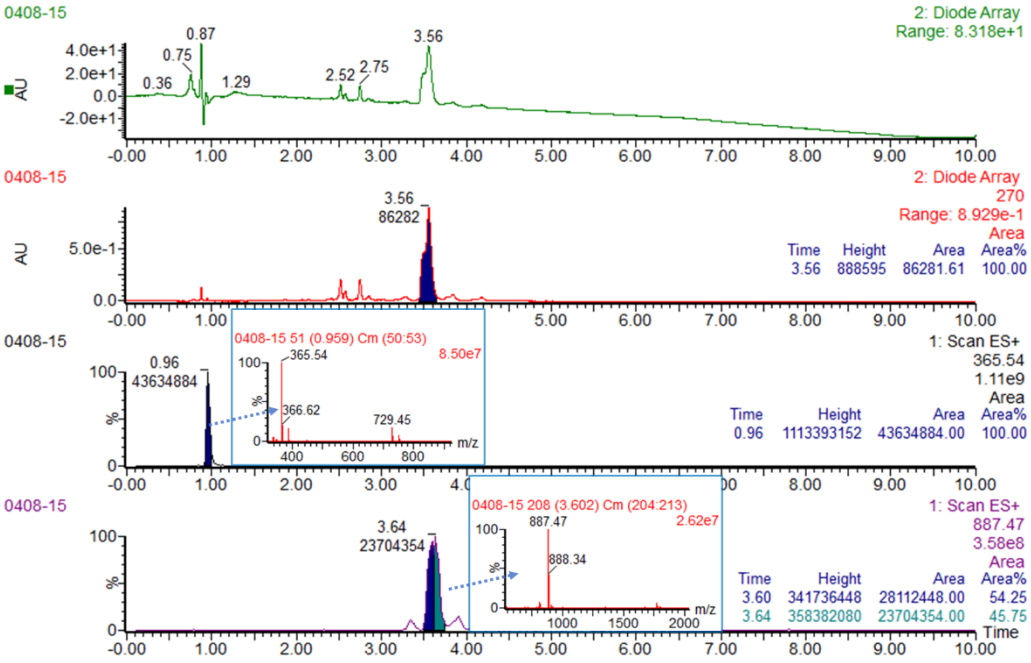

Fig S160. UPLC-MS chromatogram of **L26** and 3,6-DCT reaction mixture including TIC, UV curves (full-wavelength and extracted at 270 nm) and ESI-MS spectrum. Extract mass chromatograms from full scan data. The yield of the corresponding cyclodimerization products was determined to be 43% using equation 1.

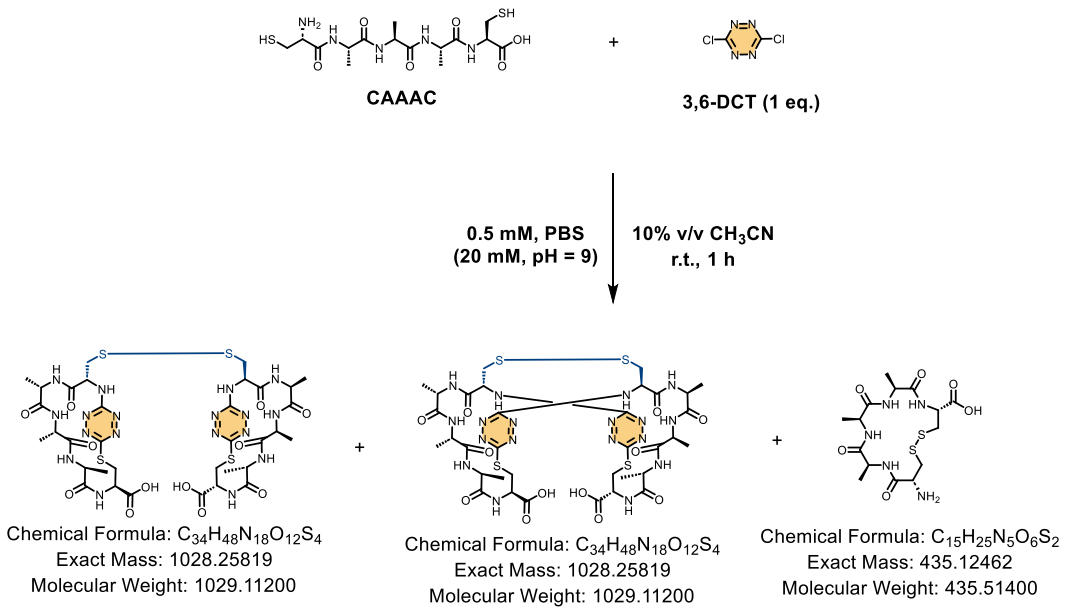

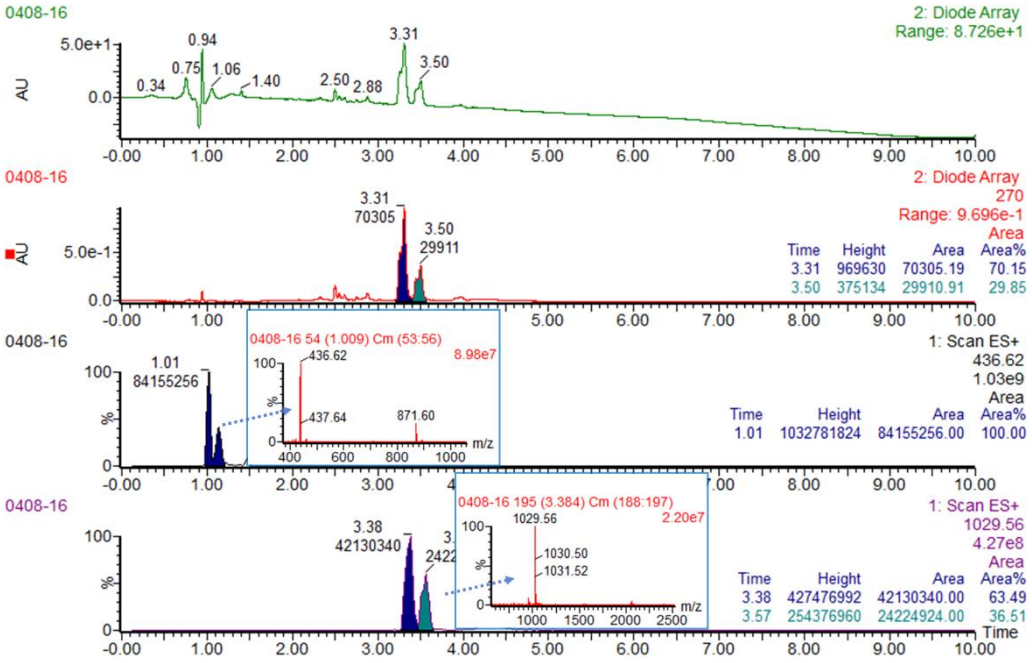

Fig S161. UPLC-MS chromatogram of **L27** and 3,6-DCT reaction mixture including TIC, UV curves (full-wavelength and extracted at 270 nm) and ESI-MS spectrum. Extract mass chromatograms from full scan data. The yield of the corresponding cyclodimerization products was determined to be 50% using equation 1.

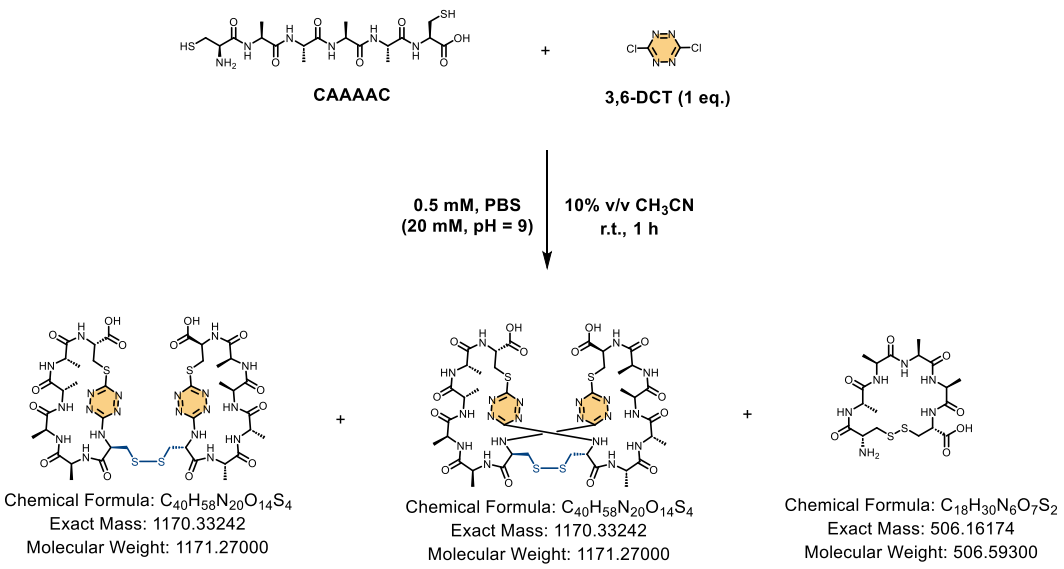

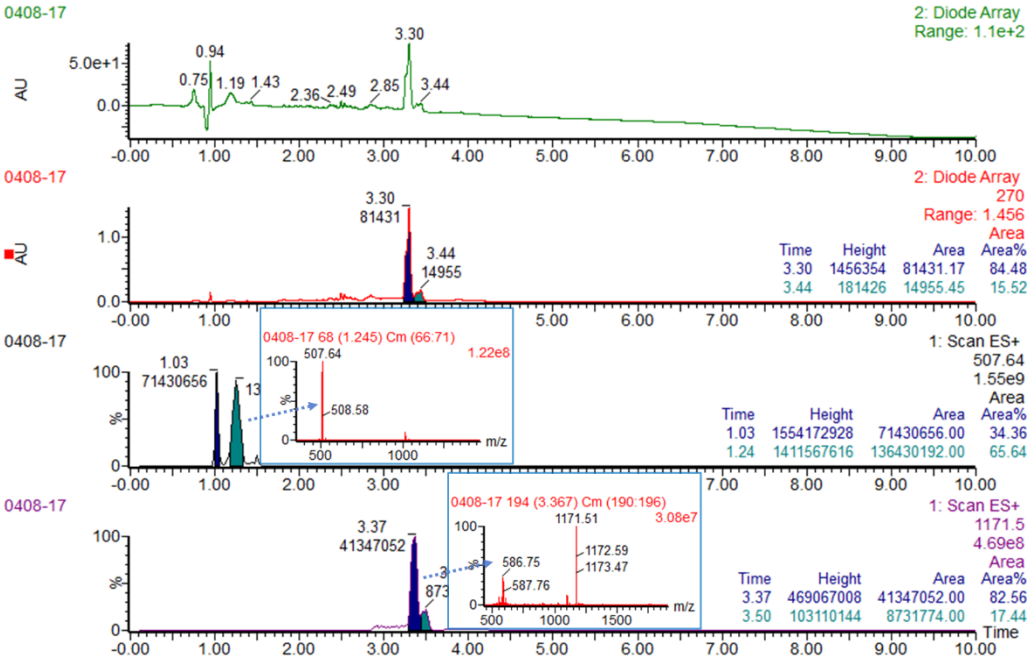

Fig S162. UPLC-MS chromatogram of **L28** and 3,6-DCT reaction mixture including TIC, UV curves (full-wavelength and extracted at 270 nm) and ESI-MS spectrum. Extract mass chromatograms from full scan data. The yield of the corresponding cyclodimerization products was determined to be 48% using equation 1.

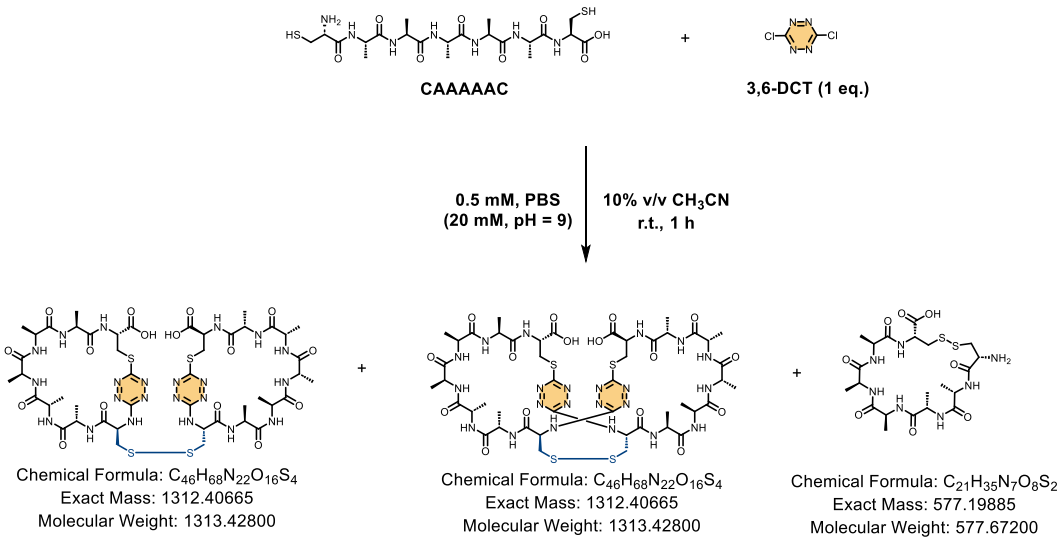

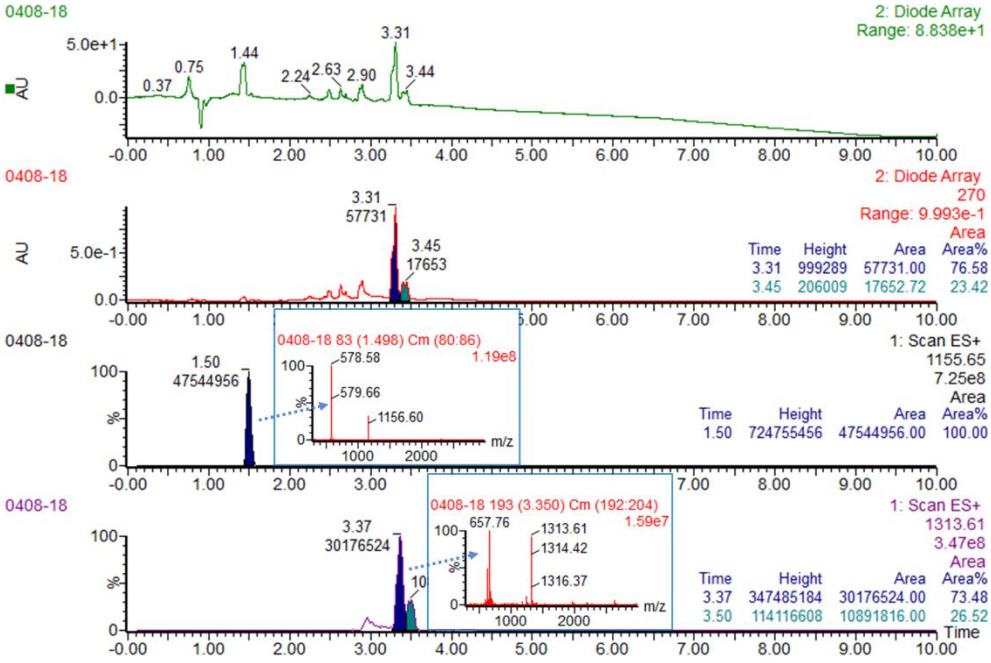

Fig S163. UPLC-MS chromatogram of **L29** and 3,6-DCT reaction mixture including TIC, UV curves (full-wavelength and extracted at 270 nm) and ESI-MS spectrum. Extract mass chromatograms from full scan data. The yield of the corresponding cyclodimerization products was determined to be 37% using equation 1.

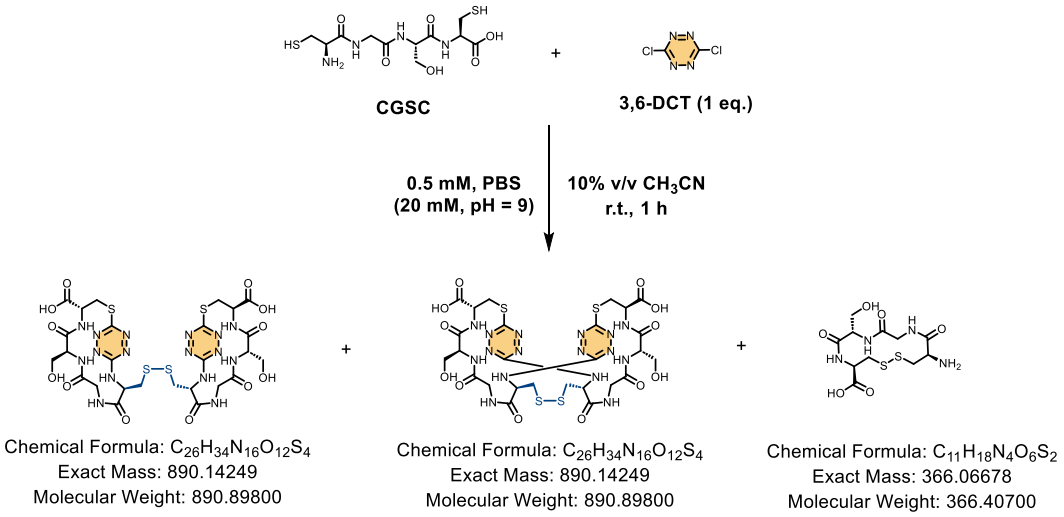

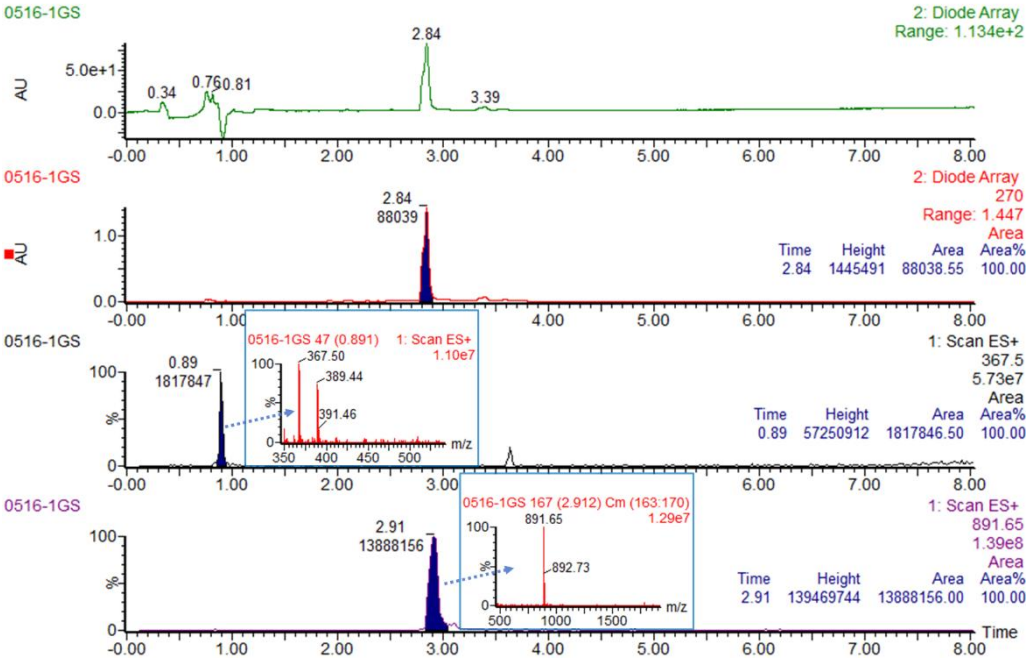

Fig S164. UPLC-MS chromatogram of **L30** and 3,6-DCT reaction mixture including TIC, UV curves (full-wavelength and extracted at 270 nm) and ESI-MS spectrum. Extract mass chromatograms from full scan data. The yield of the corresponding cyclodimerization products was determined to be 44% using equation 1.

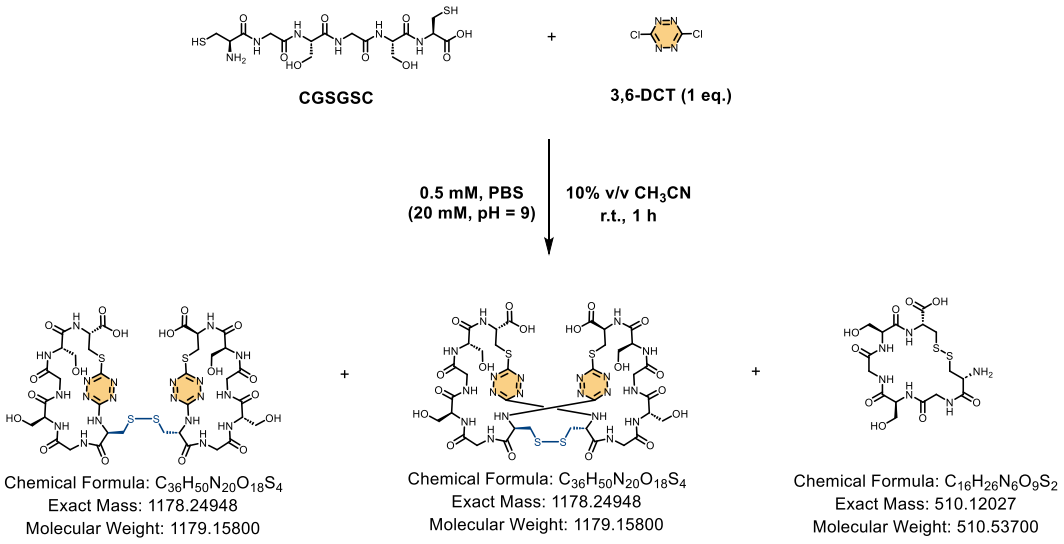

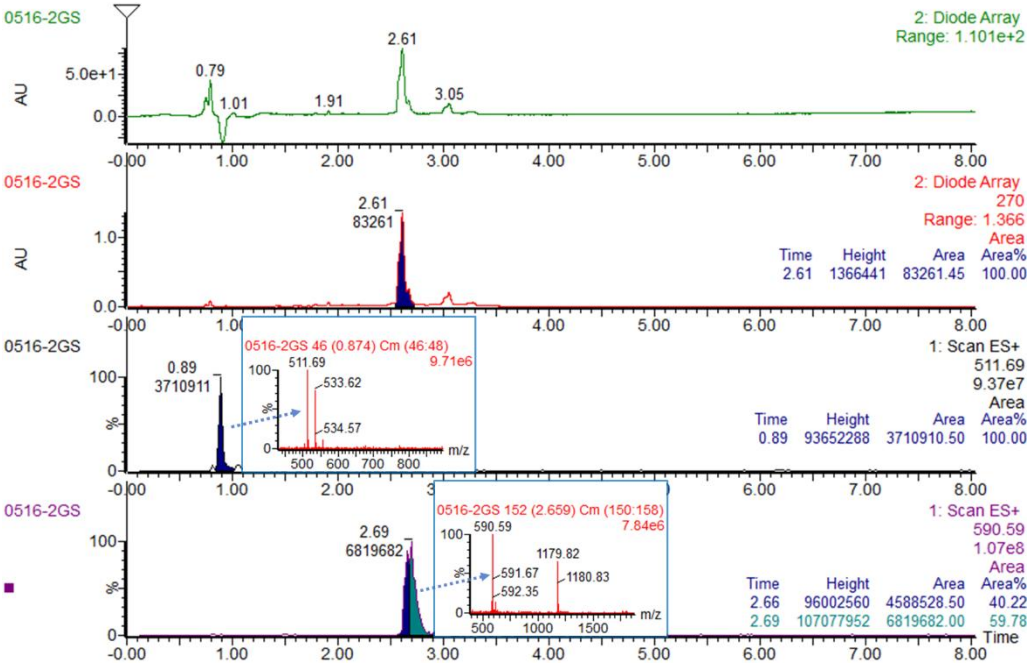

Fig S165. UPLC-MS chromatogram of **L31** and 3,6-DCT reaction mixture including TIC, UV curves (full-wavelength and extracted at 270 nm) and ESI-MS spectrum. Extract mass chromatograms from full scan data. The yield of the corresponding cyclodimerization products was determined to be 41% using equation 1.

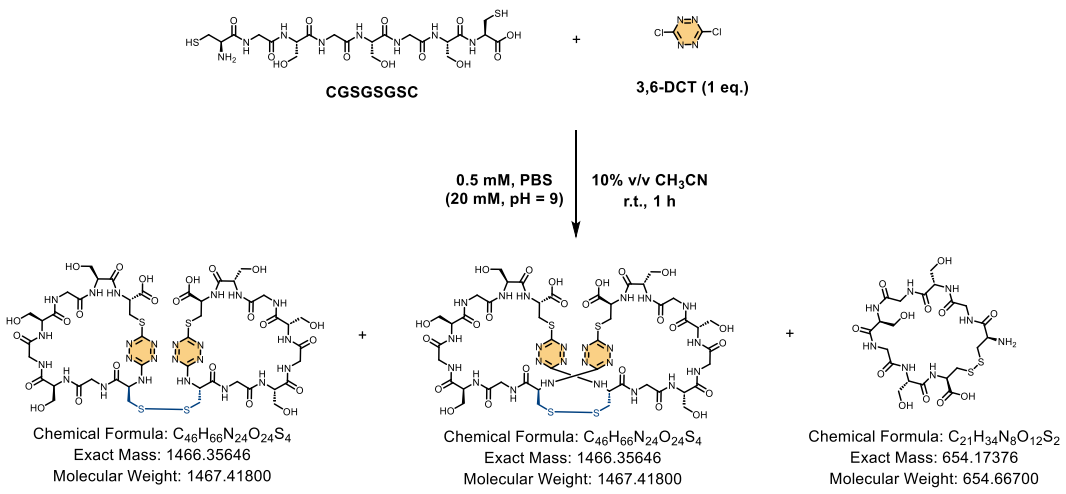

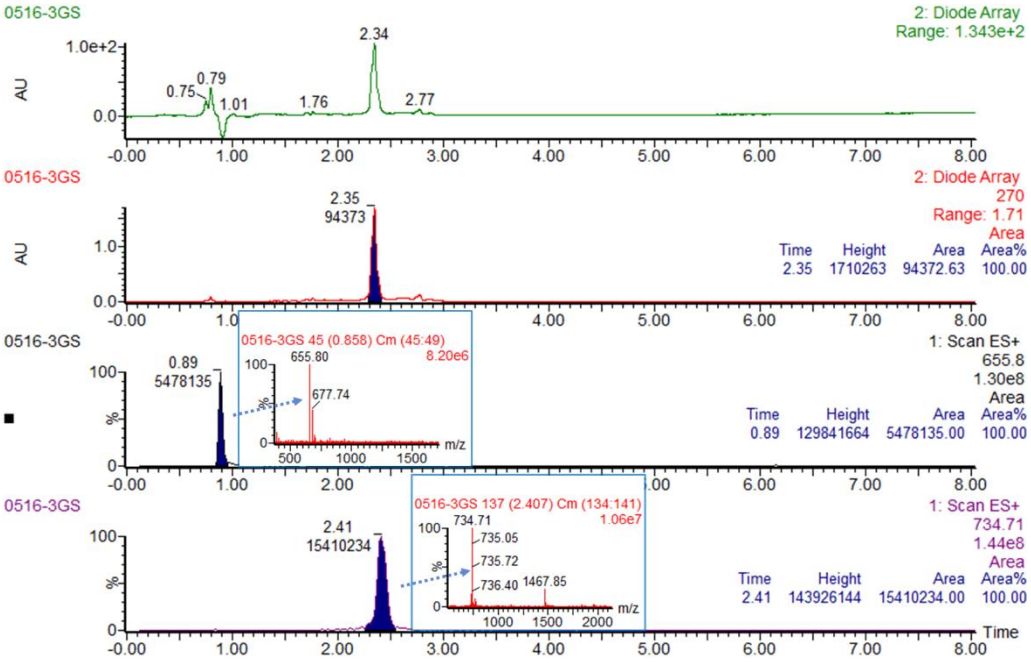

Fig S166. UPLC-MS chromatogram of **L32** and 3,6-DCT reaction mixture including TIC, UV curves (full-wavelength and extracted at 270 nm) and ESI-MS spectrum. Extract mass chromatograms from full scan data. The yield of the corresponding cyclodimerization products was determined to be 47% using equation 1.

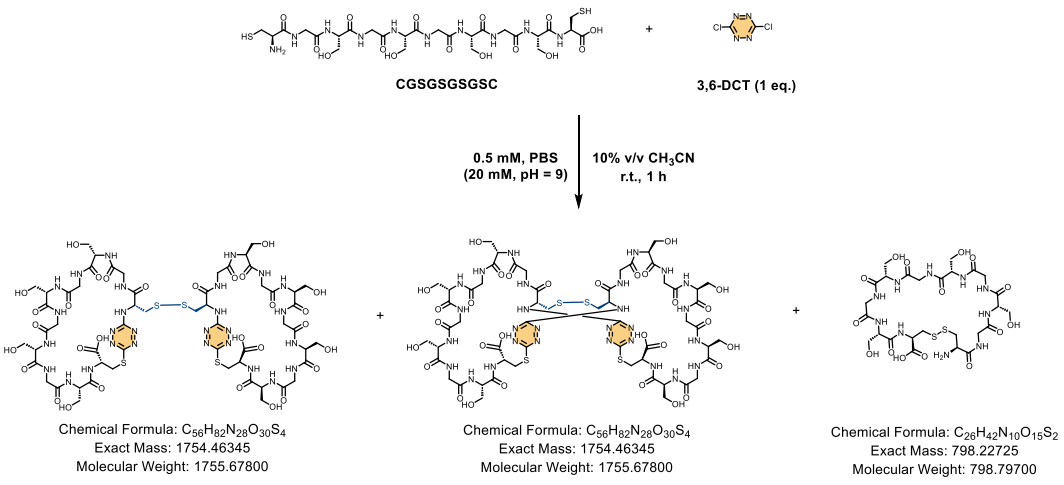

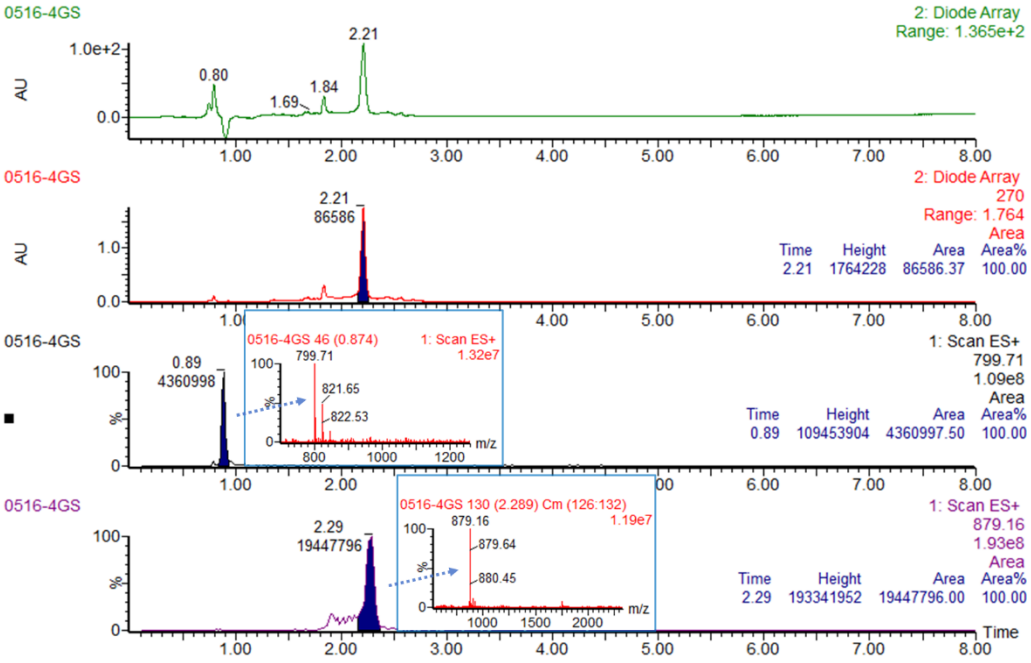

Fig S167. UPLC-MS chromatogram of **L33** and 3,6-DCT reaction mixture including TIC, UV curves (full-wavelength and extracted at 270 nm) and ESI-MS spectrum. Extract mass chromatograms from full scan data. The yield of the corresponding cyclodimerization products was determined to be 43% using equation 1.

6.2 Calculation of LC-MS yield of monocyclic products

（1）Construction of LC-MS-based yield calculation method using the standard monocyclic products

The dried peptide substrate with **L2**, was dissolved in appropriate amount of PBS (20 mM, pH = 9.0) to reach a concentration of 0.56 mM. To this solution, 3,6-DCT (1.0 equiv.) dissolved in acetonitrile (1/9 of the volume of buffer) was added. The final concentrations in the reaction were 0.5 mM peptide, 0.5 mM 3,6-DCT and 10% acetonitrile, followed by thorough mixing. The reaction mixture was shaken at 25 °C and 800 rpm for 1 h on a thermostatic shaker, and the standard monocyclic products was obtained after purification by HPLC.

The lyophilized products, standard monocyclic products (**M2-tz**) were dissolved in H_2O to prepare standard solutions of different concentrations. Under the conditions of Method A, 10 μL of each solution were injected into the LC-MS in equal volumes. Considering that all monocyclic products with Tz have a 285nm characteristic absorption peak, MassLynx V4.2 software was used to integrate the peak area at 285nm

for calibration curve calculation.

Tab S11 The LC-MS data for M2-tz at different concentrations

Entry	Concentration of M2-tz	Peak area of M2-tz in 285 nm
1	0.0625 mM	14934
2	0.125 mM	35214
3	0.25 mM	76467
4	0.5 mM	139326
5	1 mM	273801

A high-precision calibration curve was established within the linear dynamic range of 0.0625 mM to 1.0 mM (5 points), where the UV detector exhibited an excellent linear response: **y = 273146x + 2105 (R^2 = 0.9987)**

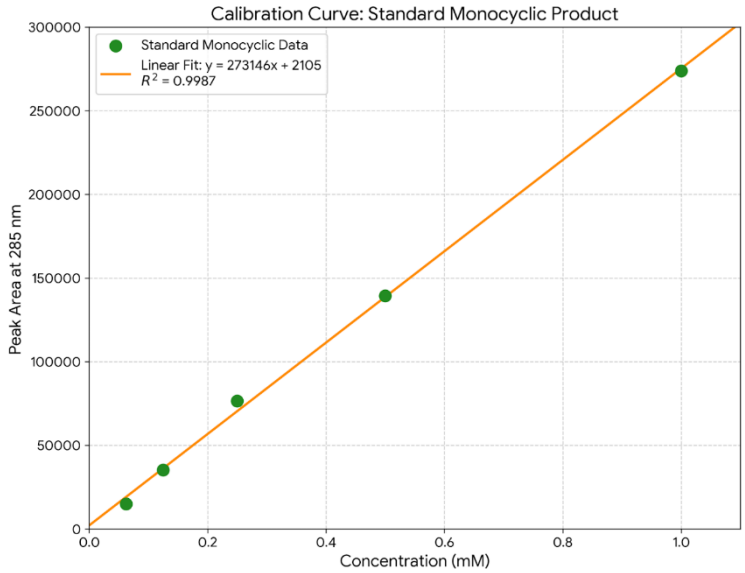

Fig S168. Calibration curve of purified **M2-tz** (0.0625–0.25 mM) at 285 nm, **y = 273146x + 2105 (R^2 = 0.9987)**

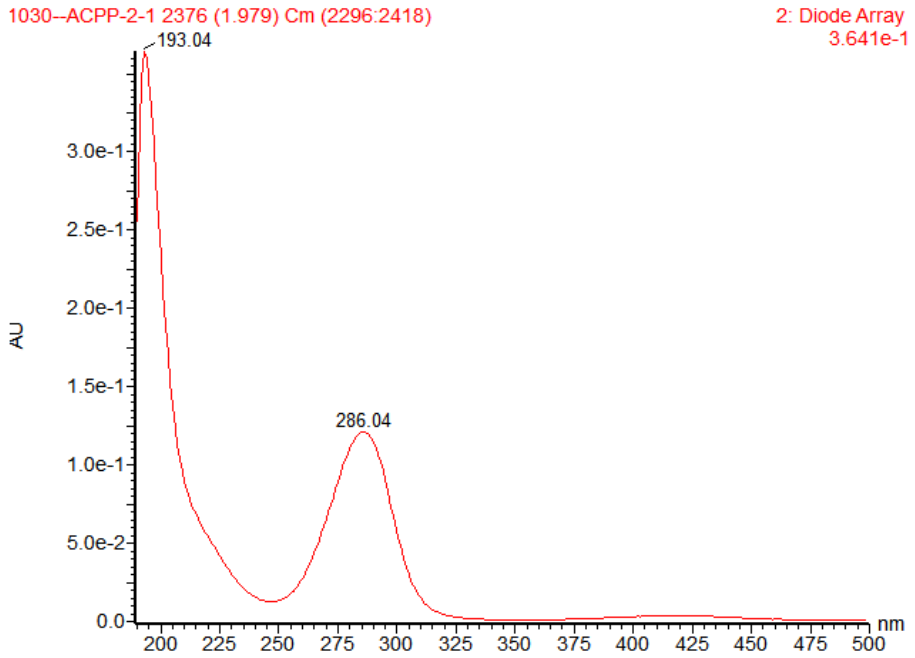

Fig S169. The UV characteristic absorption of **M2-tz**.

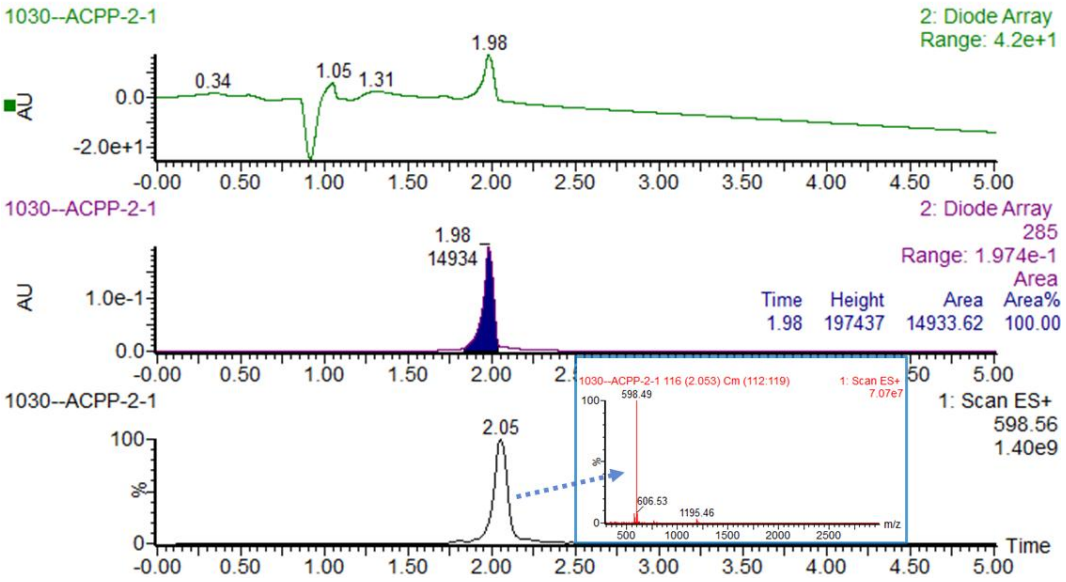

Fig S170. LC-MS for **M2-tz** (0.0625 mM) including TIC, UV curves (full-wavelength and extracted at 285 nm) and ESI-MS spectrum. Extract mass chromatograms from full scan data.

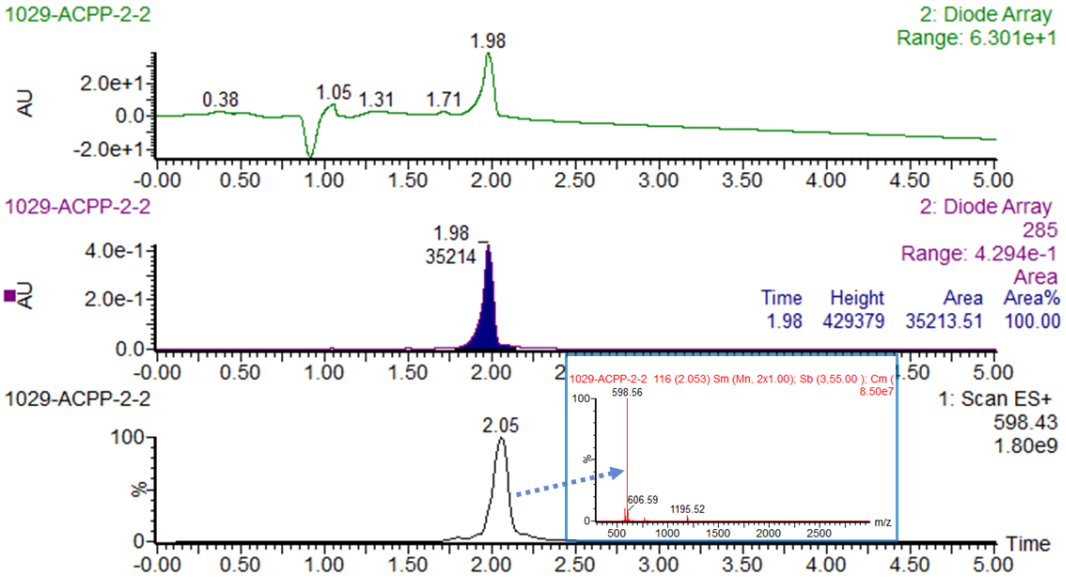

Fig S171. LC-MS for **M2-tz** (0.125 mM) including TIC, UV curves (full-wavelength and extracted at 285 nm) and ESI-MS spectrum. Extract mass chromatograms from full scan data.

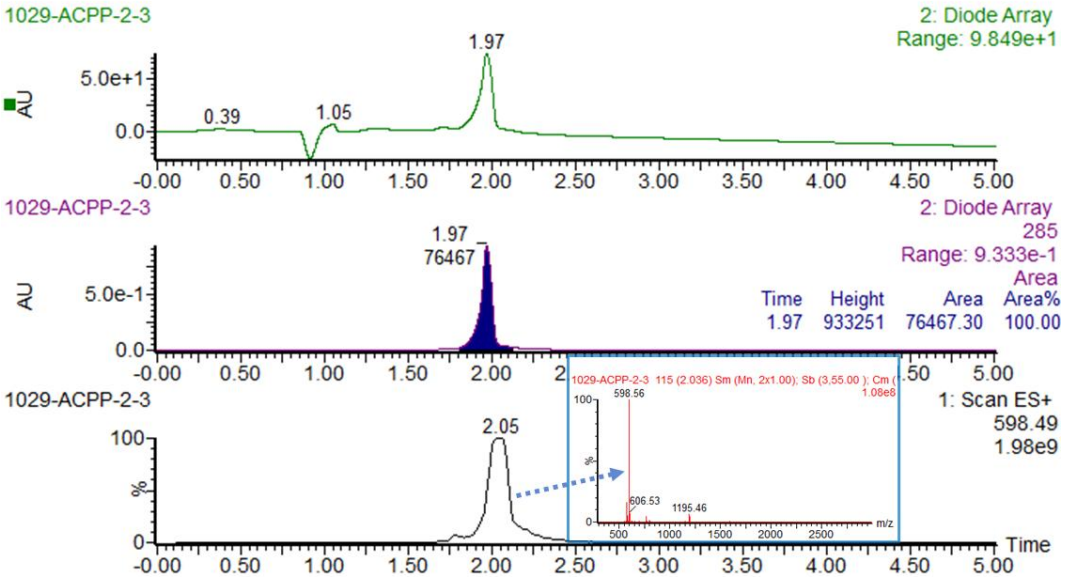

Fig S172 LC-MS for **M2-tz** (0.25 mM) including TIC, UV curves (full-wavelength and extracted at 285 nm) and ESI-MS spectrum. Extract mass chromatograms from full scan data.

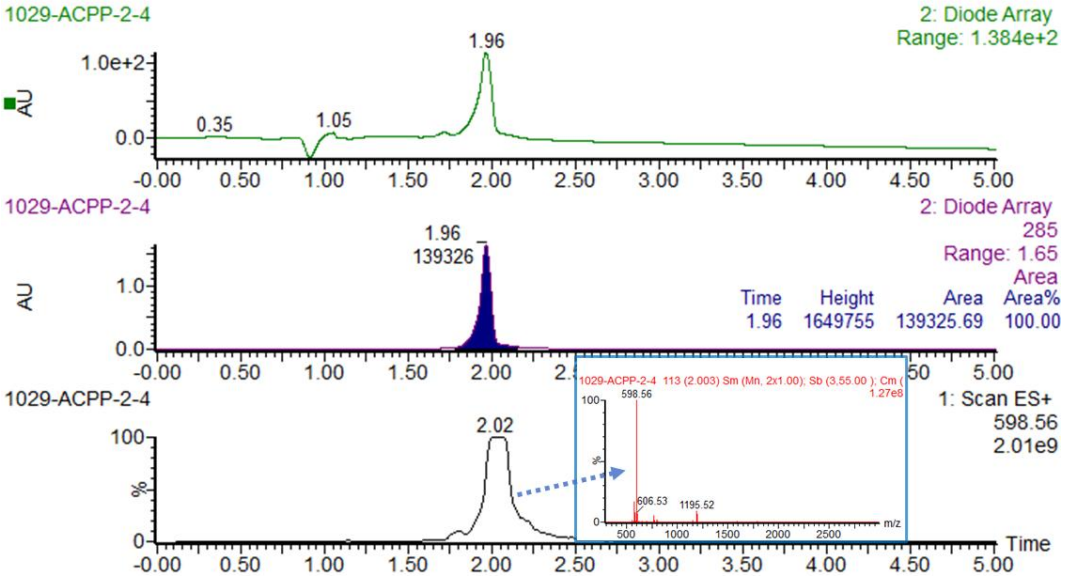

Fig S173 LC-MS for **M2-tz** (0.5 mM) including TIC, UV curves (full-wavelength and extracted at 285 nm) and ESI-MS spectrum. Extract mass chromatograms from full scan data.

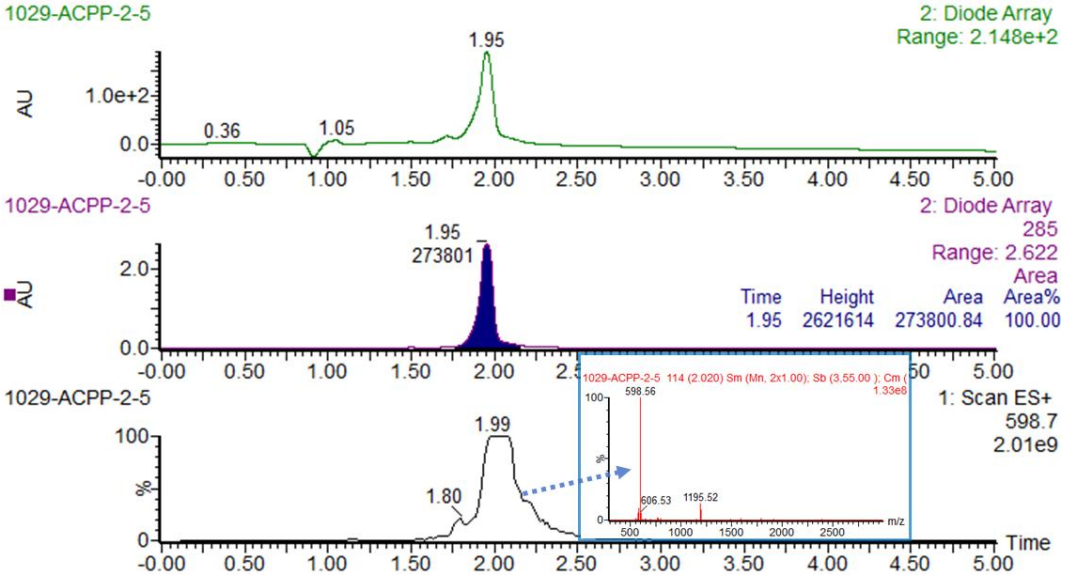

Fig S174 LC-MS for **M2-tz** (1 mM) including TIC, UV curves (full-wavelength and extracted at 285 nm) and ESI-MS spectrum. Extract mass chromatograms from full scan data.

（2）Calculation Equation

The peak area recorded at 285 nm was converted into concentration using the linear regression equation derived from the calibration curve.

Equation 3:

$$\text{Yield (\%)} = \frac{(A_{\text{sample}} - 2105)/273146}{C_{\text{theoretical}}} \times 100\%$$

Where A_{sample} is the measured peak area at 285 nm. $C_{theoretical}$ is the theoretical maximum

concentration of the monocyclic product.

6.3 Reaction of peptides without N-Cys

The dried peptide substrate without N-Cys (1.0 equiv.), such as Ac-CRGDAARGDC (**L12**), was dissolved in appropriate amount of PBS (20 mM, pH = 9.0) to reach a concentration of 0.56 mM. To this solution, 3,6-DCT (1.0 equiv.) dissolved in acetonitrile (1/9 of the volume of buffer) was added. The final concentrations in the reaction were 0.5 mM peptide, 0.5 mM 3,6-DCT and 10% acetonitrile, followed by thorough mixing. The reaction mixture was shaken at 25 °C and 800 rpm for 1 h on a thermostatic shaker.

After completion, 50 μL of the reaction mixture was collected, and 10 μL was injected into the UPLC-MS for analysis. The peak area of the monocyclic products at 285 nm was recorded. Determine the LC-MS yield using **Equation 3**. Detailed data are shown in **Table S12**.

Tab S12. The LC-MS data for peptides without N-Cys using Method A

Peptide sequence	Peak area	HPLC Yield (%)[a]
Ac-CRGDAARGDC	72473	51.53
Ac-CRGDGGRGDC	81956	58.47
Ac-CRGDpPRGDC	89435	63.95
Ac-CRGDNGRGDC	69616	49.43
Ac-CRGDPGRGDC	93140	66.66
Ac-CRGDAibPRGDC	75115	53.46
Ac-CRGDAibGRGDC	86529	61.82
GSCRGDAARGDC	41071	28.53
GSCRGDAARGDCGS	51119	35.89

[a]Yields were determined by LC-MS analysis using **Equation 3**

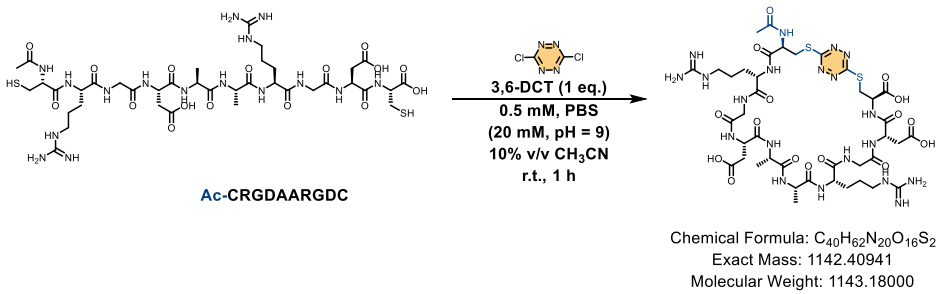

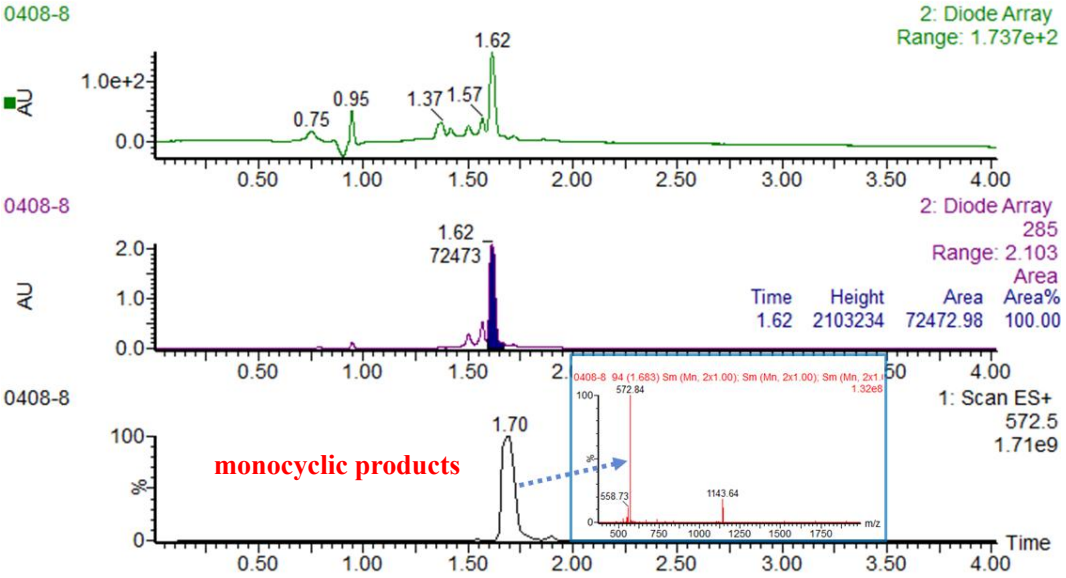

Fig S175. UPLC-MS chromatogram of **L12** and 3,6-DCT reaction mixture including TIC, UV curves (full-wavelength and extracted at 285 nm) and ESI-MS spectrum. Extract mass chromatograms from full scan data. The yield of the corresponding monocyclic products was determined to be 52% using Equation 3.

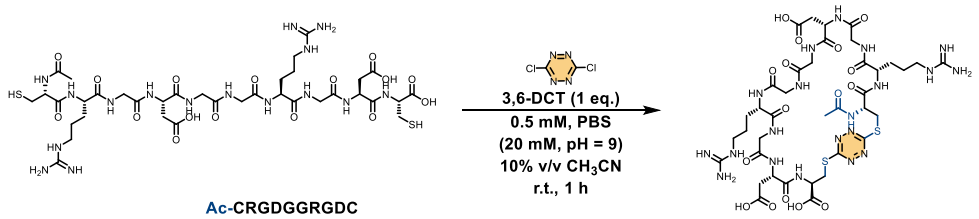

Chemical Formula: $C_{38}H_{58}N_{20}O_{16}S_2$
Exact Mass: 1114.37811
Molecular Weight: 1115.12600

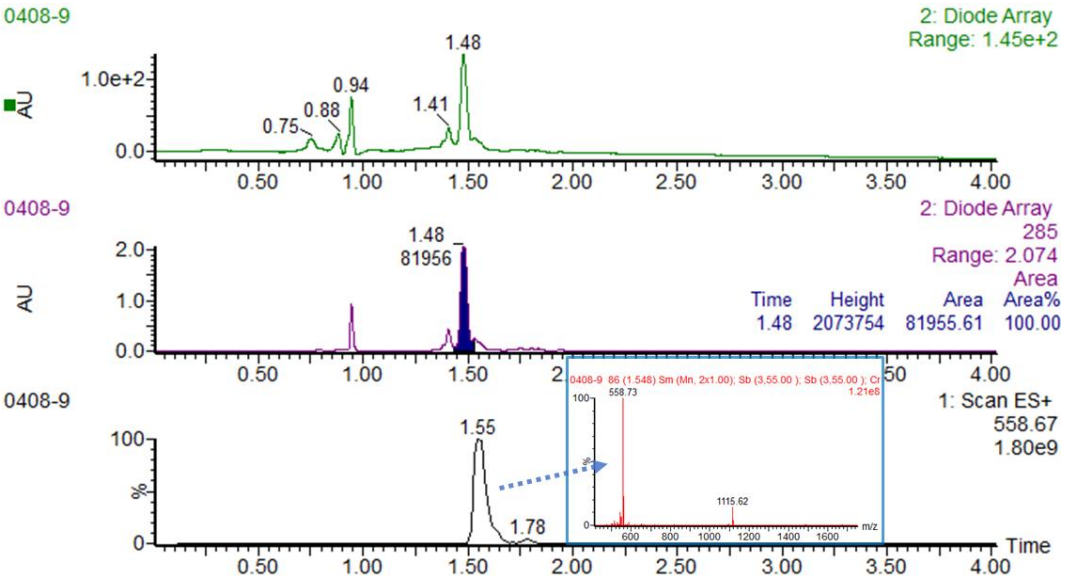

Fig S176. UPLC-MS chromatogram of **L13** and 3,6-DCT reaction mixture including TIC, UV curves (full-wavelength and extracted at 285 nm) and ESI-MS spectrum. Extract mass chromatograms from full scan data. The yield of the corresponding monocyclic products was determined to be 58% using Equation3.

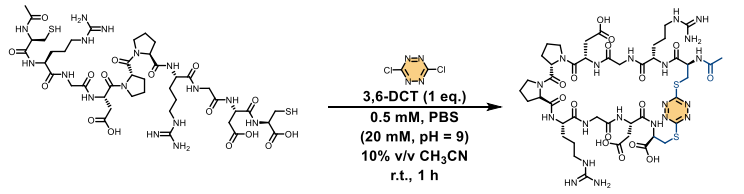

Ac-CRGDpPRGDC

Chemical Formula: $C_{44}H_{66}N_{20}O_{16}S_2$
Exact Mass: 1194.44071
Molecular Weight: 1195.25600

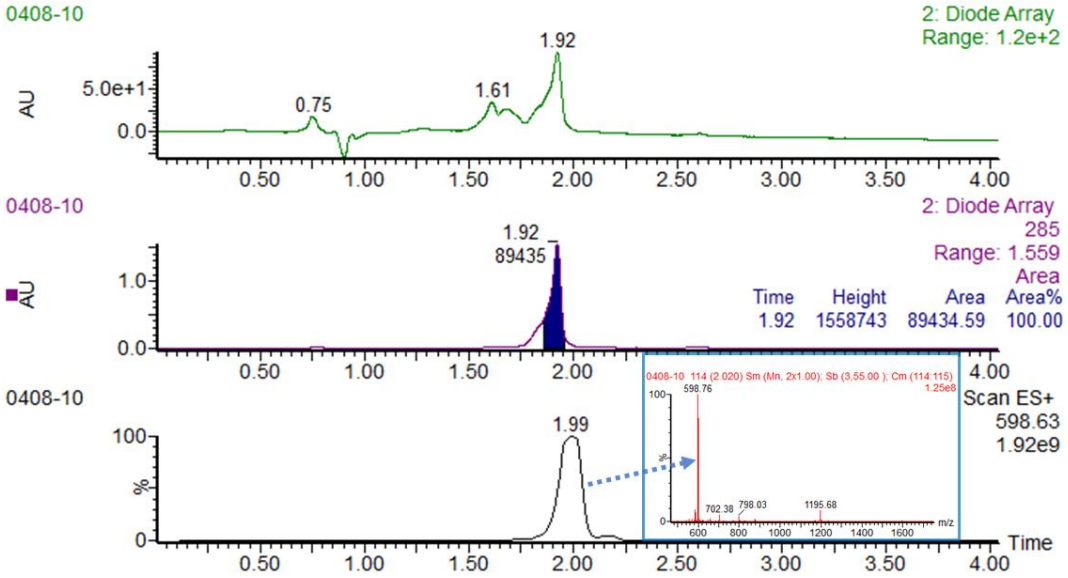

Fig S177. UPLC-MS chromatogram of **L2** and 3,6-DCT reaction mixture including TIC, UV curves (full-wavelength and extracted at 285 nm) and ESI-MS spectrum. Extract mass chromatograms from full scan data. The yield of the corresponding monocyclic products was determined to be 64% using Equation 3.

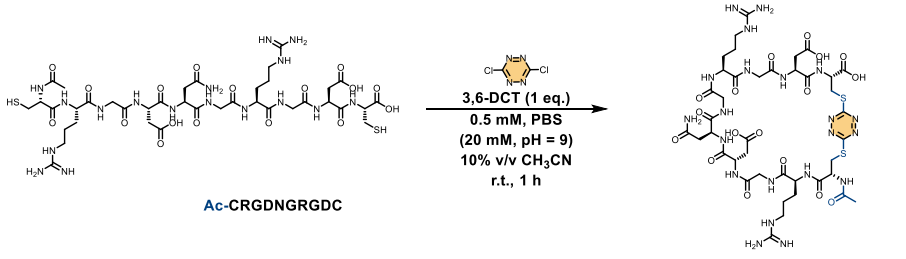

Ac-CRGDNGRGDC

Chemical Formula: $C_{40}H_{61}N_{21}O_{17}S_2$
Exact Mass: 1171.39957
Molecular Weight: 1172.17800

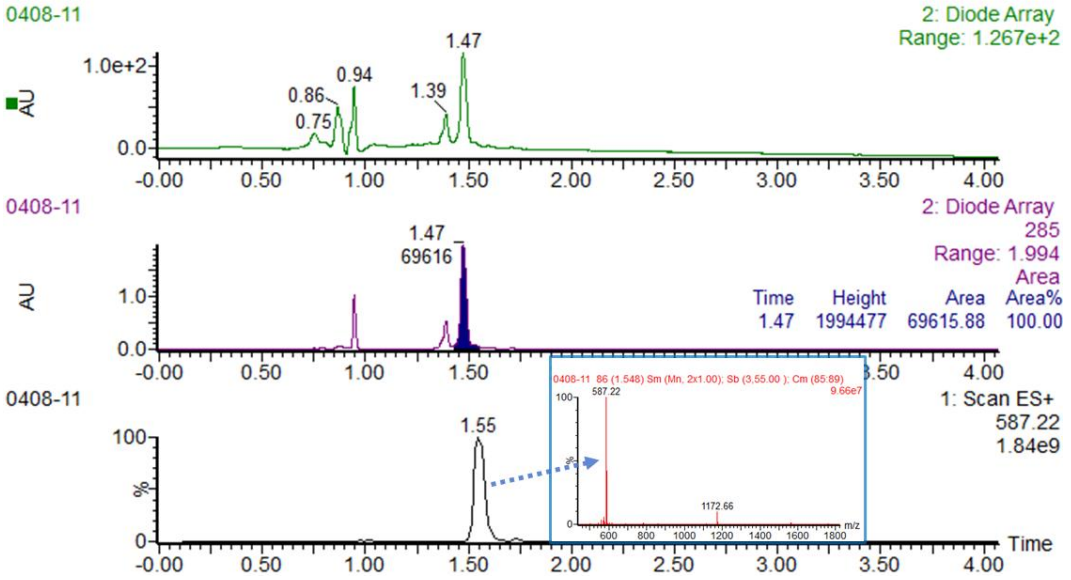

Fig S178. UPLC-MS chromatogram of **L14** and 3,6-DCT reaction mixture including TIC, UV curves (full-wavelength and extracted at 285 nm) and ESI-MS spectrum. Extract mass chromatograms from full scan data. The yield of the corresponding monocyclic products was determined to be 49% using Equation 3.

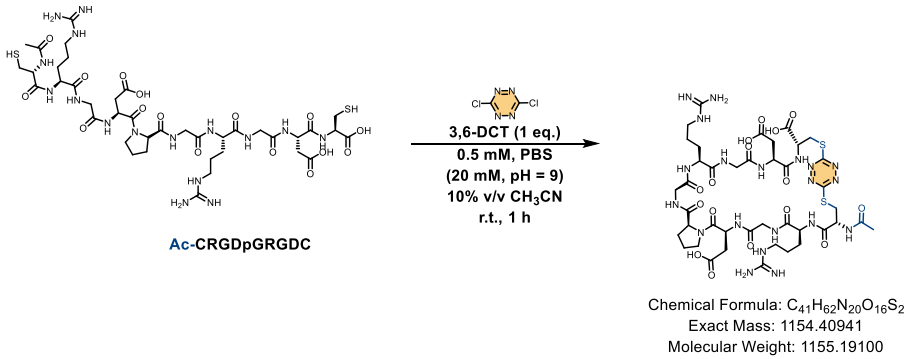

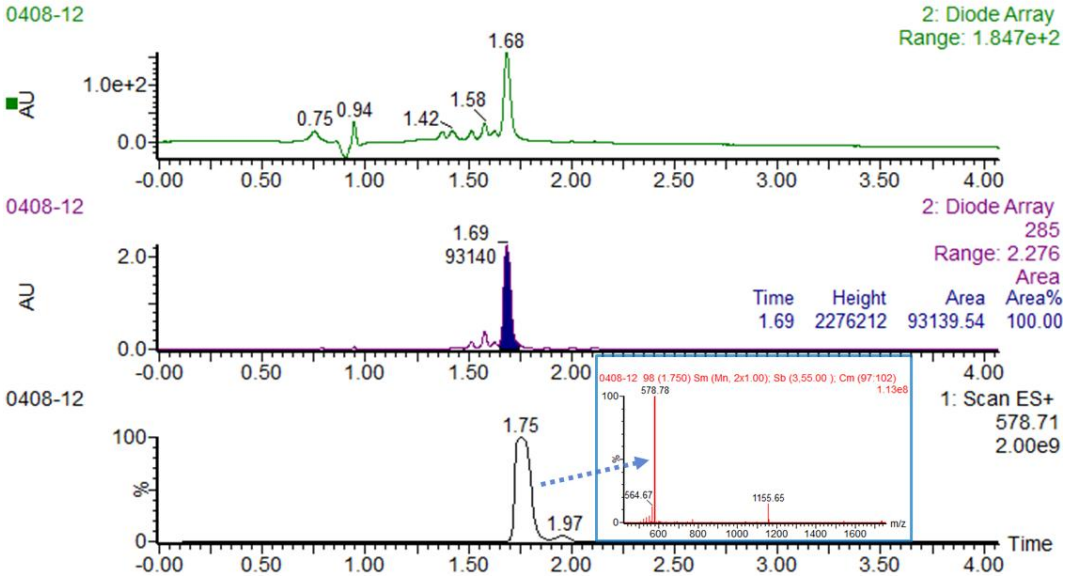

Fig S179. UPLC-MS chromatogram of **L15** and 3,6-DCT reaction mixture including TIC, UV curves (full-wavelength and extracted at 285 nm) and ESI-MS spectrum. Extract mass chromatograms from full scan data. The yield of the corresponding monocyclic products was determined to be 67% using Equation 3.

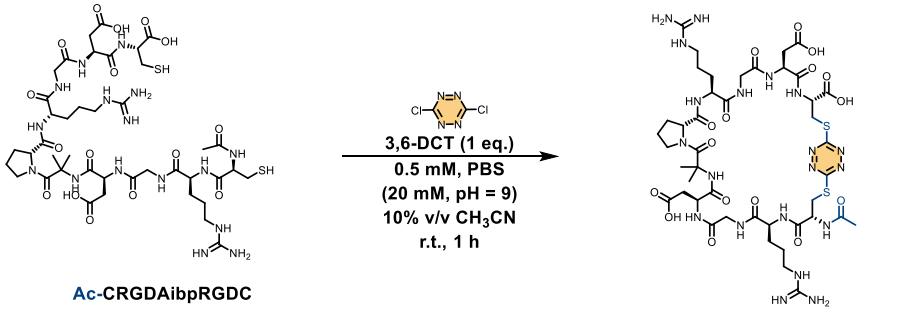

Ac-CRGDAibpRGDC

Chemical Formula: $C_{43}H_{66}N_{20}O_{16}S_2$
Exact Mass: 1182.44071
Molecular Weight: 1183.24500

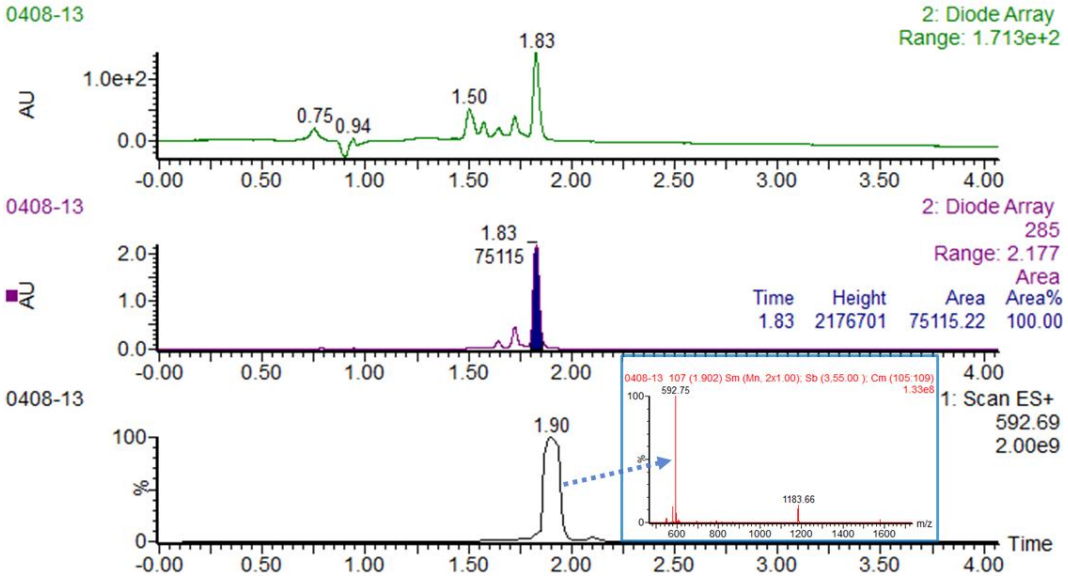

Fig S180. UPLC-MS chromatogram of **L16** and 3,6-DCT reaction mixture including TIC, UV curves (full-wavelength and extracted at 285 nm) and ESI-MS spectrum. Extract mass chromatograms from full scan data. The yield of the corresponding monocyclic products was determined to be 53% using Equation 3.

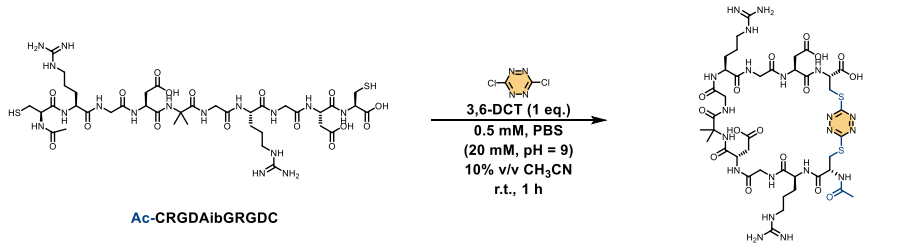

Ac-CRGDAibGRGDC

Chemical Formula: $C_{40}H_{62}N_{20}O_{16}S_2$
Exact Mass: 1142.40941
Molecular Weight: 1143.18000

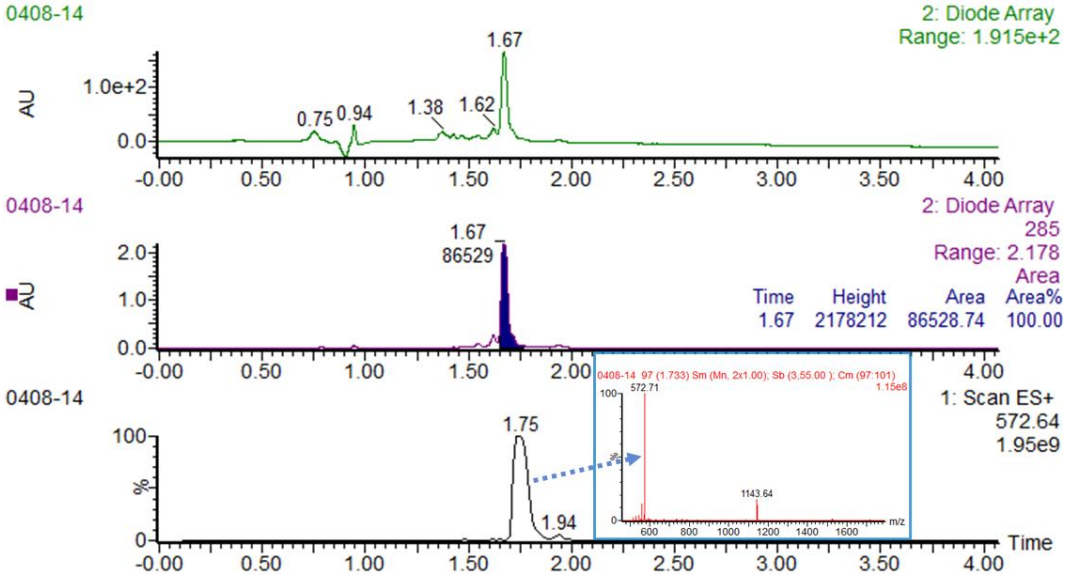

Fig S181. UPLC-MS chromatogram of **L17** and 3,6-DCT reaction mixture including TIC, UV curves (full-wavelength and extracted at 285 nm) and ESI-MS spectrum. Extract mass chromatograms from full scan data. The yield of the corresponding monocyclic products was determined to be 62% using Equation 3.

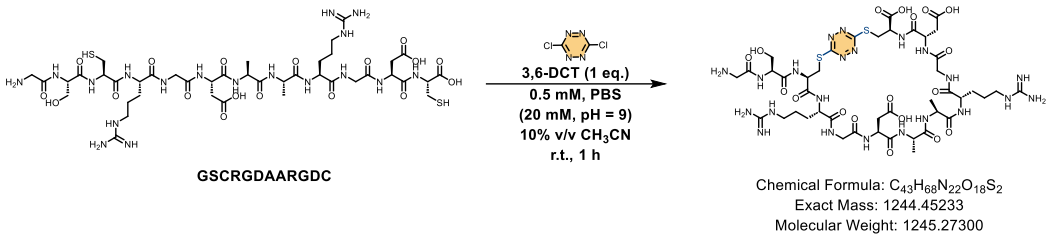

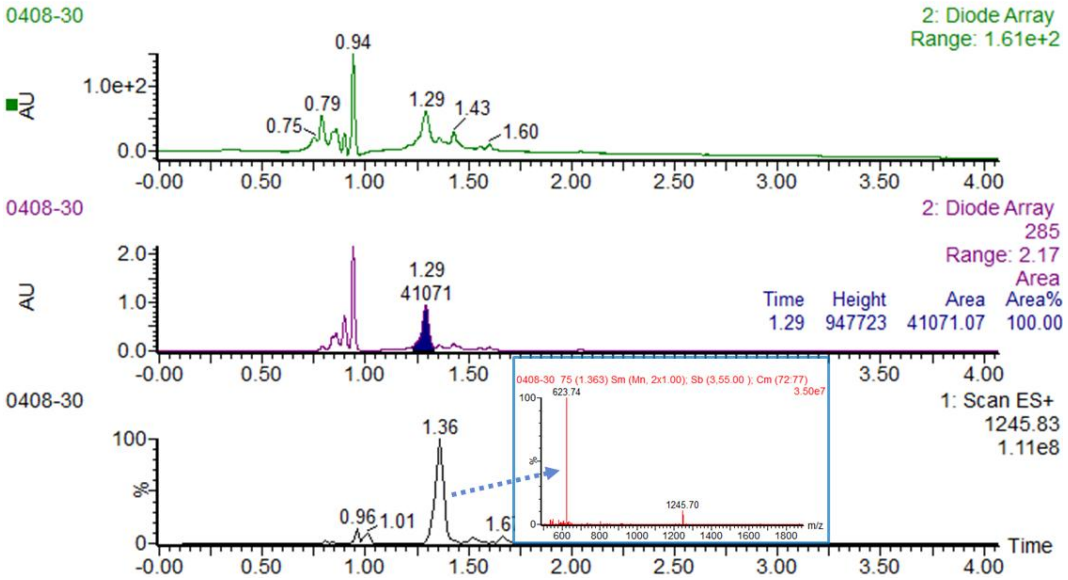

Fig S182. UPLC-MS chromatogram of **L19** and 3,6-DCT reaction mixture including TIC, UV curves (full-wavelength and extracted at 285 nm) and ESI-MS spectrum. Extract mass chromatograms from full scan data. The yield of the corresponding monocyclic products was determined to be 29% using Equation 3.

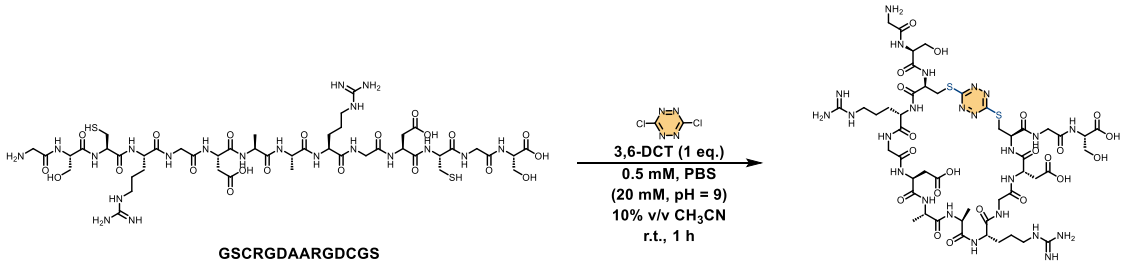

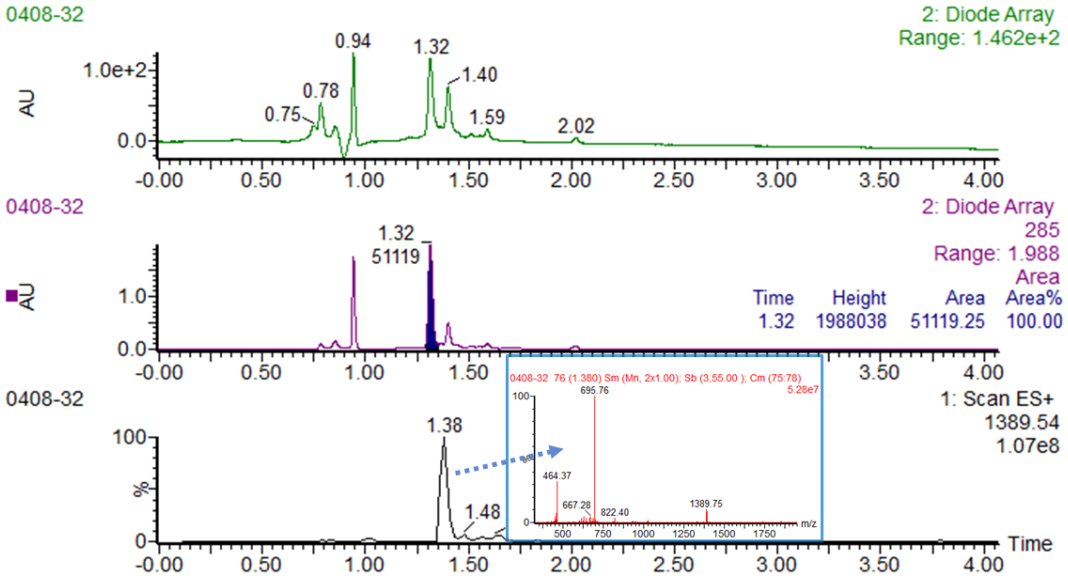

Fig S183. UPLC-MS chromatogram of **L20** and 3,6-DCT reaction mixture including TIC, UV curves (full-wavelength and extracted at 285 nm) and ESI-MS spectrum. Extract mass chromatograms from full scan data. The yield of the corresponding monocyclic products was determined to be 36% using Equation 3.

7. Substrate scope of the 3,6-DCT mediated cyclodimerization reaction

7.1 Substrate scope expansion and validation experiment

Various peptide substrates were reacted with 3,6-DCT under the standard reaction conditions (Entry 1). After completion, 50 μL of the reaction mixture was collected, and 10 μL was injected into the UPLC-MS for analysis. The peak area of the cyclodimerization products at 270 nm was recorded. Determine the LC-MS yield using Equation 1. Detailed data are shown in **Table S13.**

Tab S13. The LC-MS data for substrate scope collected using Method A

Peptide	Peak area of cyclodimerization products	Theoretical conc.	HPLC Yield (%)[a]
L34	78445	0.25 mM	38.88
L35	86861	0.25 mM	43.37
L36	71283	0.25 mM	35.06
L37	97785	0.25 mM	49.19
L38	78453	0.25 mM	38.88
L39	118490	0.25 mM	60.23
L40	79295	0.25 mM	39.33

L41	94686	0.25 mM	47.54
L42	19997	0.0625 mM	30.88
L43	40644	0.125 mM	37.45

[a]Yields were determined by LC-MS analysis using **Equation 1**

After completion of the 3,6-DCT mediated cyclodimerization reaction, TCEP (10 equiv.) was added to the reaction mixture, and reacted at room temperature for 3h. Then, 50 μL of the reaction mixture was collected, and 10 μL was injected into the UPLC-MS for analysis.

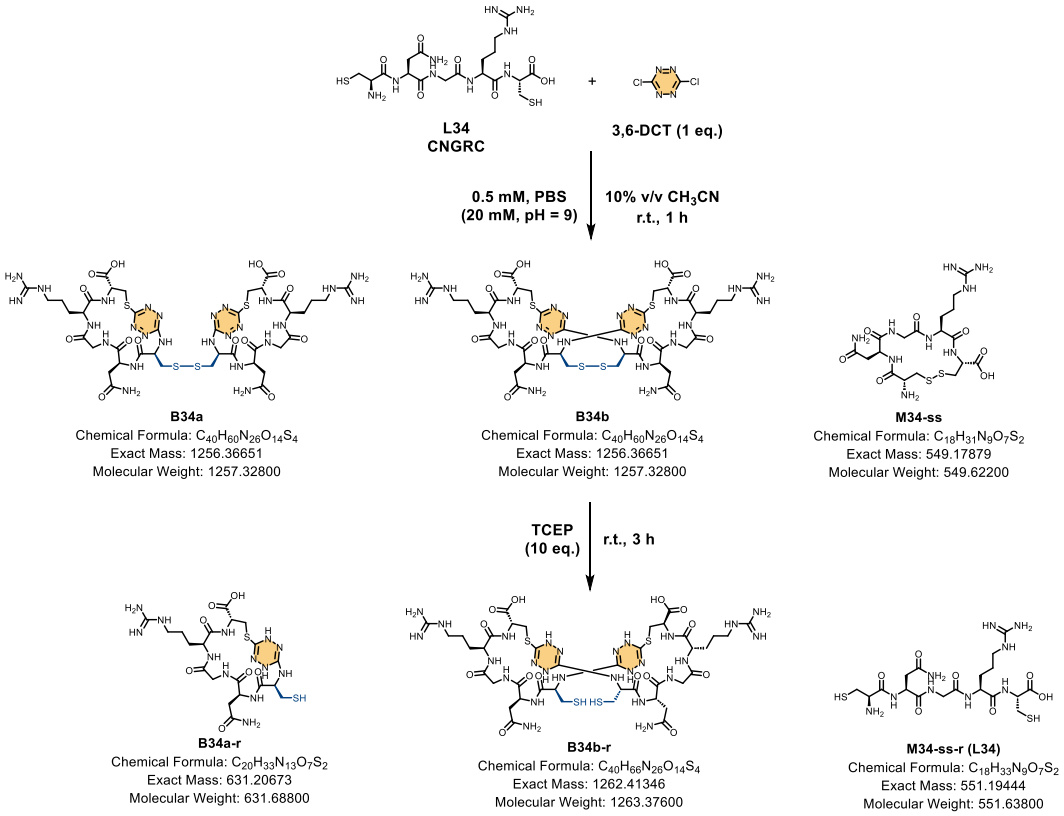

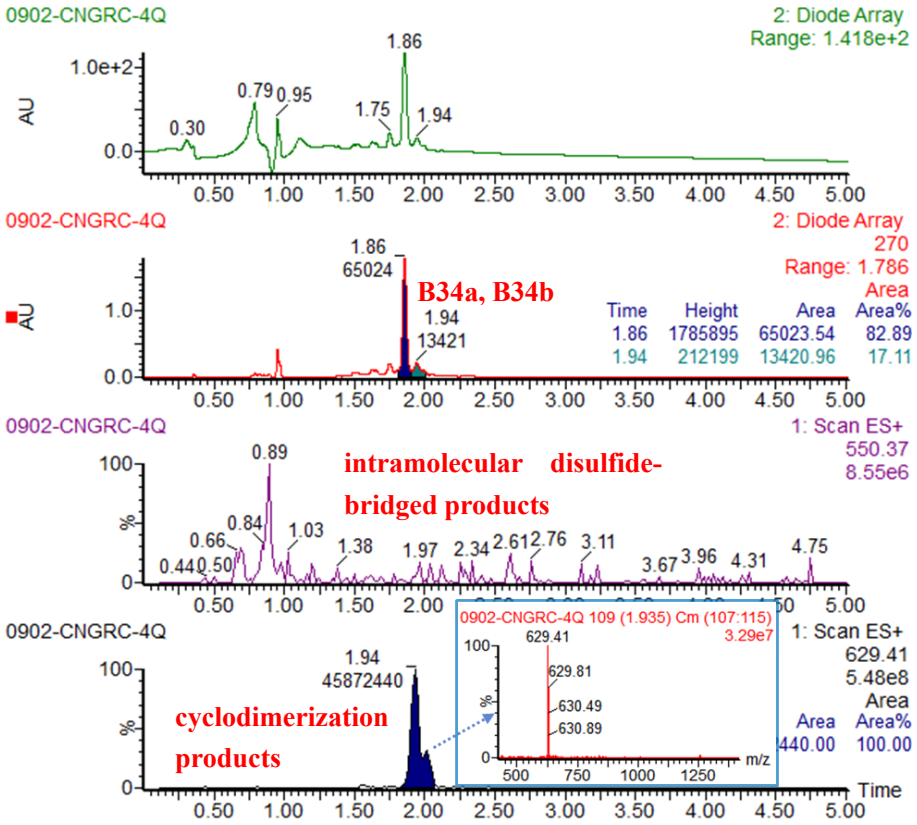

Fig S184. UPLC-MS chromatogram of reaction mixture including TIC, UV curves (full-wavelength and extracted at 270 nm) and ESI-MS spectrum of **B34a** and **B34b**. Extract mass chromatograms from full scan data. The yield of cyclodimerization products was determined to be 39% using Equation 1.

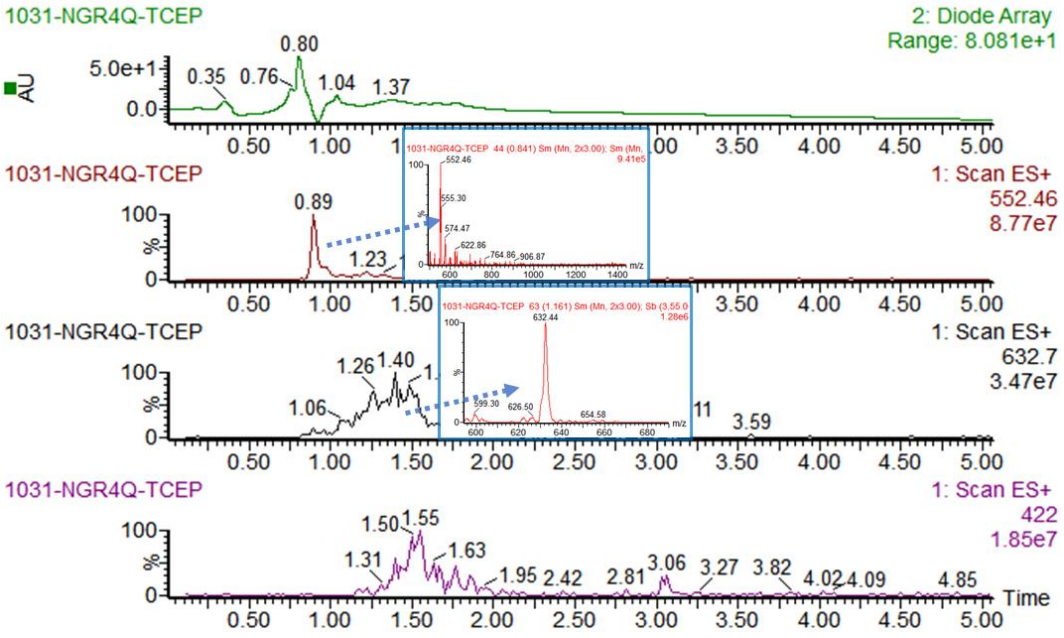

Fig S185. UPLC-MS chromatogram of reaction mixture with TCEP including TIC, UV curve (full-wavelength) and ESI-MS spectrum. Extract mass chromatograms from full scan data.

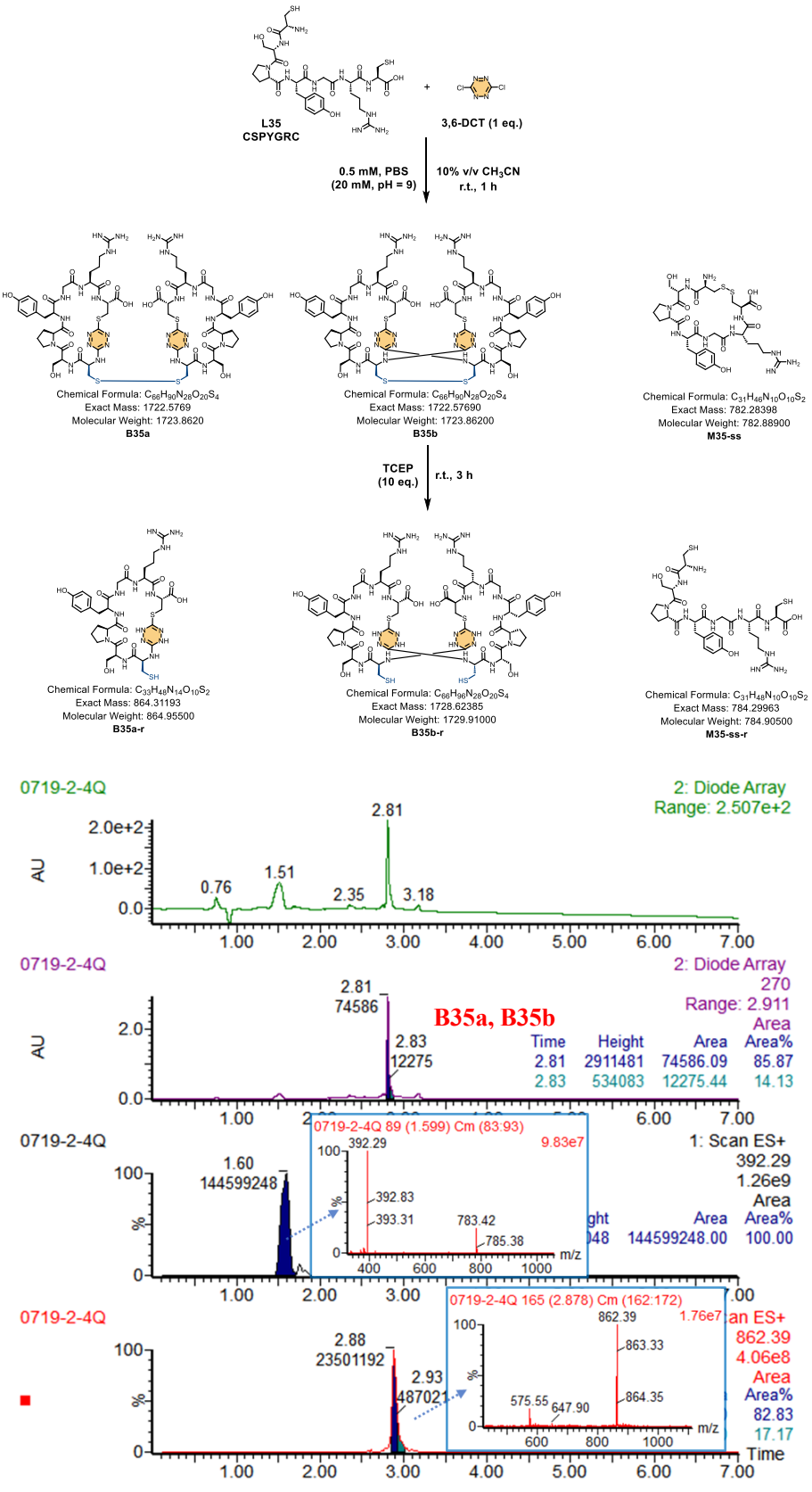

Fig S186 UPLC-MS chromatogram of reaction mixture including TIC, UV curves (full-wavelength and extracted at 270 nm) and ESI-MS spectrum of **B35a** and **B35b**. Extract mass chromatograms from

full scan data. The yield of cyclodimerization products was determined to be 43% using Equation 1.

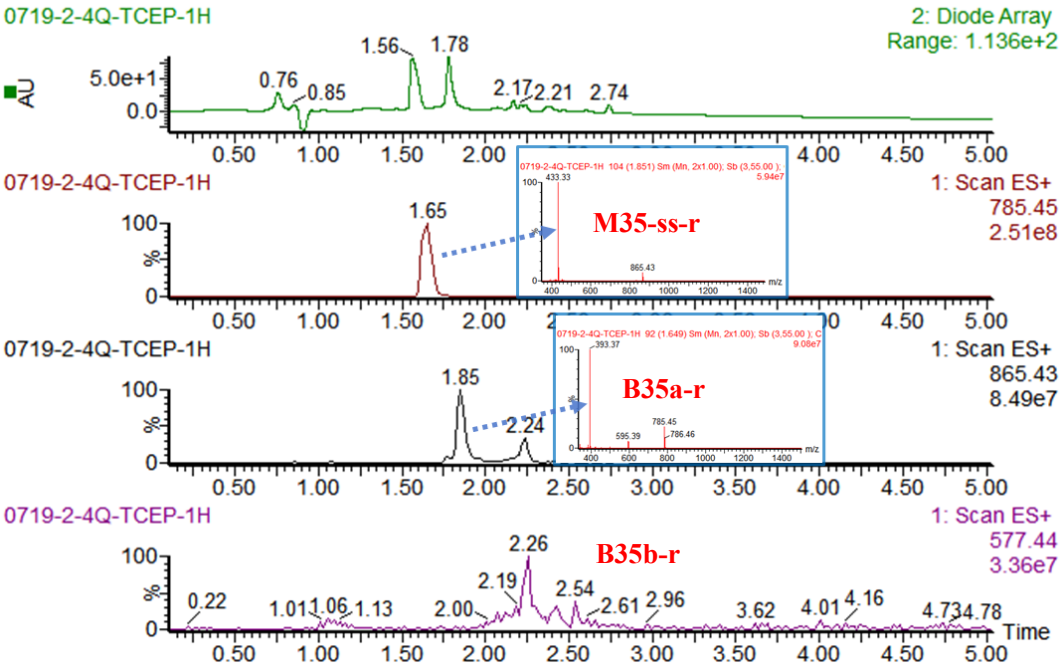

Fig S187. UPLC-MS chromatogram of reaction mixture with TCEP including TIC, UV curve (full-wavelength) and ESI-MS spectrum. Extract mass chromatograms from full scan data.

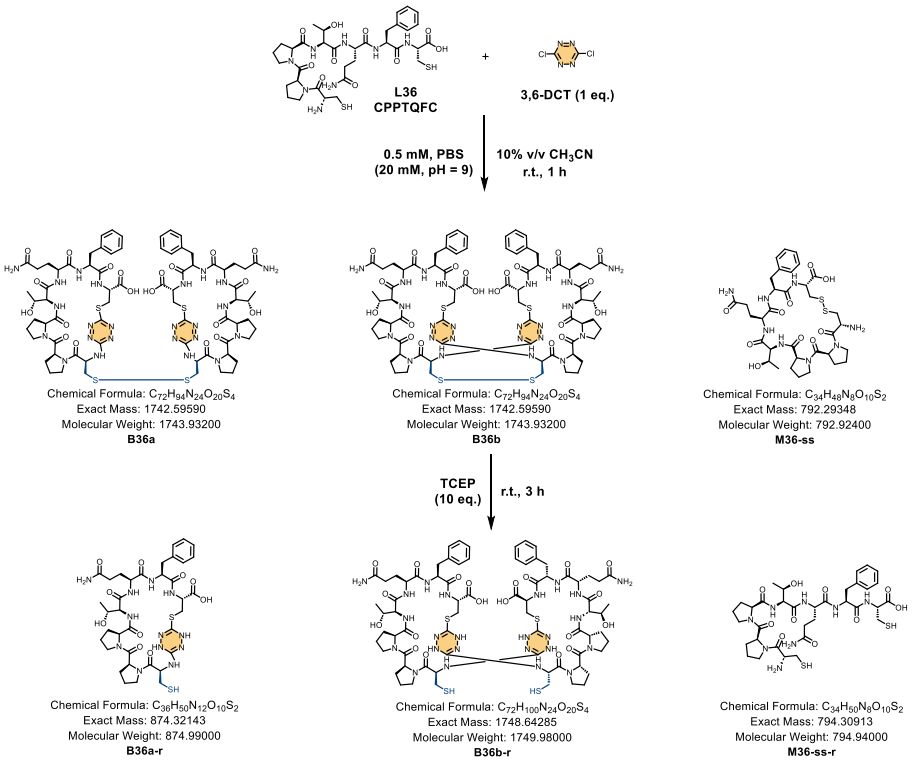

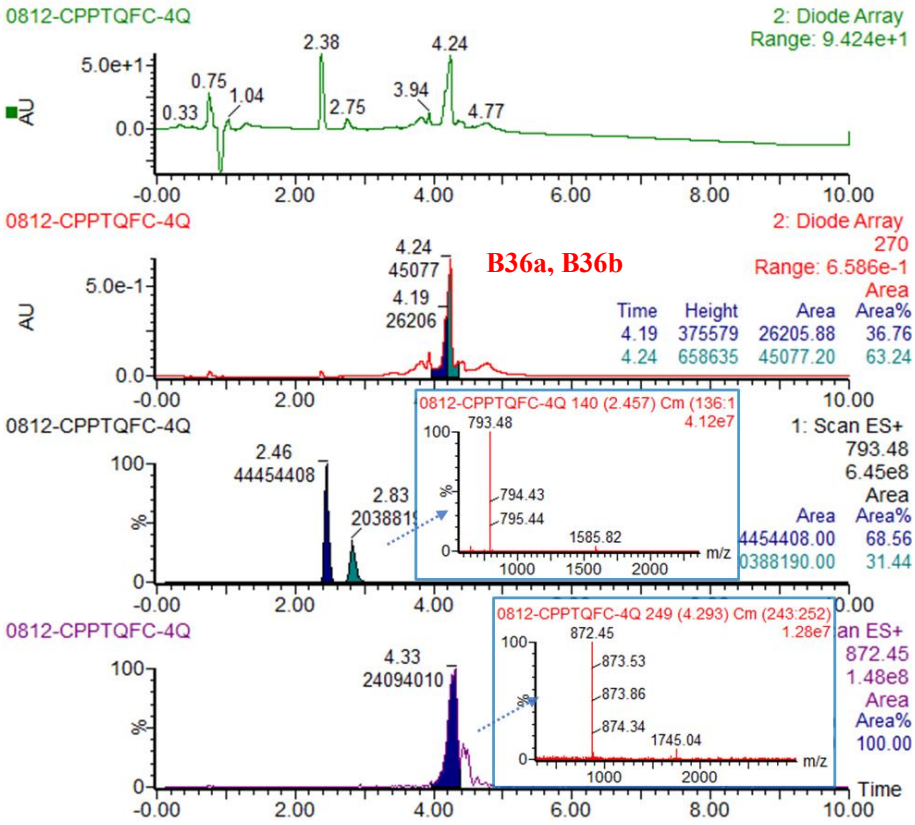

Fig S188 UPLC-MS chromatogram of reaction mixture including TIC, UV curves (full-wavelength and extracted at 270 nm) and ESI-MS spectrum of **B36a** and **B36b**. Extract mass chromatograms from full scan data. The yield of cyclodimerization products was determined to be 35% using Equation 1.

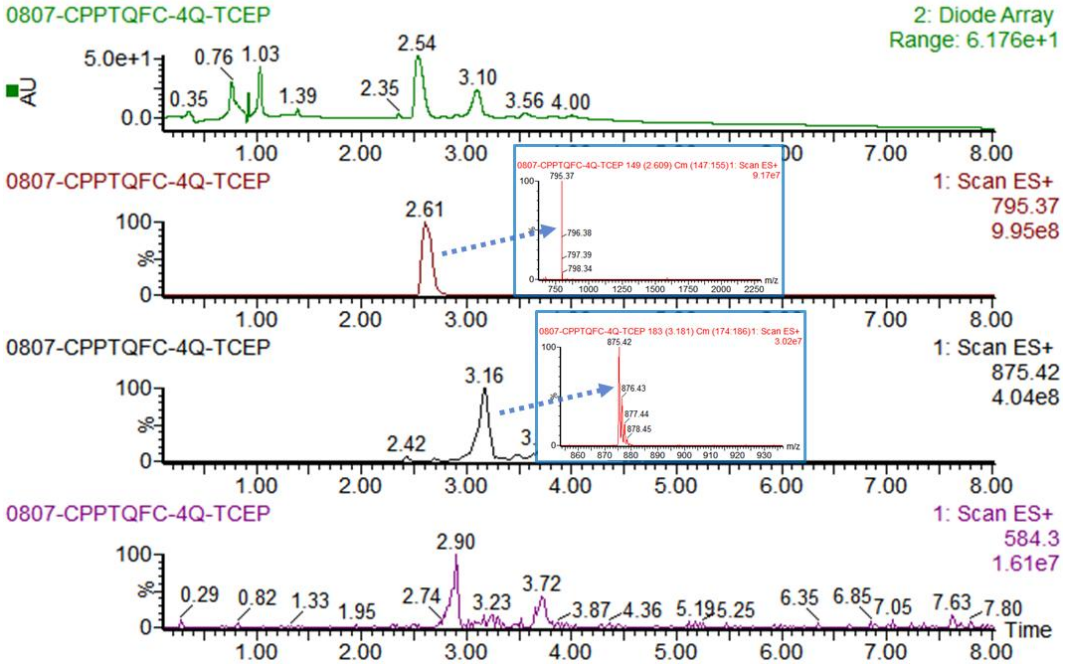

Fig S189. UPLC-MS chromatogram of reaction mixture with TCEP including TIC, UV curve (full-wavelength) and ESI-MS spectrum. Extract mass chromatograms from full scan data.

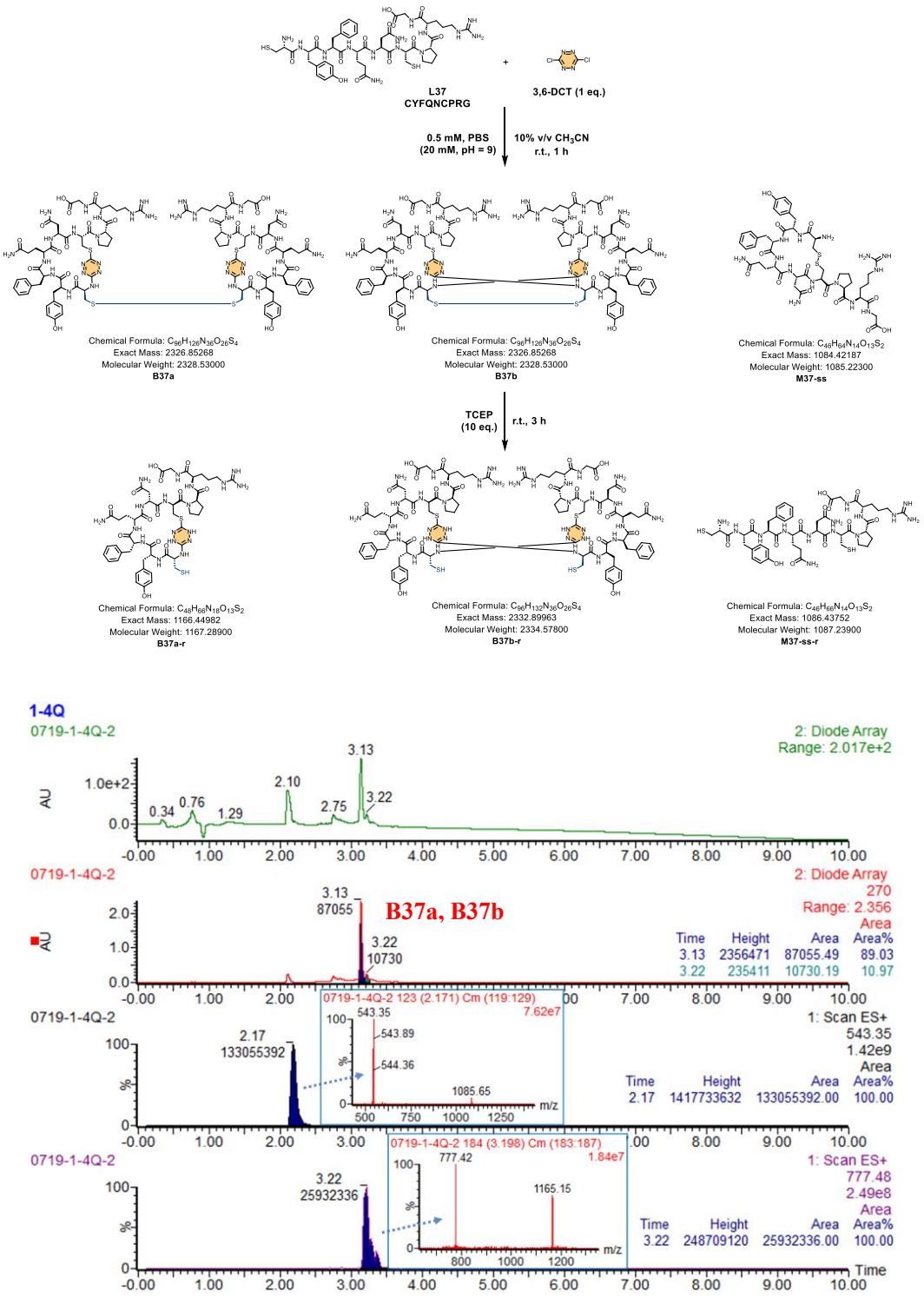

Fig S190 UPLC-MS chromatogram of reaction mixture including TIC, UV curves (full-wavelength and extracted at 270 nm) and ESI-MS spectrum of **B37a** and **B37b**. Extract mass chromatograms from full scan data. The yield of cyclodimerization products was determined to be 49% using Equation 1.

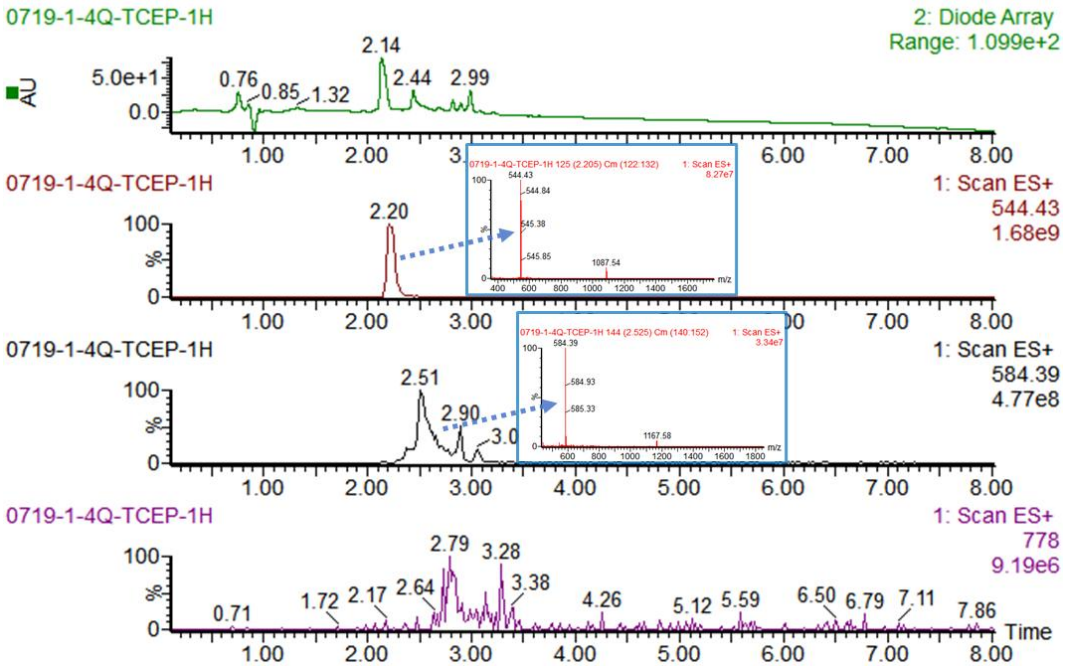

Fig S191. UPLC-MS chromatogram of reaction mixture with TCEP including TIC, UV curve (full-wavelength) and ESI-MS spectrum. Extract mass chromatograms from full scan data.

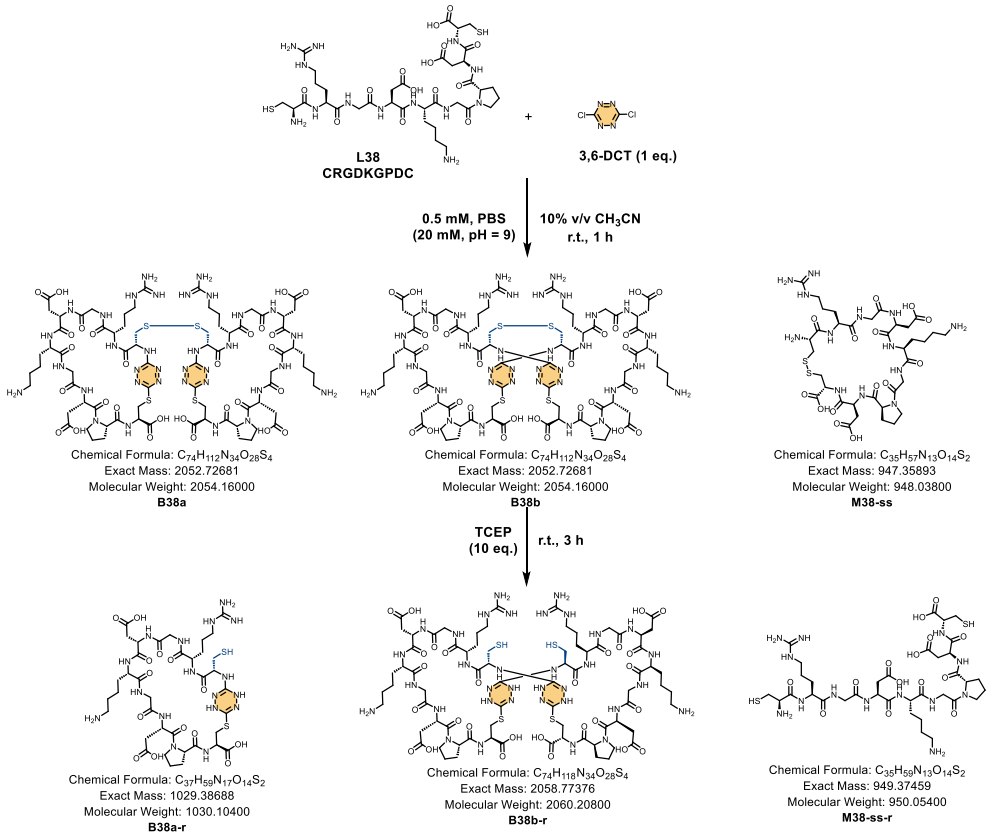

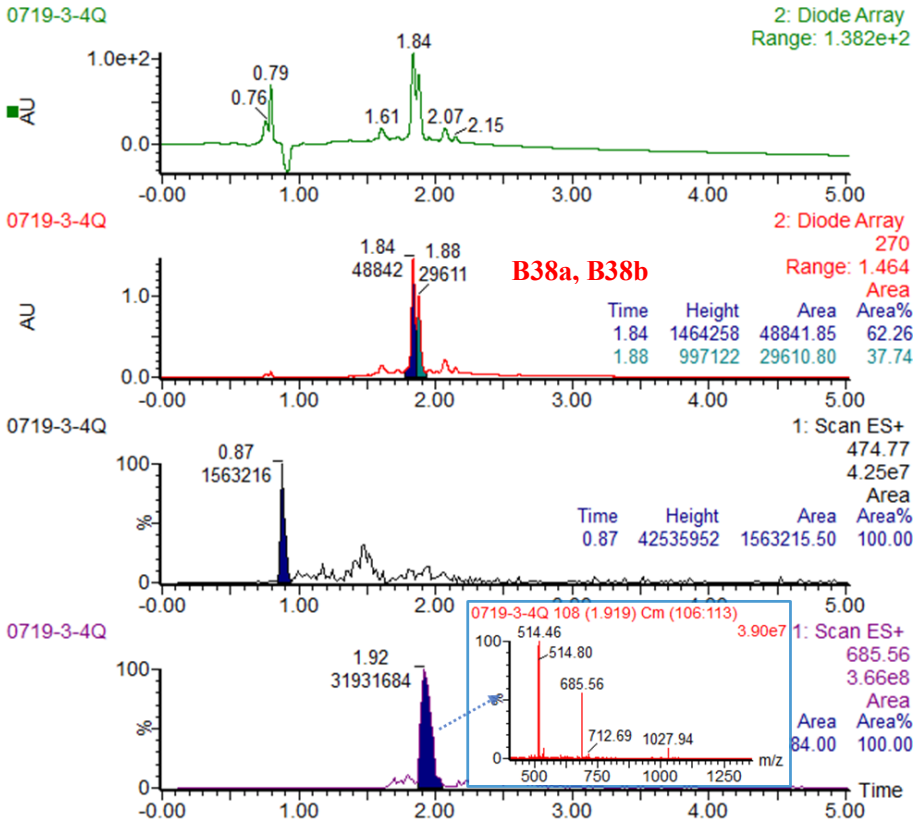

Fig S192. UPLC-MS chromatogram of reaction mixture including TIC, UV curves (full-wavelength and extracted at 270 nm) and ESI-MS spectrum of **B38a** and **B38b**. Extract mass chromatograms from full scan data. The yield of cyclodimerization products was determined to be 39% using Equation 1.

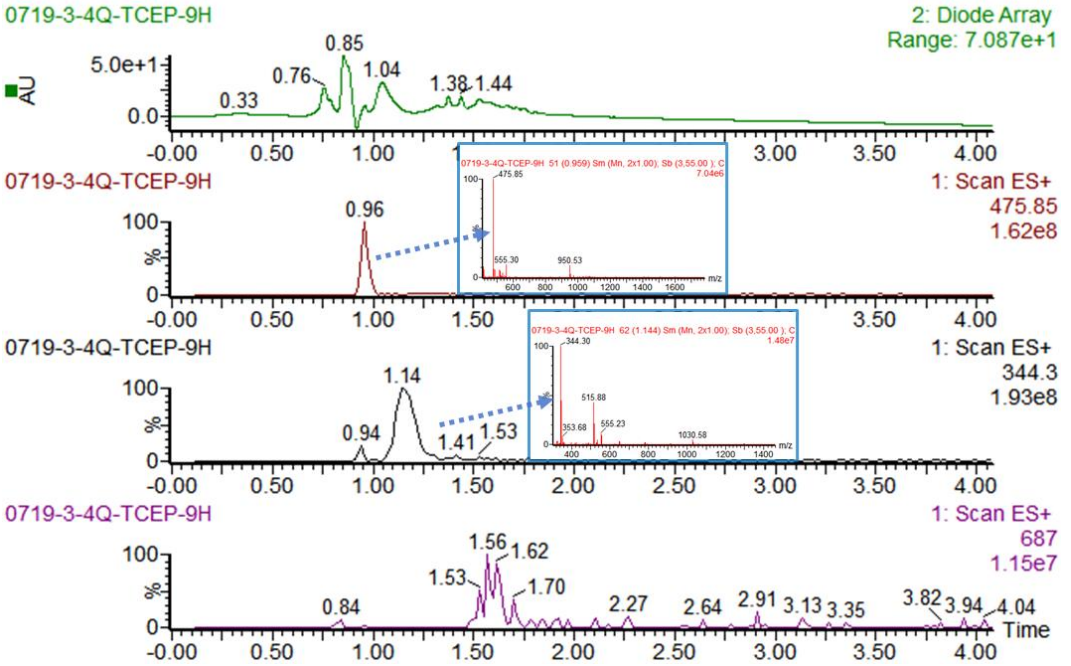

Fig S193. UPLC-MS chromatogram of reaction mixture with TCEP including TIC, UV curve (full-wavelength) and ESI-MS spectrum. Extract mass chromatograms from full scan data.

Control experiments with L44:

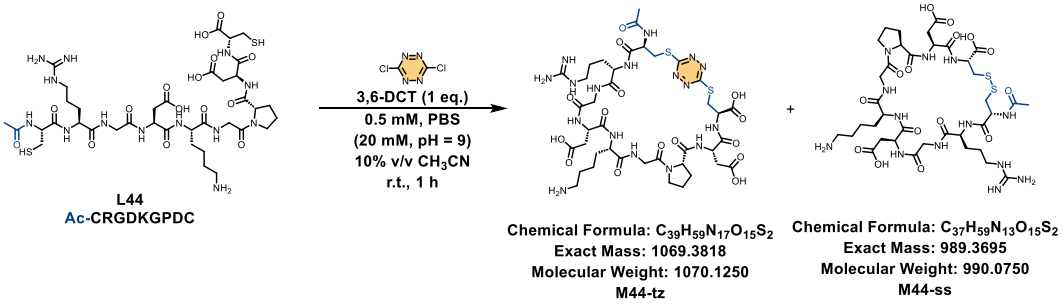

The dried peptide **L44** (1.0 equiv.) was dissolved in appropriate amount of PBS (20 mM, pH = 9.0) to reach a concentration of 0.56 mM. To this solution, 3,6-DCT (1.0 equiv.) dissolved in acetonitrile (1/9 of the volume of buffer) was added. The final concentrations in the reaction were 0.5 mM peptide, 0.5 mM 3,6-DCT and 10% acetonitrile, followed by thorough mixing. The reaction mixture was shaken at 25 °C and 800 rpm for 1 h on a thermostatic shaker.

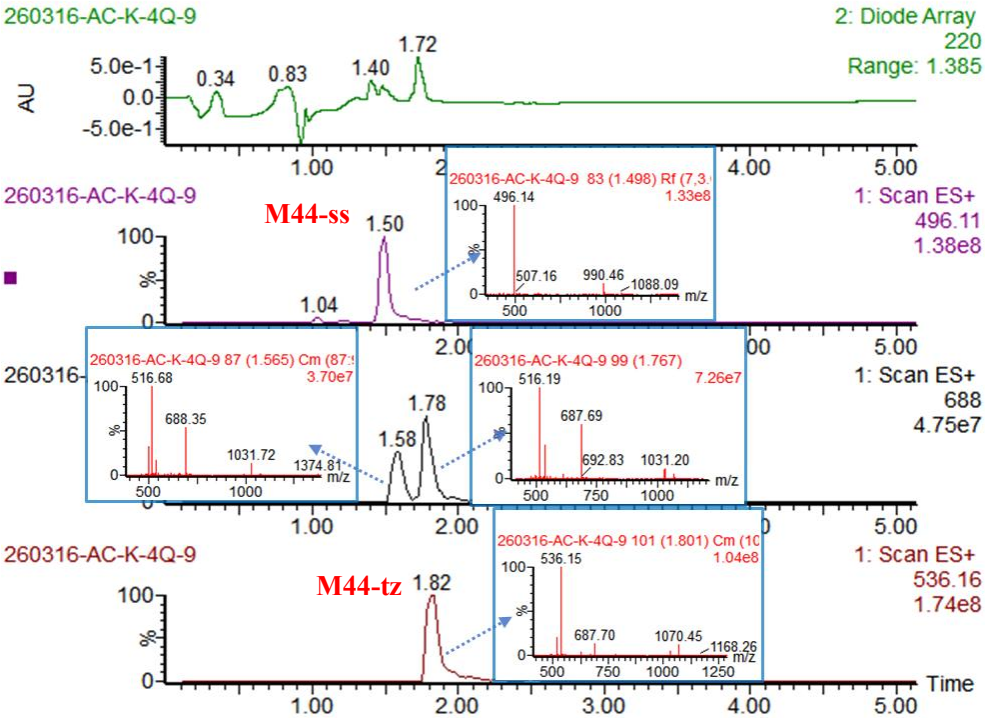

Fig S194. UPLC-MS chromatogram of **L44** and 3,6-DCT reaction mixture including TIC, UV curve (extracted at 220 nm) and ESI-MS spectrum. Extract mass chromatograms from full scan data.

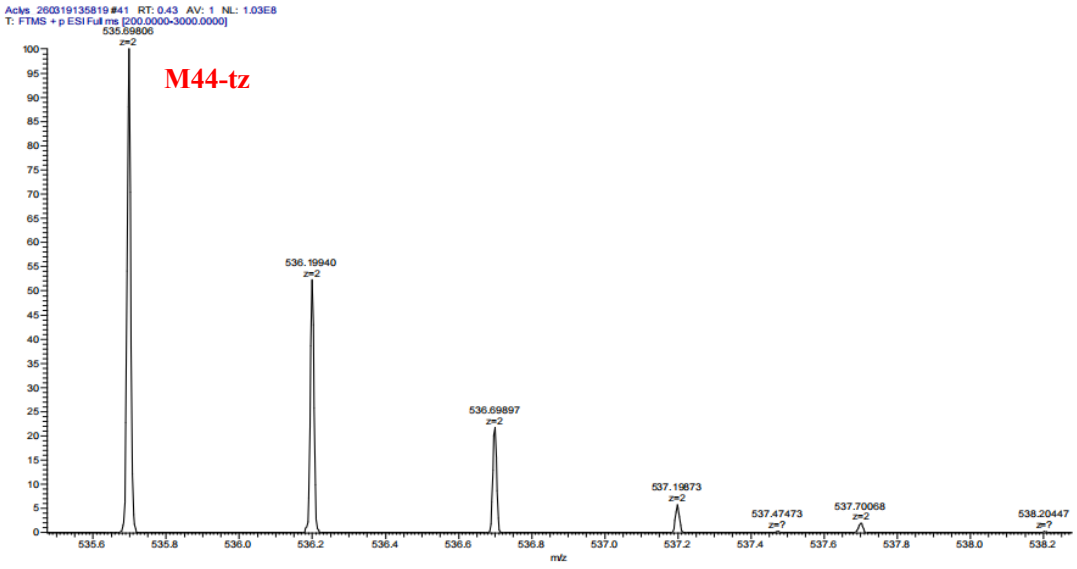

m/z	Theo. Mass	Delta (ppm)	RDB equiv.	Composition	
535.69806	535.69817	-0.21	18	C39 H61 O15 N17 S2	$[M+2H]^{2+}$

Fig S195. Q-TOF-HRMS spectrum of **M44-tz**. HRMS (ES+) m/z: $[M+2H]^{2+}$ calcd for $C_{39}H_{59}N_{17}O_{15}S_2$ 535.69, found 535.70.

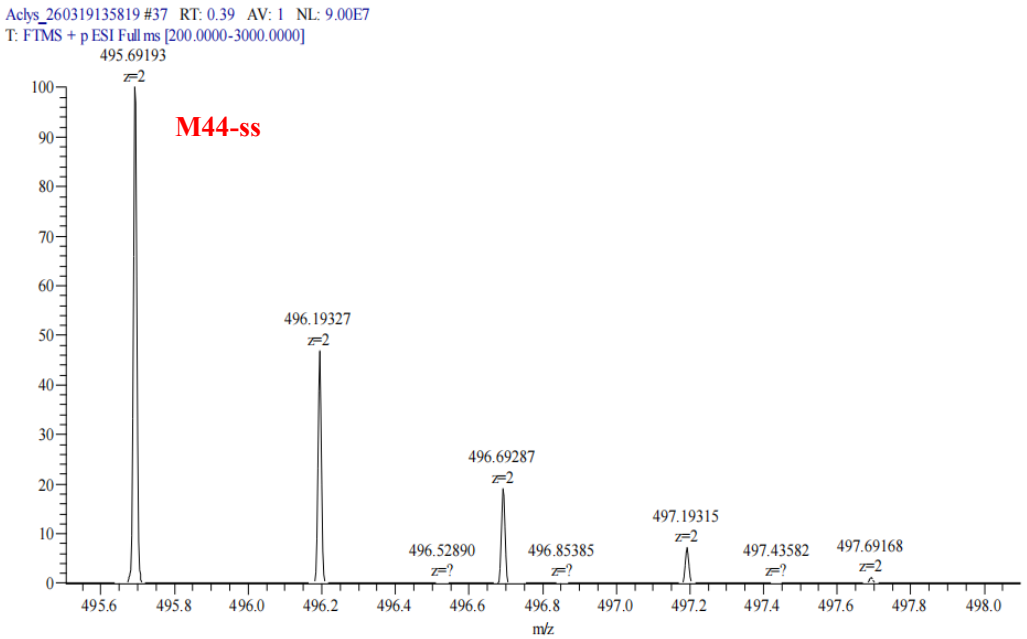

m/z	Theo. Mass	Delta (ppm)	RDB equiv.	Composition	
495.69193	495.69203	-0.19	14	C37 H61 O15 N13 S2	$[M+2H]^{2+}$

Fig S196. Q-TOF-HRMS spectrum of **M44-ss**. HRMS (ES+) m/z: $[M+2H]^{2+}$ calcd for $C_{37}H_{58}N_{13}O_{15}S_2$ 495.69, found 496.69.

To verify the selectivity of the 3,6-DCT-mediated cyclodimerization reaction, **L38** was selected as a model substrate. The cyclodimerization products **B38a** and **B38b** were isolated and purified by RP-HPLC for subsequent structural characterization by NMR spectroscopy. Meanwhile, the cyclodimerization product was dissolved in PBS buffer (20 mM, pH 7.4), treated with TCEP (10 equiv), and allowed to react at room temperature for 3 h.

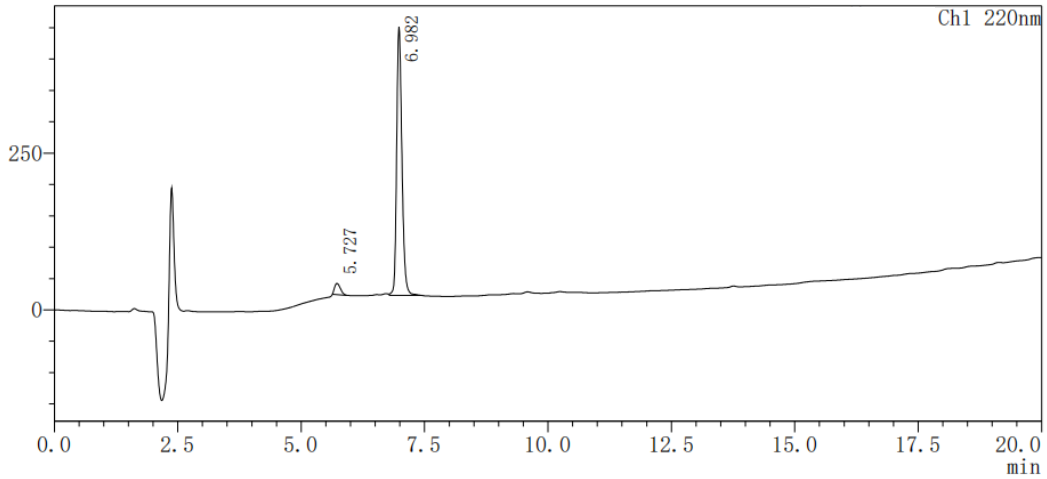

Fig S197. HPLC-UV chromatogram at 220 nm of **B38a**. Analytical HPLC using Method F, RT = 6.982 min, the HPLC purity is 96%.

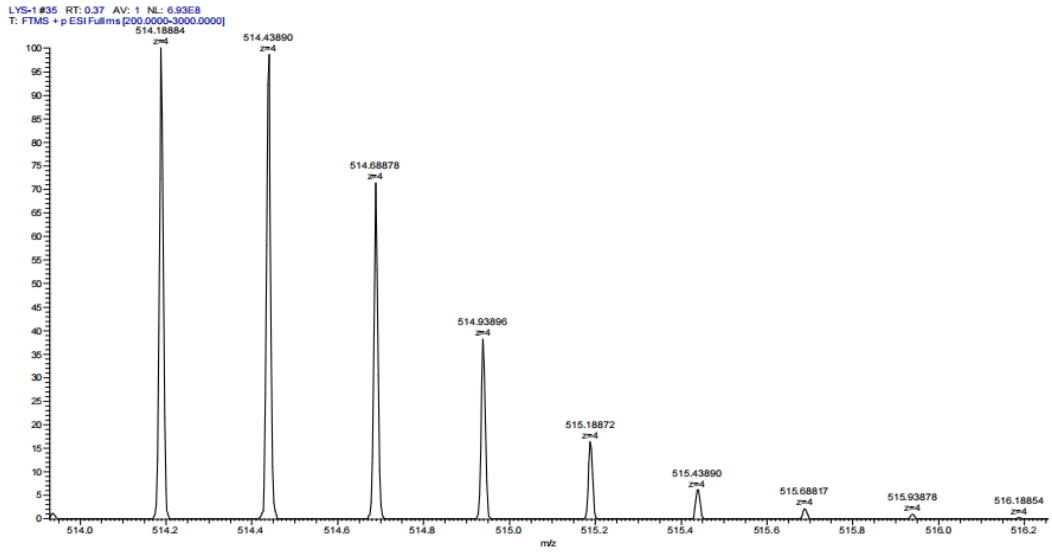

m/z	Theo. Mass	Delta (ppm)	RDB equiv.	Composition	
514.18884	514.18898	-0.27	34	C74 H116 O28 N34 S4	$[M+4H]^{4+}$

Fig S198. Q-TOF-HRMS spectrum of **B38a**. HRMS (ES+) m/z: $[M+4H]^{4+}$ calcd for $C_{74}H_{112}N_{34}O_{28}S_4$ 514.18, found 514.19.

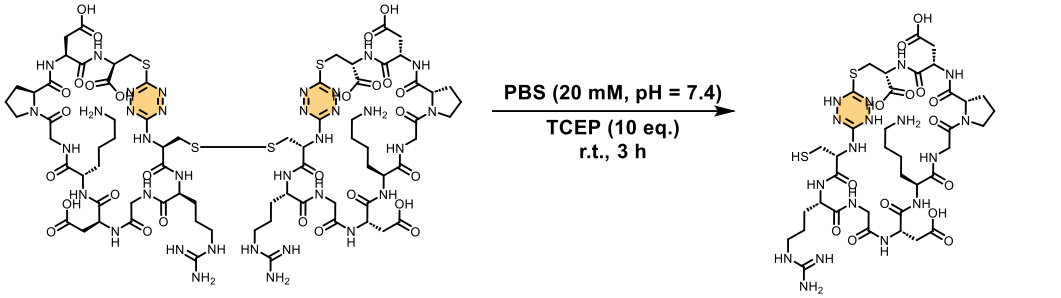

Chemical Formula: $C_{74}H_{112}N_{34}O_{28}S_4$
Exact Mass: 2052.7268
Molecular Weight: 2054.1600
B38a

Chemical Formula: $C_{37}H_{59}N_{17}O_{14}S_2$
Exact Mass: 1029.3869
Molecular Weight: 1030.1040
B38a-r

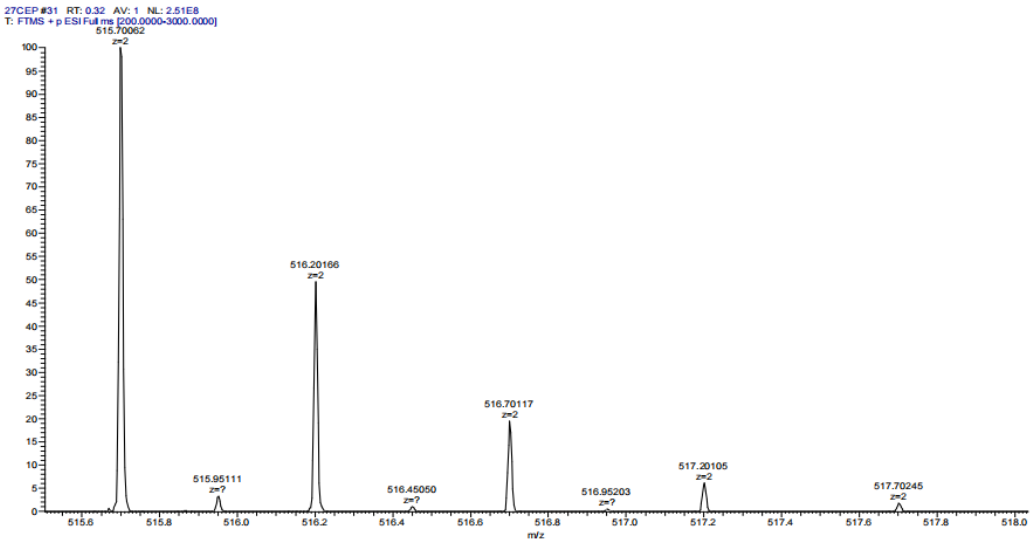

m/z	Theo. Mass	Delta (ppm)	RDB equiv.	Composition	
515.70062	515.70072	-0.19	16	C37 H61 O14 N17 S2	$[M+2H]^{2+}$

Fig S199. Q-TOF-HRMS spectrum of **B38a-r**. HRMS (ES+) m/z: $[M+4H]^{4+}$ calcd for $C_{37}H_{59}N_{17}O_{14}S_2$ 515.69, found 515.70.

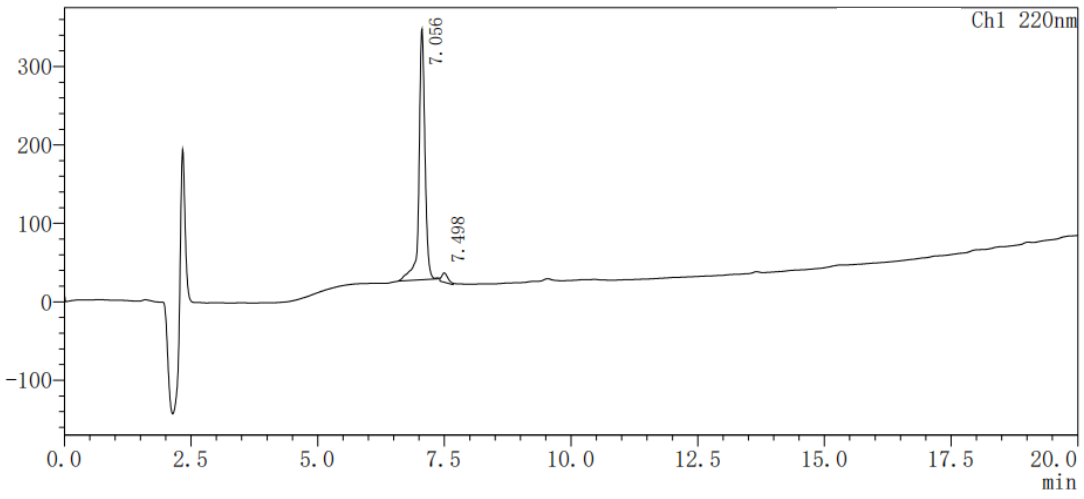

Fig S200. HPLC-UV chromatogram at 220 nm of **B38b**. Analytical HPLC using Method F, RT =

6.982 min, the HPLC purity is 96%.

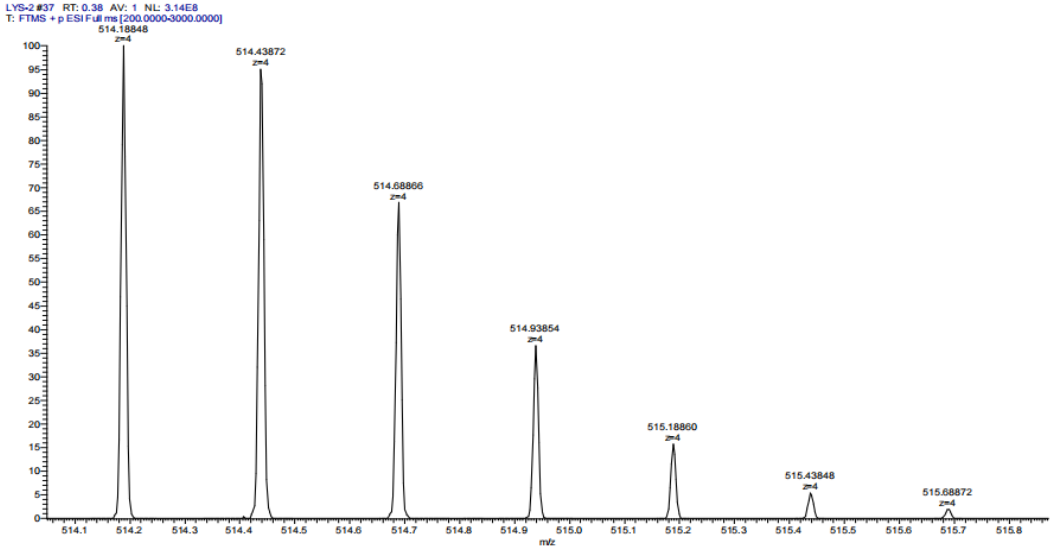

m/z	Theo. Mass	Delta (ppm)	RDB equiv.	Composition	
514.18848	514.18898	-0.97	34	C74 H116 O28 N34 S4	$[M+4H]^{4+}$

Fig S201. Q-TOF-HRMS spectrum of **B38b**. HRMS (ES+) m/z: $[M+4H]^{4}+$ calcd for $C_{74}H_{112}N_{34}O_{28}S_4$ 514.18, found 514.19.

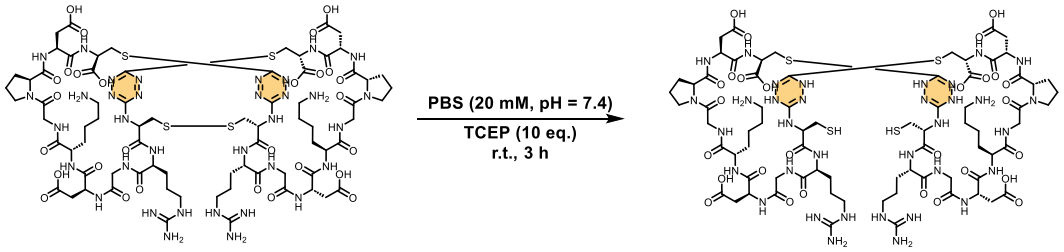

Chemical Formula: $C_{74}H_{112}N_{34}O_{28}S_4$
Exact Mass: 2052.7268
Molecular Weight: 2054.1600
B38b

Chemical Formula: $C_{74}H_{118}N_{34}O_{28}S_4$
Exact Mass: 2058.7738
Molecular Weight: 2060.2080
B38b-r

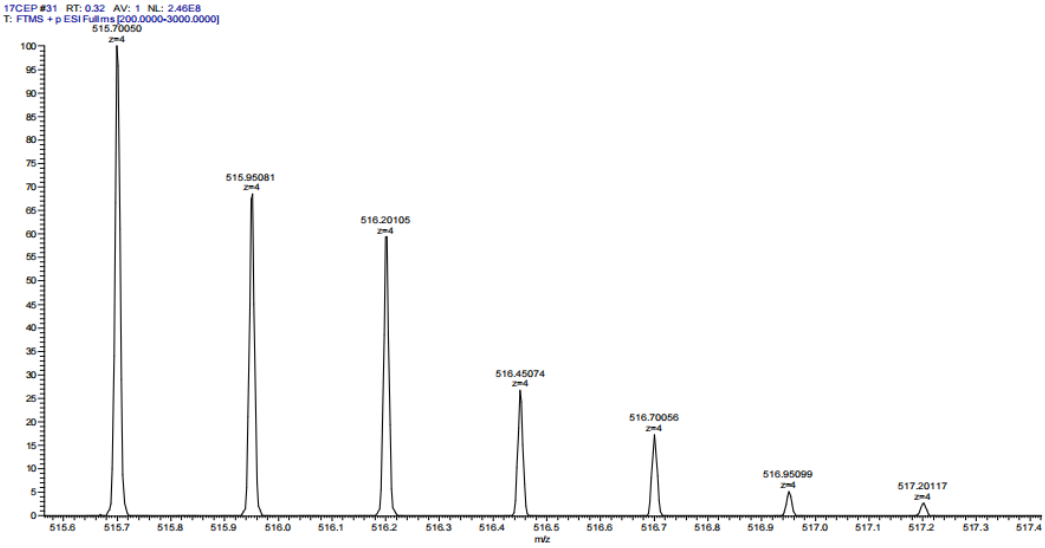

m/z	Theo. Mass	Delta (ppm)	RDB equiv.	Composition	
515.7005	515.70072	-0.42	31	C74 H122 O28 N34 S4	$[M+4H]^{4+}$

Fig S202. Q-TOF-HRMS spectrum of **B38b-r**. HRMS (ES+) m/z: $[M+4H]^{4}+$ calcd for $C_{74}H_{118}N_{34}O_{28}S_4$ 515.69, found 515.70.

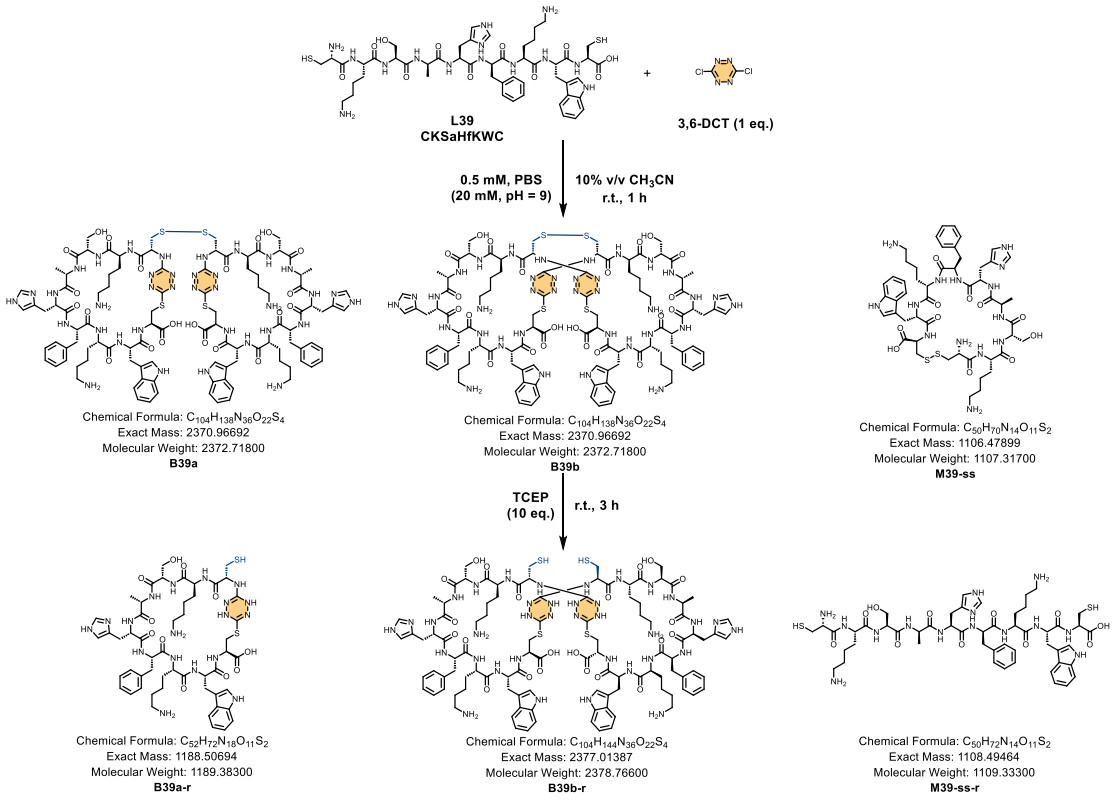

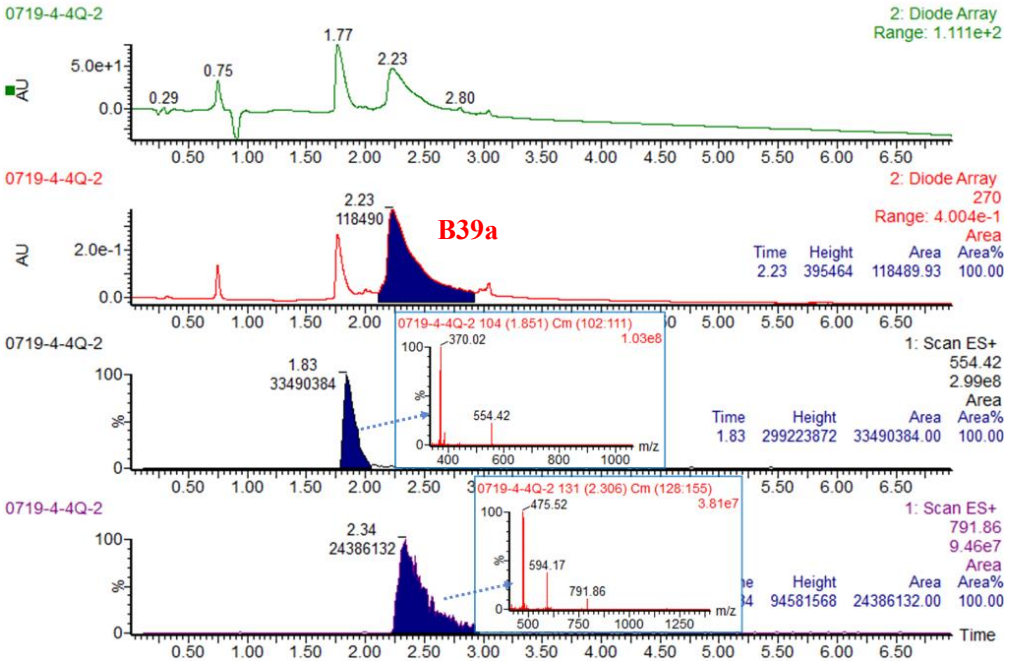

Fig S203 UPLC-MS chromatogram of reaction mixture including TIC, UV curves (full-wavelength and extracted at 270 nm) and ESI-MS spectrum of **B39a**. Extract mass chromatograms from full scan data. The yield of cyclodimerization products was determined to be 60% using Equation 1.

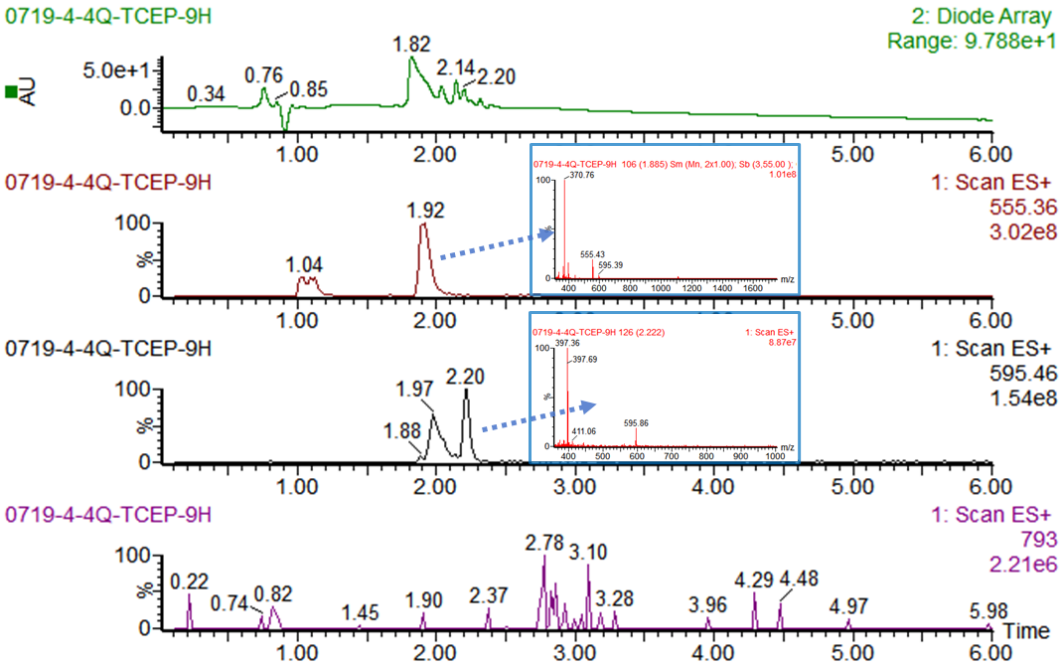

Fig S204. UPLC-MS chromatogram of reaction mixture with TCEP including TIC, UV curve (full-wavelength) and ESI-MS spectrum. Extract mass chromatograms from full scan data.

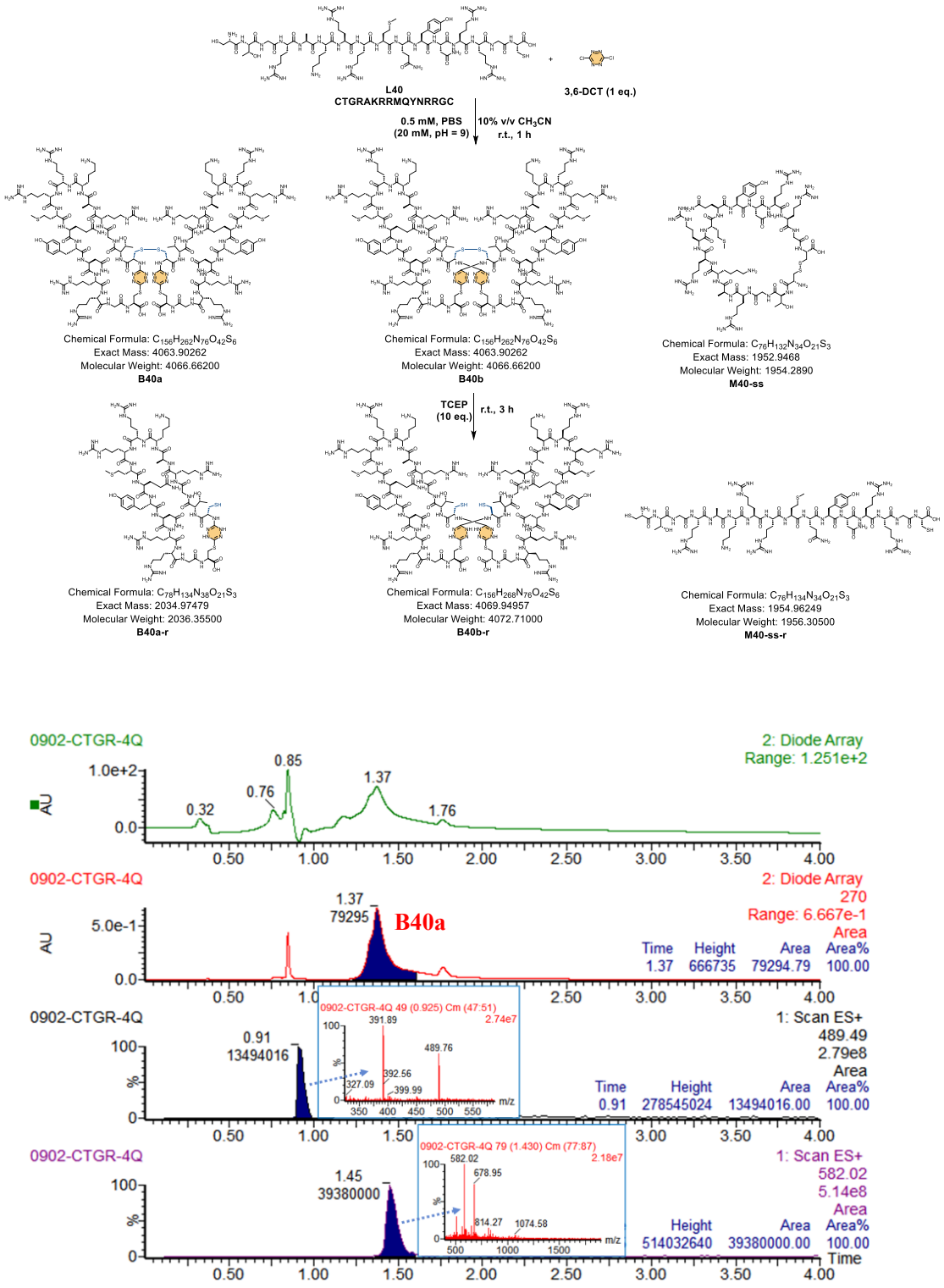

Fig S205. UPLC-MS chromatogram of reaction mixture including TIC, UV curves (full-wavelength and extracted at 270 nm), and ESI-MS spectrum of **B40a**. Extract mass chromatograms from full scan data. The yield of cyclodimerization products was determined to be 39% using Equation 1.

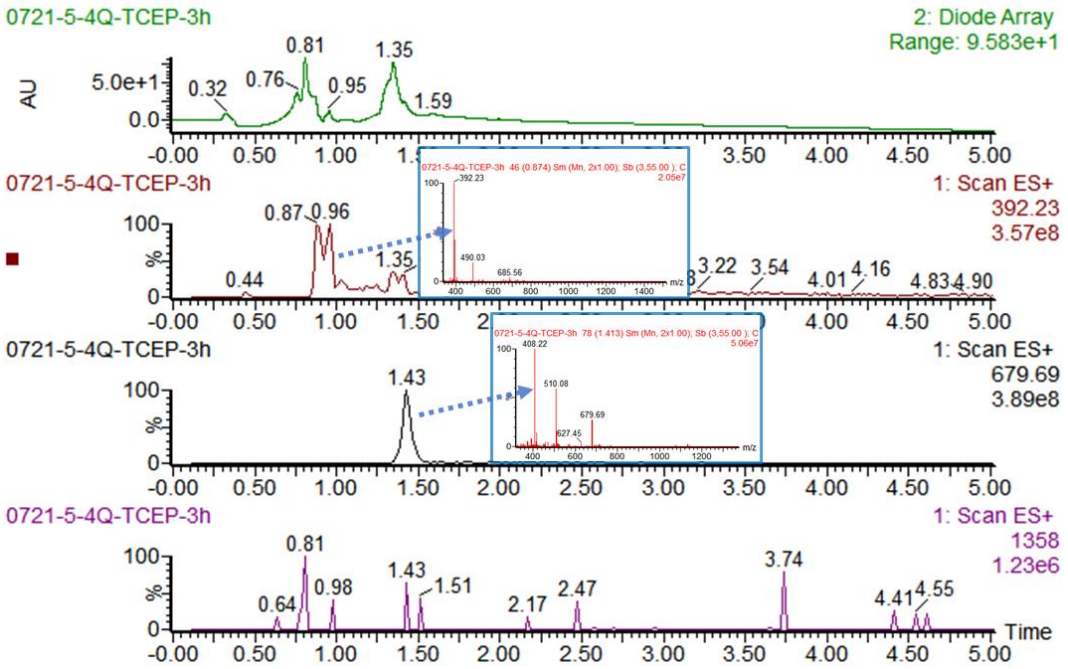

Fig S206. UPLC-MS chromatogram of reaction mixture with TCEP including TIC, UV curve (full-wavelength) and ESI-MS spectrum. Extract mass chromatograms from full scan data.

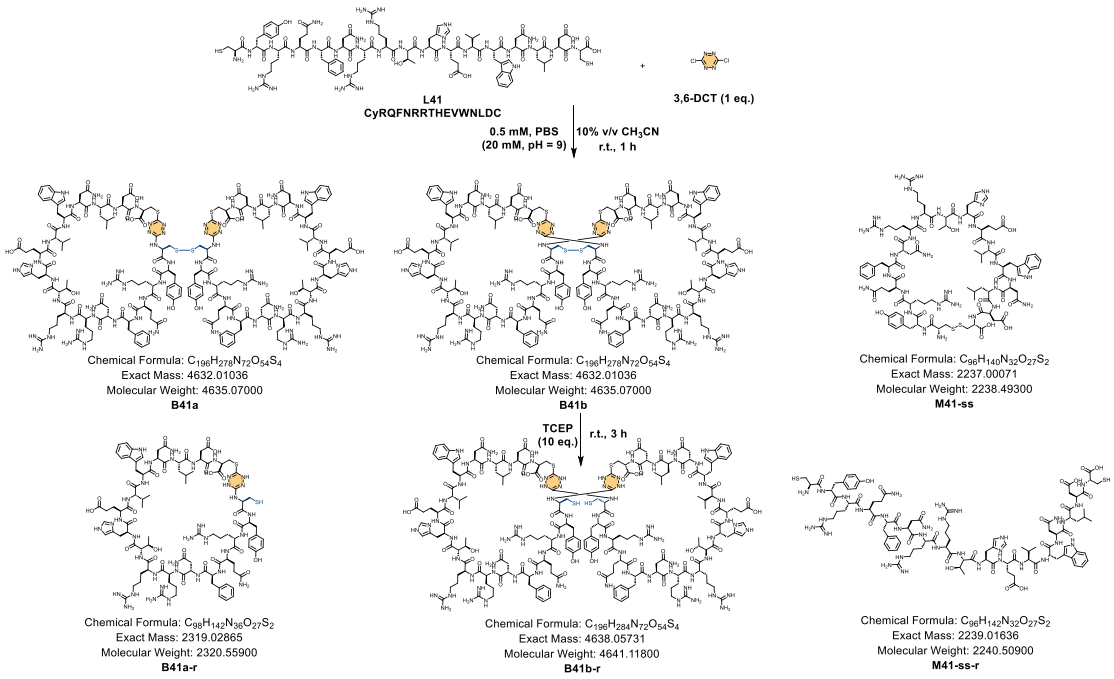

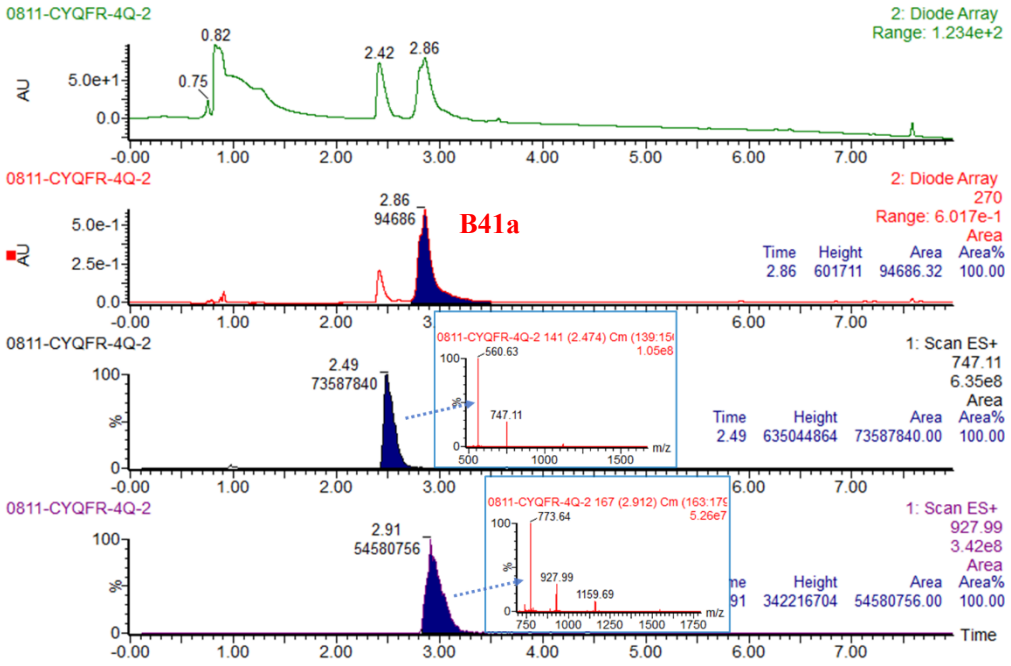

Fig S207 UPLC-MS chromatogram of reaction mixture including TIC, UV curves (full-wavelength and extracted at 270 nm) and ESI-MS spectrum of **B41a**. Extract mass chromatograms from full scan data. The yield of cyclodimerization products was determined to be 48% using Equation 1.

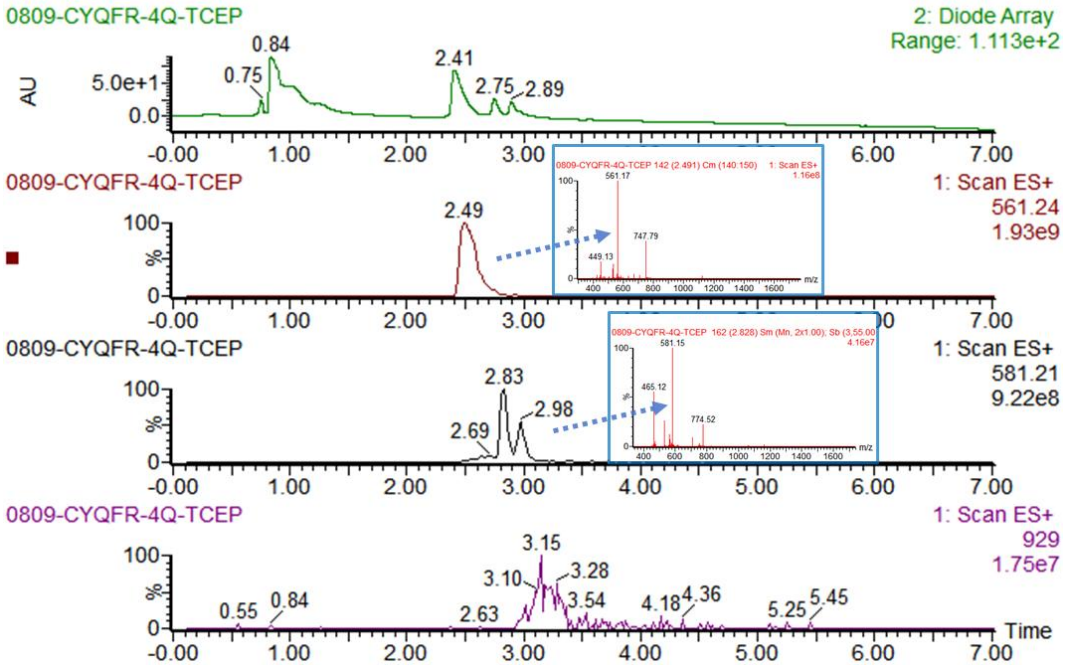

Fig S208. UPLC-MS chromatogram of reaction mixture with TCEP including TIC, UV curve (full-wavelength) and ESI-MS spectrum. Extract mass chromatograms from full scan data.

The **B41a** was isolated, purified by RP-HPLC, and lyophilized for subsequent circular dichroism (CD) experiments. In parallel, the cyclic peptide **aMD4** was

synthesized for CD experiments. Meanwhile, **B41a** was then dissolved in PBS buffer (20 mM, pH 7.4), treated with TCEP (10 equiv.), and allowed to react at room temperature for 3 h.

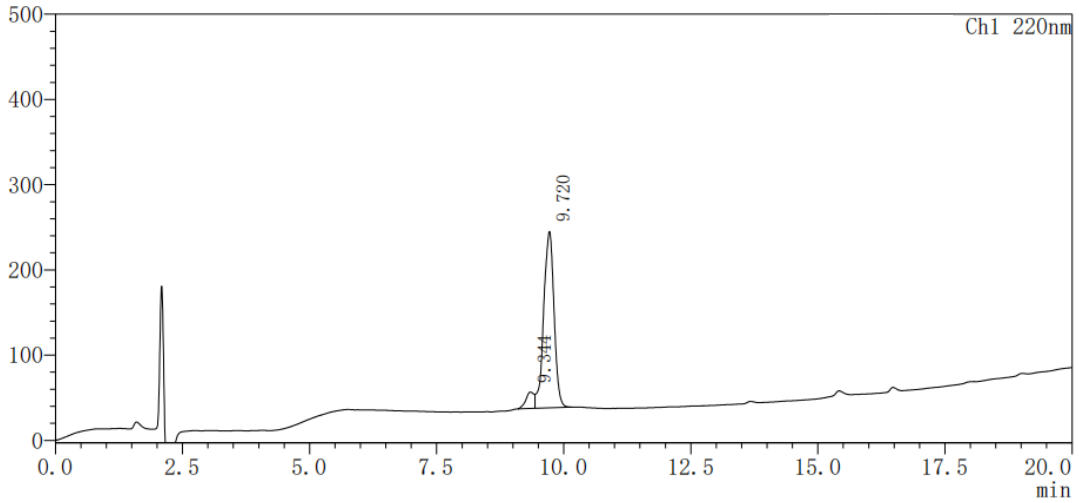

Fig S209. HPLC-UV chromatogram at 220 nm of **B41a**. Analytical HPLC using Method F, RT = 9.720 min, the HPLC purity is 93%.

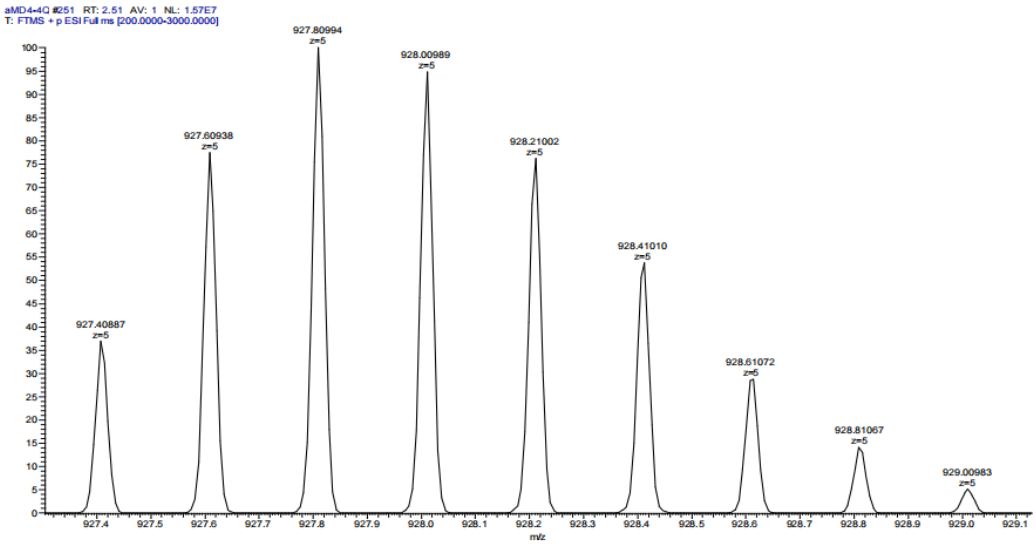

m/z	Theo. Mass	Delta (ppm)	RDB equiv.	Composition	
927.40887	927.40935	-0.52	91.5	C196 H283 O54 N72 S4	$[M+5H]^{5+}$

Fig S210. Q-TOF-HRMS spectrum of **B41a**. HRMS (ES+) m/z: $[M+5H]^{5+}$ calcd for $C_{196}H_{278}N_{72}O_{54}S_4$ 927.40, found 927.41.

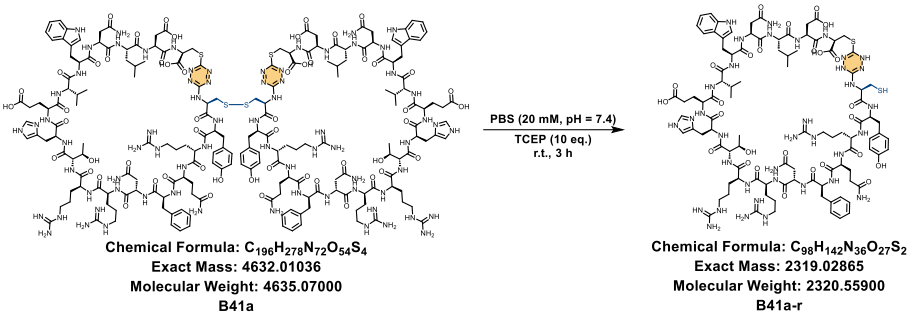

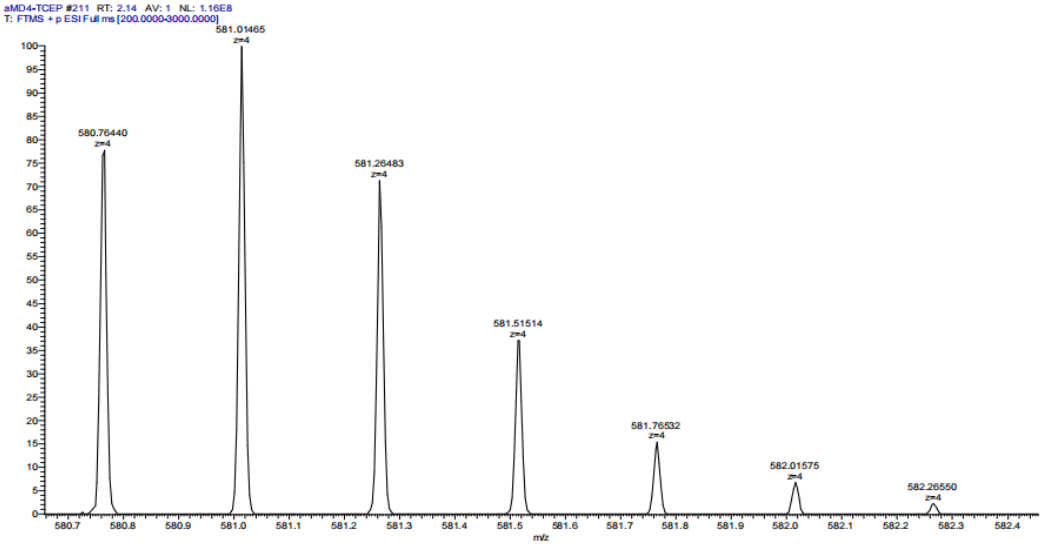

m/z	Theo. Mass	Delta (ppm)	RDB equiv.	Composition	
580.76440	580.76444	-0.07	44	C98 H146 O27 N36 S2	$[M+4H]^{4+}$

Fig S211. Q-TOF-HRMS spectrum of **B41a-r**. HRMS (ES+) m/z: $[M+4H]^{4+}$ calcd for $C_{98}H_{142}N_{36}O_{27}S_2$ 580.76, found 580.76.

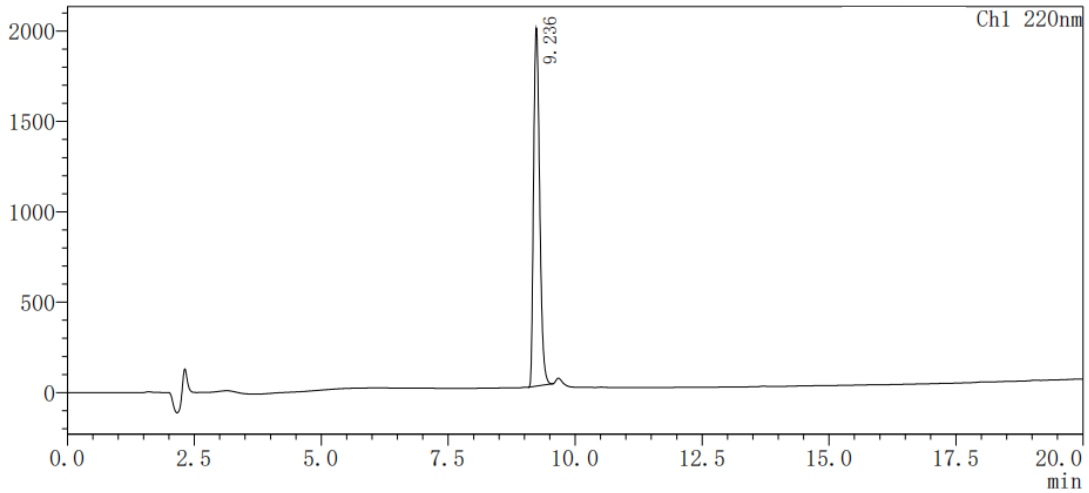

Fig S212. HPLC-UV chromatogram at 220 nm of **aMD4**. Analytical HPLC using Method F, RT = 9.236 min, the HPLC purity is 99%.

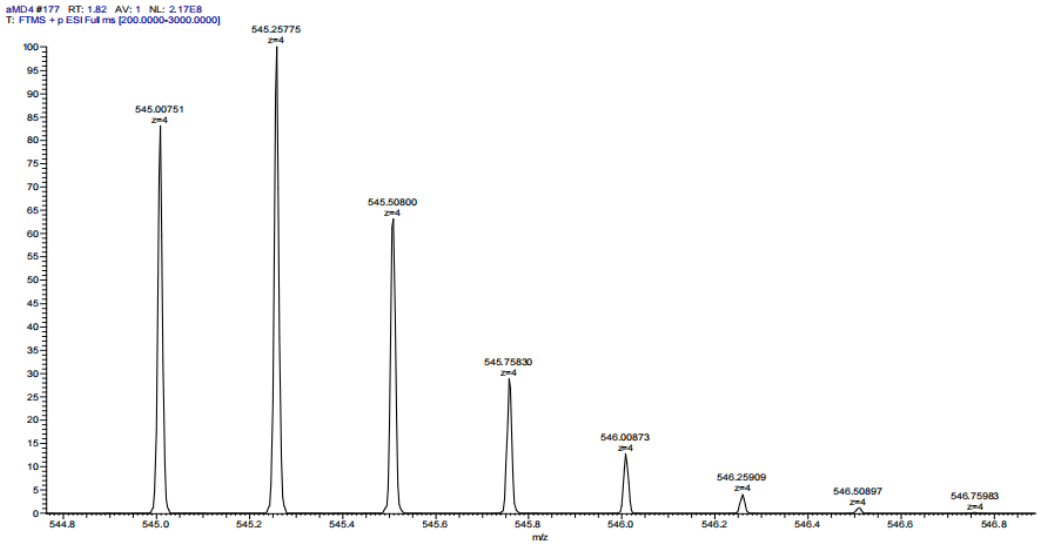

m/z	Theo. Mass	Delta (ppm)	RDB equiv.	Composition	
545.00751	545.0078	-0.53	41	C95 H141 O27 N31 S	$[M+4H]^{4+}$

Fig S213. Q-TOF-HRMS spectrum of **aMD4**. HRMS (ES+) m/z: $[M+4H]^{4+}$ calcd for $C_{95}H_{137}N_{31}O_{27}S_2$ 545.01, found 545.01.

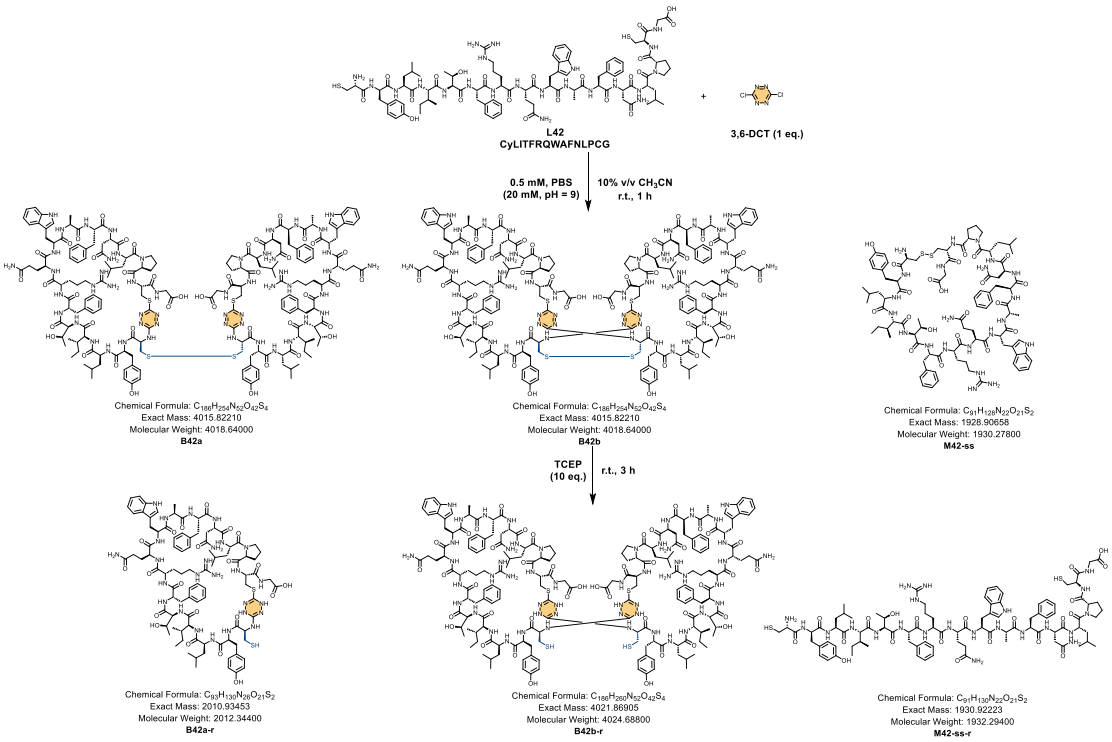

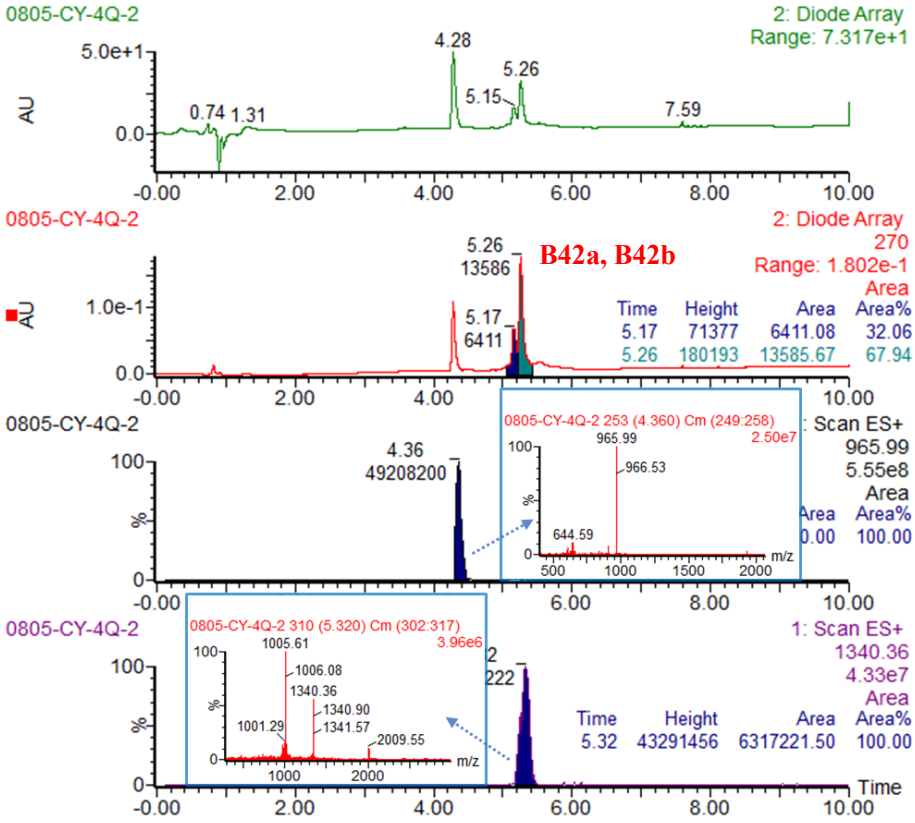

Fig S214 UPLC-MS chromatogram of reaction mixture including TIC, UV curves (full-wavelength and extracted at 270 nm) and ESI-MS spectrum of **B42a** and **B42b**. Extract mass chromatograms from full scan data. The yield of cyclodimerization products was determined to be 31% using Equation 1.

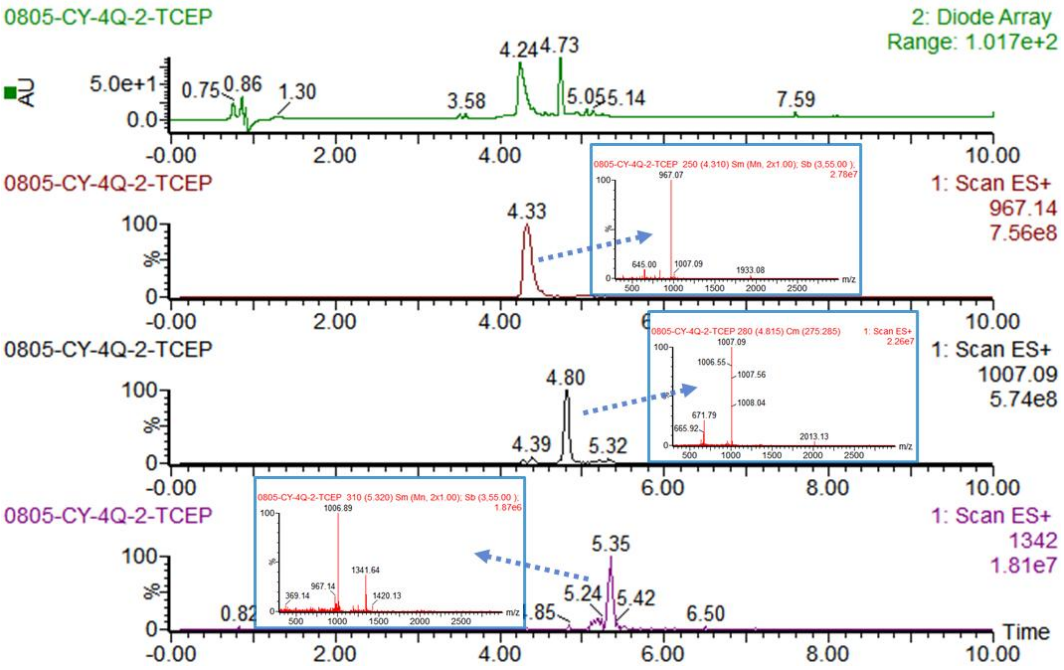

Fig S215. UPLC-MS chromatogram of reaction mixture with TCEP including TIC, UV curve (full-wavelength) and ESI-MS spectrum. Extract mass chromatograms from full scan data.

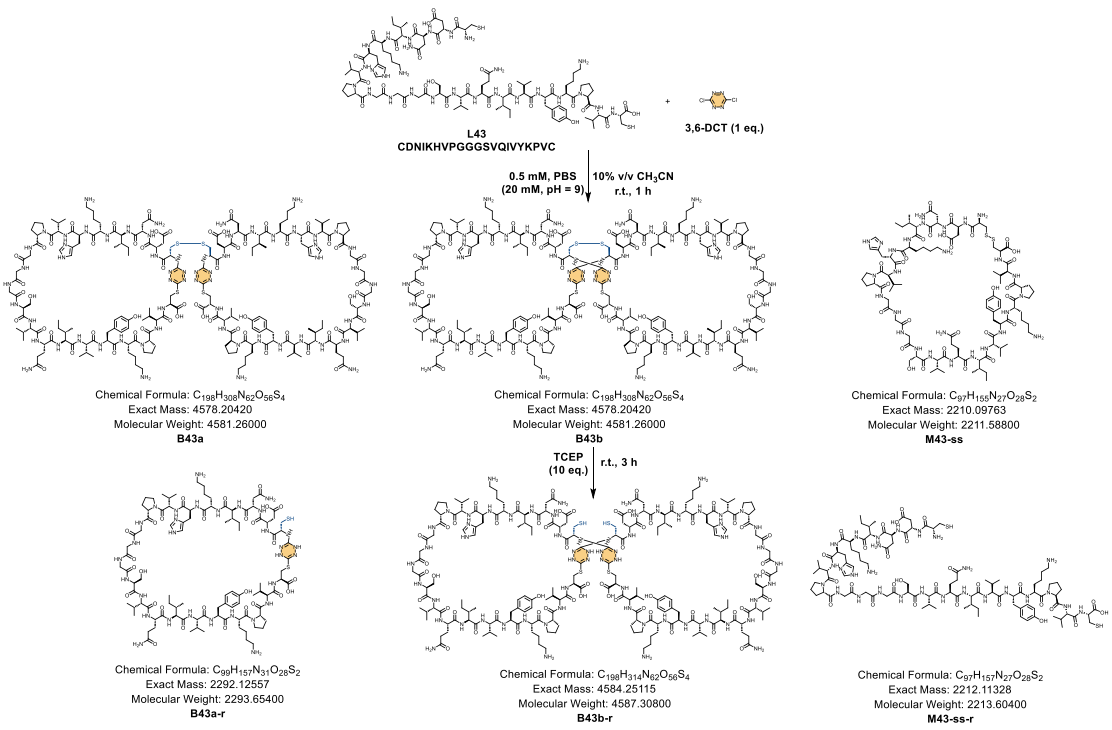

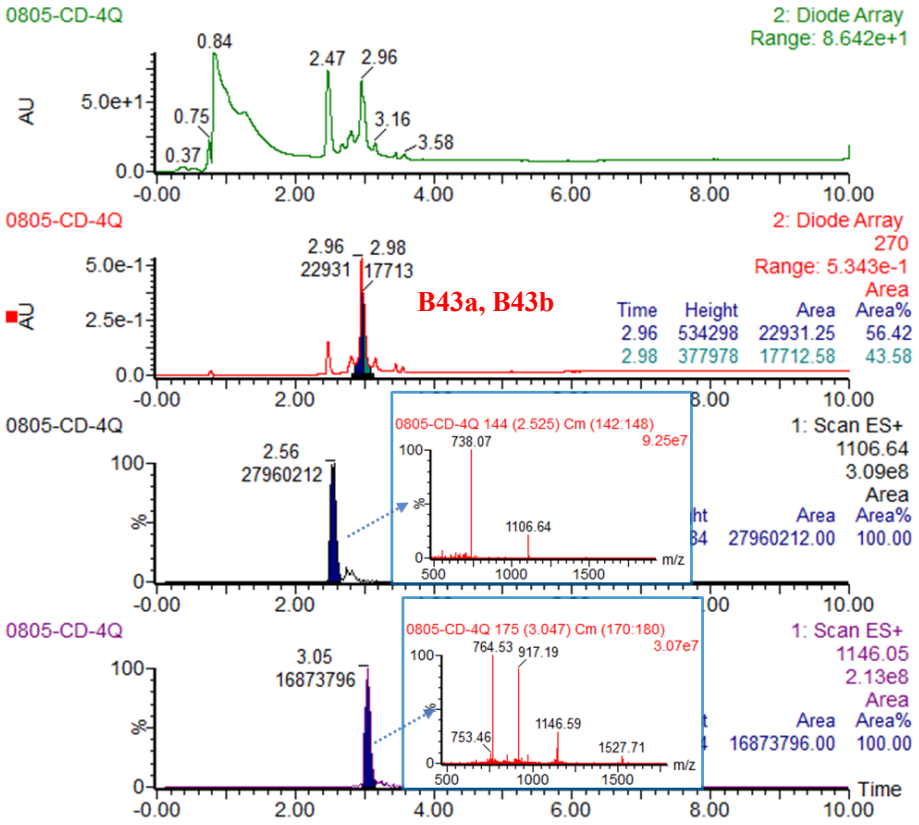

Fig S216 UPLC-MS chromatogram of reaction mixture including TIC, UV curves (full-wavelength

and extracted at 270 nm) and ESI-MS spectrum of **B43a** and **B43b**. Extract mass chromatograms from full scan data. The yield of cyclodimerization products was determined to be 37% using Equation 1.

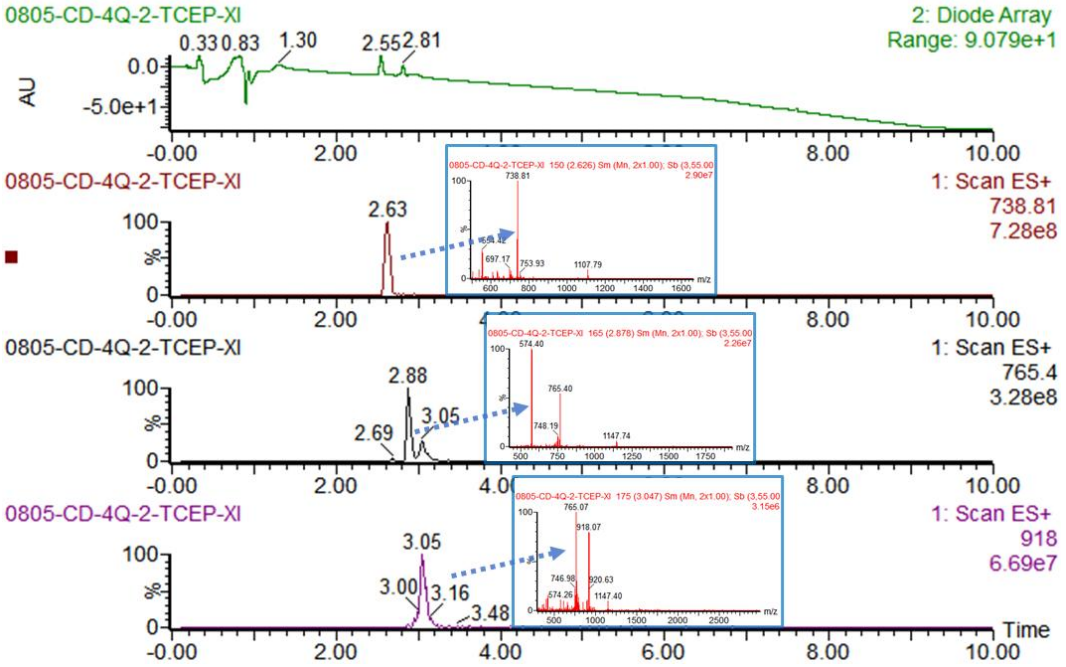

Fig S217. UPLC-MS chromatogram of reaction mixture with TCEP including TIC, UV curve (full-wavelength) and ESI-MS spectrum. Extract mass chromatograms from full scan data.

7.2 Circular dichroism assay

Before sample measurement, **L41, B41a,** and **aMD4** was diluted to a final concentration of 10 μM in ultrapure water. Subsequently, spectral data were recorded using a Jasco J-815 CD spectrometer, with the wavelength range set from 260 to 190 nanometers at a precision of 0.1 nanometer intervals. The scan speed was set at 50 nanometers per minute, with a data integration time of 4 seconds, a bandwidth of 1 nanometer, and an optical path length of 1 millimeter. Measurements were repeated three times to enhance data reliability. The entire measurement process was conducted under a constant temperature of 25°C. Finally, all recorded spectral data required subtraction of the background signal containing only the ultrapure water.

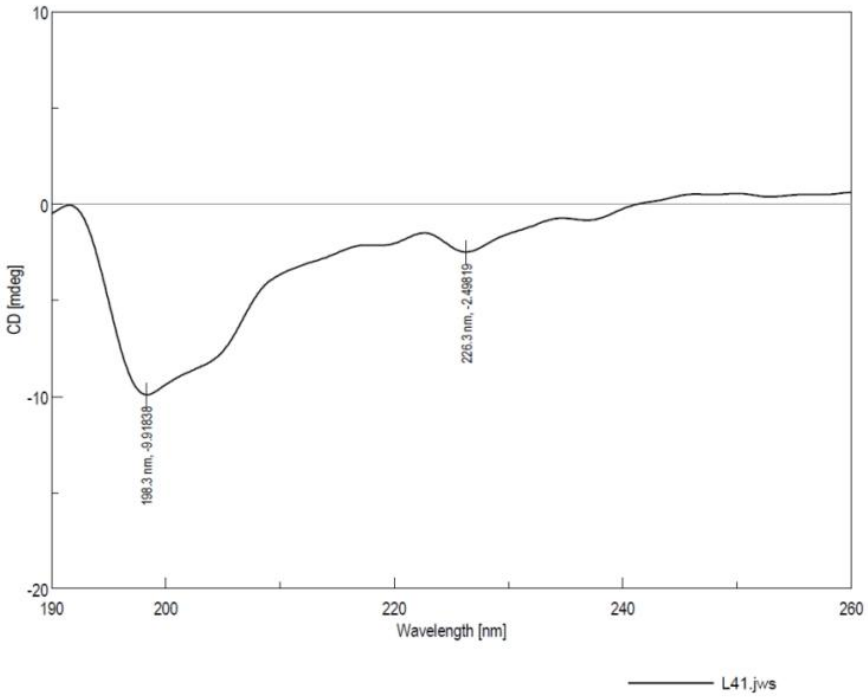

[Measurement Information]

Instrument name	IMMCD
Model name	J-815
Serial No.	A024461168
Accessory	Standard
Accessory S/N	A005461185
Cell length	1 mm
Measurement date	2026/3/27 16:29
Photometric mode	CD, HT, Abs
Measure range	260 - 190 nm
Data pitch	0.1 nm
Sensitivity	Standard
D.I.T.	4 sec
Bandwidth	1.00 nm
Start mode	Immediately
Scanning speed	50 nm/min
Baseline correction	Baseline
Shutter control	Auto
CD detector	PMT
PMT voltage	Auto
Accumulations	2
Concentration	0.1 mmol/L
Solvent	H2O

[Detailed Information]

Creation date	2026/3/30 16:32
Data array type	Linear data array * 3
Horizontal axis	Wavelength [nm]
Vertical axis(1)	CD [mdeg]
Vertical axis(2)	HT [V]
Vertical axis(3)	Abs
Start	260 nm
End	190 nm
Data interval	0.1 nm
Data points	701

Fig S218. Circular dichroism spectrum of **L41**.

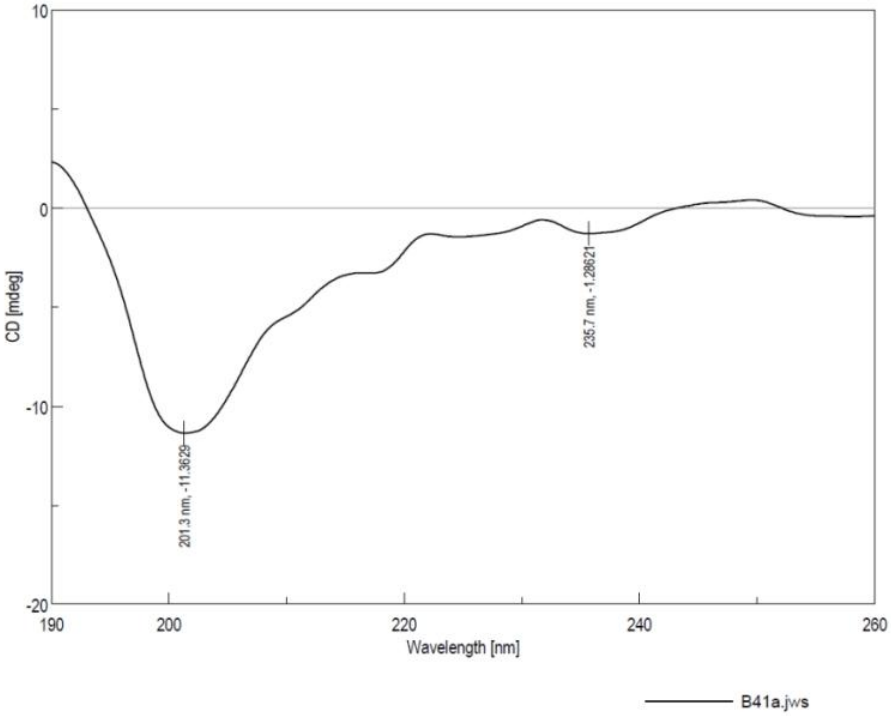

[Measurement Information]

Instrument name	IMMCD
Model name	J-815
Serial No.	A024461168
Accessory	Standard
Accessory S/N	A005461185
Cell length	1 mm
Measurement date	2026/3/27 16:39
Photometric mode	CD, HT, Abs
Measure range	260 - 190 nm
Data pitch	0.1 nm
Sensitivity	Standard
D.I.T.	4 sec
Bandwidth	1.00 nm
Start mode	Immediately
Scanning speed	50 nm/min
Baseline correction	Baseline
Shutter control	Auto
CD detector	PMT
PMT voltage	Auto
Accumulations	2
Concentration	0.1 mmol/L
Solvent	H2O

[Detailed Information]

Creation date	2026/3/30 16:31
Data array type	Linear data array * 3
Horizontal axis	Wavelength [nm]
Vertical axis(1)	CD [mdeg]
Vertical axis(2)	HT [V]
Vertical axis(3)	Abs
Start	260 nm
End	190 nm
Data interval	0.1 nm
Data points	701

Fig S219. Circular dichroism spectrum of **B41a**.

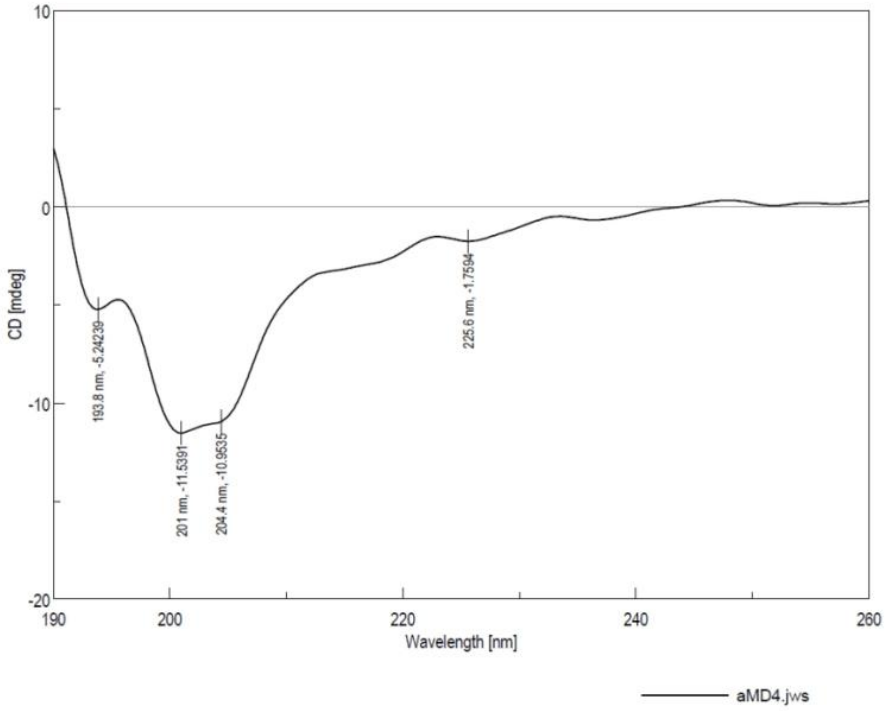

[Measurement Information]

Instrument name	IMMCD
Model name	J-815
Serial No.	A024461168
Accessory	Standard
Accessory S/N	A005461185
Cell length	1 mm
Measurement date	2026/3/27 16:48
Photometric mode	CD, HT, Abs
Measure range	260 - 190 nm
Data pitch	0.1 nm
Sensitivity	Standard
D.I.T.	4 sec
Bandwidth	1.00 nm
Start mode	Immediately
Scanning speed	50 nm/min
Baseline correction	Baseline
Shutter control	Auto
CD detector	PMT
PMT voltage	Auto
Accumulations	2
Concentration	0.1 mmol/L
Solvent	H2O

[Detailed Information]

Creation date	2026/3/30 16:33
Data array type	Linear data array * 3
Horizontal axis	Wavelength [nm]
Vertical axis(1)	CD [mdeg]
Vertical axis(2)	HT [V]
Vertical axis(3)	Abs
Start	260 nm
End	190 nm
Data interval	0.1 nm
Data points	701

Fig S220. Circular dichroism spectrum of **aMD4**.

7.3 Detailed NMR assignment of key residues in L38, B38a, and B38b

The unambiguous determination of the three-dimensional topologies for the bicyclic isomers **B38a** and **B38b**, as well as their linear precursor **L38**, relies heavily on the precise ^{1}H and ^{13}C NMR assignments of three cornerstone residues: the N-terminal Cys1, the C-terminal Cys9, and the internal Lys. The assignment strategy utilized a rigorous combination of 2D TOCSY, COSY, HSQC, and HMBC experiments,

employing a bottom-up spin-system extraction approach to confirm the covalent connectivity and the strict regioselectivity of the dual-cyclization.

7.3.1 NMR Assignment of linear peptide L38

The resonance assignment for the linear peptide **L38** served as the conformational baseline. Starting from the distinct Hα proton (4.47 ppm), TOCSY and COSY spectra revealed the complete, unconstrained aliphatic spin network of the Lys side chain, terminating at the ε-CH_2 protons (2.75 ppm). HSQC analysis mapped these ε-protons to a Cε chemical shift of 38.35 ppm.

7.3.2 NMR assignment of B38a

Verification of the Unreacted Internal Lysine:

The assignment was anchored by confirming the chemical integrity of the Lys residue. Using the Lys Hα (4.21 ppm) as a starting point, the TOCSY sequence extracted an uninterrupted spin system down to the ε-CH_2 protons at 2.72 ppm. HSQC correlations verified the corresponding carbon shift as Cε (38.40 ppm). Crucially, the ε-CH_2 and Cε shifts showed virtually no perturbation compared to the linear precursor **L38**. Furthermore, COSY spectra captured a direct correlation between the ε-CH_2 (2.72 ppm) and a broad signal at 7.73 ppm, typical of a free ammonium ion (-NH_3^+). This stationary behavior physically proves the Lys side chain remained completely unreacted during the macrocyclization.

Assignment of the C-terminal Cys9:

With the Lys orthogonality confirmed, the C-terminal Cys9 spin system was identified. TOCSY and COSY linked its Hα (4.51 ppm) to highly diastereotopic Hβ protons (3.43 and 3.86 ppm). HSQC analysis mapped these Hβ protons to a Cβ chemical shift of 30.88 ppm. The Cβ shift at ~30 ppm is an exclusive hallmark of an aromatic thioether, confirming the S-Ar linkage. Most importantly, HMBC cross-peaks from these Cys9 Hβ protons directly to a quaternary carbon at 165.71 ppm (tetrazine core) provided definitive proof of the C-terminal covalent attachment.

Assignment of the N-terminal Cys1:

The N-terminal Cys1 experienced significant deshielding. Its secondary amide proton (NH) was located at an unusually downfield position of 8.76 ppm, characteristic of an arylamine (-NH-Ar) proton forced into the deshielding cone of the tetrazine ring. TOCSY cross-peaks linked this NH to its Hα at 4.79 ppm and Hβ at 3.14 ppm. HSQC

analysis mapped the Cys1 Hβ to a Cβ shift of 38.40 ppm. This specific downfield carbon shift confirms that the Cys1 thiol is oxidized, participating in the intramolecular disulfide (S-S) bond. The final structural loop—the N-Ar covalent linkage—was verified by a clear ^{3}JCH HMBC cross-peak extending from the Cys1 Hα (4.79 ppm) across the secondary amine nitrogen to the tetrazine quaternary carbon (169.66 ppm).

7.3.3 NMR assignment of B38b

The resonance assignment for the second topological isomer, **B38b**, followed the identical logical pathway, revealing highly conserved chemical environments for the local covalent nodes, representing a distinct architectural folding of the bicyclic framework.

Lys and Cys Residues in B38b:

The Lys residue in **B38b** was extracted via its Hα at 4.33 ppm. The sequential TOCSY walk identified the ε-CH_2 protons at 2.75 ppm, mapped via HSQC to a Cε of 38.36 ppm. The absolute stability of these Lys chemical shifts across both isomers reinforces that the side chain acts strictly as a structural bystander. The Cys1 and Cys9 residues exhibited variations in their Hα shifts reflecting the new topological expansion, but the core connectivity nodes (S-Ar, S-S, N-Ar) remained functionally intact, confirming **B38a** and **B38b** as true topological isomers.

Tab S14. Detailed ^{1}H and ^{13}C NMR Chemical Shifts (ppm) of key residues in L38, B38a, and B38b

Isomer	Residue	CONH	α (H/C)	β (H/C)	γ (H/C)	δ (H/C)	ε (H/C)	NH_2	Key 2D Correlations
L38	Lys	8.39	4.47 / 49.61	1.69, 1.63/ 31.05	1.27, 1.34/ 21.77	1.52/ 26.19	2.75/ 38.35	7.86	
B38a	Lys	7.67	4.21 / 52.09	1.75 / 30.44	1.22 / 21.83	1.47 / 26.17	2.72 / 38.40	7.73	COSY: ε-H (2.72) → NH_2 (7.73)
	Cys1	8.76	4.78 / 54.08	3.14 / 38.40	—	—	—	—	HMBC: Hα → Tz C (169.66); N-Ar bond
	Cys9	8.24	4.51 / 51.65	3.42, 3.86/ 30.88	—	—	—	—	HMBC: Hβ → Tz C (165.71); S-Ar bond

B38b	Lys	—	4.33 / 51.84	1.74 / 30.63	1.33, 1.24 / 21.79	1.51 / 26.21	2.75 / 38.36	7.75	COSY: ε-H (2.75) → NH_2 (7.75)
	Cys1	8.79	4.85 / 53.61	3.22 / 40.13	—	—	—	—	N-Ar NH at 8.79; Cβ (40.13) indicates S-S
	Cys9	8.23	4.51 / 49.63	3.42, 3.84 / 30.85	—	—	—	—	HMBC: Hβ → Tz C (167.13); S-Ar bond

8. Functionalization of tetrazine-containing cyclodimerization products and construction of three FAP-targeted radiotracers

8.1 Construction of three FAP-targeted radiotracers

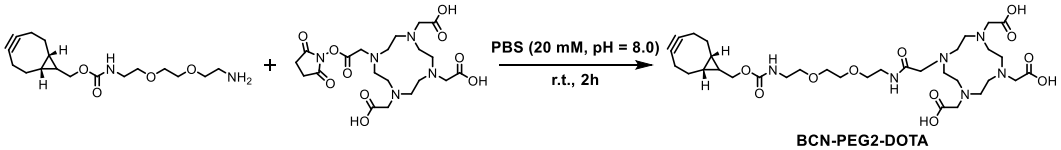

Chemical Formula: $C_{17}H_{28}N_2O_4$
Exact Mass: 324.2049
Molecular Weight: 324.4210

Chemical Formula: $C_{20}H_{31}N_5O_{10}$
Exact Mass: 501.2071
Molecular Weight: 501.4930

BCN-PEG2-DOTA
Chemical Formula: $C_{33}H_{54}N_6O_{11}$
Exact Mass: 710.3851
Molecular Weight: 710.8260

Equimolar amounts of rel-((1R,8S,9s)-bicyclo[6.1.0]non-4-yn-9-yl)methyl (2-(2-(2-aminoethoxy)ethoxy)ethyl)carbamate and NHS-DOTA were dissolved in PBS (20 mM, pH = 8.0) and allowed to react at room temperature for 2 h. The reaction mixture was purified by HPLC to afford **BCN-PEG2-DOTA**.

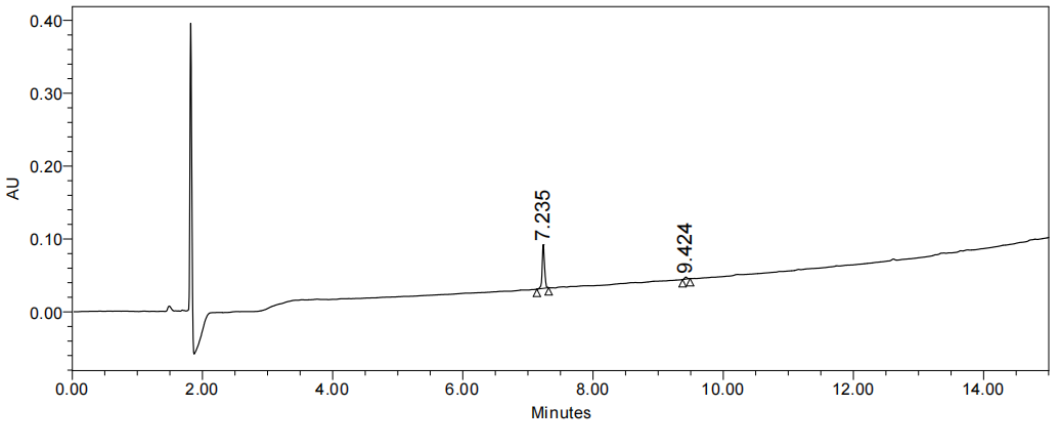

Processed Channel Descr.: 2998 Ch1 220nm@4.8nm

	Processed Channel Descr.	RT	Area	% Area	Height
1	2998 Ch1 220nm@4.8nm	7.235	150621	95.33	59948
2	2998 Ch1 220nm@4.8nm	9.424	7374	4.67	2647

Fig S221. HPLC-UV chromatogram at 220 nm of **BCN-PEG2-DOTA**. Analytical HPLC using Method B, RT = 7.235 min, the HPLC purity is 95%.

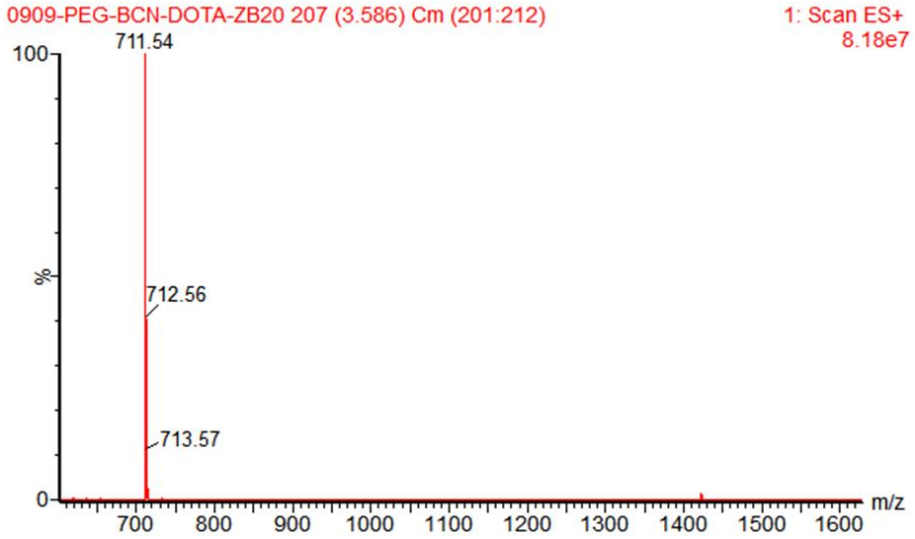

Fig S222. LRMS spectrum of **BCN-PEG2-DOTA**. LRMS (ESI+) m/z: 711.54 $[M + H]^+$.

Under the standard reaction conditions, the cyclodimerization product **B36a** was re-synthesized and purified in sufficient quantity via the 3,6-DCT-mediated cyclodimerization reaction, one of the isomeric products was isolated and purified for further experiments. The purified **B36a** was dissolved in PBS (20 mM, pH = 7.4), followed by the addition of BCN-PEG2-DOTA conjugate (2.5 equiv.). The mixture was shaken at room temperature and 800 rpm for 48 h on a thermostatic shaker, and the product **FAP-B36** was obtained after purification by HPLC.

Similarly, the lyophilized product **FAP-B36** was dissolved in PBS (20 mM, pH = 7.4), treated with TCEP (10 equiv.), and reacted at room temperature for 30 min to cleave the disulfide bond. The reaction mixture was purified by HPLC to afford **FAP-B36-r**.

The lyophilized product **FAP-B36-r** was dissolved in PBS (20 mM, pH = 7.4) and reacted with N-butyl-2-chloroacetamide (10 equiv.) at room temperature for 2 h. After purification by HPLC, the desired product **FAP-B36-m** was obtained. All compounds **FAP-B36**, **FAP-B36-r**, and **FAP-B36-m** exhibited isomeric species, attributed to the presence of the BCN functionality. And their radiolabeled analogs also displayed isomeric species.

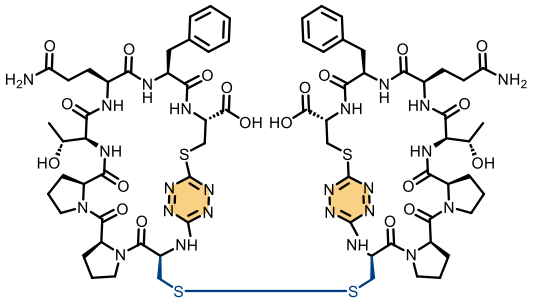

B36a

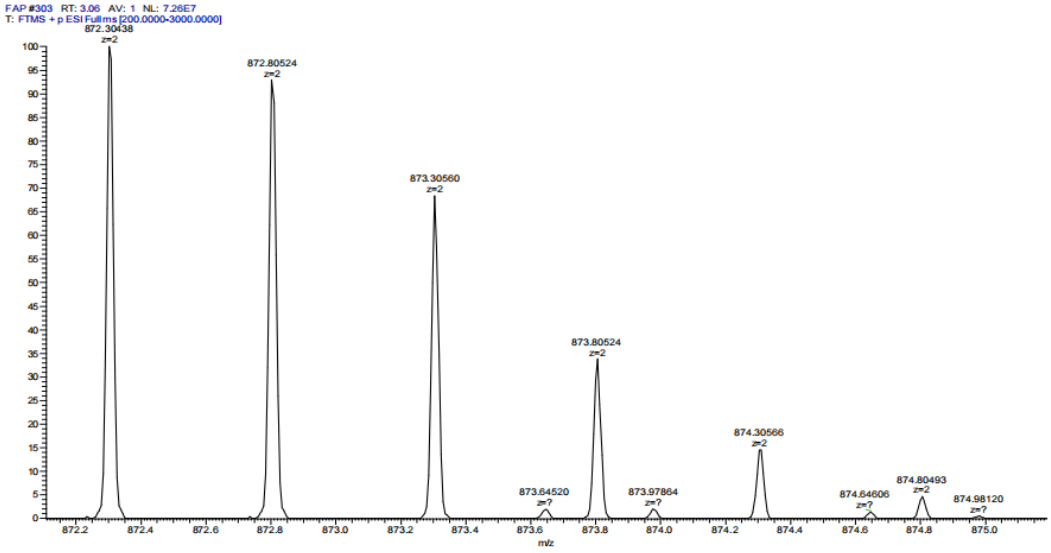

m/z	Theo. Mass	Delta (ppm)	RDB equiv.	Composition	
872.30438	872.30523	-0.97	37	C72 H96 O20 N24 S4	$[M+2H]^{2+}$

Fig S223. Q-TOF-HRMS spectrum of **B36a**. HRMS (ES+) m/z: $[M+2H]^{2+}$ calcd for $C_{72}H_{94}N_{24}O_{20}S_4$ 872.30, found 872.30.

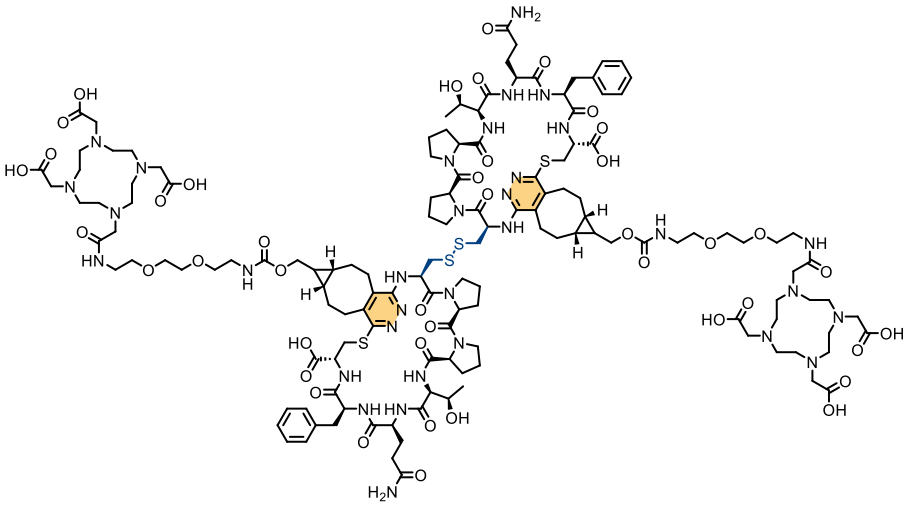

FAP-B36

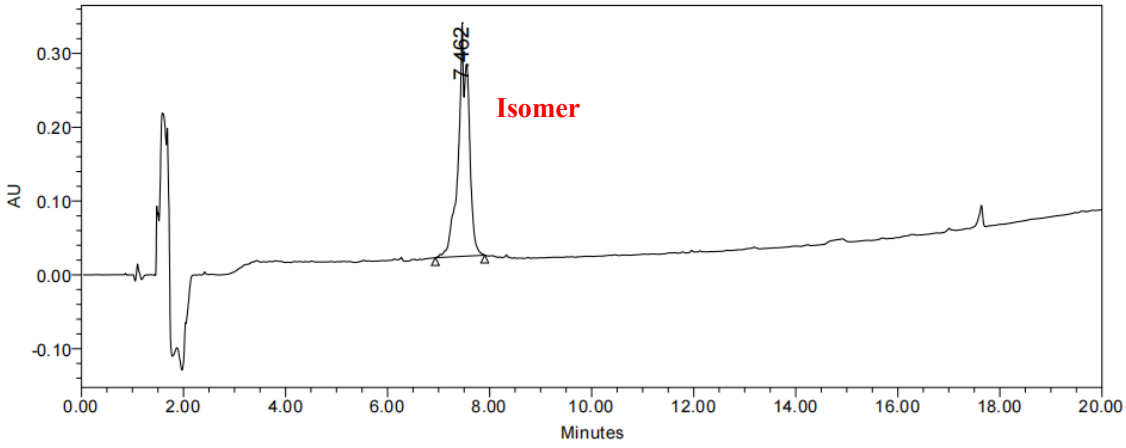

Processed Channel Descr.: 2998 Ch1 220nm@4.8nm

	Processed Channel Descr.	RT	Area	% Area	Height
1	2998 Ch1 220nm@4.8nm	7.462	4418749	100.00	316357

Fig S224. HPLC-UV chromatogram at 220 nm of **FAP-B36**. Analytical HPLC using Method B, RT = 7.462 min, the HPLC purity is 99%.

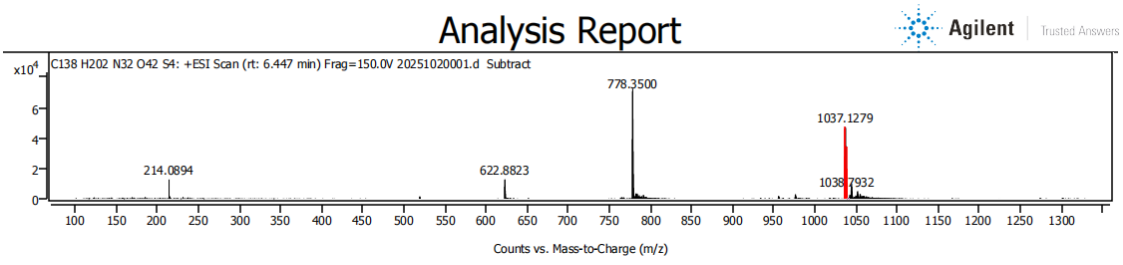

Spectrum Identification Table

Best ID Source	Name	Formula	Species	m/z	Diff (ppm)	CAS	Score	Score (Lib)	Score (DB)	Score (MFG)	Lib/DB
Yes MFG		C138 H202 N32 O42 S4	(M+3H)+3	1036.7923	1.20		99.93			99.93	

Fig S225. Q-TOF-HRMS spectrum of **FAP-B36**. HRMS (ES+) m/z: $[M+3H]^{3+}$ calcd for $C_{138}H_{202}N_{32}O_{42}S_4$ 1036.7846, found 1036.7923.

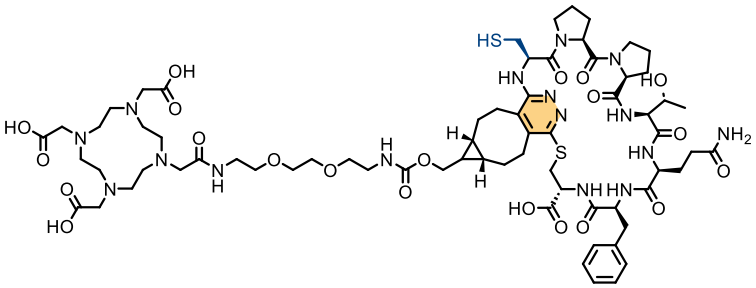

FAP-B36-r

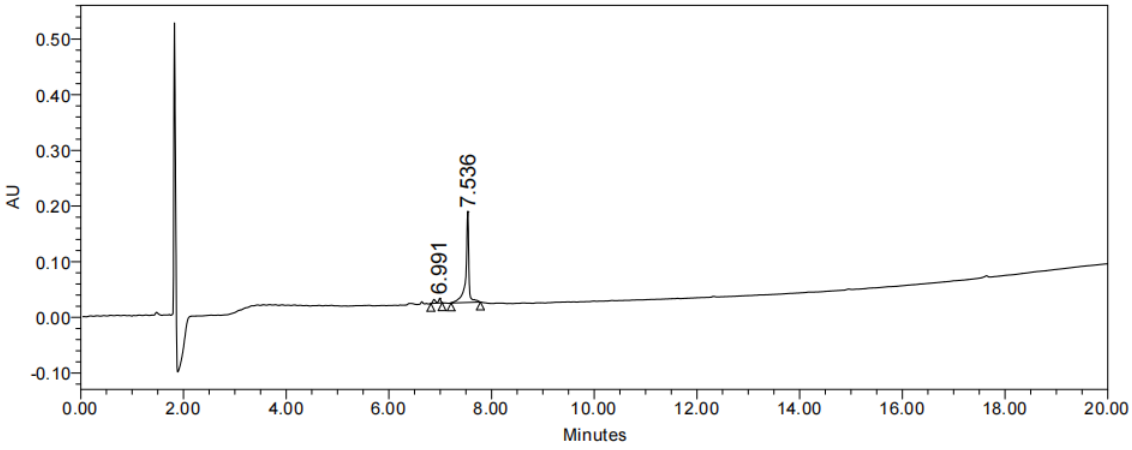

Processed Channel Descr.: 2998 Ch1 220nm@4.8nm

	Processed Channel Descr.	RT	Area	% Area	Height
1	2998 Ch1 220nm@4.8nm	6.991	48182	6.68	8349
2	2998 Ch1 220nm@4.8nm	7.536	673236	93.32	163846

Fig S226. HPLC-UV chromatogram at 220 nm of **FAP-B36-r**. Analytical HPLC using Method B, RT = 7.536 min, the HPLC purity is 93%.

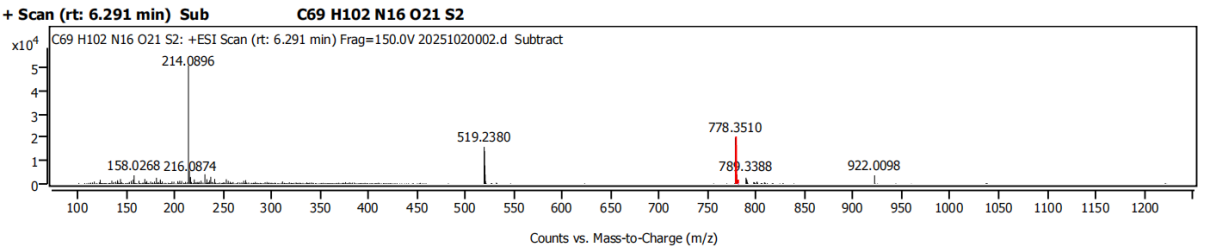

Analysis Report

Agilent Trusted Answers

Spectrum Identification Table

Best	ID Source	Name	Formula	Species	m/z	Diff (ppm)	CAS	Score	Score (Lib)	Score (DB)	Score (MFG)	Lib/DB
Yes	MFG		C69 H102 N16 O21 S2	(M+2H)+2	778.3510	1.79		99.90			99.90	

Fig S227. Q-TOF-HRMS spectrum of **FAP-B36-r**. HRMS (ES+) m/z: $[M+2H]^{2+}$ calcd for $C_{69}H_{102}N_{16}O_{21}S_2$ 778.3424, found 778.3510.

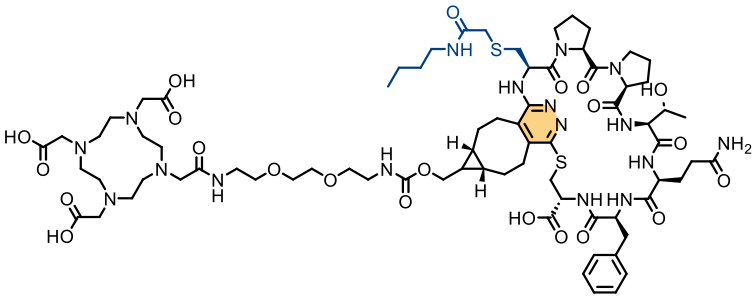

FAP-B36-m

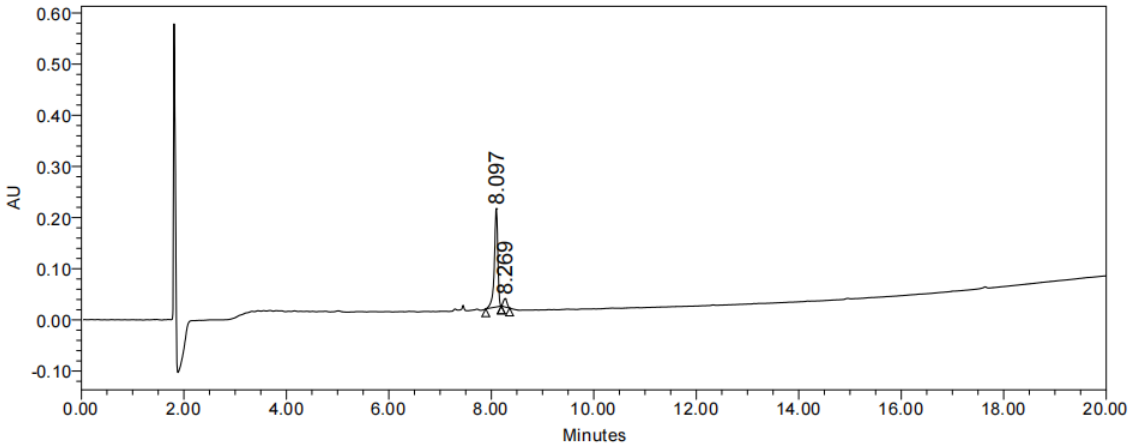

Processed Channel Descr.: 2998 Ch1 220nm@4.8nm

	Processed Channel Descr.	RT	Area	% Area	Height
1	2998 Ch1 220nm@4.8nm	8.097	886909	91.72	192351
2	2998 Ch1 220nm@4.8nm	8.269	80024	8.28	16204

Fig S228. HPLC-UV chromatogram at 220 nm of **FAP-B36-m**. Analytical HPLC using Method B, RT = 8.097 min, the HPLC purity is 92%.

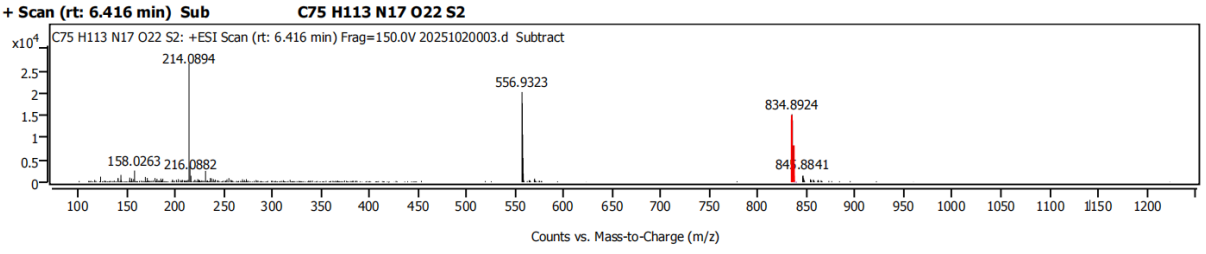

Analysis Report

Agilent Trusted Answers

Spectrum Identification Table

Best ID Source	Name	Formula	Species	m/z	Diff (ppm)	CAS	Score	Score (Lib)	Score (DB)	Score (MFG)	Lib/DB
Yes MFG		C75 H113 N17 O22 S2	(M+2H)+2	834.8924	0.64		99.98			99.98	

Fig S229. Q-TOF-HRMS spectrum of **FAP-B36-m**. HRMS (ES+) m/z: $[M+2H]^{2+}$ calcd for $C_{75}H_{113}N_{17}O_{22}S_2$ 834.8844, found 834.8924.

8.2 Radiolabeling

FAP-B36, **FAP-B36-r**, and **FAP-B36-m** (20 μg) was first dissolved in 0.01 mL of H_2O, and then the peptide solution was placed in 1 mL of 0.25 M sodium acetate. Another 4 mL of 0.05 M hydrochloric acid solution was passed through a $^{68}Ge/^{68}Ga$ generator to generate a hydrochloric acid solution containing ^{68}Ga. ^{68}Ga was mixed with the precursor solution at a ratio of 1:4 and incubated at 100 °C for 15 min. After radiolabeling, the cooled crude reaction was passed through a preconditioned C-18 Sep-Pak cartridge and eluted with 200ul of ethanol and the solution was analyzed for radiolabeling purity by RP-HPLC (Radio column, YMC-Triat-C18 (4.6 mm i.d. 150 mm, 5 mm); solvent A, deionized water; solvent B, acetonitrile (0.1% trifluoroacetic acid (TFA)); flow time, 15 min with acetonitrile from 10% to 100%.

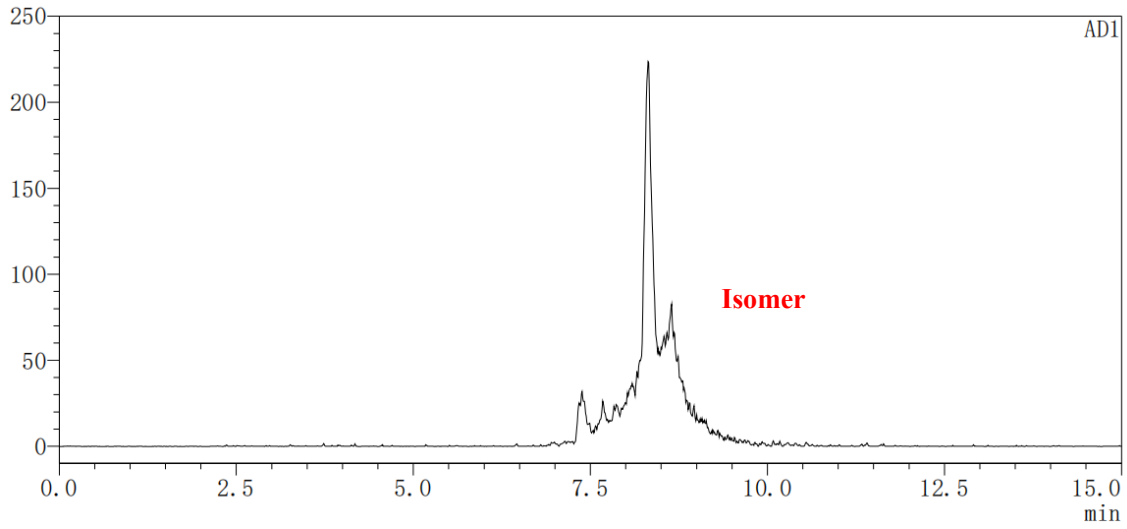

Fig S230. The radio-HPLC of **[^{68}Ga]-FAP-B36.**

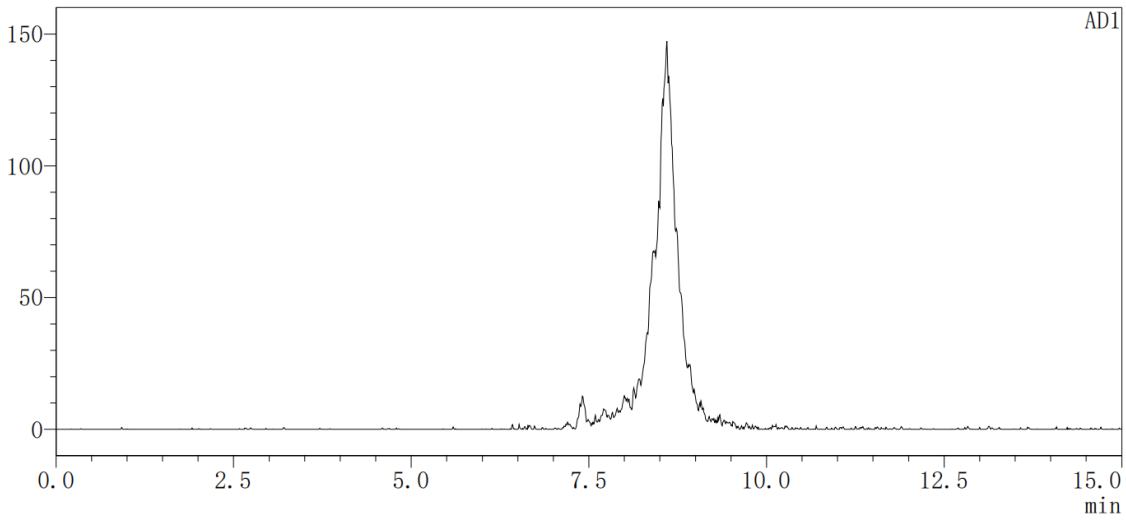

Fig S231. The radio-HPLC of **[^{68}Ga]-FAP-B36-r.**

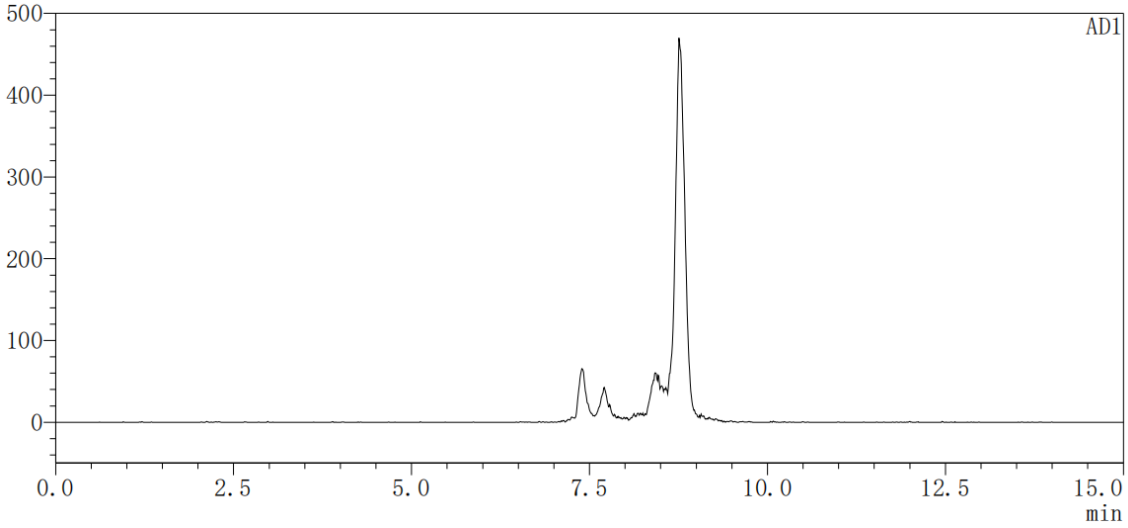

Fig S232. The radio-HPLC of **[^{68}Ga]-FAP-B36-m.**

8.3 Lipid-water partition coefficient

[^{68}Ga]-FAP-B36, [^{68}Ga]- FAP-B36-r, and **[^{68}Ga]- FAP-B36-m** (0.1 MBq each) were added to a mixture containing 5.0 mL of H_2O and 5.0 mL of n-octanol. The mixture was vigorously shaken for 2 min and then allowed to stand for 1 h until complete phase separation was observed (vigorous shaking should be avoided during the standing period). Using a pipette, four samples (0.1 mL each) were collected from both the upper (n-octanol) and lower (H_2O) layers. The radioactivity of each layer was measured with a gamma counter. The lipid-water partition coefficient was calculated as LogP = Log (n-octanol counts / H_2O counts), the lipid-water partition coefficient of **[^{68}Ga]-FAP-B36, [^{68}Ga]- FAP-B36-r, [^{68}Ga]- FAP-B36-m** are shown in **Tab S15**.

Tab S15. The lipid-water partition coefficient of **[^{68}Ga]-FAP-B36** to **[^{68}Ga]-FAP-B36-m**

Name	^{68}Ga water	^{68}Ga n-octanol	LogP
[^{68}Ga]-FAP-B36	493	273052.3	-2.74
[^{68}Ga]-FAP-B36	514	279211.5	-2.73
[^{68}Ga]-FAP-B36	421	277518.5	-2.82
[^{68}Ga]-FAP-B36-r	1107.13	819223.3	-2.87
[^{68}Ga]-FAP-B36-r	1144	830946.9	-2.86
[^{68}Ga]-FAP-B36-r	1407	817239.5	-2.76
[^{68}Ga]-FAP-B36-m	434	275285.9	-2.80
[^{68}Ga]-FAP-B36-m	1174	254193.9	-2.34
[^{68}Ga]-FAP-B36-m	1125.9	262411.4	-2.37

8.4 Western Blot

PC12 cells with high FAP expression were lysed via radioimmunoprecipitation assay (RIPA, R0010, Solarbio, Beijing, China) buffer, sonicated, and then centrifuged (12000 rpm, 20 min, 4 °C), after which the supernatants were collected. The total protein concentration was measured via a bicinchoninic acid (BCA) Kit (P0012, Beyotime, Shanghai, China). First, electrophoresis was performed via sodium dodecyl sulfate–polyacrylamide gel electrophoresis (SDS–PAGE) at 90 V for 20 min, followed by further electrophoresis for 40 min at 126 V. Then, membrane transfer was performed, and the proteins were transferred to polyvinylidene difluoride (PVDF) membranes for 50 min in an ice bath at 400 mA. After being blocked at RT for 3 h in 5% skim milk, the PVDF membranes were incubated with anti-FAP primary antibody (1:1000, diluted in 5% skim milk) overnight at 4 °C. Then, the secondary antibody (1:5000, diluted in 1% TBST) against the primary antibody was added, and the samples were incubated for 1 h at RT. After the samples were washed three times with 1% Tris-buffered saline with Tween (TBST, T1082, Solarbio, Beijing, China), immunoblotting was performed via a Western blotting detection system after treatment with enhanced chemiluminescence reagent (ECL, E411-04, Nanjing, China).

8.5 Tumor cell line culture and tumor-bearing mouse model establishment

The PC12 cell line (characterized by high FAP expression) was obtained from Procell Life Science & Technology Co., Ltd. and utilized as the tumor cell model. Cells were maintained in high-glucose DMEM supplemented with 10% fetal bovine serum, 100 U/mL penicillin, and 50 μg/mL streptomycin. The culture medium was refreshed every two days, and cells were passaged upon reaching 80%–90% confluency.

For the in vivo studies, BALB/c nude mice (4–5 weeks old) were sourced from GemPharmatech (Beijing, China). To establish the tumor-bearing model, PC12 cells (1×10^6 cells/mouse, 1 tumor/mouse) were subcutaneously injected into the left flank of each mouse. Tumor growth was monitored biennially. Generally, PET imaging was performed 10 days after transplantation.

All animal experiments and protocols were strictly performed in accordance with the instructions of the Committee for the Care and Use of Laboratory Animals and were

approved by the Institutional Animal Care and Use Committee (IACUC) of the Institute of Materia Medica, Chinese Academy of Medical Sciences & Peking Union Medical College (IMM-S-25-0053).

8.6 Small Animal PET/CT Study in Tumor-Bearing Mice

PC12 tumor-bearing nude mice models (n = 3) were injected with 100 μCi of **[^{68}Ga]-FAP-B36, [^{68}Ga]- FAP-B36-r,** and **[^{68}Ga]- FAP-B36-m** anesthetized under isoflurane to being placed on PET/CT scanner (Imviscan, France). The whole-body PET images were acquired at 30, 60, 120 and 240 min p.i. The analysis of PET/CT data was performed at the IMALYTICS Preclinical 3.1 with the decay correction of radioactivity. The uptake levels of radiotracers in tumors and organs of interest are presented as percentage of the injected dose per gram (%ID/g).

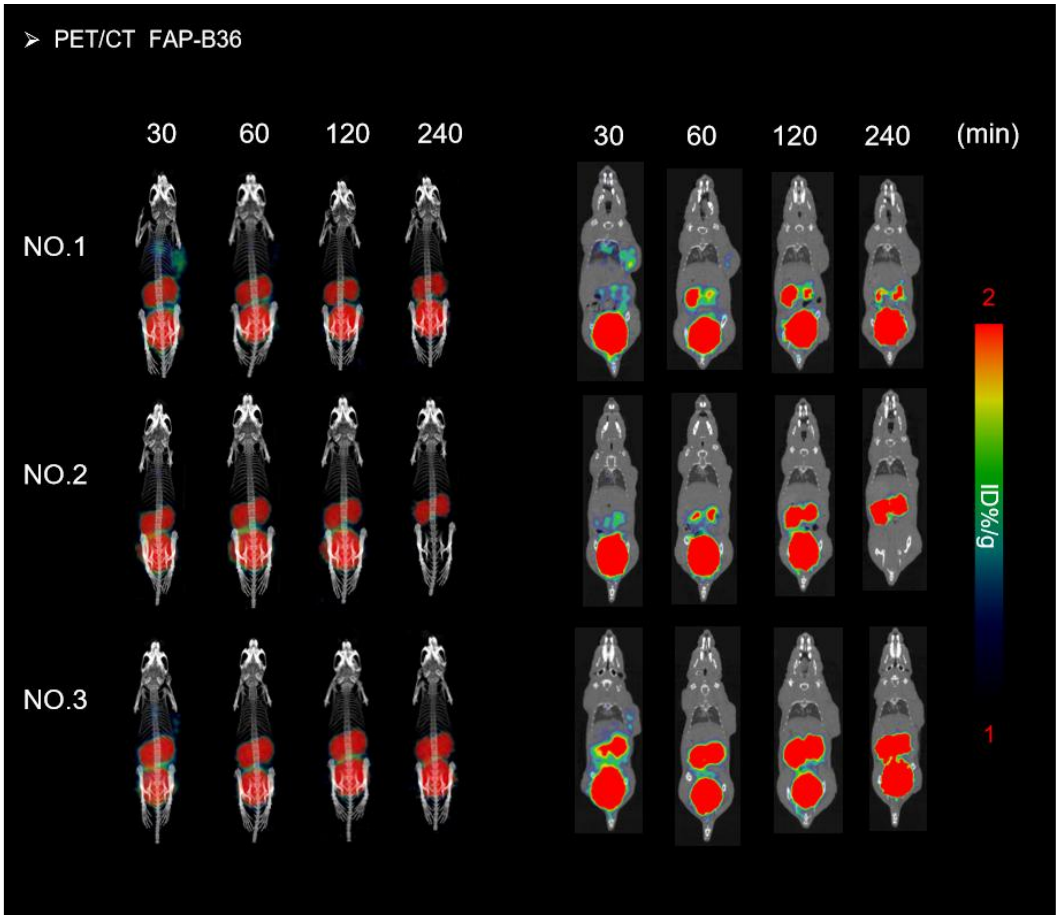

Fig S233. PET/CT images of BALB/c nude mice with **[^{68}Ga]-FAP-B36**.

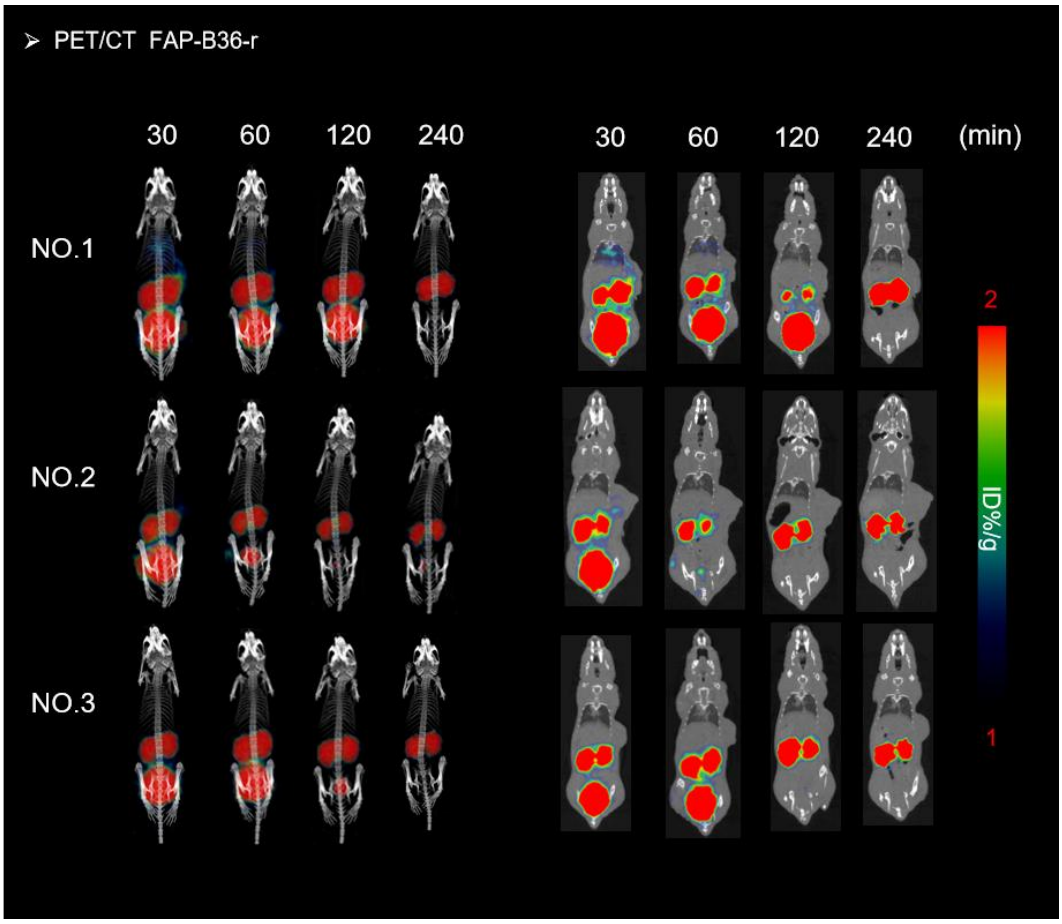

Fig S234. PET/CT images of BALB/c nude mice with **[^{68}Ga]-FAP-B36-r**.

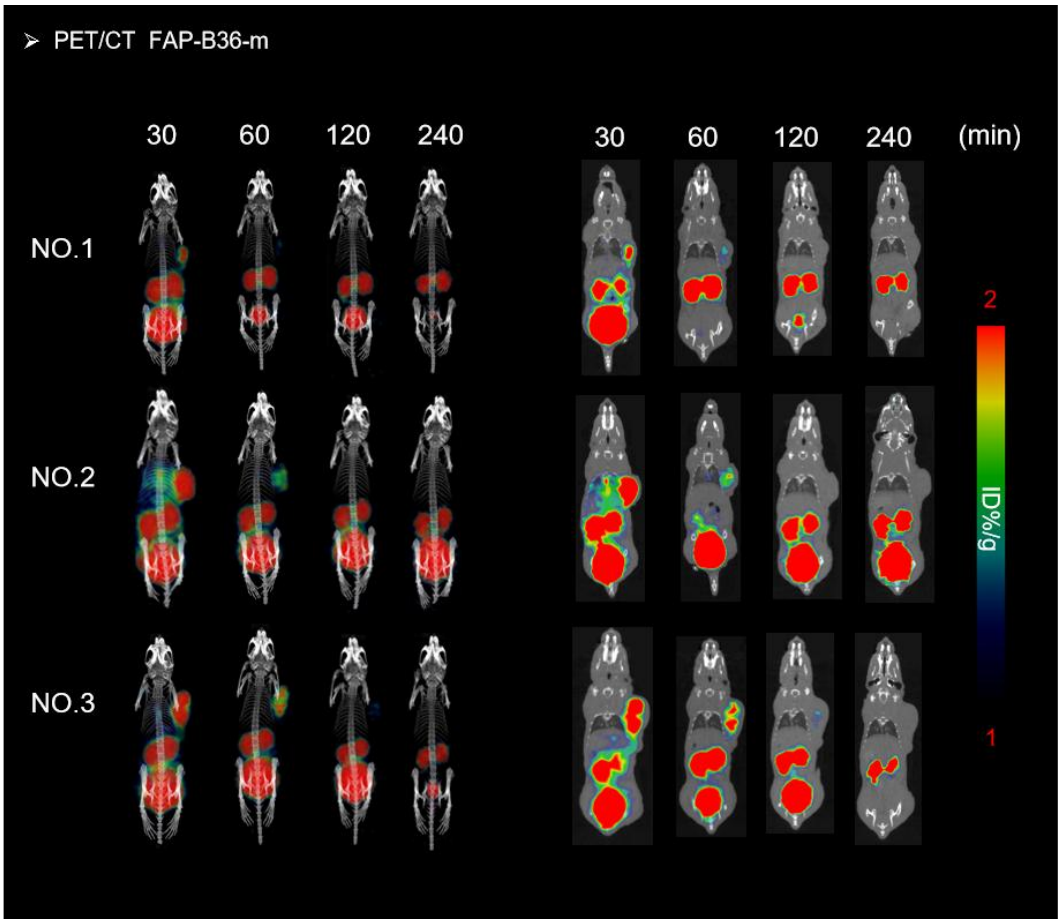

Fig S235. PET/CT images of BALB/c nude mice with **[^{68}Ga]-FAP-B36-m**.

Tab S16. The uptake values of **[^{68}Ga]-FAP-B36** to **[^{68}Ga]- FAP-B36-r** in the heart, liver, kidney, and tumor tissues of PC12 tumor-bearing nude mice at 0.5, 1, 2, and 4 h post-administration.

Name	Number	Tumor (%ID/g)				Liver (%ID/g)				Kidney (%ID/g)				Heart (%ID/g)			
		0.5h	1h	2h	4h	0.5h	1h	2h	4h	0.5h	1h	2h	4h	0.5h	1h	2h	4h
[^{68}Ga]-FAP-B36	1	1.878	1.440	1.289	1.628	0.930	0.748	0.644	0.521	4.517	3.774	3.734	3.839	1.189	0.870	0.580	0.544
	2	0.986	0.844	0.809	0.940	0.816	0.652	0.584	0.559	4.519	4.423	4.437	4.693	0.8998	0.645	0.5482	0.477
	3	1.635	1.076	1.043	1.267	1.066	0.731	0.629	0.578	7.209	6.380	6.805	6.330	1.142	0.725	0.478	0.413
[^{68}Ga]-FAP-B36-m	1	1.460	1.256	0.8104	1.175	0.952	0.759	0.523	0.384	6.551	6.087	6.120	6.089	1.043	0.848	0.530	0.377
	2	1.449	1.289	0.858	0.774	0.785	0.627	0.473	0.394	3.943	3.556	3.384	2.969	0.726	0.706	0.371	0.269
	3	0.994	0.998	0.785	0.850	0.686	0.652	0.470	0.333	4.444	4.845	4.099	3.914	0.747	0.675	0.491	0.378
[^{68}Ga]-FAP-B36-r	1	2.488	1.615	1.211	1.230	0.900	0.607	0.498	0.403	4.211	3.295	2.882	3.240	0.970	0.566	0.406	0.312
	2	3.434	1.986	1.239	1.077	1.312	0.832	0.590	0.508	4.22	2.931	2.784	3.013	1.409	0.837	0.499	0.363
	3	2.963	2.379	1.666	1.316	1.041	0.790	0.540	0.450	3.689	3.077	2.701	2.731	1.171	0.786	0.443	0.319

9. N^2-level expansion of peptide library throughput and topological diversity via 3,6-DCT mediated cyclodimerization

Peptides with different sequences, lengths, and biological activities were randomly combined and subjected to 3,6-DCT-mediated cyclodimerization reactions under equimolar concentrations and standard reaction conditions.

Example procedure (Standard reaction conditions):

The dried peptide substrates (a total of n peptides, bis-cysteine peptides, each containing one N-cysteine, 1.0 equiv. per peptide) were accurately weighed together and dissolved in an appropriate amount of PBS (20 mM, pH = 9.0) to ensure that the concentration of each peptide in the reaction mixture was 0.56 mM. To this solution, 3,6-DCT (n equiv. in total, corresponding to 1.0 equiv. relative to each peptide) dissolved in acetonitrile (1/9 of the buffer volume) was added. The final concentrations in the reaction were 0.5 mM for each peptide, 0.5*n mM for 3,6-DCT, and 10% acetonitrile, followed by thorough mixing. The reaction mixture was shaken at 25 °C and 800 rpm for 1 h on a thermostatic shaker. After completion, 50 μL of the reaction mixture was collected, and 10 μL was injected into the UPLC-MS for analysis.

For **reaction 1**, The dried peptide substrates (**L1** and **L35**, 1.0 equiv. per peptide) were accurately weighed together and dissolved in an appropriate amount of PBS (20 mM, pH = 9.0) to ensure that the concentration of each peptide in the reaction mixture was 0.56 mM. To this solution, 3,6-DCT (2 equiv.) dissolved in acetonitrile (1/9 of the buffer volume) was added. The final concentrations in the reaction were 0.5 mM for each peptide, 1 mM for 3,6-DCT, and 10% acetonitrile, followed by thorough mixing. The reaction mixture was shaken at 25 °C and 800 rpm for 1 h on a thermostatic shaker. After completion, 50 μL of the reaction mixture was collected, and 10 μL was injected into the UPLC-MS for analysis.

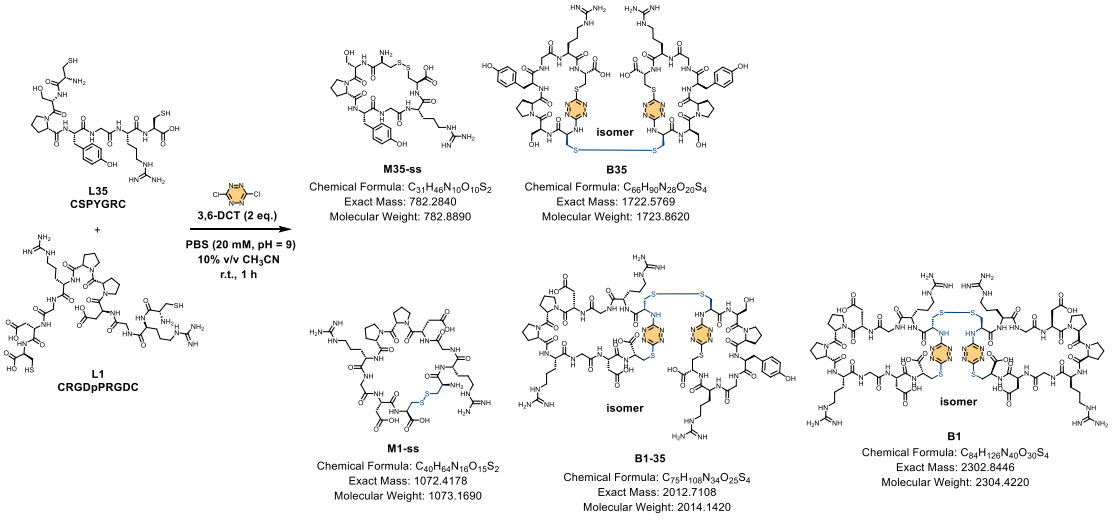

Reaction 1

intramolecular disulfide-bridged products

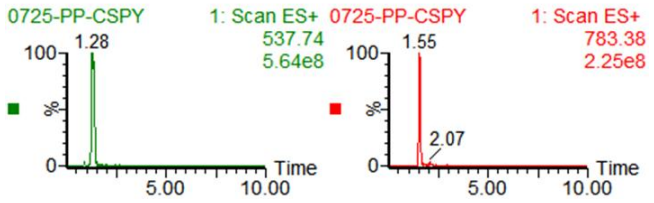

cyclodimerization products

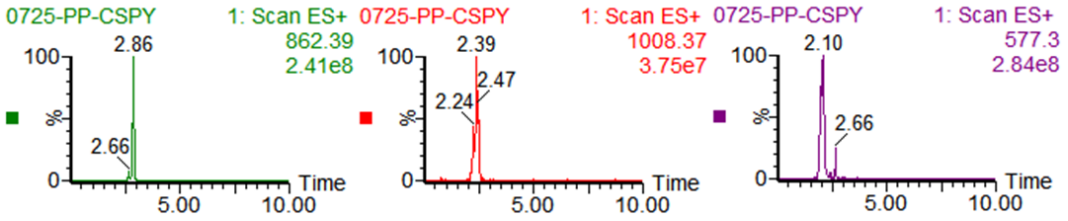

Fig S236. LRMS spectrum of intramolecular disulfide-bridged products and cyclodimerization products in **reaction 1**. Extract mass chromatograms from full scan data.

Tab S17. The LRMS spectrum analysis of **reaction 1.**

Sequence	Products	m/z	
		Theoretical	Measured
L35 (CSPYGRC) L1 (CRGDpPRGDC)	M35-ss	783.89 (z=1)	783.38 (z=1)
	M1-ss	1074.17 (z=1)	537.74 (z=2)
	B35	1724.86 (z=1)	862.39 (z=2)
	B35-1	2015.14 (z=1)	1008.37 (z=2) ; 672.67 (z=3)
	B1	2305.42 (z=1)	769.45 (z=3) ; 577.30 (z=4)

Reaction 2

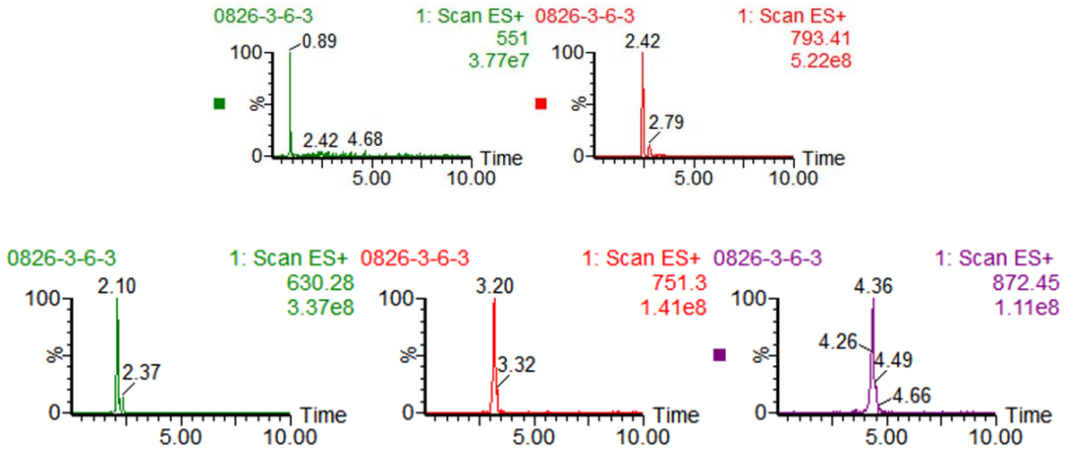

Fig S237. LRMS spectrum of intramolecular disulfide-bridged products and cyclodimerization products in **reaction 2**. Extract mass chromatograms from full scan data.

Tab S18. The LRMS spectrum analysis of **reaction 2.**

Sequence	Products	m/z	
		Theoretical	Measured
L25 (CRGDC) L36 (CPPTQFC)	M25-ss	551.61 (z=1)	551.05 (z=1)
	M36-ss	793.92 (z=1)	793.41 (z=1)
	B25	1260.30 (z=1)	630.28 (z=2)
	B36-25	1502.61 (z=1)	751.30 (z=2)
	B36	1744.93 (z=1)	1744.84 (z=1) ; 872.45 (z=2)

Reaction 3

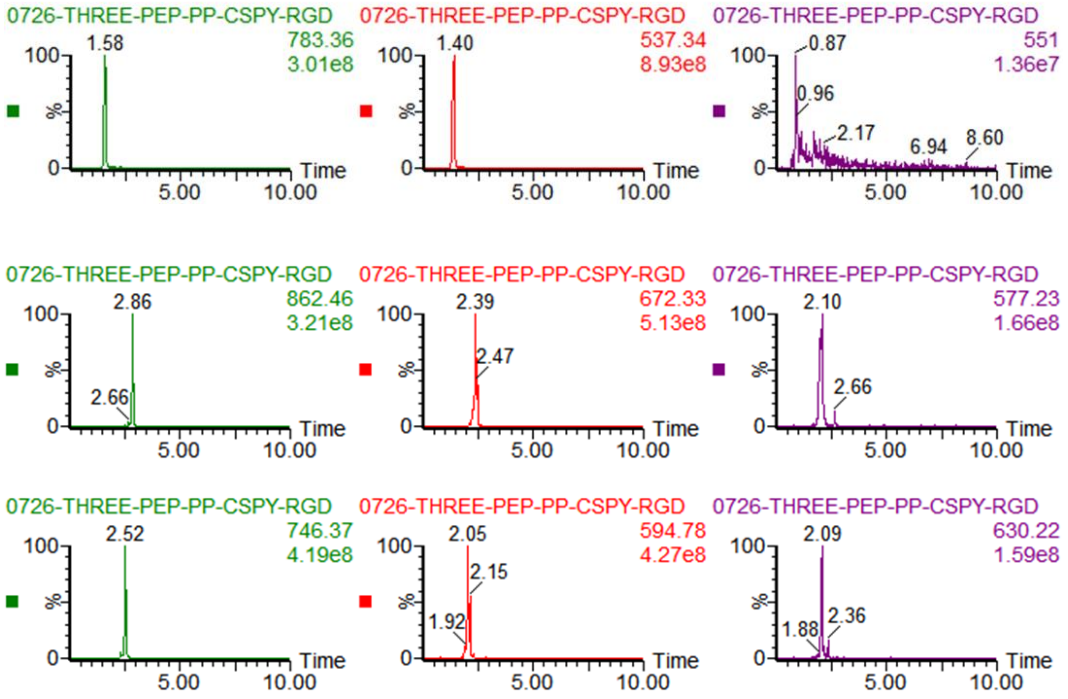

Fig S238. LRMS spectrum of intramolecular disulfide-bridged products and cyclodimerization products in **reaction 3**. Extract mass chromatograms from full scan data.

Tab S19. The LRMS spectrum analysis of **reaction 3.**

Sequence	Products	m/z	
		Theoretical	Measured
	M35-ss	783.89 (z=1)	783.36 (z=1)
	M1-ss	1074.17 (z=1)	537.34 (z=2)
	M25-ss	551.61 (z=1)	551.05 (z=1)
L35 (CSPYGRC)	B35	1724.86 (z=1)	862.46 (z=2)
L1 (CRGDpPRGDC)	B35-1	2015.14 (z=1)	1008.04 (z=2) ; 672.33 (z=3)
L25 (CRGDC)	B1	2305.42 (z=1)	769.52 (z=3) ; 577.23 (z=4)
	B35-25	1492.58 (z=1)	746.37 (z=2)
	B25-1	1782.86 (z=1)	891.41 (z=2) ; 594.78 (z=3)
	B25	1260.30 (z=1)	630.22 (z=2)

Reaction 4

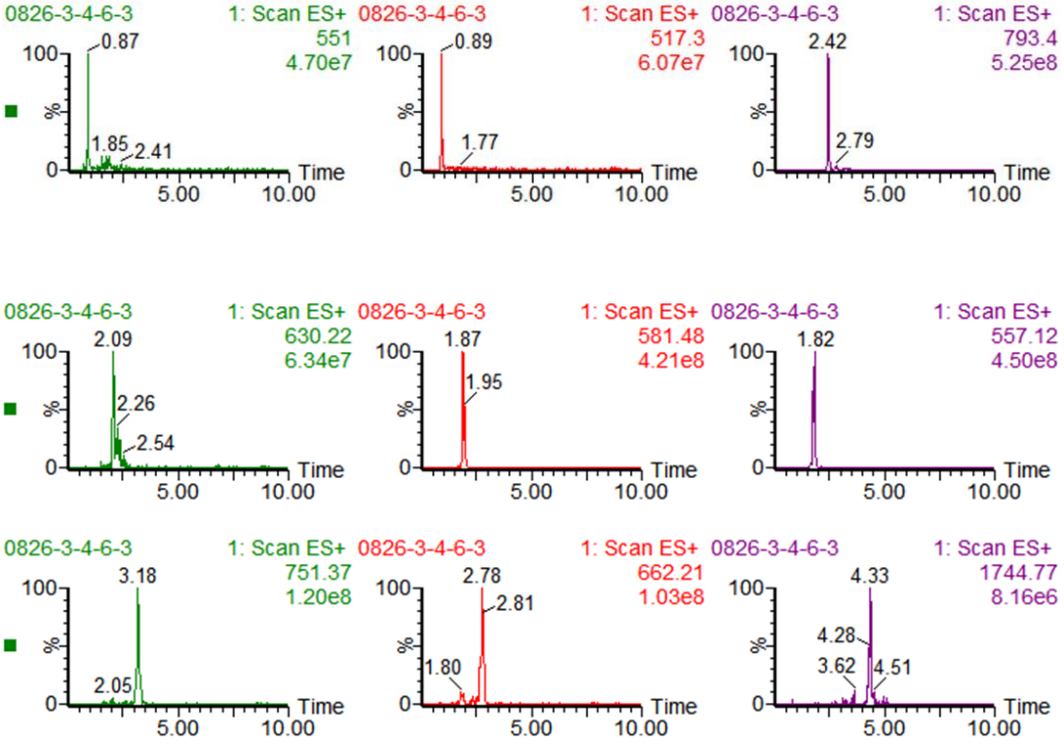

Fig S239. LRMS spectrum of intramolecular disulfide-bridged products and cyclodimerization products in **reaction 4**. Extract mass chromatograms from full scan data.

Tab S20. The LRMS spectrum analysis of **reaction 4.**

Sequence	Products	m/z	
		Theoretical	Measured
	M25-ss	551.61 (z=1)	551.05 (z=1)
	M9-ss	1034.10(z=1)	517.30 (z=2)
	M36-ss	793.92 (z=1)	793.40 (z=1)
L25 (CRGDC)	B25	1260.30 (z=1)	630.22 (z=2)
L9 (CRGDpGRGDC)	B25-9	1742.79 (z=1)	871.31 (z=2) ; 581.48 (z=3)
L36 (CPPTQFC)	B9	2225.29 (z=1)	742.25 (z=3) ; 557.12 (z=4)
	B36-25	1502.61 (z=1)	751.37 (z=2)
	B36-9	1985.11 (z=1)	992.92 (z=2) ; 662.21 (z=3)
	B36	1744.93 (z=1)	1744.77 (z=1) ; 872.45 (z=2)

Reaction 5

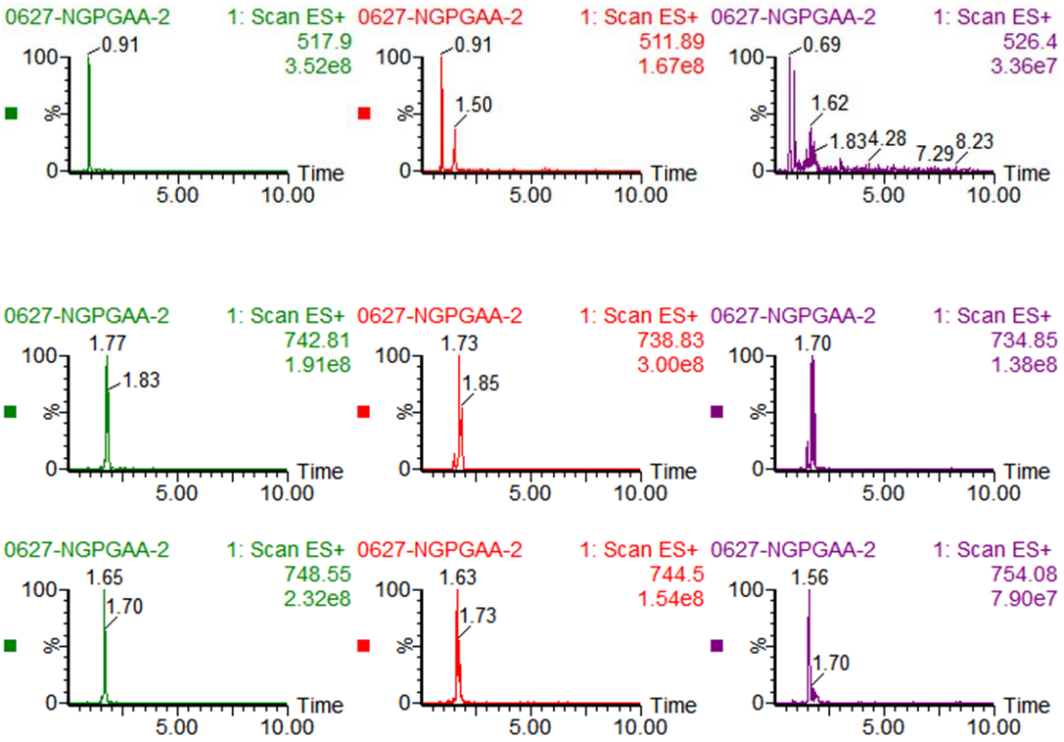

Fig S240. LRMS spectrum of intramolecular disulfide-bridged products and cyclodimerization products in **reaction 5**. Extract mass chromatograms from full scan data.

Tab S21. The LRMS spectrum analysis of **reaction 5.**

Sequence	Products	m/z	
		Theoretical	Measured
	M9-ss	1034.10 (z=1)	517.90 (z=2)
	M6-ss	1022.09 (z=1)	511.89 (z=2)
	M8-ss	1051.90 (z=1)	526.40 (z=2)
L9 (CRGDPGRGDC)	B9	2225.29 (z=1)	742.81 (z=3)
L6 (CRGDAARGDC)	B9-6	2213.28 (z=1)	738.83 (z=3)
L8 (CRGDNGRGDC)	B6	2201.27 (z=1)	734.85 (z=3)
	B9-8	2242.28 (z=1)	748.55 (z=3)
	B8-6	2230.27 (z=1)	744.50 (z=3)
	B8	2259.27 (z=1)	754.08 (z=3)

Reaction 6

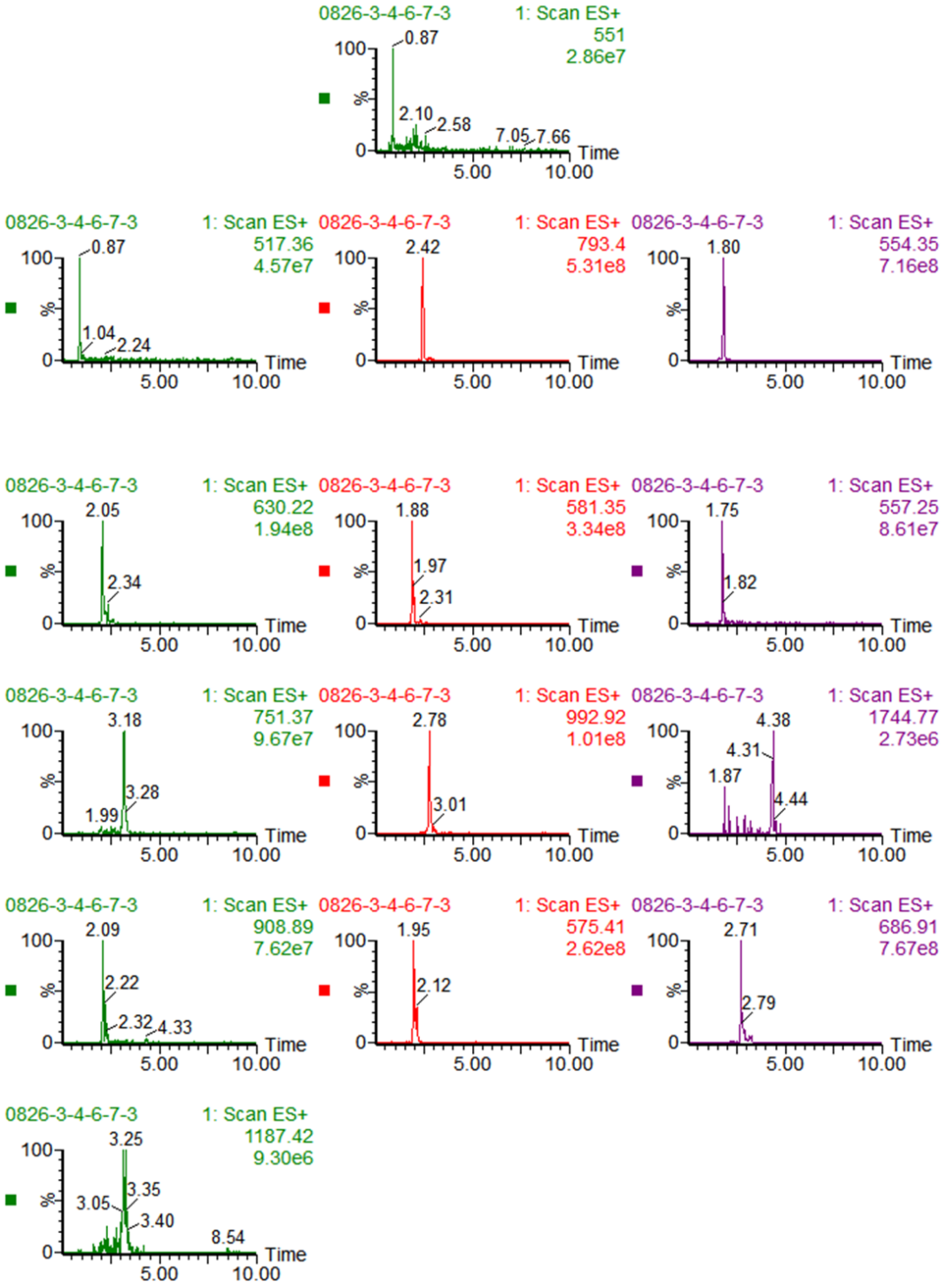

Fig S241. LRMS spectrum of intramolecular disulfide-bridged products and cyclodimerization products in **reaction 6**. Extract mass chromatograms from full scan data.

Tab S22. The LRMS spectrum analysis of **reaction 6.**

Sequence	Products	m/z	
		Theoretical	Measured
	M25-ss	551.61 (z=1)	551.05 (z=1)
	M9-ss	1034.10(z=1)	517.36 (z=2)
	M36-ss	793.92 (z=1)	793.40 (z=1)
	M39-ss	1108.32 (z=1)	554.35 (z=2)
	B25	1260.30 (z=1)	630.22 (z=2)
L25 (CRGDC)	B25-9	1742.79 (z=1)	871.16 (z=2) ; 581.35 (z=3)
L9 (CRGDpGRGDC)	B9*	2225.29 (z=1)	742.05 (z=3) ; 557.25 (z=4)
L36 (CPPTQFC)	B36-25	1502.61 (z=1)	751.37 (z=2)
L39 (CKSAHFKWC)	B36-9	1985.11 (z=1)	992.92 (z=2)
	B36	1744.93 (z=1)	1744.77 (z=1) ; 872.31 (z=2)
	B39-25	1817.01 (z=1)	908.89 (z=2) ; 606.19 (z=3)
	B39-9	2299.05 (z=1)	767.43 (z=3) ; 575.41 (z=4)
	B39-36	2059.33 (z=1)	686.91 (z=3)
	B39*	2373.73 (z=1)	1187.42 (z=2) ; 791.93 (z=3)

*The fragment ion signals of **B9** overlapped with those of the intramolecular disulfide-bridged products of **L39**. The fragment ion signals of **B39** overlapped with those of the intramolecular disulfide-bridged products of **L36**.

Reaction 7

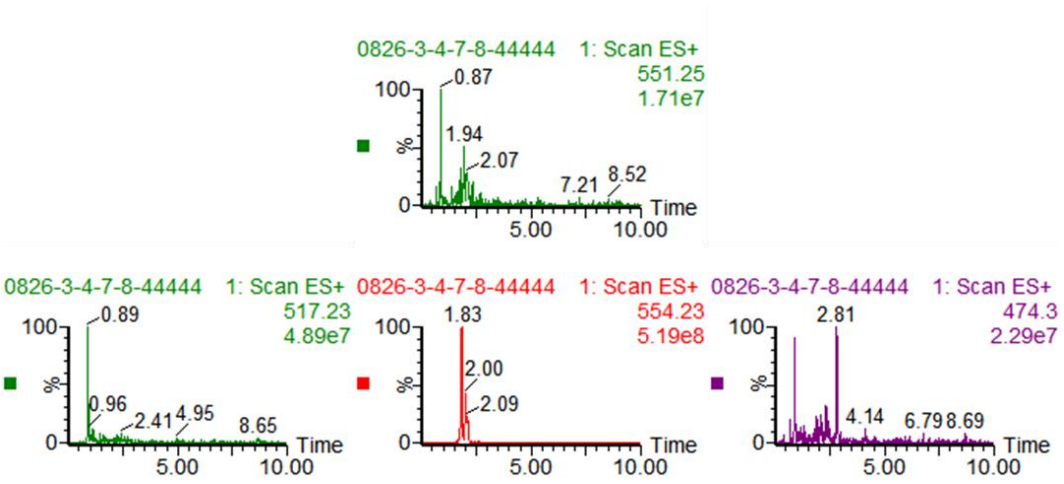

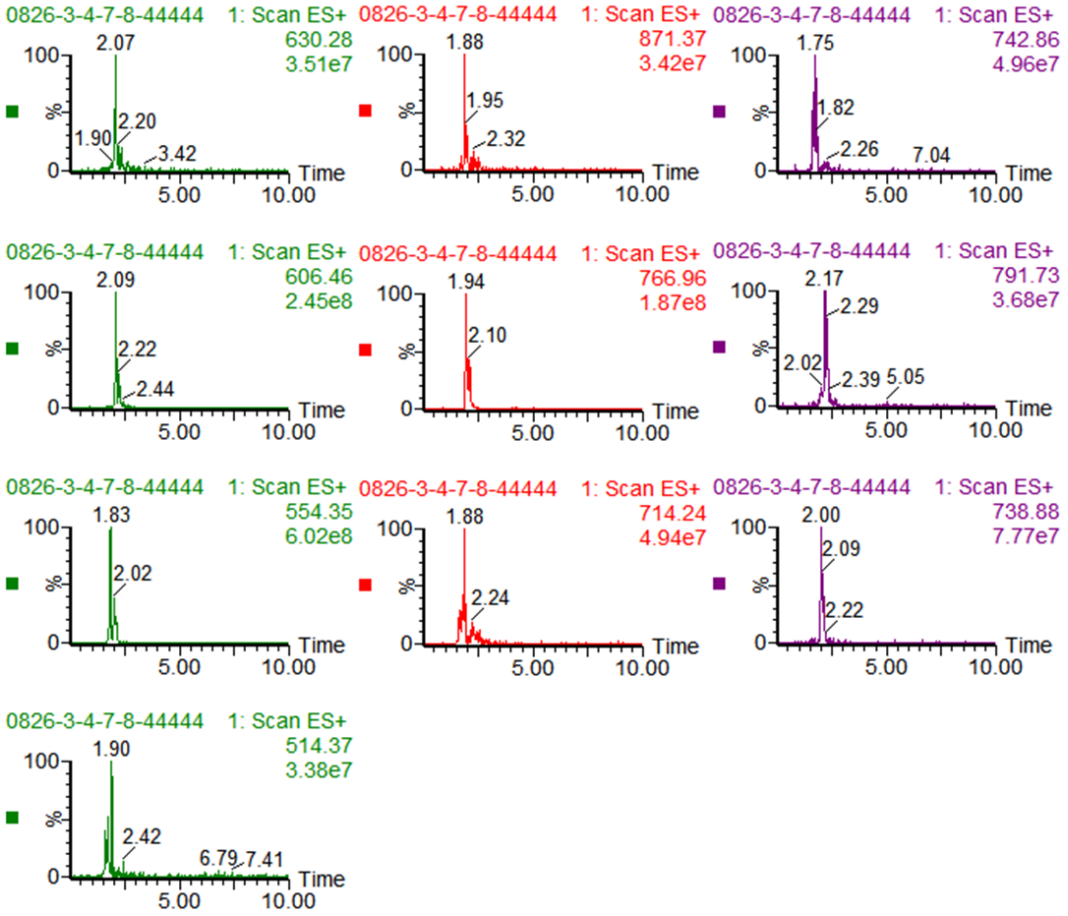

Fig S242. LRMS spectrum of intramolecular disulfide-bridged products and cyclodimerization products in **reaction 7**. Extract mass chromatograms from full scan data.

Tab S23. The LRMS spectrum analysis of **reaction 7.**

Sequence	Products	m/z	
		Theoretical	Measured
	M25-ss	551.61 (z=1)	551.25 (z=1)
	M9-ss	1034.10(z=1)	517.23 (z=2)
	M39-ss	1108.32 (z=1)	554.23 (z=2)
	M38-ss	949.04 (z=1)	474.3 (z=2)
	B25	1260.30 (z=1)	630.28 (z=2)
L25 (CRGDC)	B25-9	1742.79 (z=1)	871.37 (z=2) ; 581.89 (z=3)
L9 (CRGDpGRGDC)	B9*	2225.29 (z=1)	742.86 (z=3) ; 557.05 (z=4)
L39 (CKSAHFKWC)	B39-25	1817.01 (z=1)	908.89 (z=2) ; 606.46 (z=3)
L38 (CRGDKGPDC)	B39-9	2299.05 (z=1)	766.96 (z=3) ; 575.61 (z=4)
	B39	2373.73 (z=1)	791.73 (z=3) ; 594.24 (z=4)
	B38-25	1657.73 (z=1)	829.05 (z=2) ; 554.35 (z=3)
	B38-9	2140.23 (z=1)	714.24 (z=3) ; 535.99 (z=4)
	B39-38	2214.44 (z=1)	738.88 (z=3) ; 554.35 (z=4)
	B38	2055.16 (z=1)	686.57 (z=3) ; 514.37 (z=4)

*The fragment ion signals of **B9** overlapped with those of the intramolecular disulfide-bridged products of **L39**.

Reaction 8

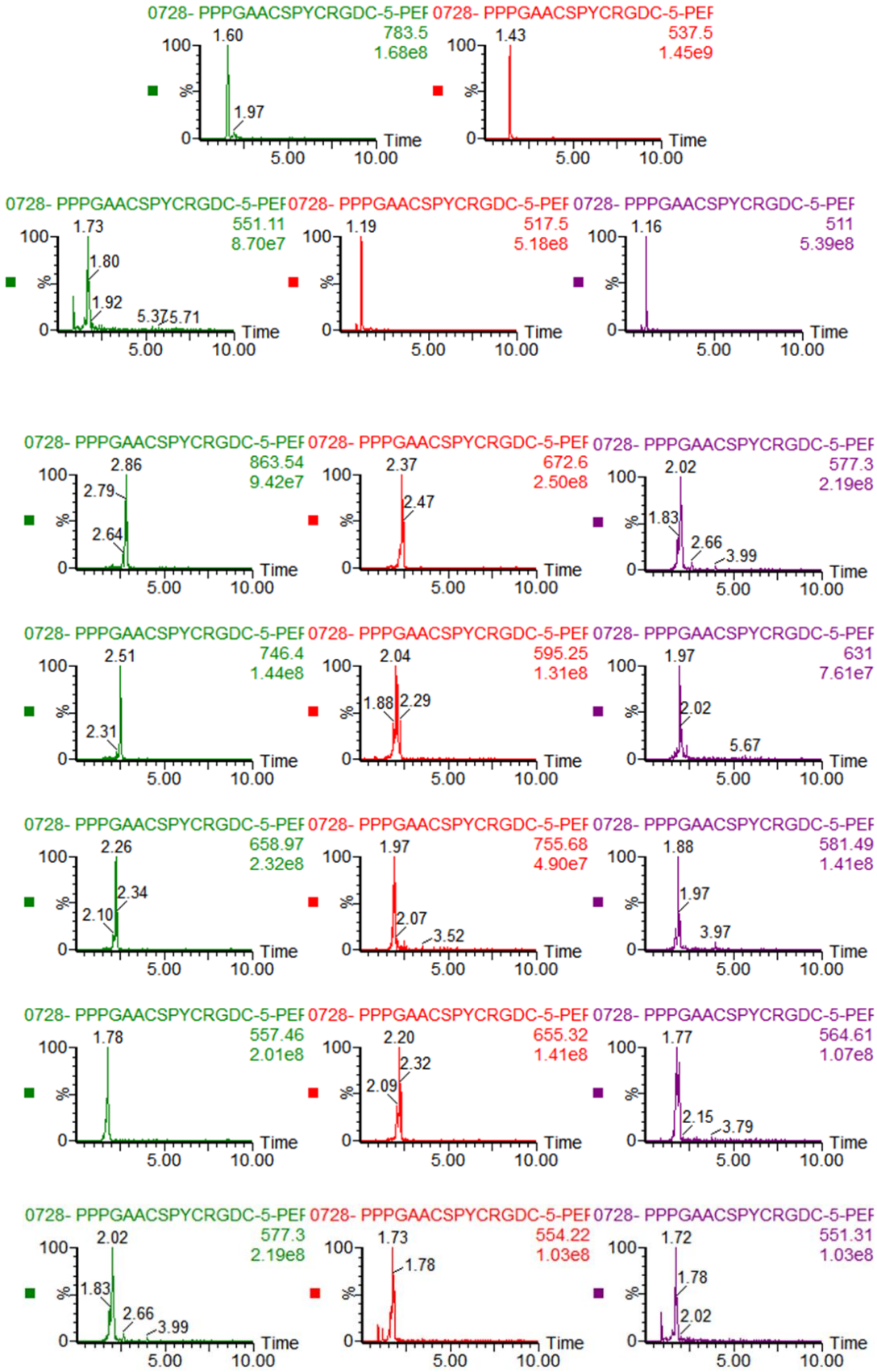

Fig S243. LRMS spectrum of intramolecular disulfide-bridged products and cyclodimerization products in **reaction 8**. Extract mass chromatograms from full scan data.

Tab S24. The LRMS spectrum analysis of **reaction 8.**

Sequence	Products	m/z	
		Theoretical	Measured
L35 (CSPYGRC) L1 (CRGDpPRGDC) L25 (CRGDC) L9 (CRGDpGRGDC) L6 (CRGDAARGDC)	M35-ss	783.89 (z=1)	783.5 (z=1)
	M1-ss	1074.17 (z=1)	537.5 (z=2)
	M25-ss	551.61 (z=1)	551.11 (z=2)
	M9-ss	1034.10(z=1)	517.50 (z=2)
	M6-ss	1022.09 (z=1)	511.05 (z=2)
	B35	1724.86 (z=1)	863.54 (z=2)
	B35-1	2015.14 (z=1)	1008.57 (z=2) ; 672.60 (z=3)
	B1	2305.42 (z=1)	769.72 (z=3) ; 577.30 (z=4)
	B35-25	1492.58 (z=1)	746.44 (z=2)
	B25-1	1782.86 (z=1)	892.09 (z=2) ; 595.25 (z=3)
	B25	1260.30 (z=1)	631.30 (z=2)
	B35-9	1975.08 (z=1)	988.53 (z=2) ; 658.97 (z=3)
	B9-1	2265.36 (z=1)	755.68 (z=3) ; 567.24 (z=4)
	B25-9	1742.79 (z=1)	871.50 (z=2) ; 581.48 (z=3)
	B9	2225.29 (z=1)	742.39 (z=3) ; 557.46 (z=4)
	B35-6	1963.06 (z=1)	982.59 (z=2) ; 655.32 (z=3)
	B6-1	2253.35 (z=1)	752.38 (z=3) ; 564.61 (z=4)
	B25-6	1730.78 (z=1)	865.49 (z=2) ; 577.30 (z=3)
	B9-6	2213.28 (z=1)	738.68 (z=3) ; 554.22 (z=4)
	B6	2201.27 (z=1)	734.29 (z=3) ; 551.31 (z=4)

Reaction 9

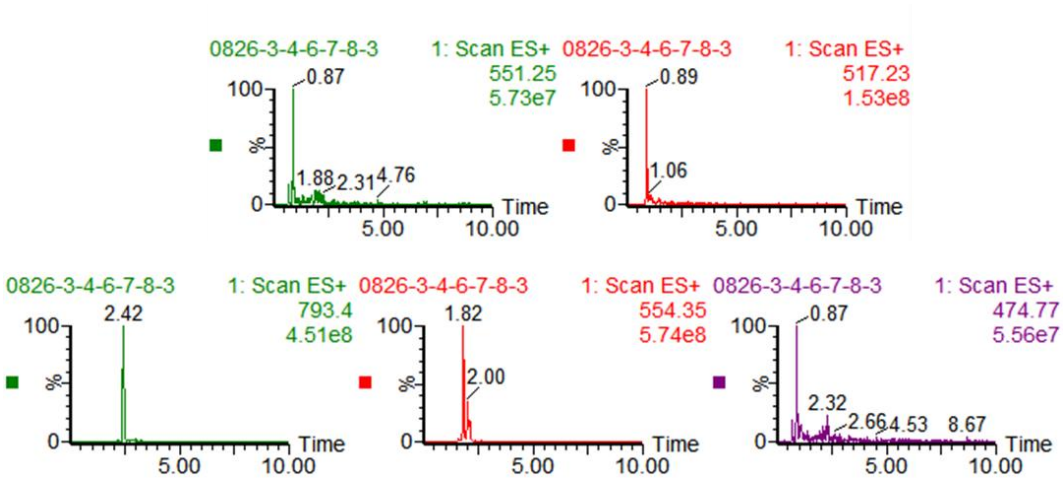

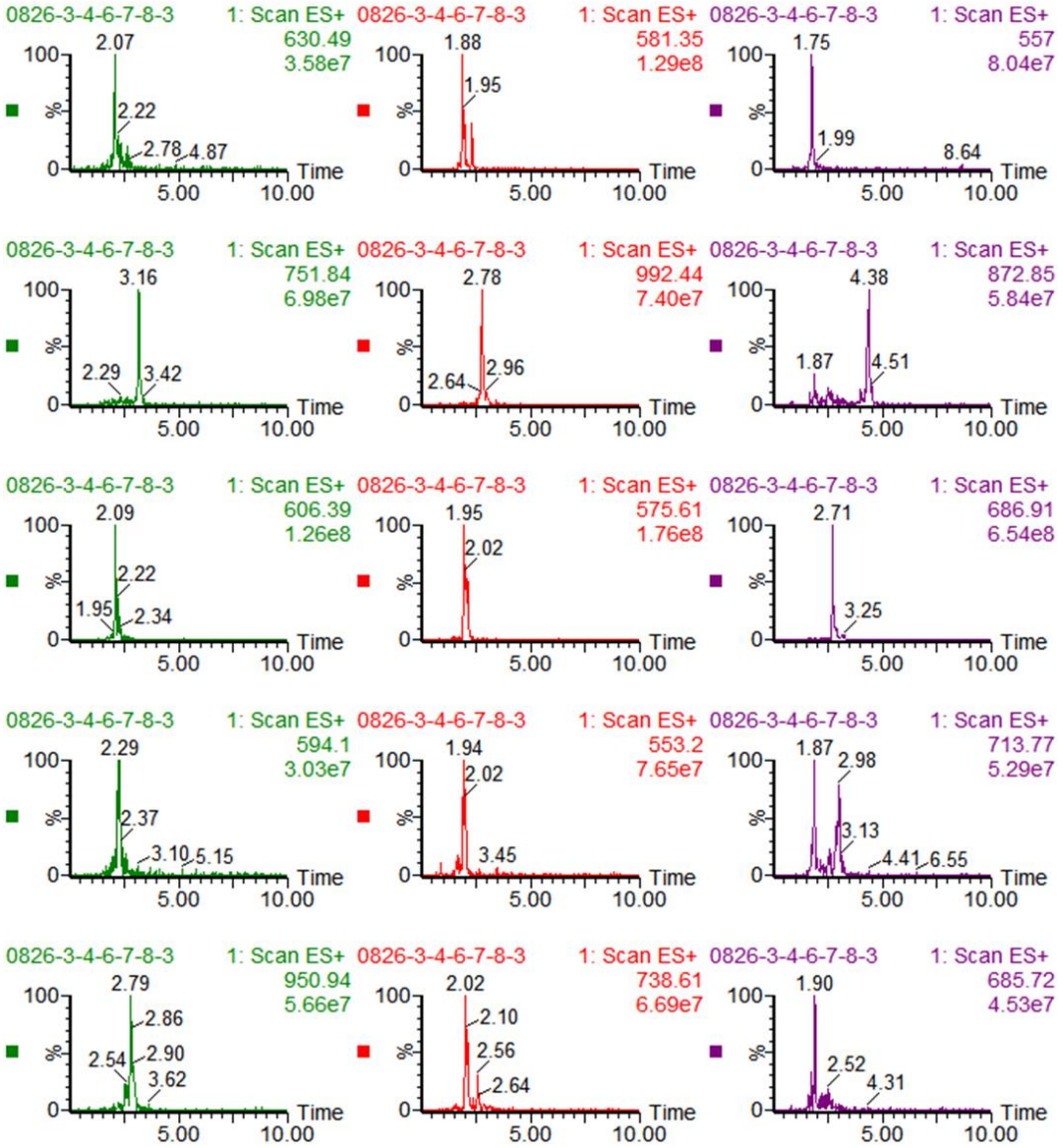

Fig S244. LRMS spectrum of intramolecular disulfide-bridged products and cyclodimerization products in **reaction 9**. Extract mass chromatograms from full scan data.

Tab S25. The LRMS spectrum analysis of **reaction 9.**

Sequence	Products	m/z	
		Theoretical	Measured
L25 (CRGDC) L9 (CRGDpGRGDC) L36 (CPPTQFC) L39 (CKSAHFKWC) L38 (CRGDKGPDC)	M25-ss	551.61 (z=1)	511.25 (z=1)
	M9-ss	1034.10 (z=1)	517.23 (z=2)
	M36-ss	793.92 (z=1)	793.40 (z=1)
	M39-ss	1108.32 (z=1)	554.35 (z=2)
	M38-ss	949.04 (z=1)	474.77 (z=2)
	B25	1260.30 (z=1)	630.49 (z=2)
	B25-9	1742.79 (z=1)	871.37 (z=2) ; 581.35 (z=3)
	B9*	2225.29 (z=1)	742.39 (z=3)
	B36-25	1502.61 (z=1)	1501.66 (z=1) ; 751.84 (z=2)
	B36-9	1985.11 (z=1)	992.44 (z=2)
	B36	1744.93 (z=1)	1744.84 (z=1) ; 872.85 (z=2)
	B39-25	1817.01 (z=1)	908.96 (z=2) ; 606.39 (z=3)
	B39-9	2299.05 (z=1)	766.89 (z=3) ; 575.61 (z=4)
	B39-36	2059.33 (z=1)	686.91 (z=3) ; 1029.97 (z=2)
	B39*	2373.73 (z=1)	1187.76 (z=2) ; 594.18 (z=4)
	B38-25	1657.73 (z=1)	828.91 (z=2) ; 553.20 (z=3) ;
	B38-9	2140.23 (z=1)	713.77 (z=3)
	B38-36	1900.05 (z=1)	950.94 (z=2) ; 634.47 (z=3)
	B39-38	2214.44 (z=1)	738.61 (z=3) ; 554.35 (z=4)
	B38	2055.16 (z=1) **close to B39-36**	685.72 (z=3) ; 1028.08 (z=2)

*The fragment ion signals of **B9** overlapped with those of the intramolecular disulfide-bridged products of **L39**. The fragment ion signals of **B39** overlapped with those of the intramolecular disulfide-bridged products of **L36**.

Reaction 10

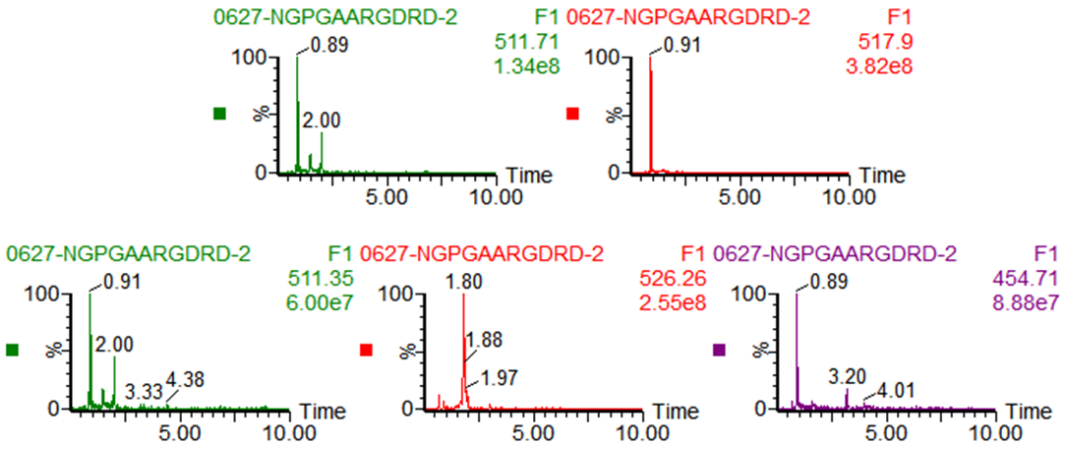

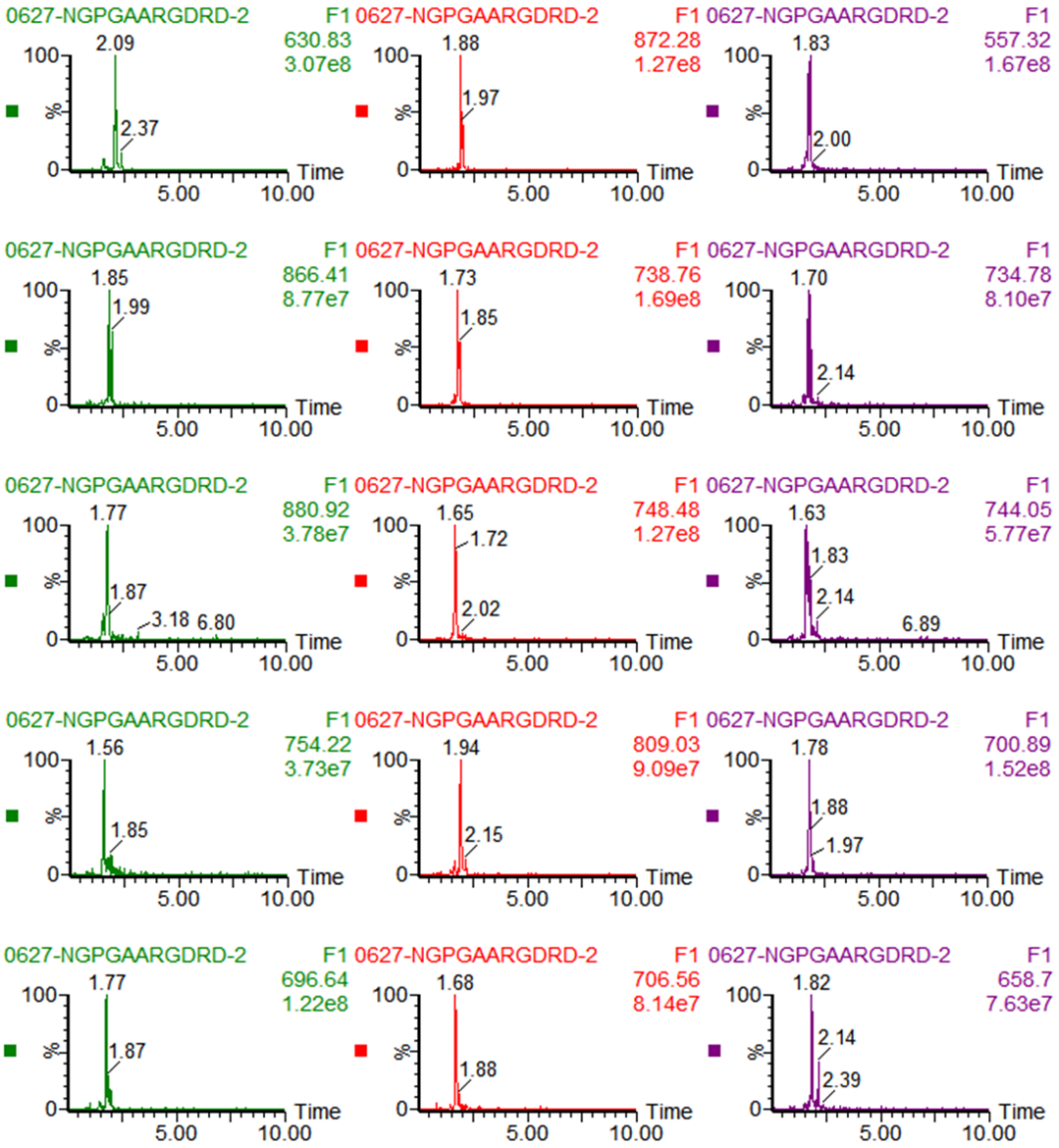

Fig S245. LRMS spectrum of intramolecular disulfide-bridged products and cyclodimerization products in **reaction 10**. Extract mass chromatograms from full scan data.

Tab S26. The LRMS spectrum analysis of **reaction 10.**

Sequence	Products	m/z	
		Theoretical	Measured
L25 (CRGDC) L9 (CRGDpGRGDC) L6 (CRGDAARGDC) L8 (CRGDNGRGDC) L24 (CRDAARDC)	M25-ss	551.61 (z=1)	551.71 (z=1)
	M9-ss	1034.10 (z=1)	517.90 (z=2)
	M6-ss	1022.09 (z=1)	511.35 (z=2)
	M8-ss	1051.90 (z=1)	526.26 (z=2)
	M24-ss	907.99 (z=1)	454.71 (z=2)
	B25	1260.30 (z=1)	630.83 (z=2)
	B25-9	1742.94 (z=1)	872.28 (z=2)
	B9	2225.29 (z=1)	743.22 (z=3) ; 557.32 (z=4)
	B25-6	1730.78 (z=1)	866.41 (z=2)
	B9-6	2213.28 (z=1)	738.76 (z=3) ; 554.48 (z=4)
	B6	2201.27 (z=1)	734.78 (z=3) ; 551.65 (z=4)
	B25-8	1759.78 (z=1)	880.92 (z=2)
	B9-8	2242.28 (z=1)	748.48 (z=3) ; 561.91 (z=4)
	B8-6	2230.27 (z=1)	744.05 (z=3) ; 558.87 (z=4)
	B8	2259.27 (z=1)	754.22 (z=3) ; 566..63 (z=4)
	B25-24	1616.68 (z=1)	809.03 (z=2)
	B24-9	2099.18 (z=1)	700.89 (z=3) ; 526.06 (z=4)
	B24-6	2087.17 (z=1)	696.64 (z=3) ; 523.03 (z=4)
	B24-8	2116.16 (z=1)	706.56 (z=3) ; 530.18 (z=4)
	B24	1973.06 (z=1)	987.17 (z=2) ; 658.70 (z=3)

10 different peptides reaction

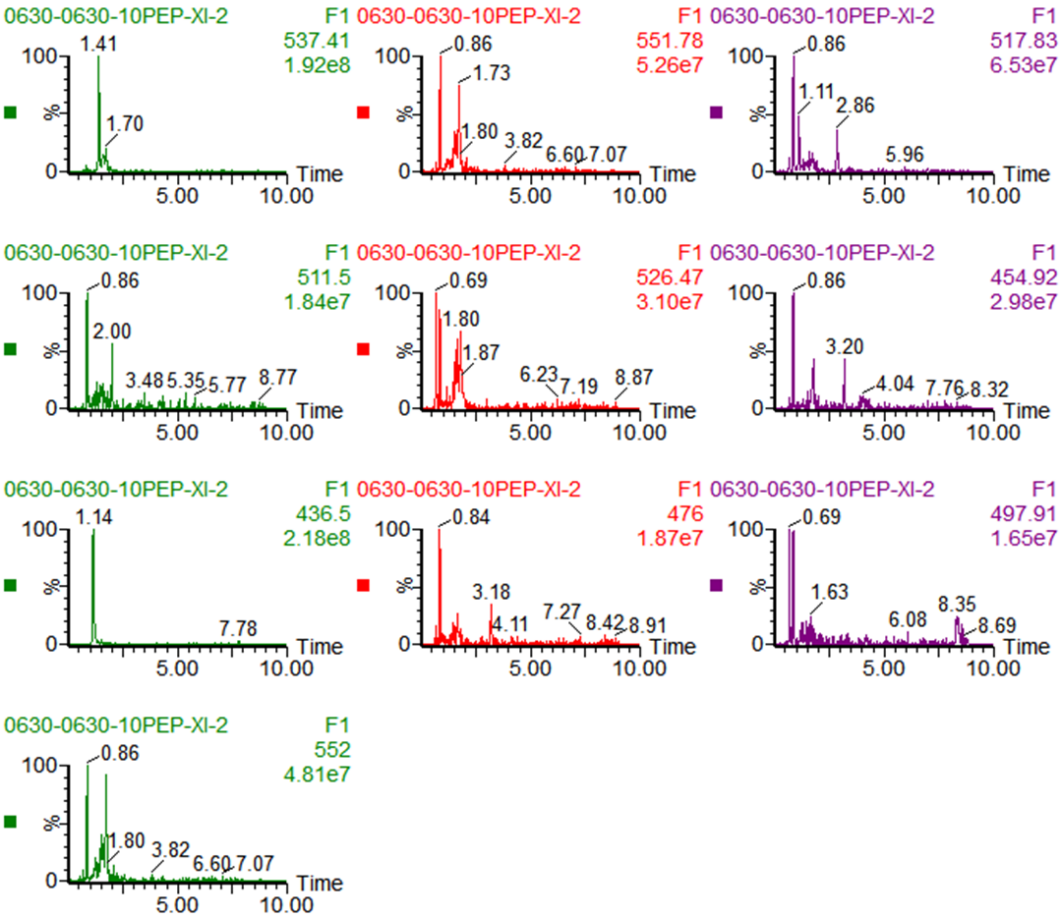

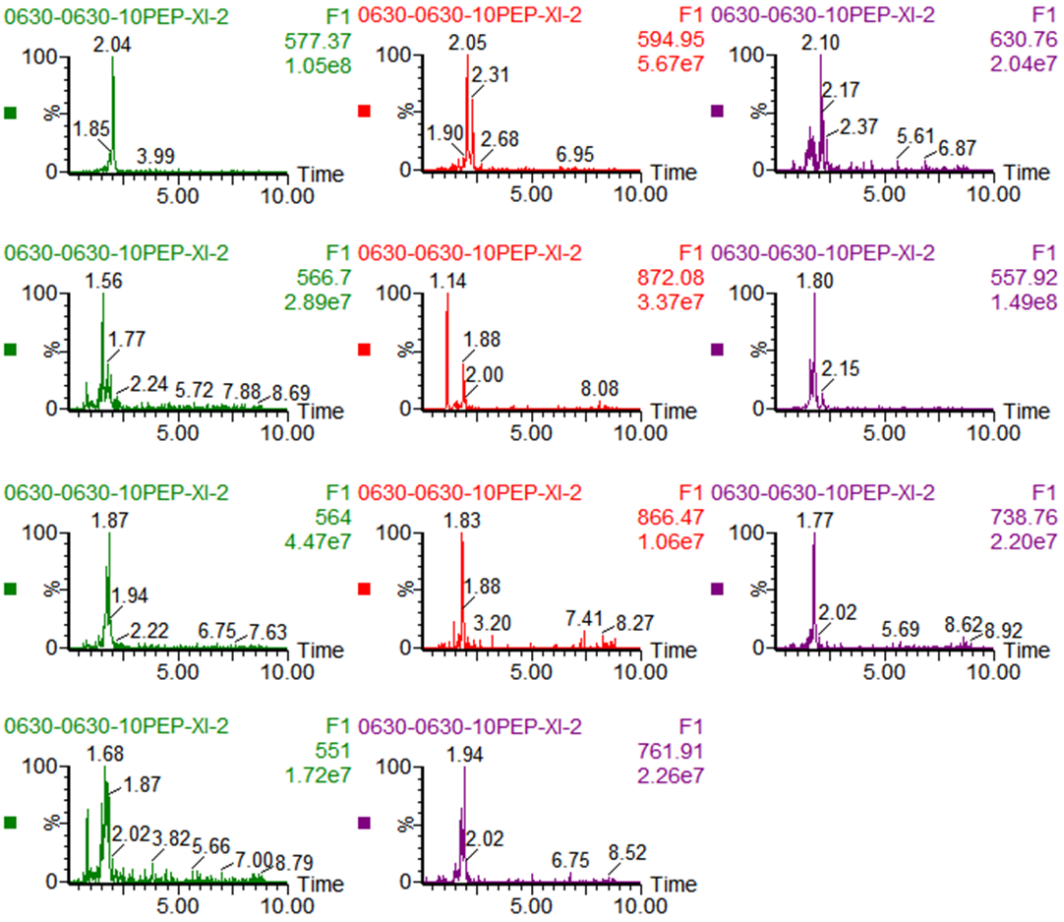
0630-0630-10PEP-XI-2 F1 577.37 1.05e8
2.04
1.85
3.99
0630-0630-10PEP-XI-2 F1 594.95 5.67e7
2.05
2.31
1.90
2.68
6.95
0630-0630-10PEP-XI-2 F1 630.76 2.04e7
2.10
2.17
2.37
5.61
6.87
0630-0630-10PEP-XI-2 F1 566.7 2.89e7
1.56
1.77
2.24 5.72 7.88 8.69
0630-0630-10PEP-XI-2 F1 872.08 3.37e7
1.14
1.88
2.00
8.08
0630-0630-10PEP-XI-2 F1 557.92 1.49e8
1.80
2.15
0630-0630-10PEP-XI-2 F1 564 4.47e7
1.87
1.94
2.22 6.75 7.63
0630-0630-10PEP-XI-2 F1 866.47 1.06e7
1.83
1.88
3.20 7.41 8.27
0630-0630-10PEP-XI-2 F1 738.76 2.20e7
1.77
2.02
5.69 8.62 8.92
0630-0630-10PEP-XI-2 F1 551 1.72e7
1.68
1.87
2.02 3.82 5.66 7.00 8.79
0630-0630-10PEP-XI-2 F1 761.91 2.26e7
1.94
2.02
6.75 8.52
Time
5.00
10.00

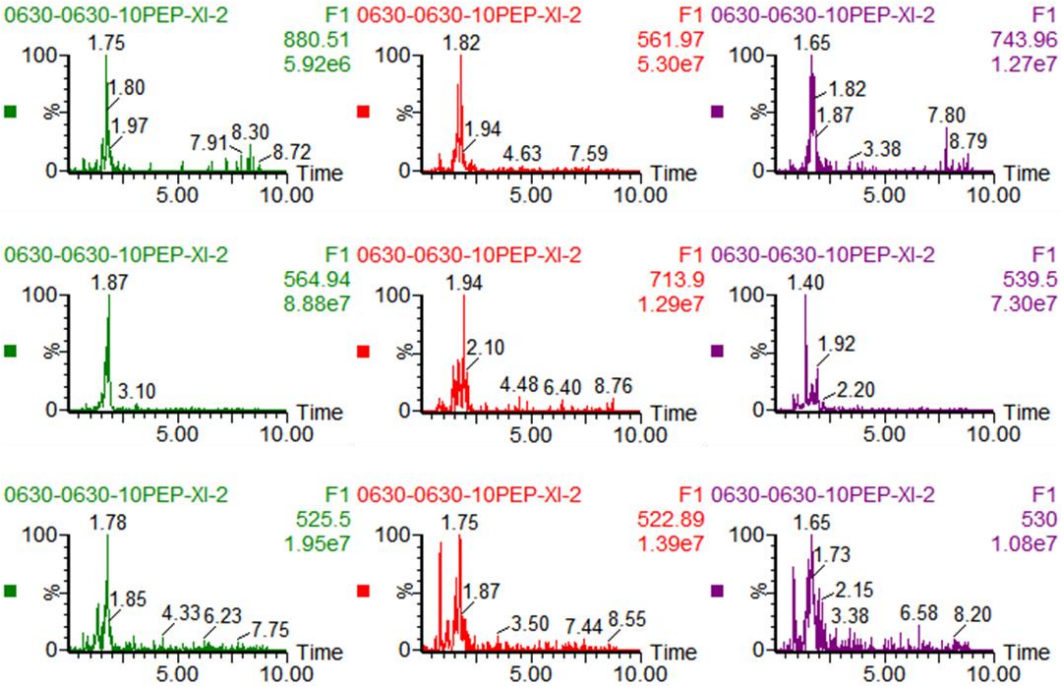
0630-0630-10PEP-XI-2 F1 880.51 5.92e6
1.75
1.80
1.97
7.91 8.30 8.72
0630-0630-10PEP-XI-2 F1 561.97 5.30e7
1.82
1.94
4.63 7.59
0630-0630-10PEP-XI-2 F1 743.96 1.27e7
1.65
1.82
1.87
3.38 7.80 8.79
0630-0630-10PEP-XI-2 F1 564.94 8.88e7
1.87
3.10
0630-0630-10PEP-XI-2 F1 713.9 1.29e7
1.94
2.10
4.48 6.40 8.76
0630-0630-10PEP-XI-2 F1 539.5 7.30e7
1.40
1.92
2.20
0630-0630-10PEP-XI-2 F1 525.5 1.95e7
1.78
1.85
4.33 6.23 7.75
0630-0630-10PEP-XI-2 F1 522.89 1.39e7
1.75
1.87
3.50 7.44 8.55
0630-0630-10PEP-XI-2 F1 530 1.08e7
1.65
1.73
2.15
3.38 6.58 8.20
Time
5.00
10.00

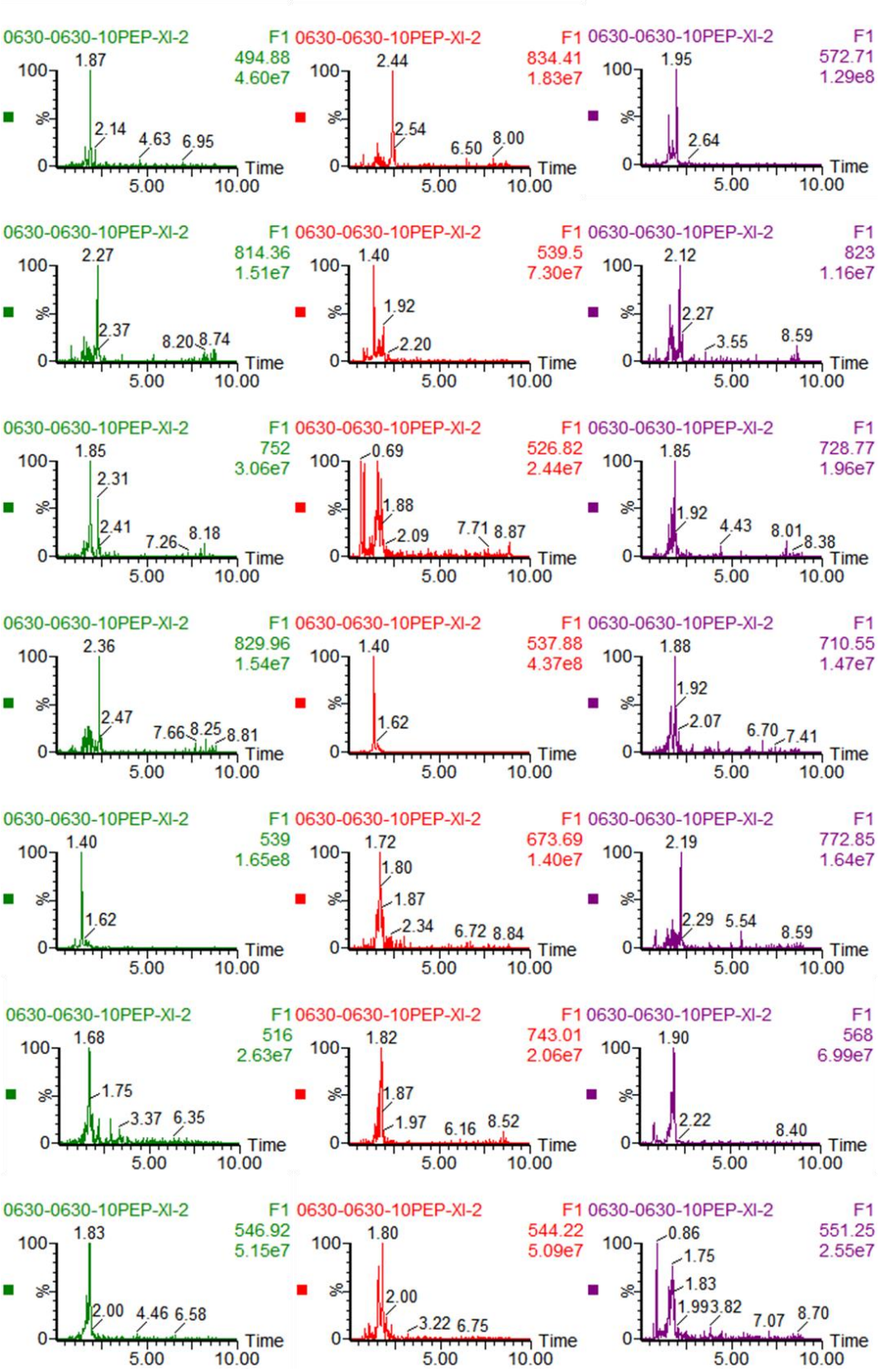
0630-0630-10PEP-XI-2 F1 494.88 4.60e7
1.87 2.14 4.63 6.95
0630-0630-10PEP-XI-2 F1 834.41 1.83e7
2.44 2.54 6.50 8.00
0630-0630-10PEP-XI-2 F1 572.71 1.29e8
1.95 2.64
0630-0630-10PEP-XI-2 F1 814.36 1.51e7
2.27 2.37 8.20 8.74
0630-0630-10PEP-XI-2 F1 539.5 7.30e7
1.40 1.92 2.20
0630-0630-10PEP-XI-2 F1 823 1.16e7
2.12 2.27 3.55 8.59
0630-0630-10PEP-XI-2 F1 752 3.06e7
1.85 2.31 2.41 7.26 8.18
0630-0630-10PEP-XI-2 F1 526.82 2.44e7
0.69 1.88 2.09 7.71 8.87
0630-0630-10PEP-XI-2 F1 728.77 1.96e7
1.85 1.92 4.43 8.01 8.38
0630-0630-10PEP-XI-2 F1 829.96 1.54e7
2.36 2.47 7.66 8.25 8.81
0630-0630-10PEP-XI-2 F1 537.88 4.37e8
1.40 1.62
0630-0630-10PEP-XI-2 F1 710.55 1.47e7
1.88 1.92 2.07 6.70 7.41
0630-0630-10PEP-XI-2 F1 539 1.65e8
1.40 1.62
0630-0630-10PEP-XI-2 F1 673.69 1.40e7
1.72 1.80 1.87 2.34 6.72 8.84
0630-0630-10PEP-XI-2 F1 772.85 1.64e7
2.19 2.29 5.54 8.59
0630-0630-10PEP-XI-2 F1 516 2.63e7
1.68 1.75 3.37 6.35
0630-0630-10PEP-XI-2 F1 743.01 2.06e7
1.82 1.87 1.97 6.16 8.52
0630-0630-10PEP-XI-2 F1 568 6.99e7
1.90 2.22 8.40
0630-0630-10PEP-XI-2 F1 546.92 5.15e7
1.83 2.00 4.46 6.58
0630-0630-10PEP-XI-2 F1 544.22 5.09e7
1.80 2.00 3.22 6.75
0630-0630-10PEP-XI-2 F1 551.25 2.55e7
0.86 1.75 1.83 1.99 3.82 7.07 8.70
100 % 0 Time 5.00 10.00

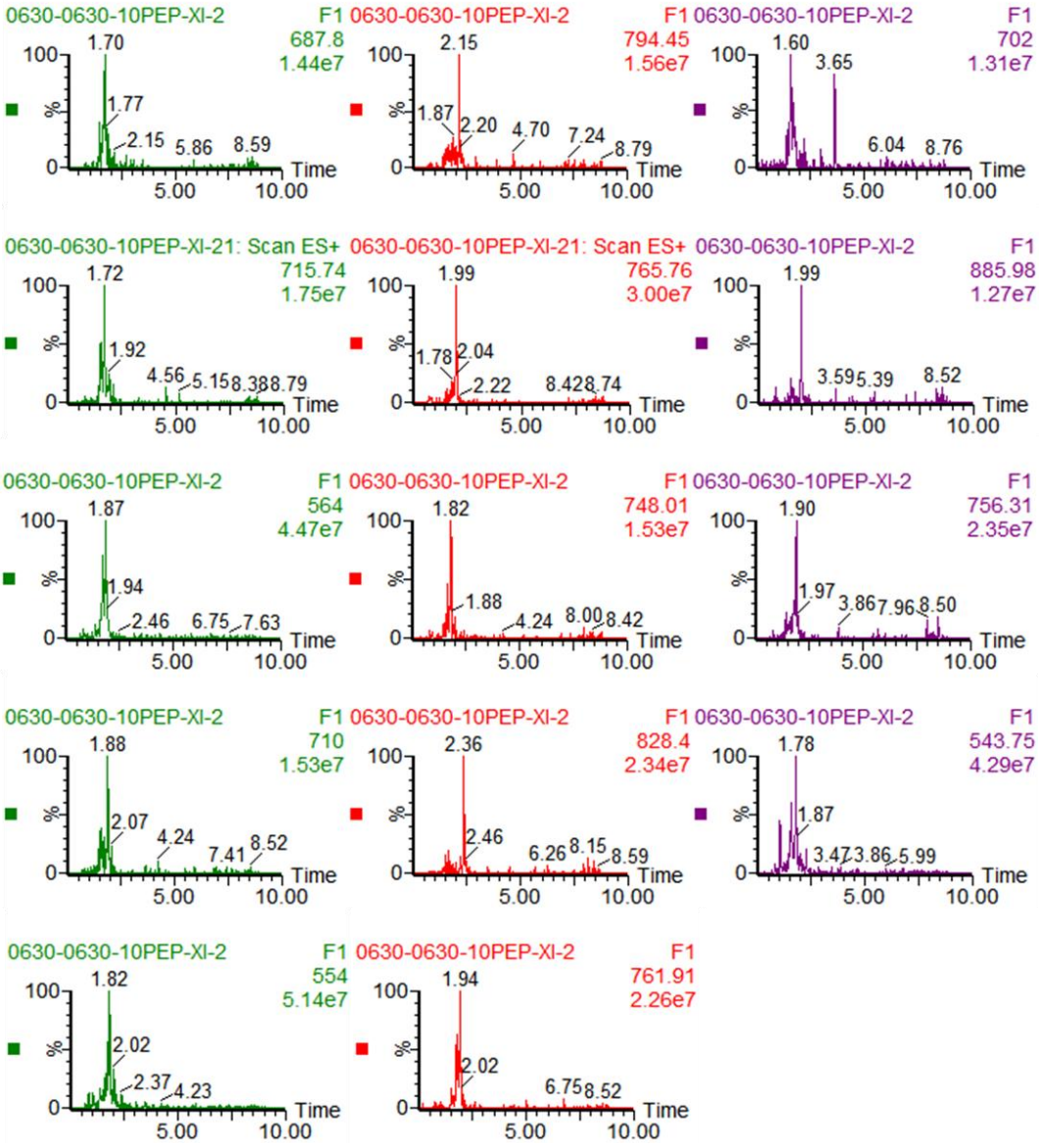

Fig S246. LRMS spectrum of intramolecular disulfide-bridged products and cyclodimerization products in reaction with 10 different peptides. Extract mass chromatograms from full scan data.

Tab S27. The LRMS spectrum analysis of 3,6-DCT-mediated cyclodimerization reactions with 10 different peptides.

Sequence	Products	m/z	
		Theoretical	Measured
L1 (CRGDpPRGDC) L25 (CRGDC) L9 (CRGDpGRGDC) L6 (CRGDAARGDC) L8 (CRGDNGRGDC) L24 (CRDAARDC) L27 (CAAAC) L45 (CRGDARGDC) L7 (CRGDGGRGDC) L10 (CRGDAibpRGDC)	M1-ss	1074.17 (z=1)	537.41 (z=2)
	M25-ss	551.61 (z=1)	551.78 (z=1)
	M9-ss	1034.10 (z=1)	517.83 (z=2)
	M6-ss	1022.09 (z=1)	511.5 (z=2)
	M8-ss	1051.90 (z=1)	526.47 (z=2)
	M24-ss	907.99 (z=1)	454.92 (z=2)
	M27-ss	436.51 (z=1)	436.5 (z=1)
	M45-ss	951.01 (z=1)	476.00 (z=2)
	M7-ss	994.04 (z=1)	497.91 (z=2)
	M10-ss	1062.16 (z=1)	552.00 (z=2)
	B1	2305.42 (z=1)	769.47 (z=3) ; 577.37 (z=4)
	B25-1	1782.86 (z=1)	891.85 (z=2) ; 594.95 (z=3)
	B25	1260.30 (z=1)	630.76 (z=2)
	B9-1	2265.36 (z=1)	755.70 (z=3) ; 566.70 (z=4)
	B25-9	1742.79 (z=1)	872.08 (z=2)
	B9	2225.25 (z=1)	743.01 (z=3) ; 557.92 (z=4)
	B6-1	2253.35 (z=1)	751.86 (z=3) ; 564.00 (z=4)
	B25-6	1544.61 (z=1)	866.47 (z=2)
	B9-6	2213.28 (z=1)	738.76 (z=3)
	B6	2201.27 (z=1)	734.85 (z=3)
	B8-1	2282.34 (z=1)	761.91 (z=3)
	B25-8	1759.78 (z=1)	880.51 (z=2)
	B9-8	2242.28 (z=1)	748.95 (z=3) ; 561.97 (z=4)
	B8-6	2230.27 (z=1)	743.96 (z=3)
	B8	2259.27 (z=1)	752.33 (z=3) ; 564.94 (z=4)
	B24-1	2139.24 (z=1)	713.92 (z=3)
	B25-24	1616.68 (z=1)	809.44 (z=2) ; 539.5 (z=3)
	B24-9	2099.18 (z=1)	525.5 (z=4)
	B24-6	2087.17 (z=1)	696.50 (z=3) ; 522.89 (z=4)
	B24-8	2116.16 (z=1)	706.63 (z=3) ; 530.05 (z=4)
	B24	1973.06 (z=1)	494.88 (z=4)
	B27-1	1667.77 (z=1)	834.41 (z=2)
	B27-25	1145.20 (z=1)	572.71 (z=2)
	B27-9	1627.70 (z=1)	814.36 (z=2)
	B27-6	1615.69 (z=1)	809.44 (z=2)
	B27-8	1644.69 (z=1)	822.94 (z=2)
	B27-24	1501.59 (z=1)	751.92 (z=2)
	B27	1030.11 (z=1)	526.82 (z=2)
	B45-1	2182.27 (z=1)	728.77 (z=3)
	B45-25	1659.70 (z=1)	829.96 (z=2)
	B45-9	2142.20 (z=1)	715.74 (z=3) ; 537.88 (z=4)
	B45-6	2130.19 (z=1)	710.55 (z=3)
	B45-8	2159.19 (z=1)	719.66 (z=3)
	B45-24	2016.09 (z=1)	673.69 (z=3) ; 504.94 (z=4)
	B45-27	1544.61 (z=1)	772.85 (z=2)
	B45	2059.11 (z=1)	687.46 (z=3) ; 516.01 (z=3)
	B7-1	2225.29 (z=1)	743.01 (z=3)
	B25-7	1702.73 (z=1)	851.96 (z=2)
	B9-7	2185.23 (z=1)	729.31 (z=3)
	B7-6	2173.22 (z=1)	725.06 (z=3)
	B8-7	2202.21 (z=1)	735.39 (z=3)
	B24-7	2059.11 (z=1)	687.80 (z=3)
	B27-7	1587.64 (z=1)	794.45 (z=2)
	B45-7	2102.14 (z=1)	702.11 (z=3)
	B7	2145.16 (z=1)	715.74 (z=3)
	B10-1	2293.41 (z=1)	765.76 (z=3)
	B25-10	1770.85 (z=1)	885.98 (z=2)
	B10-9	2253.35 (z=1)	751.86 (z=3)
	B10-6	2241.34 (z=1)	748.01 (z=3)
	B10-8	2270.33 (z=1)	756.31 (z=3)
	B24-10	2127.23 (z=1)	709.87 (z=3)
	B27-10	1655.76 (z=1)	828.40 (z=2)
	B45-10	2170.26 (z=1)	695.08 (z=3)
	B10-7	2213.28 (z=1)	738.06 (z=3)
	B10	2281.40 (z=1)	761.91 (z=3)

10. NMR spectrum

Fig S247. 1H NMR spectrum of **B1a.**

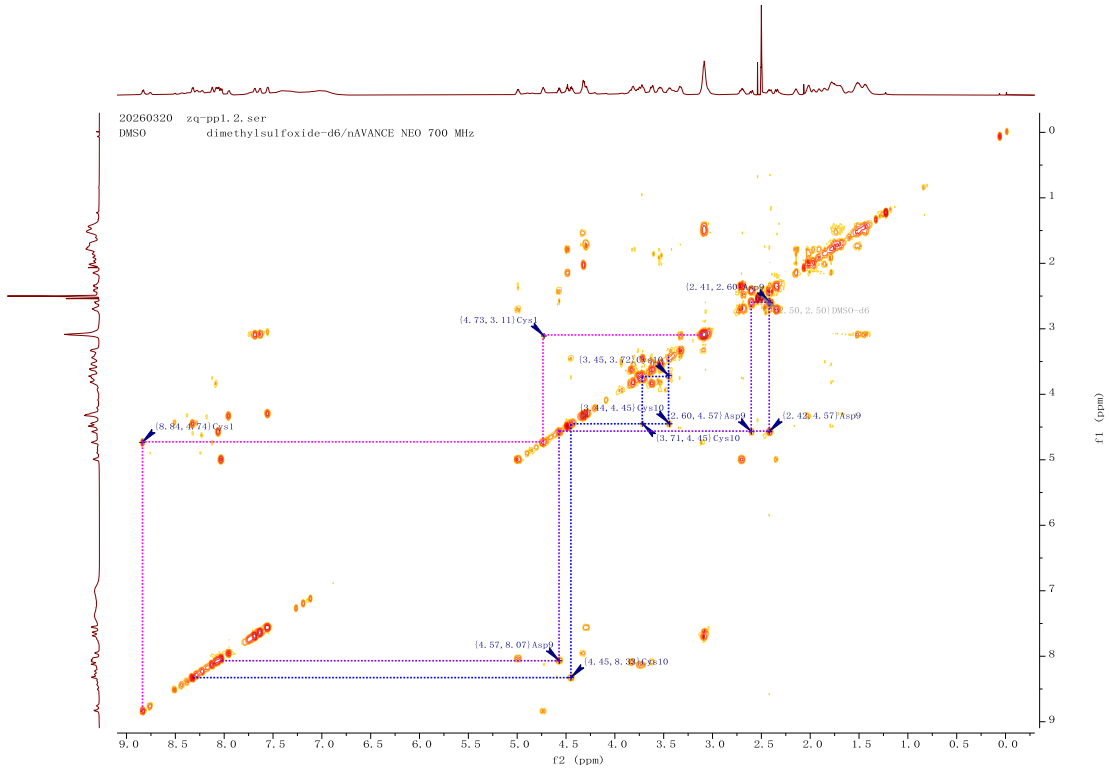

Fig S248. ^{1}H-^{1}H COSY spectrum of **B1a.** Dashed lines trace the spin systems of Cys1 (pink), Asp9 (purple), and Cys10 (blue). Annotated values represent chemical shifts (ppm).

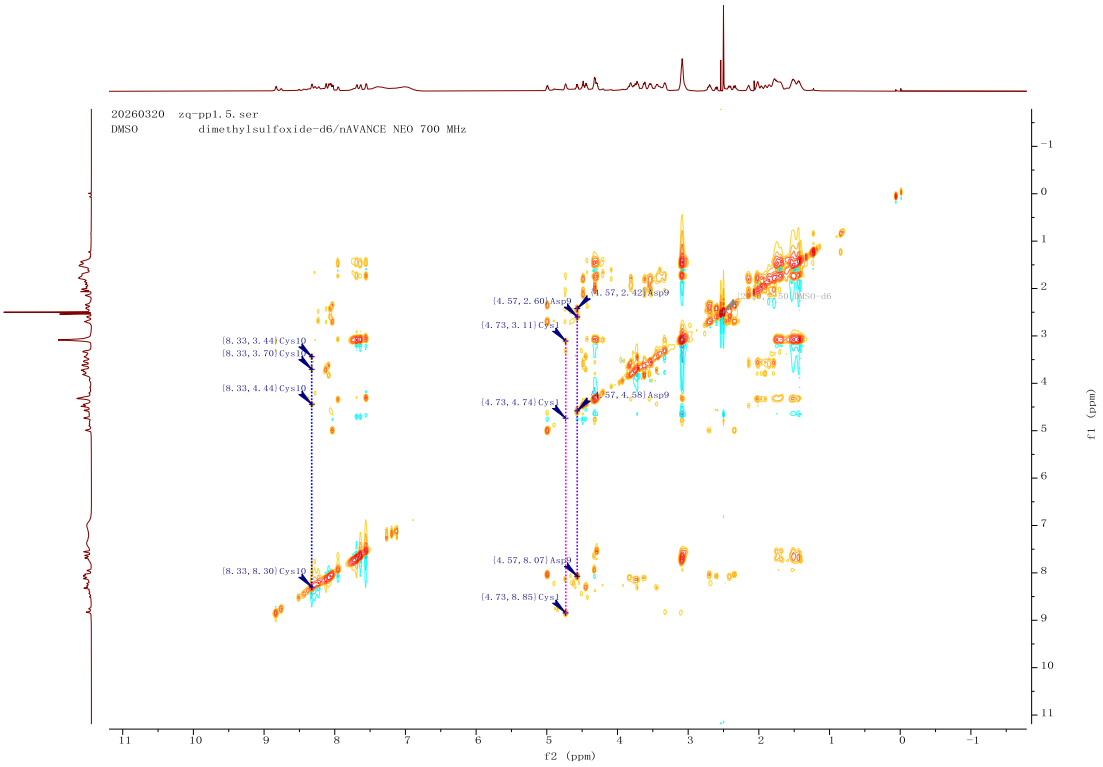

Fig S249. TOCSY spectrum of **B1a.** Dashed lines trace the spin systems of Cys1 (pink), Asp9 (purple), and Cys10 (blue). Annotated values represent chemical shifts (ppm).

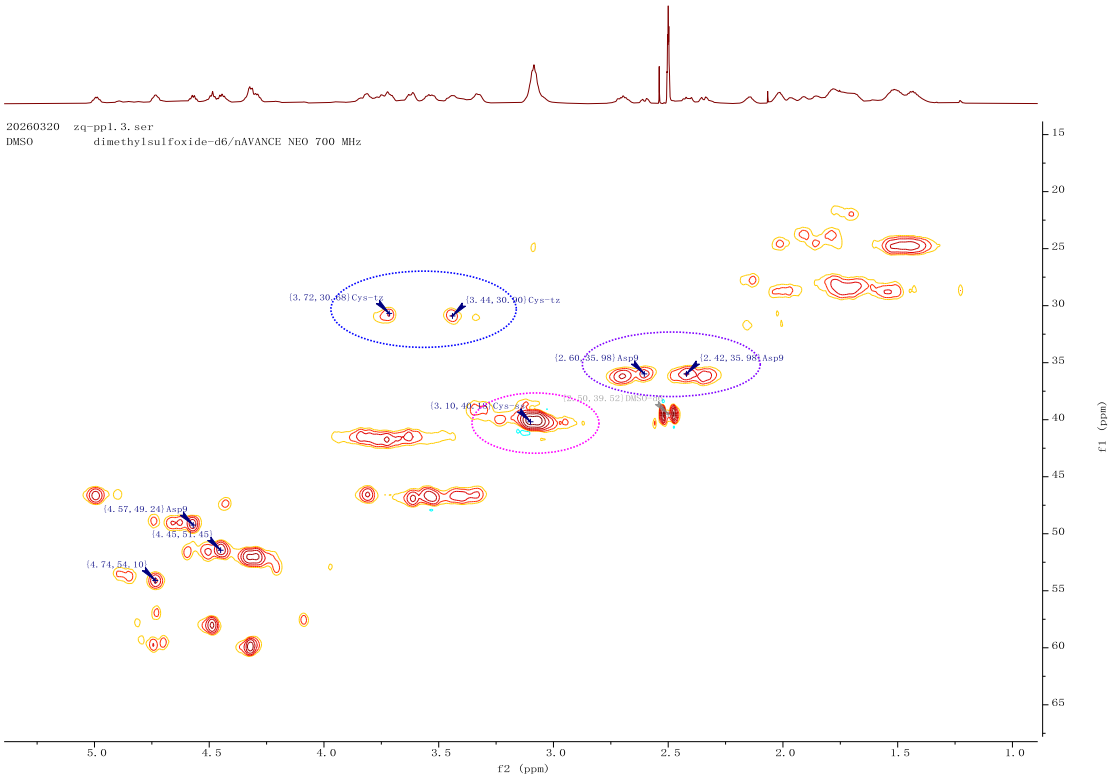

Fig S250. HSQC spectrum of **B1a.** Colored dashed ovals highlight specific cross-peaks: blue for Cys10, purple for Asp9, and pink for Cys1. Annotated values represent chemical shifts in ppm.

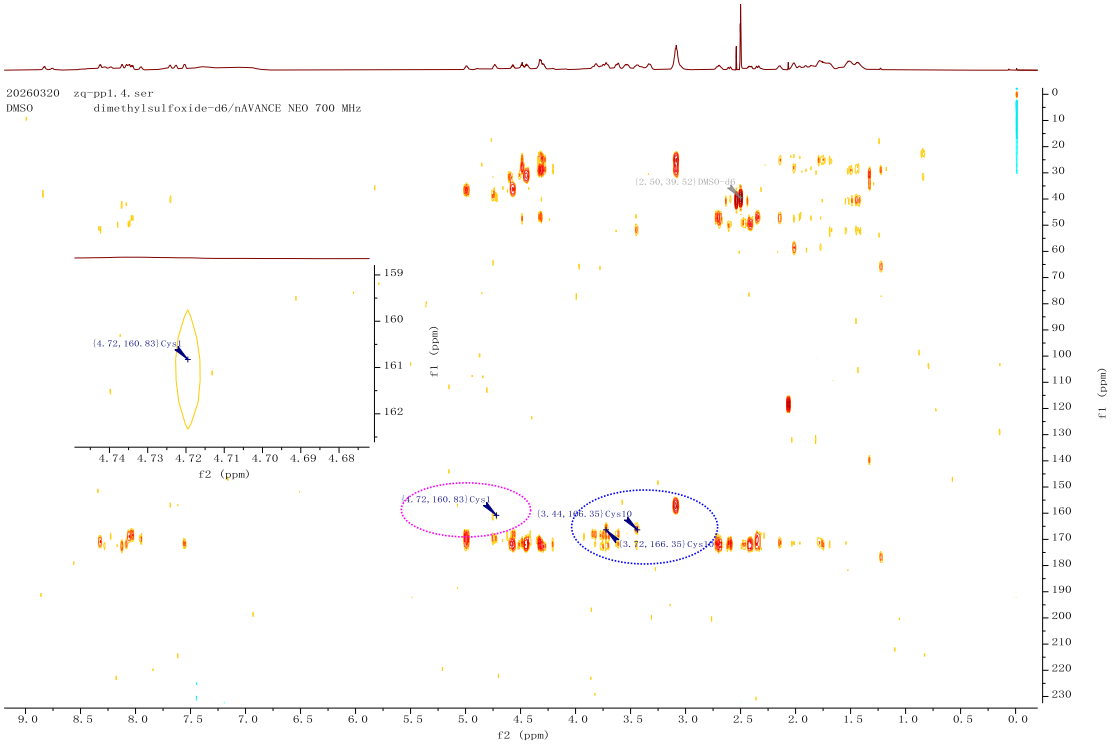

Fig S251. HMBC spectrum of **B1a.** Colored dashed ovals highlight specific cross-peaks: blue for Cys10, and pink for Cys1. Annotated values represent chemical shifts in ppm.

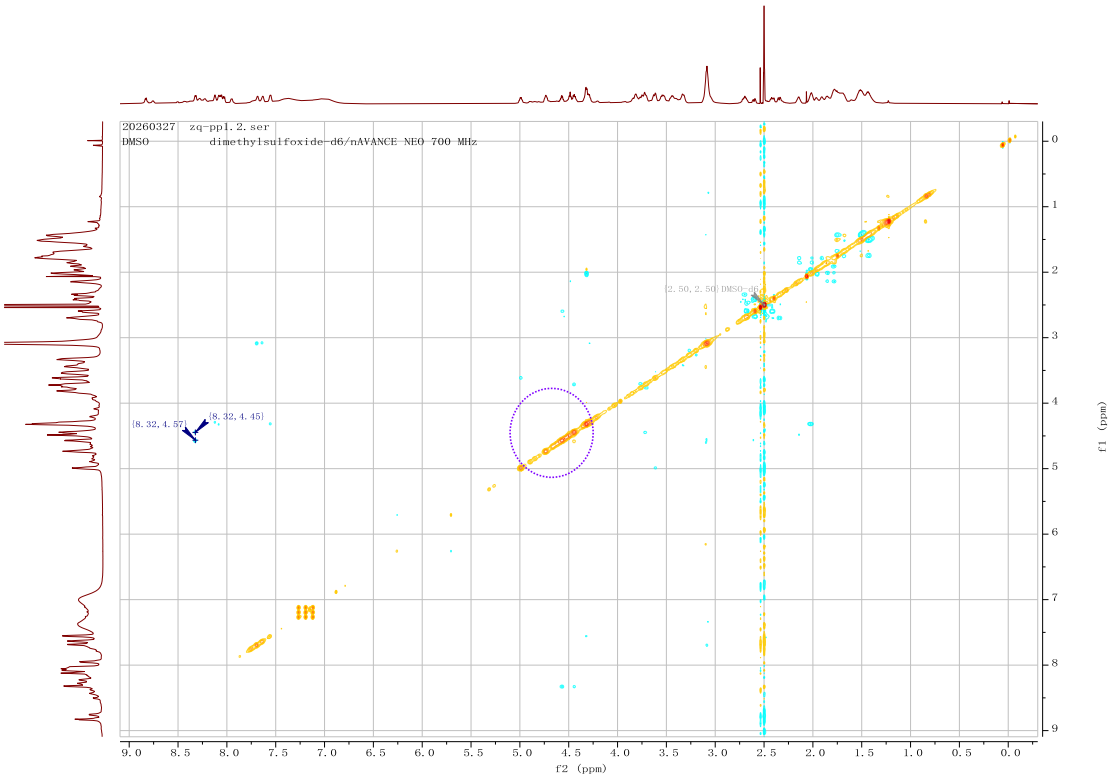

Fig S252. ROESY spectrum of **B1a.** The purple dashed circle highlights the absence of an observable NOE correlation between Cys1 and Asp9. Annotated values represent chemical shifts in ppm.

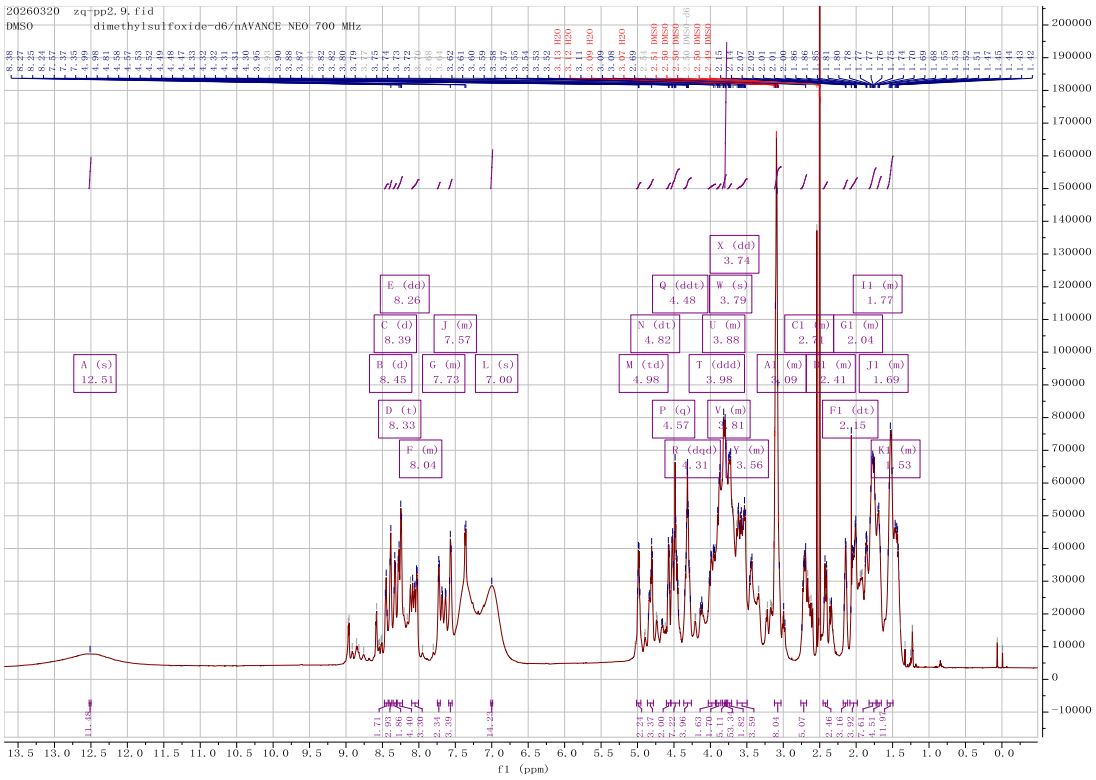

Fig S253. ^{1}H spectrum of **B1b.**

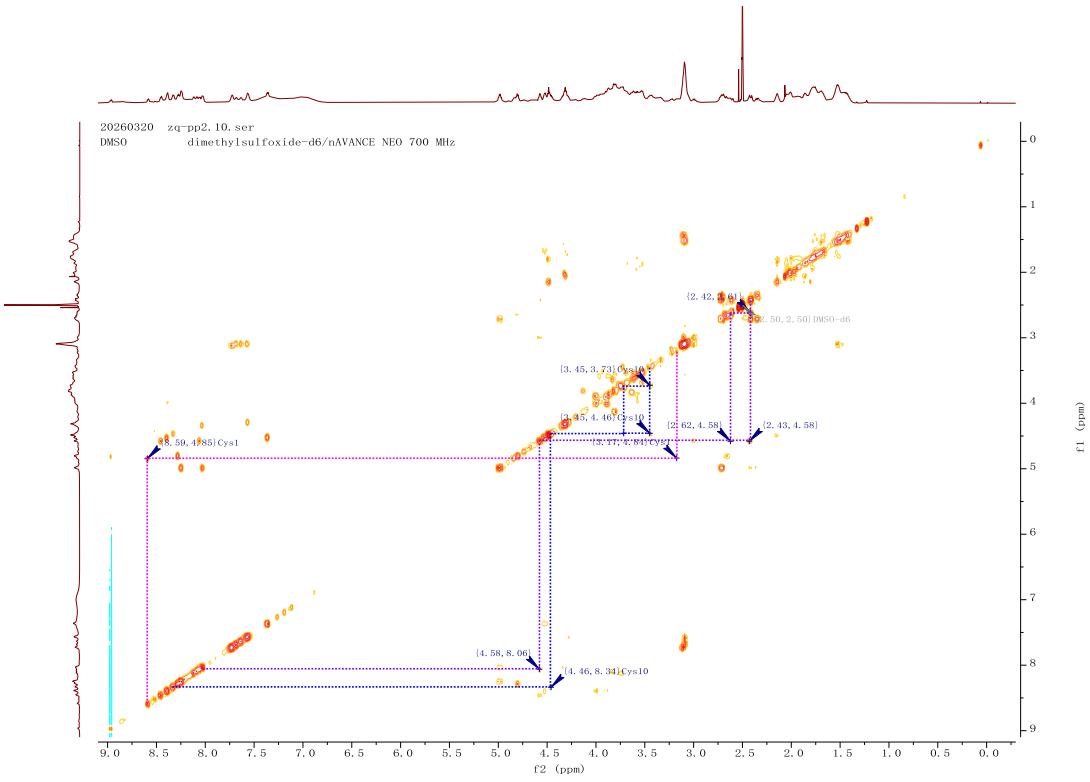

Fig S254. ^{1}H-^{1}H COSY spectrum of **B1b.** Dashed lines trace the spin systems of Cys1 (pink), Asp9 (purple), and Cys10 (blue). Annotated values represent chemical shifts (ppm).

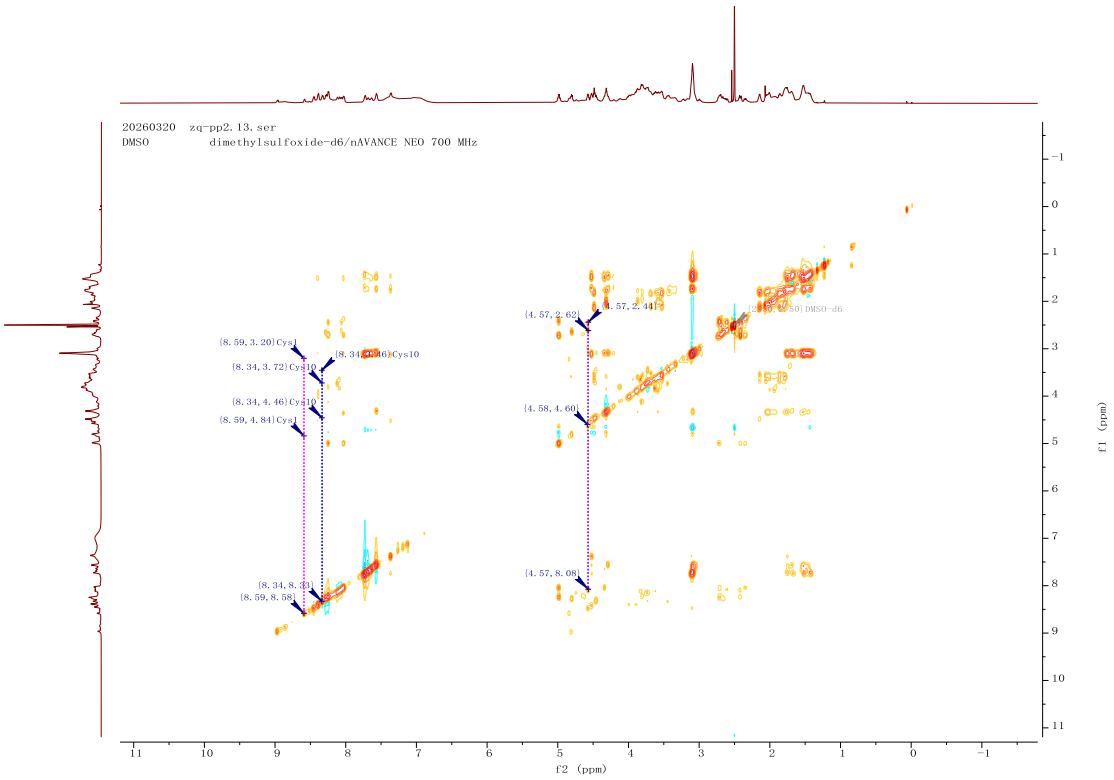

Fig S255. TOCSY spectrum of **B1b.** Dashed lines trace the spin systems of Cys1 (pink), Asp9 (purple), and Cys10 (blue). Annotated values represent chemical shifts (ppm).

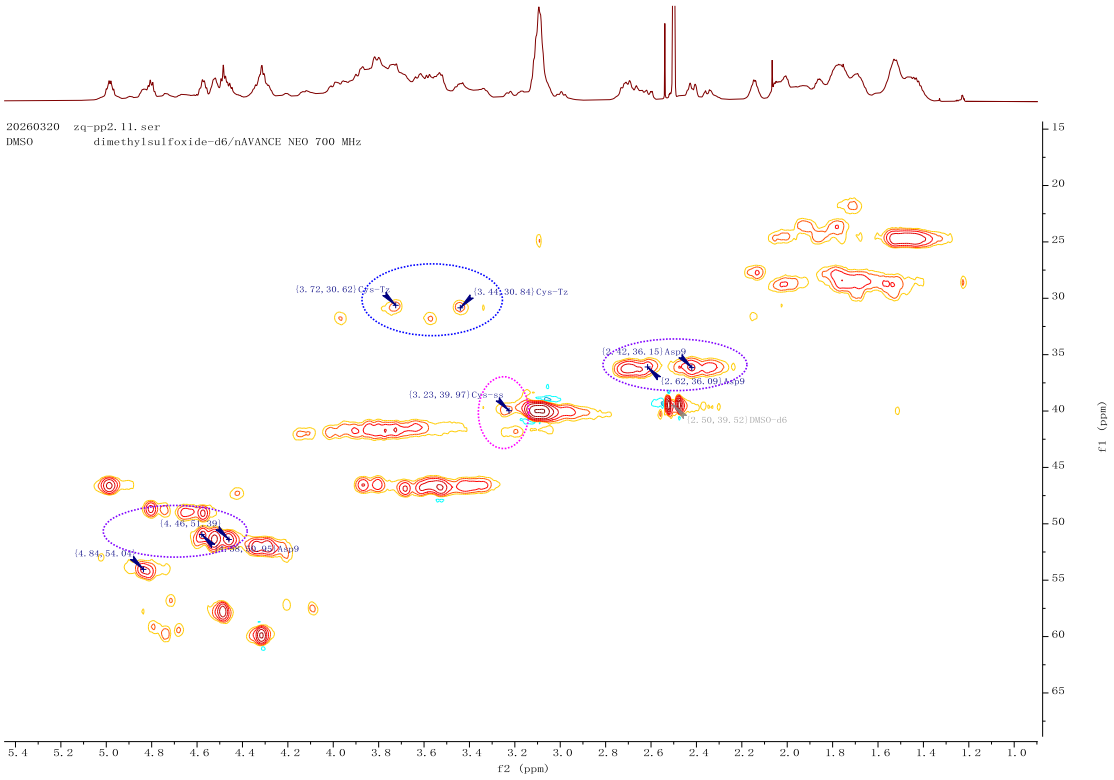

Fig S256. HSQC spectrum of **B1b.** Colored dashed ovals highlight specific cross-peaks: blue for Cys10, purple for Asp9, and pink for Cys1. Annotated values represent chemical shifts in ppm.

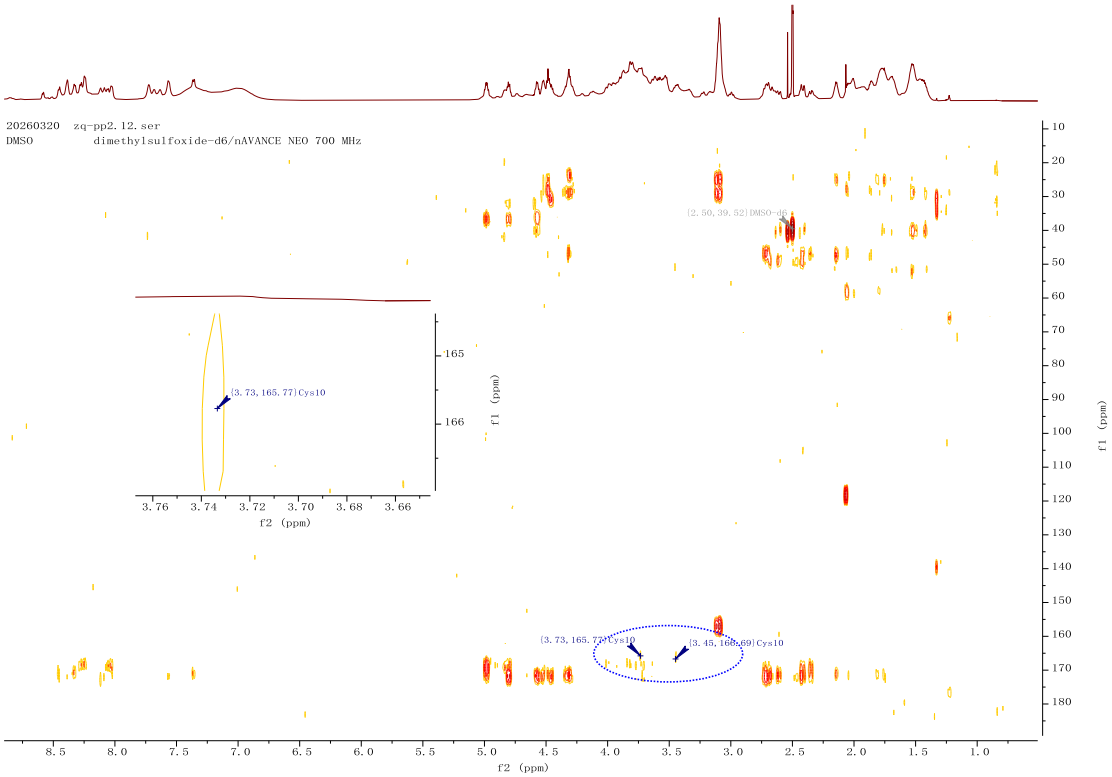

Fig S257. HMBC spectrum of **B1b.** Colored dashed ovals highlight specific cross-peaks: blue for Cys10. Annotated values represent chemical shifts in ppm.

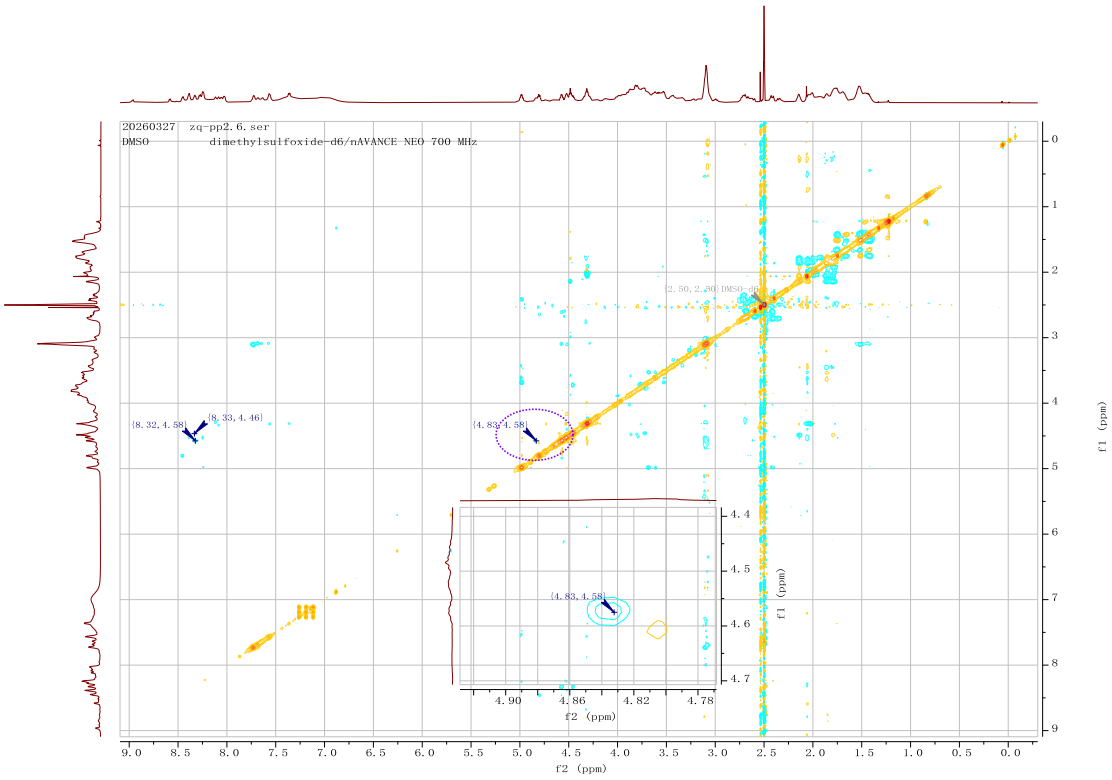

Fig S258. ROESY spectrum of **B1b.** The purple dashed oval and the corresponding magnified inset highlight the spatial NOE correlation between Cys1 and Asp9. Annotated values represent chemical shifts in ppm.

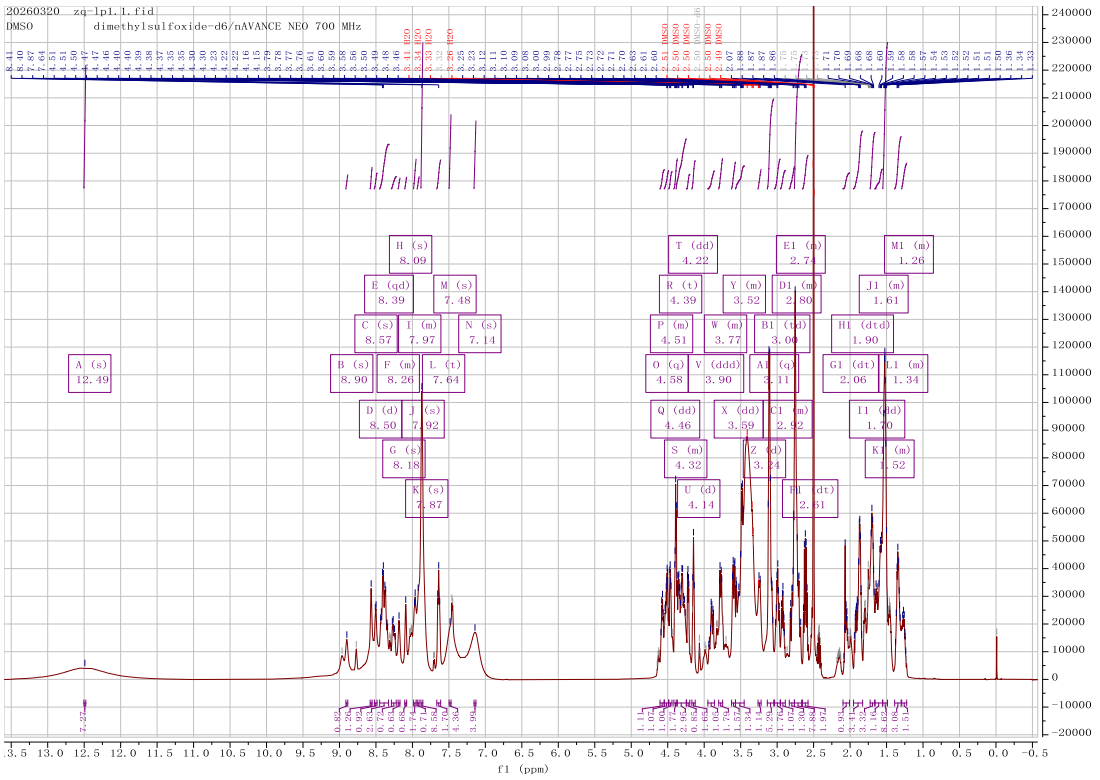

Fig S259. ^{1}H-^{1}H COSY spectrum of **L38.**

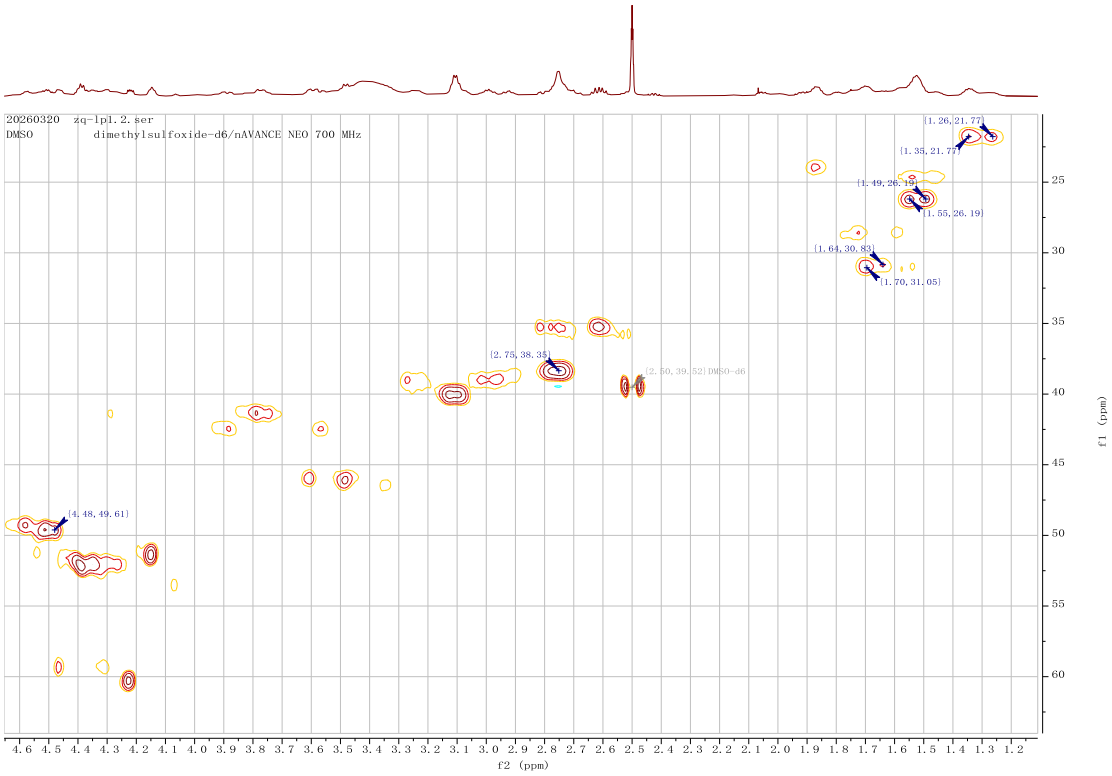

Fig S260. HSQC spectrum of **L38.** The annotated cross-peaks specifically highlight the ^{1}H and ^{13}C chemical shifts assigned to the Lysine (Lys) residue. Values next to the peaks are given in ppm.

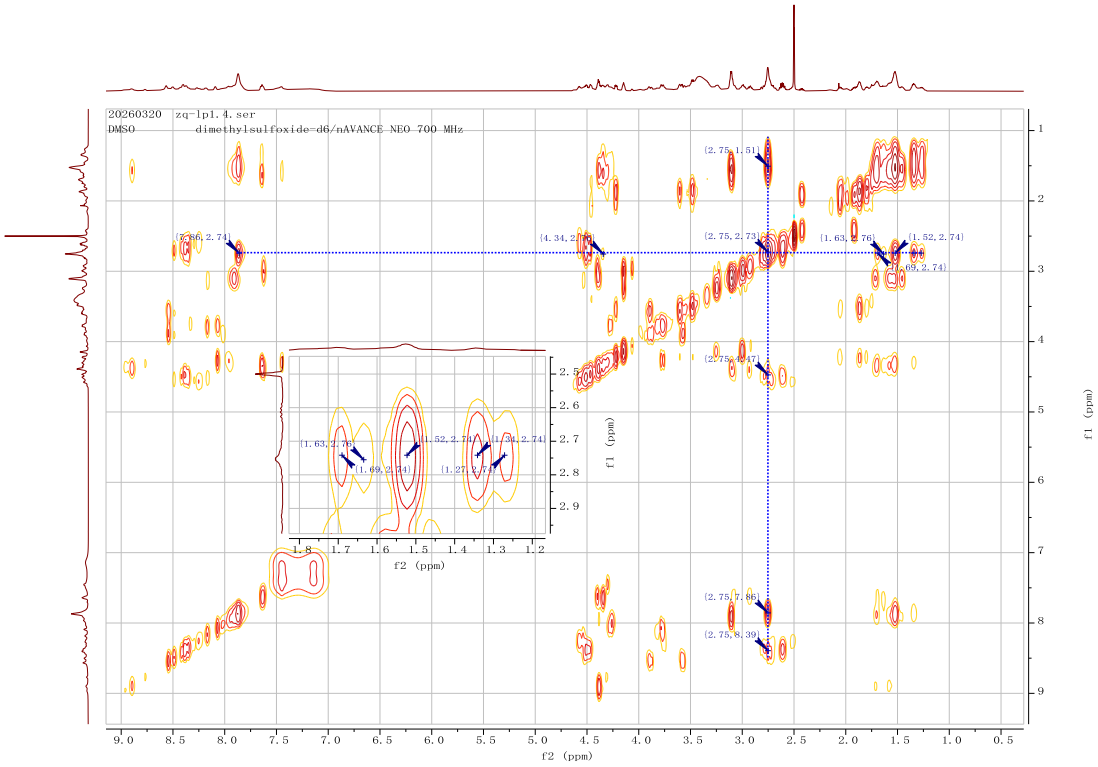

Fig S261. TOCSY spectrum of **L38.** Dashed lines trace the spin systems of Lys (blue). Annotated values represent chemical shifts (ppm).

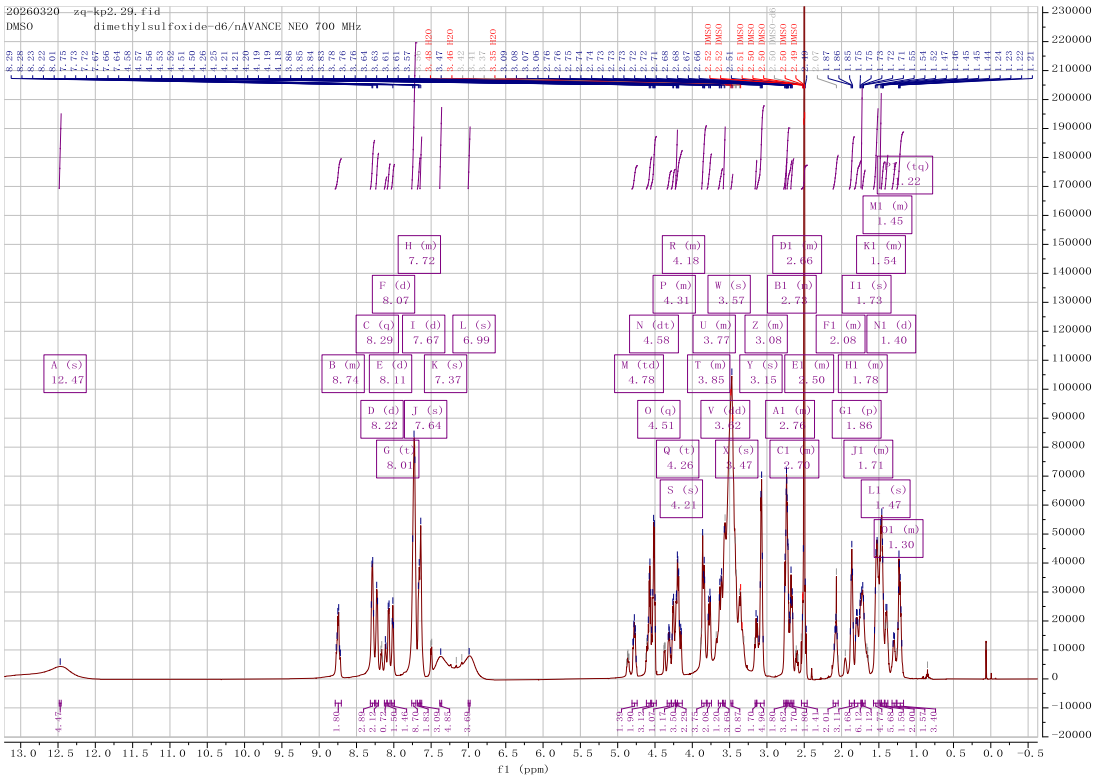

Fig S262. ^{1}H spectrum of **B38a.**

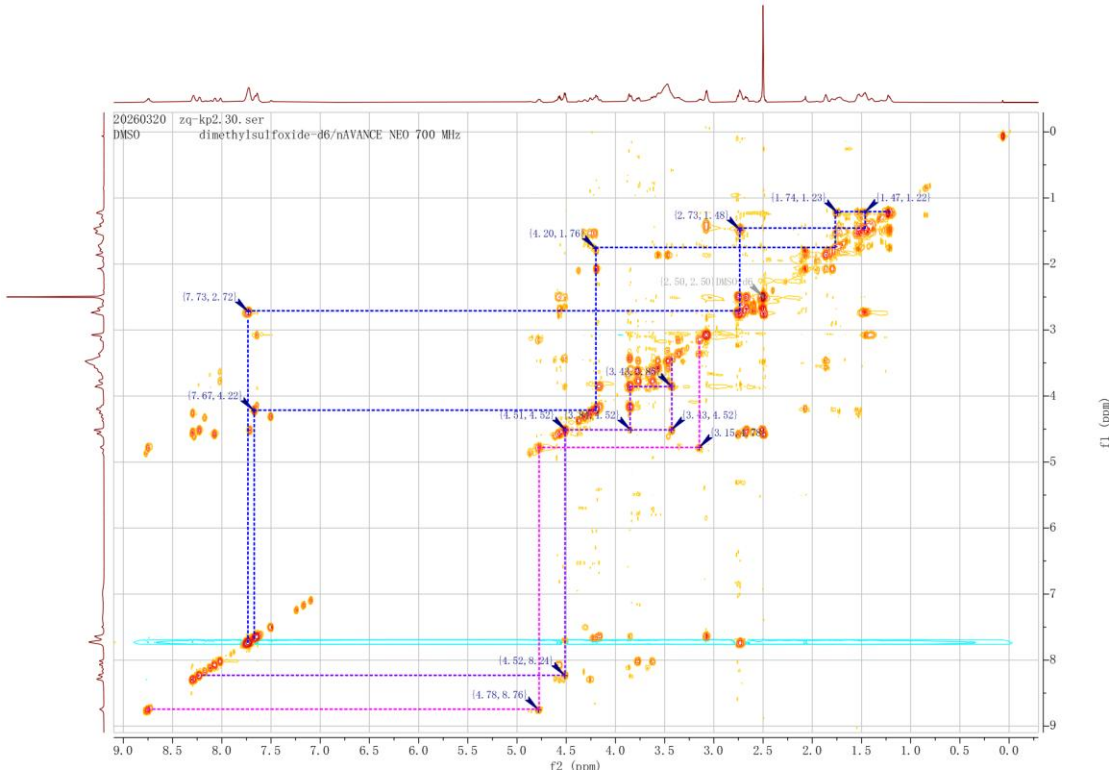

Fig S263. ^{1}H-^{1}H COSY spectrum of **B38a.** Dashed lines trace the spin systems of Cys1 (pink), Lys5 (blue), and Cys9 (purple). Annotated values represent chemical shifts (ppm).

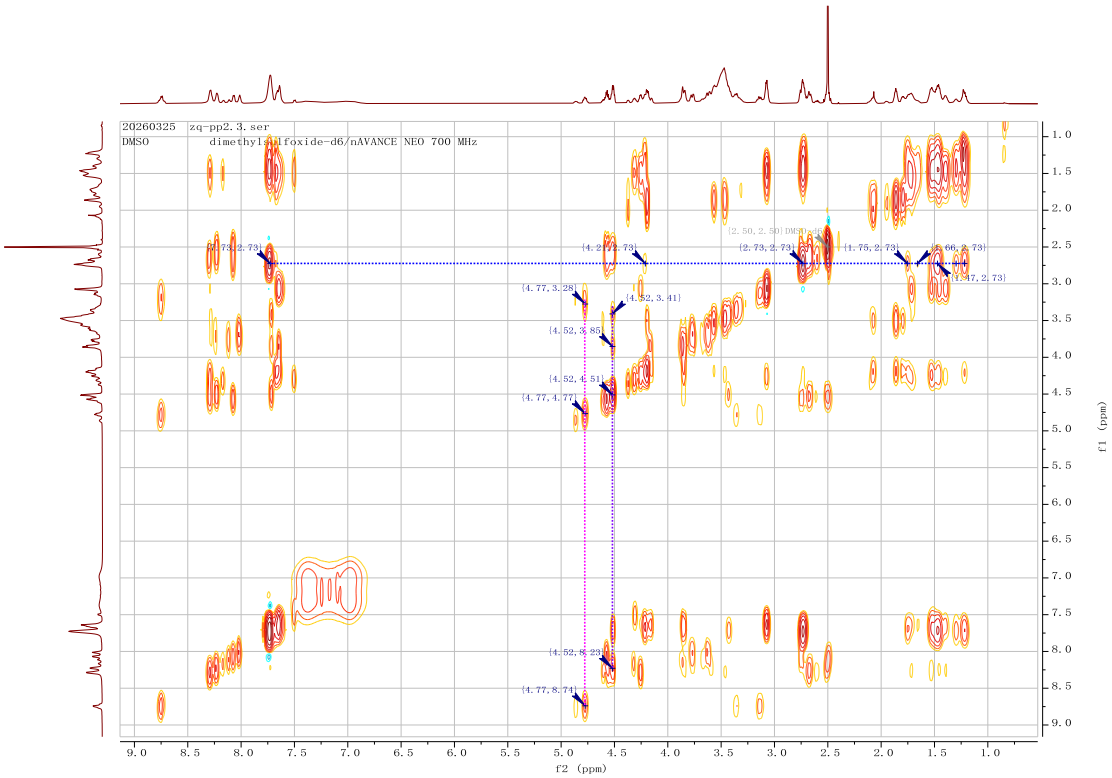

Fig S264. TOCSY spectrum of **B38a.** Dashed lines trace the spin systems of Cys1 (pink), Lys5 (blue), and Cys9 (purple). Annotated values represent chemical shifts (ppm).

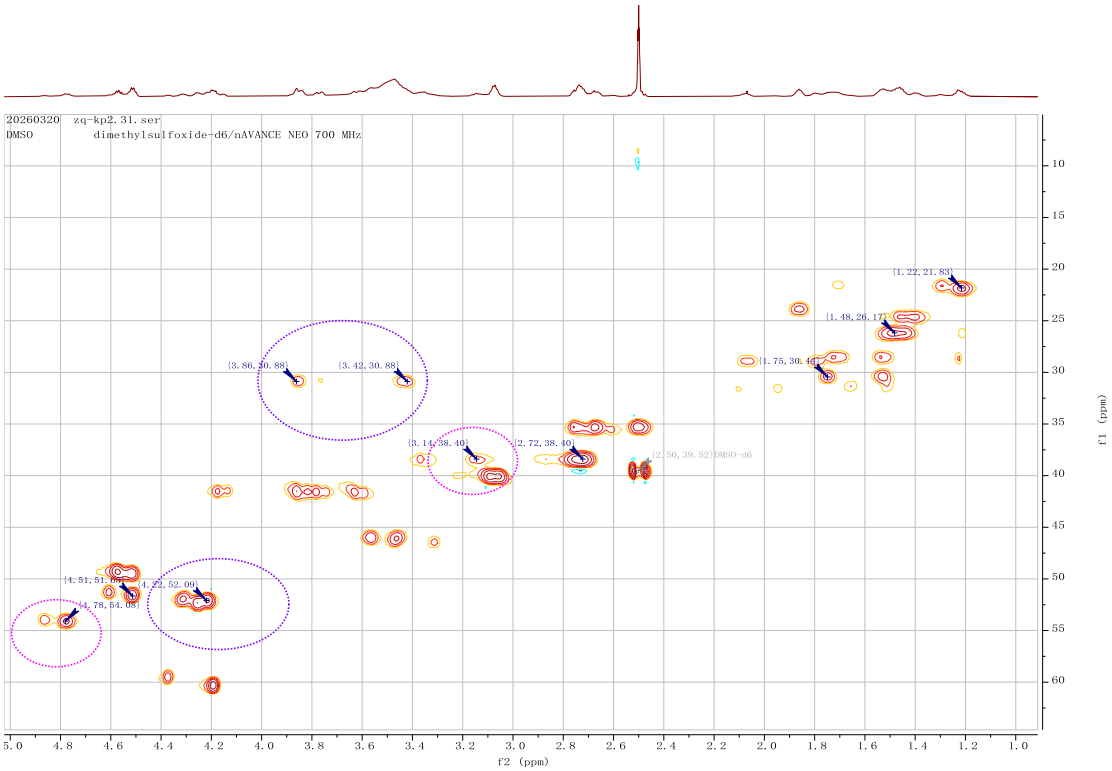

Fig S265. HSQC spectrum of **B38a.** Colored dashed ovals highlight specific cross-peaks: purple for Cys9, and pink for Cys1. Annotated values represent chemical shifts in ppm.

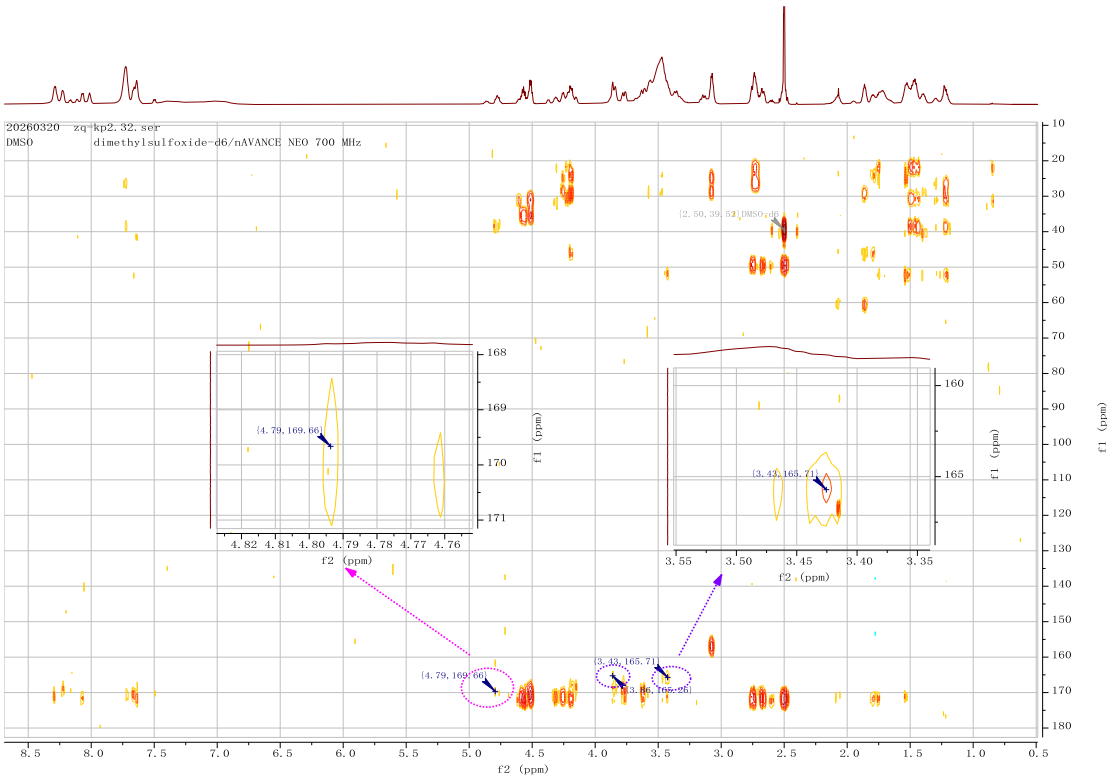

Fig S266. HMBC spectrum of **B38a.** Colored dashed ovals highlight specific cross-peaks: purple for Cys10, and pink for Cys1. Annotated values represent chemical shifts in ppm.

Fig S267. ^{1}H spectrum of **B38b.**

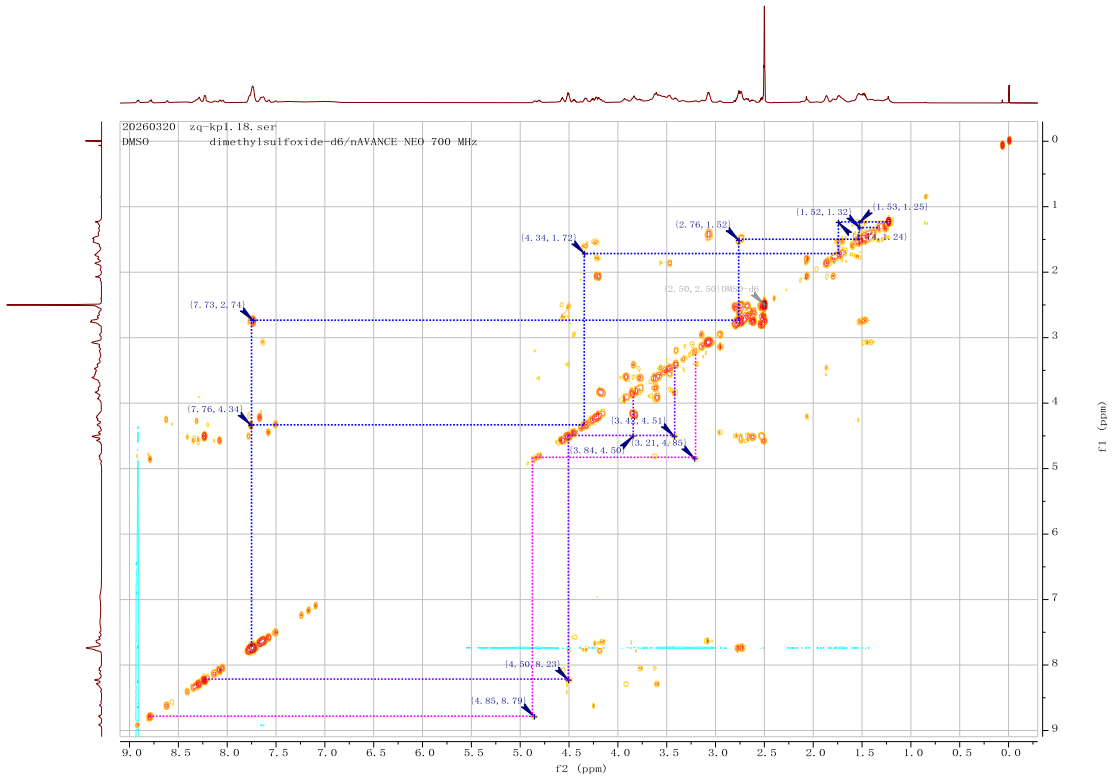

Fig S268. ^{1}H-^{1}H COSY spectrum of **B38b.** Dashed lines trace the spin systems of Cys1 (pink), Lys5 (blue), and Cys9 (purple). Annotated values represent chemical shifts (ppm).

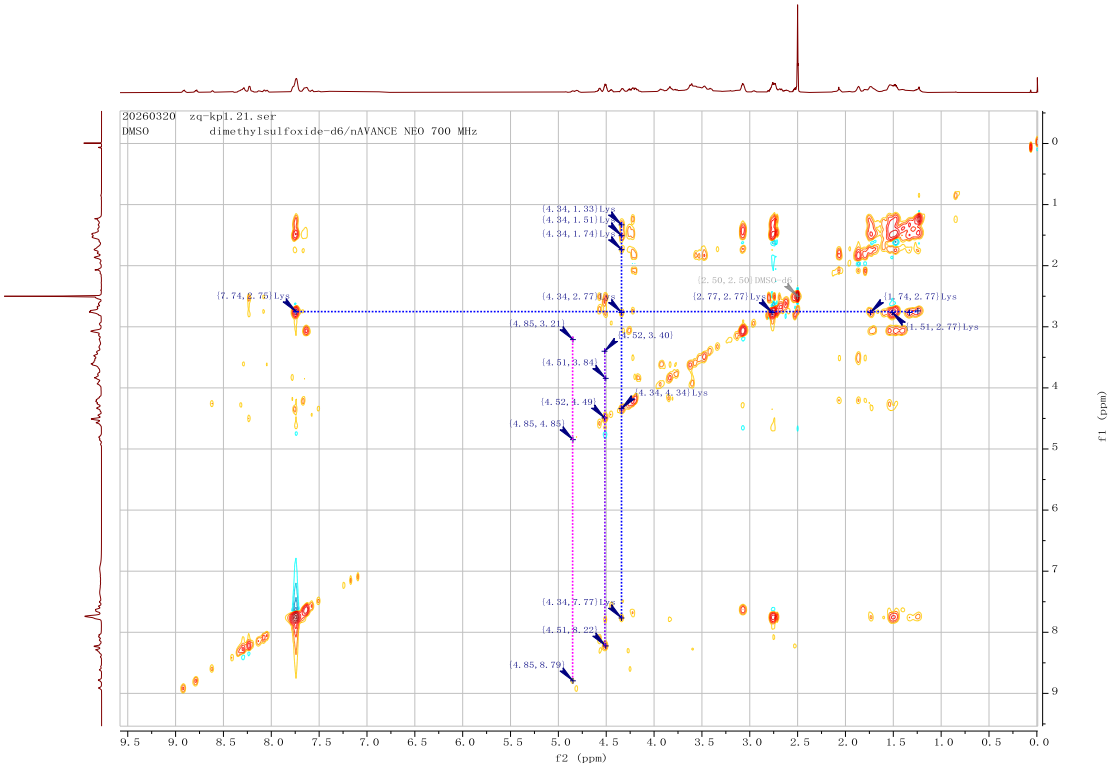

Fig S269. TOCSY spectrum of **B38b.** Dashed lines trace the spin systems of Cys1 (pink), Lys5 (blue), and Cys9 (purple). Annotated values represent chemical shifts (ppm).

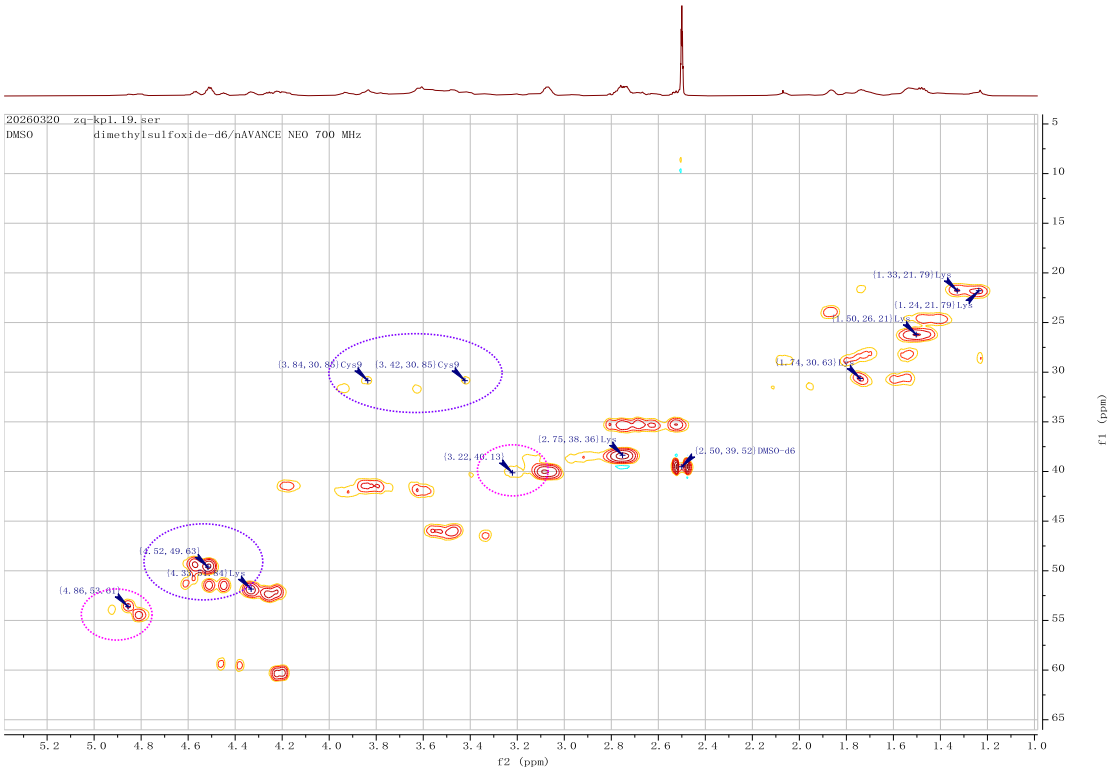

Fig S270. HSQC spectrum of **B38b.** Colored dashed ovals highlight specific cross-peaks: purple for Cys9, and pink for Cys1. Annotated values represent chemical shifts in ppm.

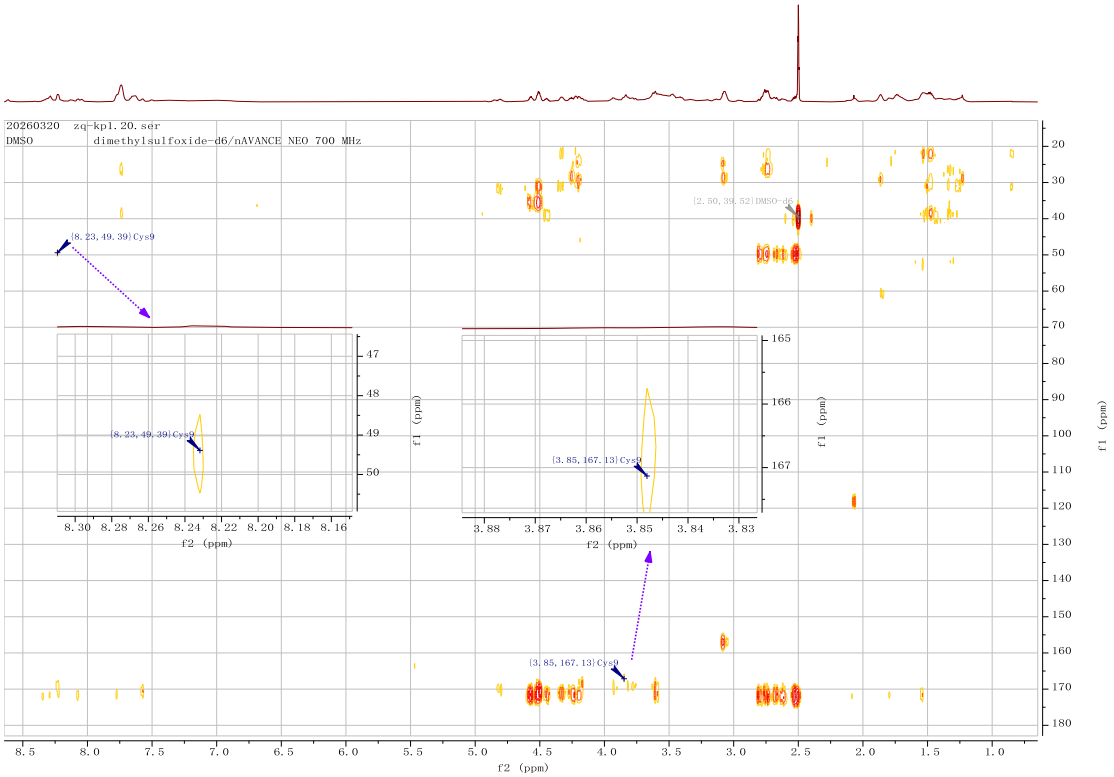

Fig S271. HMBC spectrum of **B38b.** Colored dashed ovals highlight specific cross-peaks: purple for Cys9. Annotated values represent chemical shifts in ppm.

11. Reference

1. Bao, G. *et al.* Dimethyl sulfoxide/visible-light comediated chemoselective C–S bond formation between tryptophans and thiophenols enables site-selective functionalization of peptides. *CCS Chem* **6**, 1547–1556 (2024).